The University Of Sheffield.

Macrophage Microvesicle Production and Targeting in Atherosclerosis

Taghreed Shamrani

Registration Number: 170249504

A thesis submitted in partial fulfilment of the requirements for the degree of Doctor of Philosophy

The University of Sheffield

Faculty of Medicine, Dentistry & Health

Department of Infection, Immunity & Cardiovascular Disease

December 2021

Acknowledgement

Above all, thank god for giving me the opportunity to hold the title (dr) for the second time. Secondly, a special thanks goes to my parents and sisters for supporting me and being always there whenever I need. And for King Abdulaziz University for this opportunity.

I can't thank my supervisor, Dr.Heather Wilson, enough for so many things; her supervision, providing unlimited support, offering help whenever I need, also for being a great person. A special thanks to Dr.Victoria Ridger for her supervision and providing protocols and always offering help and advice. Another special thank you to Prof. Endre Kiss-toth who also provided great advice and help.

A huge thank you to Dr.Merete Long for her unlimited help and advice (much appreciated), and to my lab group : Dr.Chiara Niespolo, Dr. Kajus Baidzajevas, and Dr. Laura Martinez Campesino for answering all of my questions regarding lab work and for teaching me a lot. A great help from Charlotte Moss for performing qPCR , thank you so much. Also, from Dr. Jaime Canedo for SEM, thank you a lot. Thank you to Areej Al-Ahmadi, Dr.Klaudia Kocsy, Favour Felix, Dr. Majid Al-Mansouri, Lucy Urwin, Meltem Catalbas, and Arshnous Marandi for your help and for being great friends.

Laila Allihaybi, was more than just a close friend to me, she was a friend, a sister, a mentor, a life-coach, who was always there for me to help me taking the right decisions. A pure soul who will not be forgotten easily, losing her had a huge impact on me, May her soul rest in peace.

A special thanks to my best friend Dr.Borooj Alzahrani for being a great person and for her help and advice in my life choices.

Big thank you to the technicians team specially to Mr.Jonathan Kilby for helping a lot with cell culture, to Dr. Benjamin Durham for phlebotomy work, to Miss.Pooja Patel for her help in cell culture, lastly to Dr.Mark Ariaans for his efforts in health and safety.

Declaration

The work in this PhD thesis was performed and analysed by myself except stated otherwise in the methods section. A huge thank you to Charlotte Moss for performing the whole qPCR presented in this thesis, and to Dr. Klaudia Kocsy for performing qPCR for HUVECs samples and for designing MerTK primers. A huge thank you to Dr. Jaime Canedo for performing SEM (secondary fixation and imaging), for multiple times. Thank you to Dr. Daniella Pirri for providing HUVECs samples and to Prof. Sheila Francis (Pooja Patel) for providing SMCs samples.

Table of Contents

Table of Figures

Table of Tables

List of Abbreviations

MV	Microvesicle
PS	phosphatidylserine
IL-1β	Interleukin-1 beta
MerTK	Mer Tyrosine Kinase receptor
ATP	Adenosine Triphosphate
BzATP	2'(3')-O-4-benzoylbenzoyl- ATP
iBMDMs	Immortalised Bone Marrow-Derived Macrophages
hMDMs	Human Monocyte-Derived Macrophages
PBMCs	Peripheral Blood Mononuclear Cells
HUVECs	Human Umbilical Vein Endothelial Cells
HMEC	Human microvascular endothelial cells
HAECT	Human aortic endothelial cell line
ECs	Endothelial Cells
SMCs	Smooth Muscle Cells
LPS	Lipopolysaccharide
MCP-1	Monocyte Chemoattractant Protein-1
VCAM-1	Vascular Cell Adhesion Molecule-1
ICAM-1	Intracellular Adhesion Molecule-1
NLRP3	Nucleotide-binding domain Leucine-Rich repeat containing family, Pyrin domain containing 3
TNF	Tumor Necrosis Factor
IFN	Interferon
LDL	Low Density Lipoprotein
oxLDL	Oxidized Low Density Lipoproteins
siRNA	small interfering RNA
Fig.	Figure

PMA	Phorbol 12-Myristate 13-Acetate
PBS	Phosphate-Buffered Saline
M-CSF	Macrophage Colony Stimulating Factor
ELISA	Enzyme-Linked ImmunoSorbent Assay
GFP	Green Fluorescent Protein
SEM	Standard Error of the Means
SD	Standard Deviation
ANOVA	Analysis of Variance
NT	Non-Targeting

Abstract

Extracellular vesicles (EVs) are cell-derived membrane structures that include exosomes and microvesicles (MVs). They are found circulating in the blood of healthy individuals, but increased levels have been observed in pathological conditions such as cardiovascular disease. MVs are shed from a variety of cells including monocytes and macrophages that are involved in atherosclerotic plaque development and instability. Macrophage-derived MVs were shown previously to contain pro-inflammatory cytokines including IL-1β, with the potential to induce inflammation in atherosclerosis in their delivery of biological cargo. The original study selectively isolated phosphatidylserine (PS)-exposed MVs found to contain IL-1β, following LPS and $P2X_7$-dependent ATP stimulation. Since the time of this study, differential centrifugation methods have been standardised for the isolation of extracellular vesicles, quantified using bead-calibrated flow cytometry where vesicles are often found to be composed of a mixed PS-positive and PS-negative population. MerTK has been identified as a key PS-receptor; preliminary work in our group using a zebrafish line lacking MerTK showed attenuated targeting of IL-1β to the head region following tail-fin injury, which was speculated to be mediated by MV delivery.

It was hypothesised that macrophages shed PS-exposed MVs containing IL-1β, which is targeted to endothelial cells via the MerTK PS receptor contributing to atherosclerosis. Macrophage-derived MVs were isolates using differential centrifugation to characterise their number, size and PS-exposure by annexin V-labelling using flow cytometry in order to determine whether production and PS-exposure was stimulus dependent. The proportion of IL-1β secretion in MVs was assessed, compared to vesicle-independent release. The dependency of targeting of IL-1β-containing MVs on MerTK expression, and whether expression of this receptor alters with stimulus and cell-type, was also assessed.

The number of macrophage-derived MVs produced in differentiated THP-1 human monocytic cells, in immortalised mouse bone-marrow derived macrophages and in human primary monocyte-derived macrophages was not found to be stimulus dependent in response to LPS and BzATP treatment. The proportion of PS-positive MVs did not alter with these stimuli compared to untreated control cells. Microvesicle

numbers and PS-positivity were unaffected by $P2X_7$ receptor and caspase-1 inhibition. Secretion of IL-1β was increased in human primary monocyte-derived macrophages following LPS and BzATP treatment. Separation of MVs using differential centrifugation showed that the highest proportion of IL-1β was in the MVs-free fraction compared to the MV pellet.

Differential expression of MerTK was shown in a variety of cell types associated with atherosclerotic plaque progression, with an absence in vascular smooth muscle cells and higher expression in endothelial cells and macrophages. MerTK expression was not induced by a variety of stimuli and conditions including inflammation, infection and altered shear stress, the latter relating to disturbed blood flow at atheroprone regions of the endothelium. Expression of MerTK was detected in epithelial cells including the HeLa cell line. The role of MerTK in regulating IL-1β targeting from MVs was tested using HeLa-cell IL-6 induction as a bioassay for IL-1β targeting. Knock-down of MerTK in HeLa cells did not inhibit MV IL-1β-targeting in this IL-6 bioassay; we wish to test this in endothelial cells going forward.

Overall, these findings indicate that macrophage MVs production is not stimulus dependent, that most IL-1β is secreted via vesicle-independent mechanisms, and that MVs do not appear to target their IL-1β-content in a Mer-TK-dependent manner.

Chapter 1 . Introduction

Cardiovascular disease (CVD) remains the leading cause of morbidity and mortality worldwide. The global deaths in 2013 and 2015 were estimated at around 17 million attributed to cardiovascular diseases, this being the main cause of non-communicable disease mortality (Wang et al., 2016).

Atherosclerosis is the underlying cause of cardiovascular diseases including coronary artery disease (CAD), peripheral arterial disease, and carotid artery disease. It is a disease of the arterial wall leading to hardening and stiffness, fuelled by the continuous build-up of lipids inside the arterial wall and an inflammatory response. It is a chronic, immunoinflammatory, progressive disease that affects the large and medium-sized conduit arteries (Woollard and Geissmann, 2010), resulting from the interaction between vascular cells, immunoinflammatory cells including monocytes, macrophages, and T cells together with modified lipoproteins. It is widely recognized to have a slowly progressing pattern and is characterized by the development of atherosclerotic plaques (atheroma) in the intimal layer of the artery protruding towards the lumen. The atherosclerotic plaque consists of fatty streaks, recruited inflammatory cells, calcium deposits, and fibrous elements. The plaque grows and expands due to the rapid accumulation of lipid under a continuous inflammatory process leading to either narrowing of the vessel lumen thus decreasing the blood flow, occlusion, or plaque rupture that induces the formation of thrombus which can ultimately culminate in the development of serious acute conditions such as myocardial infarction, stroke, and peripheral arterial disease (Lusis, 2000).

1.1 Atherosclerosis pathophysiology

1.1.1 Atherosclerosis initiation

Atherosclerosis development is a result of several cardiovascular environmental and genetic risk factors that provoke and may accelerate the progression of plaque formation, such as smoking, hypertension, diabetes, obesity, and elevated serum levels of cholesterol (Glass and Witztum, 2001). As these risk factors participate in triggering inflammatory pathways culminating in arterial wall cells altered functions.

The principal factor that can trigger atherosclerosis development is hypercholesterolemia, the presence of elevated levels of low density lipoproteins (LDL) , which can induce disease even in the absence of other risk factors (Glass and Witztum, 2001).

The fatty streaks, which are the result of lipid droplets phagocytosed by macrophages, accumulate in the arterial wall which serves as a key initiating event in atherosclerosis development (Melaku and Dabi, 2021). When LDL particles are present in high levels in plasma, they are modified to become oxidative either enzymatically or non-enzymatically to become pro-inflammatory, highly atherogenic molecules that induce an immune response (oxLDL) (Insull, 2009, Poznyak et al., 2021). Endothelial cell dysfunction also plays a role in the initiation of the plaque, where endothelial cell injury and subsequent activation caused by the presence of oxidized LDL particles, shear stress disturbances, free radical generation from smoking, diabetes mellitus, genetic modifications, or other risk factors which may damage the endothelium (Ross, 1999). This in turn affects endothelial permeability by an enhanced expression of chemoattractant molecules, such as vascular cell adhesion molecule-1 (VCAM-1) that allow leukocyte adherence to the activated endothelium (Libby, 2002). Another potent chemoattractant chemokine that contributes to leukocyte recruitment and adhesion to the endothelium is monocyte chemotactic protein-1 (MCP-1) which is upregulated by activated endothelial cells, macrophages, and smooth muscle cells (Libby, 2002). Subsequently, monocytes infiltrate into the intimal layer via diapedesis through endothelial cells junctions and then differentiate into macrophages (Fig. 1.1). Macrophages increase their expression of scavenger receptors that recognize and engulf modified lipoproteins which accumulate in the cytoplasm, forming foam cells. This lipid accumulation is initially observed as fatty streaks, which is a pathological hallmark of early stage atherosclerosis (Libby, 2002). These arterial wall changes occur at susceptible sites such as at the arterial bifurcation points where blood flow is disturbed, and walls are exposed to low shear stress, hence enhancing lipid accumulation (Insull, 2009).

1.1.2 Atherosclerotic plaque progression

The atherosclerotic plaque expands over time, mainly due to the accumulation of foam cells and other inflammatory cells such as T lymphocytes alongside smooth muscle

cell migration and proliferation in the intima. Macrophages replicate inside the intima and secrete inflammatory cytokines and growth factors enhancing inflammation and lesion progression. In addition, oxLDL accumulates in the cytoplasm of smooth muscle cells where these cells proliferate in response to growth factors released by macrophages, contributing to continued plaque expansion (Insull, 2009). When the foam cells die oxLDL particles accumulate extracellularly and pool inside the atheroma (Insull, 2009, Libby, 2002). The extracellular matrix of the plaque contains macromolecules such as interstitial collagen and elastin that promote entrapping and pooling of lipids (Libby et al., 2019). The pooling of lipids provokes further release of cytokines, hydrolytic enzymes, and growth factors thus amplifying inflammation that eventually leads to macrophage, lymphocyte, and smooth muscle cell death forming the lipid-rich necrotic core (Fig. 1.1) (Insull, 2009) which further provokes inflammation and lesion expansion. Neovascularization is also a crucial factor in plaque expansion (Camare et al., 2017). Thin, fragile microvasculature form inside the atheroma due to the release of vascular endothelial growth factor (VEGF) and other angiogenic mediators by plaque macrophages (Libby, 2002). These microvasculature predispose the artery to intraplaque haemorrhage and may serve as a marker for lesion progression (Camare et al., 2017). Collectively, these events promote lesion progression and expansion resulting in stenosis or occlusion of the arterial lumen.

1.1.3 Plaque rupture and thrombus formation

The thrombogenic lipid-rich core is surrounded by a fibrous cap composed of smooth muscle cells and collagen-rich matrix generated by these cells to separate it from the blood flow. While the plaque continues to expand, the fibrous cap is weakened and may fracture exposing intimal thrombogenic stimuli, tissue factor (TF) and lipids to the bloodstream, initiating the coagulation cascade and thrombosis (Libby, 2002).

Deposition of calcium nodules on the arterial wall also enhances thrombosis; these deposits occur through all stages of plaque development starting with small nodules and progressing to large deposits that harden the plaque (Insull, 2009).

Plaque rupture is primarily caused by the excessive amounts of proteolytic enzymes such as collagenases and elastases, and matrix metalloproteinases (MMP) released by macrophages that degrade the extracellular matrix (Ramel et al., 2019). Alongside continuous plaque expansion, thinning and fracture of the fibrous cap leads to plaque

instability and eventually rupture forming a thrombus which may result in arterial occlusion causing myocardial infarction, stroke or other acute cardiovascular events (Ross,1999).

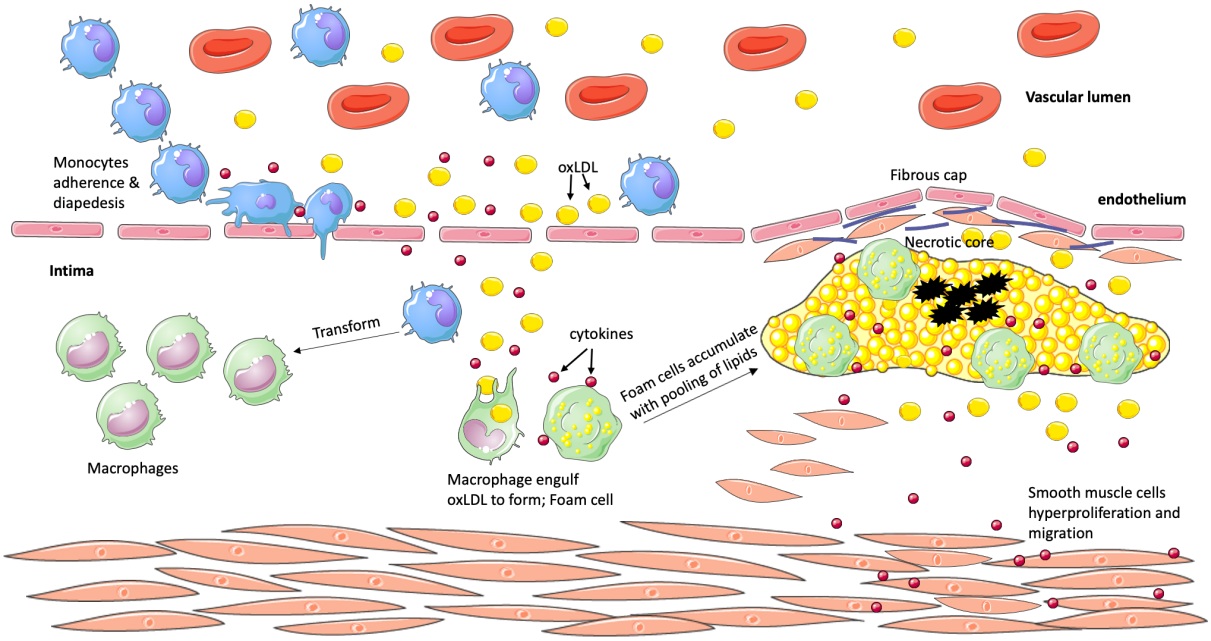

Figure 1.1 Pathophysiological events in atherosclerosis.

Schematic representation of the main events in atherosclerosis development showing high amounts of LDL particles that are oxidized to initiate inflammatory events where circulating monocytes adhere to the endothelium followed by their diapedesis inside the intima under the effects of chemoattractant molecules such as VCAM1 and MCP-1. There monocytes differentiate into lesional macrophages expressing scavenger receptors to facilitate oxLDL engulfment to become foam cells that accumulate together with pooling of oxLDL particles to form the lipid-rich core. Meanwhile, vascular smooth muscle cells proliferate to contribute to plaque progression. The foam cell death contributes to the formation of necrotic core.

1.2 Monocytes and Macrophages

1.2.1 Monocytes in Host Defence

Monocytes are circulating leukocytes and a component of the mononuclear phagocyte system (MPS), derived from bone marrow hematopoietic stem cells, they are precursor of some tissue macrophages and inflammatory dendritic cells (Leon et al., 2005). They play a vital role in host defence through pathogen phagocytosis and inflammatory cytokines production, also playing a role in wound healing and neovascularization (Nahrendorf et al., 2007). Monocytes during inflammation play a role in innate and adaptive immune responses as they are recruited via tissue chemotactic factors to enter the tissues and differentiate irreversibly into macrophages and dendritic cells (Tacke and Randolph, 2006).

Monocytes are divided into two subsets according to the amount of surface markers expressed, CD14 and CD16, which are LPS co-receptor and FcγIII receptors, respectively. The $CD14^{hi}$ and $CD16^{low}$ are the major monocyte subset, comprising approximately 80-90% of circulating monocytes (Passlick et al., 1989), and known as classical monocytes. $CD14^{low}$ and $CD16^{hi}$ are the minor monocyte subset and are known as non-classical monocytes. A third subset is observed in humans, with CD14 and CD16 expression between these two main subsets, referred to as intermediate monocytes (Boyette et al., 2017). Recent studies suggest that classical monocytes confer a pro-inflammatory function in cardiovascular disease involved in cytokine production alongside with the intermediate subset, whilst the non-classical subset participates in resolving inflammation and tissue repair (Wildgruber et al., 2016).

1.2.2 Monocytes in Mouse

The mouse monocytes are classified into two subsets according to the surface expression of the monocyte inflammatory marker Ly6C (Gr1). The first subset is $Ly6C^{+}$ ($Gr1^{+}$) also referred to as $Ly6C^{high}$ and the second is $Ly6C^{-}$ ($Gr1^{-}$) also referred to as $Ly6C^{low}$ (Geissmann et al., 2003). The two subsets differ in the expression of the chemokine receptors CX_3CR1 and CCR2. The $Ly6C^{high}$ monocyte subset express $CCR2^{high}$ CX_3CR1^{low} whilst the $Ly6C^{low}$ express $CCR2^{low}$ CX_3CR1^{high} (Geissmann et al., 2003). However, both subsets were found to express the following surface markers $CD11b^{+}$ and $CD115^{+}$. The human subsets; $CD14^{hi}$ and $CD16^{low}$ or the classical

monocytes are correspondent to the mouse Ly6C^{+} inflammatory subset, while CD14^{low} and CD16^{hi} or the non-classical are correspondent to Ly6C^{-} patrolling subset (Boyette et al., 2017).

The Ly6C^{high} monocyte subset have a large diameter of around 10-14 μm and more granules intracellularly. This subset plays a vital role in inflammation as they showed migratory effect when introduced into inflamed tissue owing to the presence of the chemokine receptor CCR2 abundantly. While the Ly6C^{low} subset were termed as "resident" monocytes as they present circulating in the blood for extended periods and tend to accumulate in the non-inflamed tissues. Also, they are smaller with a diameter of 8-12 μm and less granular than the Ly6C^{high} monocytes (Geissmann et al., 2003).

1.2.3 Monocytes in Atherosclerosis

Monocytes and their descendant macrophages are crucial elements in the development of atherosclerosis as they play a significant role in the atheromatous plaque expansion. In general, the number of circulating classical monocytes; CD14^{hi} and CD16^{low} reflect cardiovascular disease progression, as their number increase, the disease progresses and worsens (Swirski et al., 2007), as they predict adverse cardiovascular events. Studies showed that the classical monocytes tend to adhere to the endothelium and migrate into the intima more than other monocyte subsets (Hilgendorf et al., 2015). Elevated levels of circulating classical and intermediate monocytes are associated with acute myocardial infarction (Tsujioka et al., 2009) as they tend to accumulate at the infarction borders in patients with acute myocardial infarctions (van der Laan et al., 2014). A recent study have found a fourth subset of circulating monocytes i.e. CD14^{hi} and no CD16 surface expression in patients diagnosed with acute coronary syndrome, whilst the non-classical subset was more abundant in patients with chronic coronary syndrome (Vinci et al., 2021). Several studies using *in-vivo* atherosclerotic models showed that hypercholesterolemia provokes monopoiesis; a process of producing excessive amounts of monocytes, in particular the CD14^{hi} subset from the bone marrow (Hilgendorf et al., 2015) and from extra-medullary organs such as the spleen (Robbins et al., 2012). Furthermore, monocytes are mobilized from bone marrow to the inflammation site which is seen atherosclerosis, this mobilization is achieved through chemokine/chemokine receptor

(CCR) responses. The study by (Boring et al., 1998), showed that blocking CCR2 in an atherosclerotic mouse model resulted in decreased lesion formation since it affected the monocyte mobilization from the bone marrow. In spite of that, the exact role of monocyte subsets in each stage of atherosclerosis has not yet been fully elucidated.

1.2.4 Macrophages in Atherosclerosis

Macrophages play a key role through all stages of atherosclerosis development. Among the inflammatory cells involved and contributing to the plaque development and initiation, macrophages are key in disease progression. It is thought that lesional macrophages are only derived from the circulating monocytes that are recruited to adhere to the endothelium and subsequently migrate across the intima where they transform into macrophages. However, recent studies showed that the intima contains resident macrophages derived from pericytes or perivascular cells; cells that surround endothelial cells characterized by pluripotent properties (Orekhov et al., 2014).

The macrophages present in atherosclerotic plaques have a diminished ability to migrate outside of the plaque due to the presence of engulfed lipid droplets that upregulate the expression of migration inhibitory molecules (van Gils et al., 2012). They replicate locally and die inside the plaque and their ability to clear apoptotic cells is impaired (Gautier et al., 2009). Plaque macrophages participate in the formation of the necrotic core and promote chronic inflammation within the intima. Notably, macrophages are the main source of plaque pro-inflammatory mediators such as cytokines, chemokines, reactive oxygen species, growth factors and matrix degradation enzymes. In turn these factors augment monocyte recruitment and transmigration, smooth muscle cell proliferation, and lipid uptake.

1.3 Inflammation driving atherosclerosis

1.3.1 Atherosclerosis is a chronic inflammatory disease

Chronic inflammation refers to a condition where inflammation persists over a prolonged period due to an inability to eliminate the cause. In atherosclerosis, disease is characterized by a slow progression and is considered a chronic condition. It is associated with recurrent destruction and repair of tissues due to the persistent presence of inflammatory mediators released by several cell types. Atherosclerosis can progress silently where no clinical symptoms appear. Multiple plaque ruptures with subsequent healing have been reported (Burke et al., 2001) which are more to contribute to plaque progression associated with sudden cardiac death due to intraplaque haemorrhage (Chistiakov et al., 2015).

Circulating inflammatory molecules that can predict cardiovascular risk include; C-reactive protein (CRP), an acute phase reactant, is a valuable biomarker which can reliably indicate atherosclerosis (Libby and Ridker, 2004). Its release is driven most apically by IL-1 that is also responsible for driving other secondary inflammatory cytokines such as IL-6 and IL-8. It was observed that IL-1 has an autocrine effect on the cells releasing this cytokine, as well as the targeted cells, which may contribute to the persistence of the disease.

1.3.2 Role of Interleukin-1 in atherosclerosis

Interleukin-1

Interleukin-1 (IL-1) comprise a family of regulatory and inflammatory cytokines that have a central role in the innate and adaptive immune response, involved in mediating both acute and chronic inflammation and in inducing local and systemic responses. The family comprises of 11 members: IL-1α, IL-1β, IL-1Ra, IL-18, IL-33, IL-36α, IL-36β and IL-36γ, IL-36Ra, IL-37, IL-38 (Dinarello, 2011). Some of the members have pro-inflammatory properties such as IL-1α, IL-1β, IL-18, IL-33, IL-36α, IL-36β and IL-36γ which activate inflammation in an autocrine and paracrine mode, whilst four have antagonistic properties including IL-1Ra, IL-36a, IL-37 and IL-38 (Dinarello, 2018). The IL-1Ra competes with IL-1α/β for IL-1Receptor 1 binding, IL-36Ra competes with IL-36α/β/γ and IL-38 for IL-36 binding, and IL-38 structure is related to IL-1Ra (Yuan et

al., 2015, Dinarello, 2018, Bensen et al., 2001). The cytokine IL-37 has anti-inflammatory properties as it supresses the inflammatory response through acting on inhibiting pro-inflammatory cytokines production and function (Tete et al., 2012). IL-1 is highly expressed by immune cells including monocytes, macrophages, dendritic cells, B lymphocytes, and natural-killer cells, and affects multiple cell types.

IL-1 has the ability to regulate its own gene expression by a positive feedback loop which results in producing further biologically active IL-1, in addition to its ability to drive secondary inflammatory cytokine gene expression such as IL-6, IL-8 and C-reactive protein (CRP) hence being apical to inflammatory cytokine responses (Ridker, 2016).

Interleukin-1 in atherosclerosis

IL-1 is strongly implicated in atherogenesis and has multiple effects on cells involved in atherosclerosis including endothelial cells, smooth muscle cells, and monocyte/macrophages. IL-1 can alter functions of vascular endothelial cells to enhance leukocyte recruitment and adhesion, by activating cell surface expression of intercellular adhesion molecule-1 (ICAM-1) and (VCAM)-1 (Marui et al., 1993), and by enhancing the production of the chemokine, MCP-1 (Kirii et al., 2003). Moreover, it promotes the proliferation of vascular smooth muscle cells by triggering them to produce platelet-derived growth factor (PDGF) (Libby et al., 1988).

1.3.3 Interleukin-1β (IL-1β)

IL-1β has gained attention due to its major contribution in atherosclerotic lesion development since it is the main cytokine found in atherosclerosis and has a potent pro-inflammatory effect acting locally and systemically. Several lines of studies showed strong indications of the involvement of IL-1β in atherogenesis. Researchers (Shimokawa et al., 1996) created an inflammatory lesion in the coronary artery of a porcine model that showed stenotic lesions and intimal thickening of the coronary arterial wall when exposed chronically to IL-1β denoting to its effect on platelet-derived growth factor production by vascular wall cells. Another *in vivo* study on hypercholesteraemic mice showed that IL-1β increases the atherosclerotic lesion size denoting to its effect on the expression of VCAM-1 and MCP-1 which is increased compared to the mice lacking IL-1β (Kirii et al., 2003).

IL-1β a therapeutic target

IL-1α and IL-1β are the most studied isoforms, they are related although both differ markedly structurally and functionally, they bind to the receptor IL-1RI, a member of IL-1 receptor family that present on almost all cells, to initiate signal transduction to a certain cell and trigger a cascade to mediate the release of secondary cytokines and chemokines. The endogenous IL-1 receptor antagonist (IL-1Ra) can also bind to IL-1RI effectively inhibiting IL-1α and IL-1β inflammatory actions (Dinarello, 2011). IL-1RI which was successfully blocked by IL-1 receptor antagonist (IL-1Ra) proved to decrease inflammation. A study was performed by generating hyperlipidaemic mice that were IL-1Ra deficient showing that IL-1Ra absence caused increased intimal thickening suggesting its role in supressing the lesion development (Isoda et al., 2004). Another study on atherosclerotic mouse model was conducted showing homozygous deficiency of IL-1Ra results in lethal arterial inflammation and increased number of macrophages in the plaque (Nicklin et al., 2000). Thus, IL-1Ra is required to limit atherosclerosis development.

The receptor antagonist (IL-1Ra) is known as anakinra and is used in a variety of diseases entail inflammation such as rheumatoid arthritis limiting the disease burden. Another anti-inflammatory agent, canakinumab a human monoclonal antibody that targets IL-1β is beneficial in the cases of atherosclerosis since IL-1β has been proved to be the apical inflammatory cytokine driving inflammation in atherosclerosis. Researchers studied the effects of canakinumab on atherosclerosis showing reduced inflammation and reduced levels of IL-6 and CRP, the secondary cytokines driven by IL-1β (Ridker et al., 2012). More recently canakinumab was shown to reduce recurrent cardiovascular events when used in clinical trials of patients with previous myocardial infarction and circulating CRP (Ridker et al., 2017).

IL-1β synthesis and secretion mechanisms

IL-1β is produced by immune cells in response to pathogen-associated molecular patterns (PAMPs), which are conserved microbial molecules, and damage-associated molecular patterns (DAMPs) such as lipid, some metabolites and cell damage products including ATP. These molecules are considered pathogenic and activate the immune response when recognized by pattern recognition receptors (PRR) of immune cells (Takeuchi and Akira, 2010) (Fig. 1.2). IL-1β is primarily produced in an inactive

form (pro-IL-1β), a precursor that needs processing to perform biological functions. A proteolytic enzyme called caspase-1 activates the precursor through cleavage from 33-kDa into 17-kDa a mature form (Thornberry et al., 1992). Caspase-1 is activated by a multiprotein complex called Nucleotide-binding domain Leucine-Rich repeat containing family, Pyrin domain containing 3 (NLRP3) inflammasome involved in cleaving pro-caspase1 (the inactive form) into caspase-1 (the active form) (Martinon et al., 2002). The NLRP3 inflammasome is assembled and activated by several conditions associated with atherosclerosis for instance, disturbed blood flow activates the formation of the inflammasome in endothelial cells (Xiao et al., 2013), hypoxia (Folco et al., 2014) and acidic environments (Rajamaki et al., 2013) act as endogenous danger signals triggering inflammasome assembly and activation.

Most proteins secreted by cells are exported extracellularly through endoplasmic reticulum (ER) to Golgi apparatus route of secretion, which is known as the conventional or classical pathway. The protein's nascent peptide is translated in the ribosome requiring the presence of a signal sequence in order to be translocated to the lumen of the ER. However, the IL-1β precursor lacks this leader sequence and so does not enter the ER-Golgi classical pathway, meaning it must follow a non-conventional route of secretion (Rubartelli et al., 1990). Researchers demonstrated the translation of IL-1β on intracellular cytoskeleton-associated free ribosomes (Stevenson et al., 1992).

The mechanism of IL-1β release is not clear yet although, several mechanisms are proposed in the literature. The first mechanism proposed is that IL-1β is secreted through exocytosis of endolysosomes, where cytosolic IL-1β is contained in vesicles to protect it from cellular enzymatic degradation (Andrei et al., 1999). These protected proteins are prone to degradation in basal conditions whilst in the presence of a stimulus such as extracellular ATP, their release is enhanced, and these IL-1β-contained vesicles are rescued from degradation. This process is also known as "autophagy". The second mechanism proposed is referred to as a "protected mechanism" is through shedding of IL-1β-containing MVs. The MVs result from a two-stage process, firstly through priming monocytes/macrophages with bacterial endotoxin lipopolysaccharide (LPS) that initiate production of pro-IL-1β then a second stimulus such as ATP acting on purinergic receptors ($P2X_7$) leading to activation of

caspase-1 to process the pro-IL-1β and extracellular release of IL-1β within MVs (Fig. 1.2) (MacKenzie et al., 2001). Another proposed protected mechanism is through exosomes, where cytosolic IL-1β are packed inside multivesicular bodies that subsequently fuse forming the exosome which then fuses with the plasma membrane to release its content (IL-1β in this case) to the extracellular space (Qu et al., 2007). The fourth mechanism proposed is via pyroptosis, this phenomenon is achieved when macrophage induce apoptosis following cellular infection with pathogens to prevent pathogen growth eventually resulting in cell lysis and cytokine release including IL-1β (Monack et al., 2001).

It has been widely shown that the protein Gasdermin D is responsible for the pyroptosis as a result of its lytic activity at the cell membrane leading to pore formation that eventually to cell death (Ding et al., 2016, Liu et al., 2016). Gasdermin D is a cytosolic protein that belongs to Gasdermin family, and consists of two domains; the carboxy C-terminal; which is autoinhibitory and the amino N-terminal; which is the cytotoxic and responsible for the cell membrane pore formation (Shi et al., 2015). Recently, the Gasdermin D pore formation in an intact cell membrane of living macrophage (not pyroptotic) has been proposed as a mechanism of IL-1β release (Evavold et al., 2018). Caspase-1 and caspase-11 and its human homologue; Caspase-4/ 5, cleave Gasdermin D at the interdomain linker region between the C-terminal and N-terminal leading to the release of the N-terminal fragment from the inhibitory C-terminal fragment (Ding et al., 2016; Shi et al., 2015). The N-terminal fragment exhibits lipid-binding characteristics that target the cell membrane leading to structural changes (Ding et al., 2016). When the Gasdermin D N-terminal is inserted or binds the membrane lipids, it assembles into oligomerized complexes forming a ring-shape like structure which then forms the transmembrane pores (Mulvihill et al., 2018) and the IL-1β is released through these formed pores. Thus, caspase dependent pore formation serves as a gate for IL-1β to exit the cell.

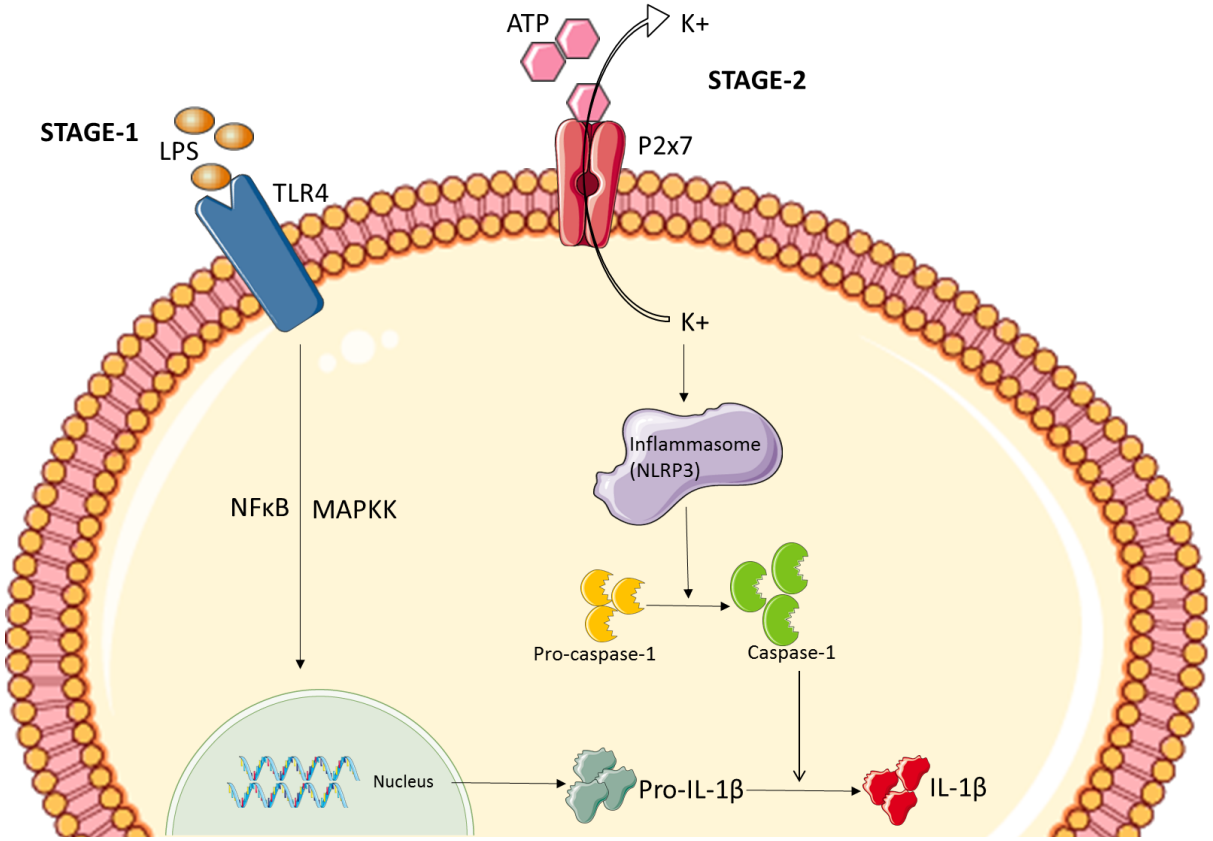

Figure 1.2 :Schematic representation showing the IL-1β two-stage synthesis.

The first stage involves immune cell recognition of microbial pathogens such as LPS through TLR4 (a PRR) activating NFκB and MAPKK signalling pathways to upregulate the gene transcription of pro-IL-1β. The second stage where cellular stimulus (ATP) acts on the purinergic receptor ($P2X_7$) inducing intracellular hypokalaemia that activates the assembly of the inflammasome (NLRP3) that activates the pro-caspase-1 into an active form (caspase-1) to cleave pro-IL-1β to IL-1β.

1.4 Microvesicles (MVs)

1.4.1 Definition of microvesicles

Extracellular vesicles (EV) refer to a family of small vesicles enclosed by membrane that are present in the extracellular space. The EV components are mainly cellular-derived proteins, lipids, and nuclear materials. The family of EVs is classified into three types: microvesicles (MVs), exosomes, and apoptotic bodies (Teng and Fussenegger, 2021). The three members vary in their size, mode of formation (biogenesis), and their components, as these are dependent on the cells they were originated from (Table1.1). However, they are related to some extent in their function since they all appear to provide a mechanism for intercellular communication and compartmentalised transfer of biological information.

Apoptotic bodies are shed during the process of cellular apoptosis and usually contain genomic material and cytosolic proteins stemmed from the parent cell. Exosomes are formed intracellularly then released through fusion of multivesicular bodies (secretory granules) with the cellular membrane, thus enabling the release of their contents to the extracellular (Loyer et al., 2014). MVs are differentiated based on the mechanism of their formation (explained below) in addition to their size range. Apoptotic bodies are the largest vesicles as their diameter is larger than 1μm, while the exosomes diameter is between 40-100 nm which are the smallest (Boulanger et al., 2017).

MVs are small-sized, spherical, vesicles with a diameter ranging from 0.1-1μm, shed from the plasma membrane of healthy or damaged cells via membrane blebbing and released to the extracellular space. They are produced by a variety of cells upon their activation or through proapoptotic stimulation such as: leukocytes, erythrocytes, platelets, endothelial cells, smooth muscle cells, and others (Boulanger et al., 2017). Importantly they also express on their surfaces essential receptors and bioactive ligands that serve in cellular crosstalk, and contain a variety of proteins, cytokines, lipids, growth factors, enzymes, mRNAs, and microRNAs for transcellular delivery, all derived from the parent cells they were originated from (Mause and Weber, 2010, Ratajczak and Ratajczak, 2020). It is worth noting that MVs are observed to represent heterogeneous populations owing to the fact that they reflect the contents and surface

molecules that are retained from the parent cells. In addition to the type of stimuli that provoke their formation and release i.e. the constituents of the parental cell, the microenvironment can also affect and alter their content and the surface molecules expressed (Ratajczak et al., 2006).

The presence of a pro-apoptotic stimulus is not an essential requirement for MV shedding (Boulanger et al., 2017). MVs are seen circulating in healthy individuals' blood as their formation and release is considered a physiological phenomenon involved in cellular activation (Berckmans et al., 2001). Pathological states such as inflammation (Mesri and Altieri, 1999), hypercoagulation diseases, cardiovascular disease (VanWijk et al., 2003), malignancy (Ratajczak et al., 2006), and stress conditions in general are accompanied by significantly increased levels of circulating MVs.

Table 1.1: Classification and characteristics of extracellular vesicles.

	Microvesicles (MVs)	**Exosomes**	**Apoptotic bodies (AB)**	**References**
Size	0.1 – 1 µm	0.04 - 0.1 µm	Up to 5 µm	
Mode of formation	Cellular membrane deformation followed by cytoskeleton reorganization resulting in membrane blebbing.	Formation of intraluminal vesicles inside the multivesicular bodies that eventually exocytose and fuse with cellular membrane.	Large membrane blebbing followed by cellular fragmentation resulting in AB formation.	(Boulanger et al., 2017)& (Loyer et al., 2014).
Contents	Proteins, lipids, cellular organelles, microRNA, and RNA	Proteins and RNA	Cellular organelles, RNA, and DNA	(Loyer et al., 2014)& (Zhang et al., 2015)& (D'Souza et al., 2021).

1.4.2 Microvesicle function

Microvesicles play a key role in cell-to-cell communication and modulate intercellular information exchange and biological signalling, they serve as vectors transcellularly. Since MVs circulate in the blood and are present in other body fluids such as saliva, urine, and inflammatory tissues (Loyer et al., 2014), the recipient cells targeted are not limited to those present in the local microenvironment that provoked their release; distant recipient cells might be targeted (Mause and Weber, 2010). MVs exert biological effects on recipient cells achieved through: (i) surface molecules expressed that bind target cells via ligand-receptor interaction; (ii) transfer of a receptor to the recipient cell's plasma membrane in order to induce target cell signalling; (iii) delivering their cargo (such as protein, mRNA, miRNA, or lipid) through internalisation resulting in recipient cells stimulation and activation that eventually alter cellular properties and regulate their functions and responses (Ridger et al., 2017). In addition, they may transfer organelles between cells (Ratajczak et al., 2006, D'Souza et al., 2021).

1.4.3 Microvesicle Biogenesis

The plasma membrane is composed of lipid bilayer anchored with several membrane proteins, which is maintained asymmetrically in eukaryotic cells in order to maintain the cellular structure during normal cell function (Contreras et al., 2010). During the cellular resting state, phospholipids are organized asymmetrically where amino phospholipids including phosphatidylethanolamine and phosphatidylserine are present on the inner leaflet facing the cytoplasm, whilst phosphatidylcholine (PC) and sphingomyelin (SM) are present on the outer leaflet facing extracellularly (Contreras et al., 2010). The lipid bilayer asymmetry is established through an active process involving three main membrane proteins, two are ATP-dependent phospholipid translocators: flippase for the inward translocation and floppase for the outward translocation, the third is scramblase an ATP-independent protein which is responsible for non-specific bidirectional transbilayer transport. The flippase is only activated during the cellular resting state with normal calcium levels to maintain the PS molecule in the inner leaflet, whereas during cellular activation intracellular calcium concentrations increase inhibiting flippase activity and activating the floppase to

translocate the PS molecule to the outer leaflet (Fig. 1.3). Additionally, scramblase is involved in movement of phospholipids across the membrane in response to increased cytosolic calcium influx, thereby favouring membrane symmetry (Morel et al., 2011). Moreover, the cytoskeleton reorganization which involves proteolytic activity of caspase and calpain enzymes acting on multiple cytoskeletal proteins such as filamin, gelsolin, myosin, and talin that are cleaved by these activated enzymes as a result of intracellular calcium influx (Fig. 1.3) (Ridger et al., 2017). In turn, membrane asymmetry collapses resulting in local membrane instability together with cytoskeleton modification leading to the formation of membrane blebbing and MV shedding.

Phosphatidylserine exposure on the surface of the MVs provides a means of detection by labelling with a fluorescently tagged Annexin V protein, which is a ligand that binds strongly to PS molecules (Vermes et al., 1995). Interestingly, some MV populations are reported to lack detectable surface PS exposure (Connor et al., 2010). The mechanism of their formation is still unknown, it is possible that PS-negative MVs may occur due to the heterogeneous nature of MV biogenesis where different mechanisms lead to their formation. The analysis techniques used to detect and label these MVs, relying on protein tools that bind to PS (such as lactadherin and annexin V) or their fusion with other vesicles, may act as obstacles limiting the detection of true MV populations (Yuana et al., 2013).

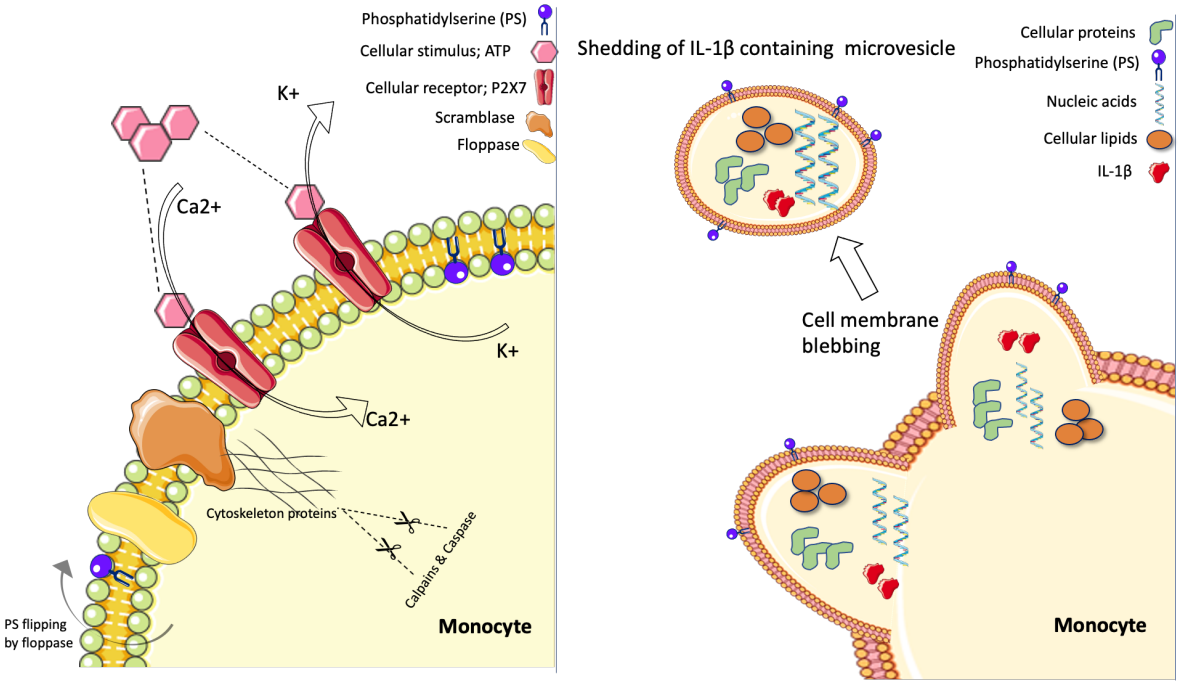

Figure 1.3: IL-1β-containing microvesicle shedding.

Schematic representation of MVs biogenesis, on the left shows the effect of a secondary cellular stimulus e.g. (ATP) binding to purinoreceptors ($P2X_7$) that allow K^+ efflux & Ca^{+2} influx activating the translocase proteins that destabilize the membrane: floppase inverts the PS molecule to the outer leaflet of the plasma membrane and scramblase disrupts membrane phospholipids contributing to membrane symmetry. Proteases (calpains & caspase) activated by Ca^{+2} influx cleave cytoskeletal proteins filamin, gelsolin, myosin and talin activating cytoskeletal reorganization and eventually formation of blebs. Inflammasome/caspase-1 activation results in IL-1β processing. The right panel shows more advanced activation with membrane blebbing and MV packaging of cellular proteins, lipids, active IL-1β and nucleic acid and externalized the PS molecules.

1.4.4 Microvesicles in CVD and Atherosclerosis

Microvesicles are present abundantly throughout all the stages of atherosclerosis development starting from disease initiation progressing to advanced lesion formation. Microvesicles exhibit pleiotropic properties that influence inflammation, angiogenesis, endothelial cell function, and thrombosis, all critical elements involved in atherosclerosis development, progression and rupture. Moreover, MVs are present in high quantities from the early cardiovascular disease initiation i.e. their numbers correlate with cardiovascular risk factors such as smoking (Mobarrez et al., 2014), hypercholesterolemia (Ferreira et al., 2004), hypertension (Preston et al., 2003), obesity (Goichot et al., 2006), and diabetes mellitus (Nomura et al., 1995).

Several *in vitro* studies demonstrated effects of MVs originating from cells present in the atherosclerotic plaque including endothelial cells and leukocytes involved in initiation of plaque formation. These effects comprise endothelial cell dysfunction, increased monocyte adhesion to the endothelium and migration into the sub-endothelial space and significantly, enhancement of pro-inflammatory cytokine production (Boulanger et al., 2017). MVs possess the ability to disrupt the endothelium due to their contents affecting cadherin-containing intercellular junctions modulating the endothelium integrity (Lapping-Carr et al., 2021). MVs were shown to stimulate the pro-inflammatory cytokine interleukin-6 (IL-6) production by endothelial cells (Mesri and Altieri, 1999), IL-1β and IL-1Ra production by monocytes (Scanu et al., 2008) promoting monocyte-endothelial adhesion. Moreover, MVs derived from platelets increase the expression of intracellular cell adhesion molecule–1; ICAM-1, by endothelial cells simultaneously upregulating monocytic CD11a receptors that also promote monocytic adherence (Barry et al., 1998). Endothelial dysfunction was promoted by endothelial-derived MVs leading to decreased nitric oxide production and altered vasorelaxation of aortic rings (Brodsky et al., 2004). Another study showed that endothelial-derived MVs contain several inflammatory cytokines and chemokines enhancing vascular inflammation and promoting trans-endothelial monocyte migration (Hosseinkhani et al., 2020). The neutrophil-derived MVs were also found to enhance vascular inflammation and atherogenesis by preferentially adhering to endothelial cells and activating them to release IL-6 and CXCL8 and other chemokines through

activating the NF-kB pathway leading to the trans-endothelial monocyte migration (Gomez et al., 2020).

During lesion progression, MVs were found to stimulate macrophages through acting on Toll-like receptors (TLR) leading to foam cell formation (Keyel et al., 2012). Furthermore, MVs induce macrophage apoptosis; the subsequent release of MVs during foam cell apoptosis promotes accumulation of extracellular lipids and lesion progression (Distler et al., 2005). Smooth muscle cell proliferation and migration play a key role in plaque progression; platelet-derived MVs were found to increase vascular smooth muscle cell proliferation (Pakala, 2004).

Plaque stability, angiogenesis, and thrombosis are influenced by MV production. For instance, plaque MVs showed high expression of the CD40 ligand that binds to the endothelial cell CD40 receptor promoting their proliferation thus, contributing to neoangiogenesis inside the atherosclerotic plaque and eventually plaque vulnerability (Leroyer et al., 2008). The presence of tissue factor (TF) and exposure of PS on the surface of MVs enhances blood coagulation where monocyte-derived MVs in particular express significant TF (Mallat et al., 1999). It is worth mentioning that these MVs serve as promising prognostic markers which can be used to predict advanced cardiac manifestations, since patients with plaque rupture showed elevated levels of leukocyte-derived MVs when compared to patients with stable plaques (Sarlon-Bartoli et al., 2013) providing an indicator of plaque instability.

1.5 $P2X_7$ receptor channel

1.5.1 Structure and function

$P2X_7$ receptor is a member of the purinergic family of receptors, which are activated by purine nucleotides, such as adenosine and adenosine triphosphate (ATP), or pyrimidine nucleotides, such as uridine 5’-triphosphate (UTP) and uridine 5’-diphosphate (UDP) (Burnstock, 2007). These purinergic receptors are divided into two families P1 and P2 receptors, where P1 receptors bind purine, adenosine and P2 receptors bind either the purine ATP, adenosine-5′-diphosphate (ADP) or the pyrimidine UTP and uridine-5’-diphosphate (UDP). The P2 family is further divided into

two subfamilies according to their structure and function, the ligand-gated ionotropic P2X, and the G-protein coupled metabotropic P2Y (Burnstock, 2007). P2X subfamily is comprised of seven members ($P2X_{1-7}$) and they are ATP-gated channels i.e. ATP is the physiologic preferred ligand.

$P2X_7$ receptor is a trimeric ligand-gated cation channel that is formed by three identical monomers assembled. The human $P2X_7$ subunit is comprised of 595 amino acids that are composed of a large extracellular loop, two transmembrane helices a short intracellular NH_4- and longer COOH-termini domains. The extracellular loop contains the binding pocket of ATP which is located between the three adjacent monomers with two monomers have specific residues contributing to the binding site (Karasawa and Kawate, 2016), whilst the two transmembrane helices form the ion channel. The intracellular COOH-terminal tail of the receptor is unique and longer than the other P2X receptors as it is responsible for cell membrane pore formation when agonist binds due to the cysteine-rich region (Allsopp and Evans, 2015). The $P2X_7$ receptor is an ATP-gated cation channel, leading to formation of membrane pores allowing passage of cations such as K^+ efflux, Ca^{2+} and Na^+ influx through plasma membrane (Fig. 1.3). This contributes to plasma membrane reorganization and changing cell ionic homeostasis and resulting in initiating intracellular downstream signalling pathways such as cell proliferation, p38 MAP kinase pathway activation and gene expression of cytokines and their release as well as, calmodulin regulation, and ectodomains shedding. The sustained exposure to high levels of ATP can lead to a larger, reversible, and non-selective “macropore” formation that allow passage of normally impermeant organic cations of MW up to 900 Da such as YO-PRO-1 and ethidium (Surprenant et al., 1996, (Virginio et al., 1999).

The ATP compound is the most ancient damage associated molecular pattern (DAMP) released by healthy and diseased cells into the extracellular space. This nucleotide plays a vital role in cellular communication acting as neurotransmitter in the nervous system, and serving as a danger signal recognized by immune and non-immune cells initiating an immune response that may lead to inflammation. The presence of ATP in the extracellular space surrounding healthy cells under physiological conditions is maintained at low nanomolar concentrations (Wilhelm et al., 2010). $P2X_7$ receptor is distinguished from other P2X receptors by its low affinity to ATP and only activated if high levels of ATP are released into the extracellular space by stressed or dying cells

such as in inflamed or damaged tissue where ATP levels can reach up to hundreds of micromolar. Studies have shown that $P2X_7$ receptor is a cytotoxic receptor if stimulated maximally and continuously (> 30 mins) with ATP leading to massive Ca^{+2} influx disrupting the mitochondrial network and eventually causing cell death. Thus, if activated maximally, its function may shift to cytolytic effects. $P2X_7$ is ordinarily maintained to some extent inactive in healthy states nevertheless, according to (Adinolfi et al., 2005) stimulation with low concentration for few seconds contributes to cellular growth via increasing the energy storage intracellularly. Also, $P2X_7$ plays a role in supporting cell proliferation as downregulation of the receptor expression leads to a decrease in microglial cell cycle progression (Bianco et al., 2006).

The $P2X_7$ receptor has been widely demonstrated to play a role in inflammation. Nonetheless, $P2X_7$ receptor is expressed by several hematopoietic lineage cells, including monocytes and macrophages, such as mast cell, microglia, eosinophil, erythrocytes, and lymphocytes. It is also expressed in cell types other than those of hematopoietic lineage including epithelial cells, endothelial cells, osteoblasts and fibroblasts (Surprenant and North, 2009). $P2X_7$ involvement in innate and adaptive immune-mediated responses has been investigated where $P2X_7$ stimulation with ATP leads to the release of pro-inflammatory cytokines including IL-1β and IL-18 through assembly and activation of the NLRP3 inflammasome which in turn activates caspase-1 when K^+ efflux occurs (Ferrari et al., 1997). The $P2X_7$ receptor is a key driver of inflammasome activation and IL-1β release thus, a key initiator of acute inflammatory responses. It also triggers the release of pro-inflammatory cytokines IL-6 and CCL2 from mouse microglia (Shieh et al., 2014). $P2X_7$ activation augments the inflammatory response through releasing intracellular ATP via pannexin-1 hemichannel pore formation promoting autocrine signalling (Pelegrin and Surprenant, 2006). The $P2X_7$ receptor also plays a role in adaptive immunity as $P2X_7$ was found to promote T cell activation and differentiation e.g. it promotes differentiation of T helper 1 into follicular T helper in malarial disease (de Salles et al., 2017). Influx of calcium caused by $P2X_7$ and the consequent downstream signalling promotes T cell activation (Yip et al., 2009).

1.5.2 Comparison of human and mouse $P2X_7$ receptors

$P2X_7$ receptor is encoded in human by *PR2X7* gene that is located on chromosome 12q24 (Buell et al., 1998) while the mouse *P2rX7* is located on chromosome 5. Several lines of studies have investigated the species differences in pharmacological criteria of $P2X_7$ receptor agonists and antagonists as the latter complicated the study of the physiological role of the receptor. The $P2X_7$ of mouse and human are 80% homologous at the encoded protein where the extended C-terminal tail and the extracellular loop were highly conserved or related at the amino acids level (Chessell et al., 1998). The lower conservation at the extracellular ATP binding site suggests differences in pharmacological criteria among the species affecting the kinetics of the receptor function.

To date, the most well-recognized $P2X_7$ receptor ligand is the endogenous nucleotide, ATP. Interestingly, $P2X_7$ receptor response to ATP stimulation varies according to the agonist concentration and length of stimulus (Surprenant et al., 1996). In general, brief stimulation with low ATP concentrations activates the receptor leading to a cation-selective channel formation while prolonged stimulation allow channel dilation and non-selective pore formation that allow the passage of large molecules. The presence of ecto-enzymes called ectonucleotidases metabolize ATP to its metabolites ADP,AMP, and adenosine, as this contributes to regulating the extracellular ATP concentration and availability thus, contributes in cellular homeostasis integration (Savio et al., 2018). 2'(3')-O-4-benzoylbenzoyl- ATP, an ATP analogue, is around 30-fold more potent than ATP at human $P2X_7$ (Surprenant et al., 1996, Bianchi et al., 1999) and is in fact, the most potent agonist in human followed by ATP, 2-methylthio-ATP (2MeSATP), adenosine-5'-O-(3-thiotriphosphate) (ATPγS), and finally ADP (Donnelly-Roberts et al., 2009). Whilst in mouse, BzATP is a less potent $P2X_7$ agonist when compared to its effect on human $P2X_7$ mediated calcium influx and YO-PRO-1 uptake (indicative of pore formation). The agonists 2MeSATP and ATPγS were shown to have no significant stimulation in mouse $P2X_7$ (Donnelly-Roberts et al., 2009). Nicotinamide adenine dinucleotide (NAD^+) makes the $P2X_7$ receptor in mouse T lymphocytes more sensitive to ATP (Seman et al., 2003) by ADP-ribosylation. The NAD-induced $P2X_7$ activation lead to pore formation, calcium influx, cell shrinkage,

DNA fragmentation and eventually lead to T cell death. This NAD-ribosylation site only occurs in rodents and not human $P2X_7$.

A number of studies have reported that the ionic composition of the extracellular affect the agonist potency and regulate the receptor function. The presence of divalent or monovalent cations extracellularly recognized as allosteric modulators as they can alter the affinity of the agonist binding. For instance, the removal of calcium and magnesium has increased the receptor response to the agonists BzATP and ATP in human $P2X_7$ (Rassendren et al., 1997) by measuring the currents evoked. Indeed, (Michel et al., 1999) have shown in $P2X_7$-overexpressing HEK293 cells that YO-PRO-1 dye uptake was decreased with the presence of extracellular calcium and magnesium while removal of monovalent sodium chloride increased the BzATP agonist potency. Similarly in mouse $P2X_7$, the removal of sodium and chloride has increased the agonist potency (Chessell et al., 1998).

The species differences have also been observed in the compounds that antagonize or inhibit the receptor function as several studies investigated the role of $P2X_7$ in multiple diseases (Table 1.2). The antagonist pyridoxalphosphate-6-azopheny-2′,4′-disulfonate (PPADS) blocks P2X receptors non-selectivity, with low $P2X_7$ affinity and non-competitive antagonism and is more potent in blocking human $P2X_7$ than mouse $P2X_7$ (Donnelly-Roberts et al.,2009). Whilst KN-62 is a non-competitive, $P2X_7$ selective antagonist blocking the human $P2X_7$ but not the mouse $P2X_7$. The commonly used antagonist Brilliant Blue G (BBG) has no effect on human $P2X_7$ activity whilst it does block mouse $P2X_7$ activity. The $P2X_7$ selective antagonists A438079 and A740003 have potently blocked both the human and mouse $P2X_7$ activation (Donnelly-Roberts et al.,2009).

Collectively, the marked species related variations in drug potency and inhibitory effects can be attributed to amino acid variation in the binding site of the agonist or antagonist while receptor splice variants are also likely to affect these responses.

Table 1.2: $P2X_7$ receptor agonists and antagonists.

Human $P2X_7$	**Agonists**	**Antagonists**
	Adenosine triphosphate (ATP)	Periodate oxidized ATP (oxATP)
	Benzoyl ester of ATP (BzATP)	Tetrazole derivatives: A438079
	2-methylthio-ATP (2MeSATP)	Cyanoguanidine derivative: A740003
	Adenosine 5'-O-(3-thiotriphosphate) (ATPγS)	KN-62
		Brilliant Blue G (BBG)
		Pyridoxalphosphate-6-azopheny-2',4'-disulfonate (PPAD)
Mouse $P2X_7$	Adenosine triphosphate (ATP)	Periodate oxidized ATP (oxATP)
	Benzoyl ester of ATP (BzATP)	Tetrazole derivatives: A438079
		Cyanoguanidine derivative: A740003
		Pyridoxalphosphate-6-azopheny-2',4'-disulfonate (PPAD).

(Donnelly-Roberts et al., 2009)

1.5.3 $P2X_7$ in Atherosclerosis

Atherosclerosis is regarded as chronic inflammatory disease of the arterial wall that is caused by accumulation of lipid and cellular proliferation forming a plaque or atheroma. The circulating oxidized lipids play a key role in initiating the inflammation via interacting with the endothelium. It is linked to $P2X_7$ receptor signalling, a study showed that the presence of certain lipids increases the potency of ATP and modulates the receptor function (Michel and Fonfria, 2007). Moreover, a high fat diet in C57BL/6J mice induced significantly increased $P2X_7$ receptor expression in brain tissues as well as in activated glial cells (Asatryan et al., 2015). In contrast, over-activation of the $P2X_7$ receptor led to alkalinized lysosomes accompanied by increased lipid oxidation (Guha et al., 2013). Collectively, these studies indicate an interaction between circulating lipids and $P2X_7$ receptor activation suggesting this may influence atherosclerosis, although further research is required to provide insights on whether circulating lipids and $P2X_7$ receptor modulate atherosclerosis.

Vascular dysfunction and expression of adhesion molecules leading to leukocyte recruitment and infiltration eventually to the intima are crucial events in initiating atherosclerosis. Several lines of studies reported the involvement of the purinergic signalling in endothelial dysfunction and the expression of chemokines and adhesion molecules such as VCAM-1 and subsequently leukocyte adherence (Dawicki et al., 1995, Smedlund and Vazquez, 2008). Under inflammatory conditions, $P2X_7$ receptor contributes to endothelial dysfunction by enhancing cell permeability and upregulating the adhesion molecules ICAM-1 and VCAM-1 (Sathanoori et al., 2015).

$P2X_7$ receptor expression and activation have been linked to atherosclerosis where expression was significantly increased in endothelial cells and macrophages in human carotid and artery plaques (Piscopiello et al., 2013). In mice lacking the low-density lipoprotein receptor (LDLR) fed on high fat diet, $P2X_7$ expression was high in atherosclerotic lesion particularly by lesional macrophages (Green et al., 2018, Stachon et al., 2017). Moreover, this study showed that mice lacking both LDLR and $P2X_7R$ had reduced atherosclerotic lesions size compared to only LDLR deficient mice and fewer lesional macrophages. This has contributed to decreased leukocyte adhesion and recruitment. Another study investigated the coronary artery plaque in apo$E^{-/-}$ deficient mice showing increased expression of $P2X_7$ compared to wild type

(Peng et al., 2015). As well as increased $P2X_7$ expression in coronary artery plaques, elevated expression of the inflammasome NLRP3 was observed. Since activation of the NLRP3 inflammasome is involved in IL-1β maturation, this indicates the role of $P2X_7$ in promoting inflammation through the release of IL-1β. ApoE $^{-/-}$ deficient mice lacking IL-1β showed smaller atherosclerotic lesions compared to wild type (Kirii et al., 2003), indicating the contribution of IL-1β in atherosclerosis progression. In addition selective $P2X_7$ receptor antagonists showed decreased IL-1β release and inflammation, as well as decreased matrix metalloproteinase-9 (MMP-9) in atherosclerotic plaques, where high levels of MMP-9 correlate with atherosclerosis pathogenesis and plaque vulnerability (Lombardi et al., 2017). The levels of mRNA expression of the $P2X_7$ receptor in circulating mononuclear cells were recently linked to the clinical prognosis in acute myocardial infarction patients i.e. higher levels indicates more severe coronary artery stenosis (Shi et al., 2021).

1.5.4 $P2X_7$ in Macrophage Function

The presence of extracellular ATP, the physiological agonist of $P2X_7$ receptor, is recognised to mediate the most investigated response i.e. initiation of pro-inflammatory response. Upon ATP binding, $P2X_7$ channel opens allowing bidirectional flux of cation and activation of downstream signalling pathways leading to release of cytokines. As mentioned previously, the persistent stimulation of the receptor with ATP leads to formation of non-specific pore allowing passage of molecules up to 900 Da in size. $P2X_7$ mediated pore formation requires the presence of high levels of ATP in the extracellular milieu (>100 μM) (Surprenant et al., 1996). Since extracellular ATP under physiological conditions is maintained at nanomolar levels, the receptor remains “silent” or in an “inactivated” state. This suggests that the $P2X_7$ may have an alternate physiological role therefore, it was noteworthy to investigate the inactive state of the receptor. Gu et al. (2010) showed the innate phagocytic role of $P2X_7$ when cells overexpress the receptor, the receptor confer the ability to phagocytose non-opsonized particles/apoptotic cells in the absence of its physiological ligand, ATP as well as the serum. The phagocytic role was investigated in human monocyte/macrophage cells showing a brisk uptake of non-opsonised beads, bacteria, apoptotic lymphocytes, and neuronal cells (Gu et al., 2011). The phagocytosis was inhibited by the addition of both ATP and oxidized ATP, which is an

irreversible $P2X_7$ antagonist. Furthermore, siRNA against $P2X_7$ and monoclonal antibody targeting $P2X_7$ receptor of an epithelial cell line with $P2X_7$ constructs have also inhibited phagocytosis (Gu et al., 2010)2011). HEK-293 cells are non-phagocytic cells, and the transfection of this cell line is a robust technique to determine the ability of $P2X_7$ receptor on the recipient cells to act as a scavenger receptor. Gu et al. (2011) used confocal microscopy to verify the presence of $P2X_7$ receptor in the phagosomes membrane that surround phagocytosed particles supporting its role in phagocytosis. As well as, it was abundantly expressed intracellularly in normal white cells including; monocytes, lymphocytes, platelets, etc, (Gu et al., 2000).

$P2X_7$ receptor stimulation is characterized by actin reorganization and membrane blebbing indicating a close relation between the receptor and the actin-myosin cytoskeleton (Pfeiffer et al., 2004). $P2X_7$ is a transmembrane trimeric ion channel present in a large multiprotein complex, and is associated with several cytoskeletal proteins. The multiprotein complex includes β_2-integrin, β-actin, heat shock protein 70 and 90, etc., but the most important anchored protein to $P2X_7$ is the non-muscle myosin heavy chain (NMMHC) (Kim et al., 2001). The composition of the multiprotein complex associated with $P2X_7$ differ between cell types or even intracellularly implying variety of functions could be carried out by the activation of $P2X_7$ receptor. The non-muscle myosin are actin-binding proteins and in general are ATP-dependent and involved in motility processes in the cell through actin filaments. NMMHC has been found to anchor to the C-terminal region of $P2X_7$ tightly in monocytic THP-1 cells and transfected HEK-293 cells (Gu et al., 2009). It rearranges the cytoskeleton through providing energy by ATP hydrolysis and contribute to phagocytose the apoptotic cells. Importantly, when ATP binds $P2X_7$, the NMMHC complex dissociates and this leads to pore formation. Moreover, it is a rate limiting step for the pore formation (Gu et al., 2009). Thus, $P2X_7$-NMMHC complex is responsible for the receptor transition from channel to form a pore abolishing the receptor mediated phagocytosis. Studies shown the ectodomain of the extracellular domain of $P2X_7$ extending from the membrane contributes in the recognition of several targets including apoptotic cells, beads, and bacteria (Gu et al., 2011).

The $P2X_7$ receptor ability to engulf particles/apoptotic cells has been largely linked to early central nervous system (CNS) development and neurogenesis as CNS development involves overproduction of neuronal cells and apoptosis (Lovelace et al., 2015, Collo et al., 1997). Lovelace and colleagues (2015), also observed that neuronal precursor cells and neuroblasts derived from human embryos were expressing high levels of $P2X_7$ receptor. Those cells confer the ability to phagocytose several targets including apoptotic neuroblasts and ReN cells (a human neural progenitor cell line) as well as latex beads. Pre-treatment of these cells with either ATP, oxidized ATP, or siRNA against $P2X_7$ reduce their ability to clear these targets. It indicates that $P2X_7$ conveys an important scavenging function during foetal CNS development. The phagocytosis is only achieved under serum-free conditions as well as the absence of ATP, which resemble the CNS conditions during development. The phagocytic role of $P2X_7$ receptor has been also studied in the neuronal cells of the human adult CNS such as microglia. Microglia are the immune cells present in CNS, and they express $P2X_7$ in high levels. A study used cultured human microglia to investigate the involvement of $P2X_7$ in their engulfing activity by showing addition of BzATP or $P2X_7$ antagonist reduced the phagocytic ability of microglia (Janks et al., 2018). Astrocytes derived from mice were also investigated by (Yamamoto et al., 2013) and found that $P2X_7$ inhibition and knock down reduce their phagocytic ability. These studies indicate that $P2X_7$ is a scavenger receptor plays a critical role regulating the CNS innate immunity.

1.6 Mer receptor tyrosine kinase as a phosphatidylserine receptor

1.6.1 Structure and function

In order to understand how PS-positive cells and possibly MVs are targeted to other cells, we will discuss the role of the PS receptor complex. The MerTK receptor belongs to the tyrosine kinase receptors family knowns as TAM, short for the three main receptors in this family: Tyro3, Axl, and Mer. They share similar structure and domain organisation but are distinct from other tyrosine kinases receptors. Their extracellular domain is composed of two tandem immunoglobulin-like domains (IgG), while the transmembrane repeat is of two fibronectin type III domains (FNIII) and lastly, the intracellular C-terminal domain which is the cytoplasmic tyrosine kinase domain (Cai

and Kasikara, 2020, Graham et al., 1994) (Fig. 1.4). The extracellular domain of the receptor specifically, the Immunoglobulin-like domain, mediates ligand binding. TAM receptors and their ligands are required for the regulation of tissue homeostasis as they mediate efferocytosis i.e. the mechanism of recognition and phagocytosis of apoptotic cell. The two ligands for TAM receptors share homologous topology; Growth Arrest-Specific gene 6 (Gas6) and Protein S (ProS) that bind in a vitamin-K dependent manner to the receptor and interact with the externalised PS molecule on cells in a Ca^{+2}-dependent manner (Stitt et al., 1995, Manfioletti et al., 1993). The ligand binding affinity to TAM receptors is variable: Gas6 activates all the TAM receptors but has higher affinity to Axl more than to Mer and Tyro3 (Nagata et al., 1996). ProS binds preferably to Tyro3 more than Mer while it does not activate Axl (Lew et al., 2014, Zagorska et al., 2014). Gas6 and ProS have N-termini regions rich in γ-carboxylated glutamic acid known as Gla domains, which bind to the PS molecule (Huang et al., 2003). Whilst the C-terminal containing laminin G domain of both Gas6 and ProS binds to the N-terminal; Ig-like domain of the TAM receptor (Lemke and Rothlin, 2008) (Fig. 1.4). Thus, Gas6 and ProS serve as a link between PS molecules on the surface of the apoptotic cells and the TAM receptor. Binding both PS and TAM receptor must occur at the same time in order to activate the intracellular tyrosine kinase of the TAM receptor and doing so leads to transduction of downstream signalling required for phagocytosis.

The MerTK receptor is expressed mainly in innate immune cells such as macrophages, dendritic cells and natural killer cells (Behrens et al., 2003). Studies have shown the importance of MerTK receptor in mediating phagocytosis and clearance of apoptotic cells. For instance, mice lacking MerTK receptor have shown decreased macrophage ability to phagocytose apoptotic cells whilst phagocytosis of other particles was not affected (Scott et al., 2001). It has been suggested that defective apoptotic cell clearance due to MerTK receptor knockdown *in vivo* is associated with accelerated atherosclerotic plaque progression by contributing to necrotic core expansion (Thorp et al., 2008). In addition, the MerTK receptor may negatively regulate inflammation. In mice lacking MerTK, pro-inflammatory tumor necrosis factor (TNF) serum levels were high and the mice had lupus-like autoimmune symptoms and were more susceptible to LPS-mediated death compared to wild-type control mice (Camenisch et al., 1999). MerTK was shown to inhibit the activation of

the transcriptional factor NF-κB pathway that induces inflammatory cytokine gene expression (Sen et al., 2007). MerTK is involved in maintaining the endothelial barrier as its depletion in microvascular endothelial cells led to increased vascular permeability by disrupting adherens junction and junction proteins, increasing trans-endothelial migration of leukocytes (Li et al., 2019). Nonetheless, the exact role of MerTK in atherosclerosis has not been elucidated yet.

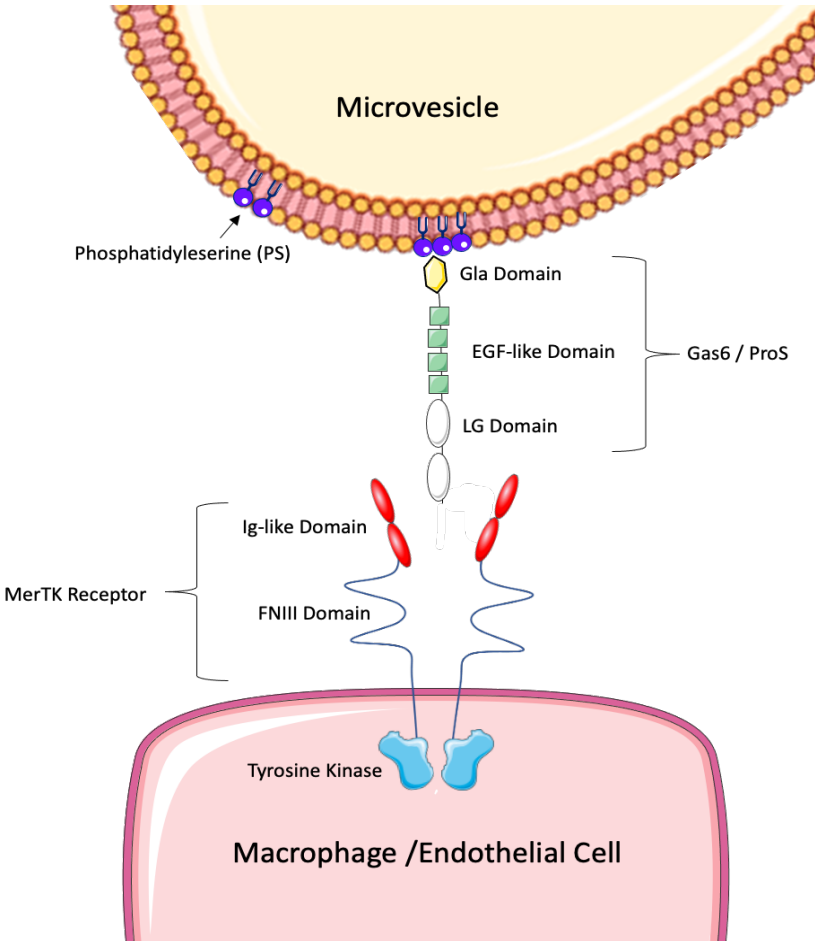

Figure 1.4: The structure of MerTK receptor and its ligands Gas6 and ProteinS.

The schematic shows the PS signal transduction by MerTK-lignad pair. MerTK receptor is comprised of three domains; Extracellular domain is ligand-binding region and composed of two Immunoglobulin-like domains (IG-like) and two fibronectin type III repeat (FNIII), followed by a single-pass transmembrane, Intracellular is of C-terminal tyrosine kinase domain. Gas6 and ProS are composed of amino terminal; γ-carboxylic acid (Gla) domain, then epidermal growth factor-like (EGF-like) repeats, ending with the sex hormone–binding globulin domain comprising; the caboxy terminus and the two laminin G domain (LG).

1.7 Targeting microvesicles

Microvesicles as described previously mediate cellular communication through either their contents or the surface molecules expressed that vary according to the cells originated from and the microenvironment promoting their release.

How the recipient cells interact and uptake MVs remains incompletely understood, although there are mechanisms of MV uptake and internalization by target cells described in the literature. For instance, researchers showed MVs adhere to primary human coronary artery endothelial cells (HCAEC) surface then are subsequently detected inside the endothelial cell cytoplasm, thus the interaction is carried out through ICAM-1-mediated surface binding initially followed by an endocytosis mechanism (Gomez et al., 2020). That study suggested an active endocytosis/micropinocytosis mechanism of MVs uptake. Another endocytosis mediated interaction was shown where, human brain endothelial cells internalized platelet-derived MVs by active endocytosis involving a phagocytosis mechanism (Faille et al., 2012). This mechanism was a ligand-receptor independent interaction. A third mechanism proposed is the fusion of membranes of both MVs and the recipient cell resulting in freeing the MVs contents inside the cell (del Conde et al., 2005). This interaction was observed following a ligand-receptor interaction and was effectively blocked by Annexin V, suggesting PS exposure potentially plays a role in MV targeting.

Phosphatidylserine externalisation was observed to enhance MV uptake and internalization by recipient cells where PS seems to interact with several proteins and cellular receptors. For instance, lactadherin facilitates MV binding and uptake via externalized PS (Otzen et al., 2012), and developmental endothelial locus-1 (Del-1) also plays a role in binding PS-expressing MVs and their uptake by endothelial cells (Dasgupta et al., 2012). Furthermore, there are receptors reported to interact with PS molecules such the receptor family Tyro3/Axl/Mer (TAM) of tyrosine kinases and their ligands: Gas6 and protein S. Researchers showed that endothelial cells of human umbilical vein and aortic artery ingest MVs through Gas6-PS interaction which was inhibited in the presence of antibodies against Axl receptors (Happonen et al., 2016). Other receptors involved in targeting the PS molecule of MVs have been identified.

For example, T-cell immunoglobulin mucin-domain-containing molecule; Tim4 expressed on macrophages acts as a PS receptor enhancing the engulfment of apoptotic cells (Miyanishi et al., 2007). Collectively, these studies suggest that the presence of PS on the MV surface may act as a signalling molecule for their engulfment and uptake by various target cells.

Preliminary work in our group using a zebrafish line lacking MerTK showed attenuated targeting of IL-1β to the head region following tail-fin injury. This targeting to the head region was independent of circulating blood cells moving to the head region, where photoconversion at the tail region showed no converted cells moved to the head within the time frame of IL-1β activation at this site. Light sheet microscopy of fluorescent macrophages in injured zebrafish also showed labelled MVs within the circulation, which were PS-positive when combined with a tagged annexin-V line. Taken together we speculated that IL-1β, produced at the site of tail injury, was delivered to the head region via PS-positive MVs and targeted via the MerTK receptor in the TAM signalling complex.

In summary, MVs are shed from a variety of cells including monocytes and macrophages that are involved in atherosclerotic plaque development and instability. Macrophage-derived MVs were shown previously to contain pro-inflammatory cytokines including IL-1β, with the potential to induce inflammation in atherosclerosis in their delivery of biological cargo. The original study selectively isolated phosphatidylserine (PS)-exposed MVs found to contain IL-1β, following LPS and $P2X_7$-dependent ATP stimulation. Since the time of this study, differential centrifugation methods have been standardised for the isolation of extracellular vesicles, quantified using bead-calibrated flow cytometry where vesicles are often found to be composed of a mixed PS-positive and PS-negative population. MerTK has been identified as a key PS-receptor; preliminary work in our group using a zebrafish line lacking MerTK showed attenuated targeting of IL-1β to the head region following tail-fin injury, which we speculated was via MV delivery.

1.8 Hypothesis & Aims

Macrophages shed PS-exposed MVs containing IL-1β which are targeted to endothelial cells via the MerTK PS receptor, contributing to atherosclerosis (Fig. 1.5).

The aims of this project were to:

1. Isolate macrophage-derived MVs using differential centrifugation to:
    a. characterise their number, size and PS-exposure by annexin V-labelling using flow cytometry
    b. determine whether production and PS-exposure is stimulus dependent.
    c. determine the proportion of IL-1β secretion in MVs, compared to vesicle-independent release.
2. Determine whether expression of MerTK alters with stimulus and cell-type.
3. Assess if targeting of IL-1β-containing MVs is dependent on MerTK expression.

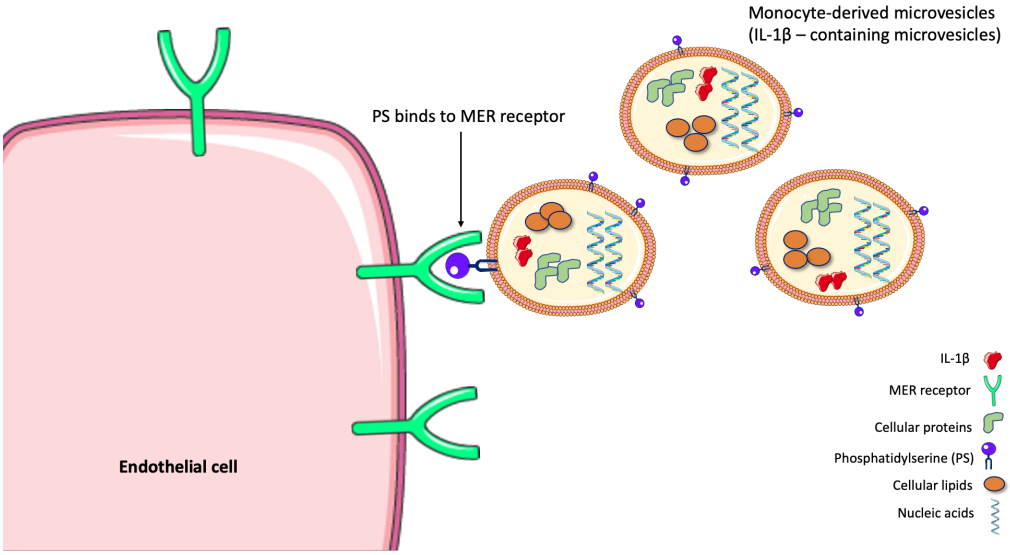

Figure 1.5: Proposed mechanism of MV targeting to the endothelium.

Our unpublished studies suggest an involvement of MerTK receptor in IL-1β targeting. In this study we will test the hypothesis that the PS exposed on the surface of IL-1β-containing MVs is required for targeting to endothelial cells via MerTK receptor to deliver IL-1β through a ligand-receptor interaction.

Chapter 2 . Material and Methods

2.1 Materials

2.1.1 Buffers and solutions preparation

For primary monocyte isolation:

- Red blood cell lysis buffer (1x): 16.6 g NH_4Cl, 2 g $KHCO_3$, 400 uL 0.5 M EDTA in 200 mL distilled, sterile H_2O.
- PBSE: 500ml 1xPBS + 2ml of 0.5M EDTA
- MACS Buffer: 2ml of 0.5M EDTA + 500ml of 1xPBS + 0.5% (w/v) BSA protein
- 1xPBS Oxoid phosphate buffered saline tablets: 137 mM NaCl, 2.7 mM KCl, 8 mM Na_2HPO_4, 1.8 mM KH_2PO_4 in distilled H_2O.

For MVs quantification:

- Annexin V Binding Buffer (1x): 100µl of Annexin V binding buffer (5x) by Invitrogen and composed of : 50 mM HEPES, 700 mM NaCl, 12.5 mM CaCl2, pH 7.4, diluted in 900µl of distilled H_2O.

For Western Blot:

- Transfer Buffer: 5% (v/v) NuPAGE transfer buffer (20x) [ThermoFisher] + 0.1% (v/v) NuPAGE antioxidant [ThermoFisher] + 20% (v/v) CH3OH in distilled H_2O.
- 1xTBST: Tris buffered saline with Tween®20 sachets [Sigma Aldrich] composed of : NaCl - 0.138 M; KCl - 0.0027 M); Tween®20 - 0.05%, pH 8.0, in distilled H_2O.
- Blocking Buffer: 5% (w/v) semi-skimmed dry milk in 1xTBST buffer.

2.2 Methods

2.2.1 Cell culture

Table 2.1: Reagents and materials for cell culture.

Material / Reagent	Supplier [Catalogue No.]
RPMI medium 1640 (1x) 500mL, (+) L-Glutamine	Gibco by Life Technologies [21875034]
Dulbecco's phosphate-buffered saline (DPBS) (1x) 500ml	Gibco™, Thermo Fisher Scientific [14040133]
LPS from E. coli, serotype R515 (Re) (TLR grade™), 2ml, 1mg/mL	Enzo ® life science [ALX-581-007-L001]
2′(3′)-O-(4-Benzoylbenzoyl) adenosine 5′-triphosphate triethylammonium salt ≥93% (BzATP)	Sigma-Aldrich [B6396-25MG]
Phorbol 12-myristate 13-acetate (PMA)	Sigma-Aldrich [8139]
Ficoll-Paque Plus	GE Healthcare [171440-02]
EDTA	Focus Bioscience
Low endotoxin-heat inactivated, Foetal Bovine Serum; FBS	PAN BIOTECH [P40-37500]
Dulbecco's Modified Eagle's Medium - high glucose (DMEM)	Gibco by Life Technologies [11965-092]
Human recombinant macrophage-colony stimulating factor (M-CSF)	Prepotech [300-25]
Sodium Pyruvate	Focus Bioscience [25-000-CIR]
RIPA Buffer	Sigma-Aldrich [R0278-50mL]
Protease inhibitor cocktails	Sigma-Aldrich [P8340-1mL]
Pierce™ BCA Protein Assay Kit	Thermo Fisher Scientific [Prod#23227]

Penicillin/Streptomycin	Gibco [15070-063]
L-glutamine	Gibco [17-605E]
0.25 % Trypsin-EDTA (1x)	Gibco [25200-072]
A 438079 hydrochloride	Tocris [2972]
Caspase-1 Inhibitor – Ac-YVAD-cmk	Invivogen [inh-yvad]
Interleukin-1 receptor antagonist; IL-1RA	PeproTech [200-01RA-250uG]
CD14+ microbeads	Miltenyi Biotech [130-050-201]
4% w/v Paraformaldehyde-PBS	ThermoFisher [15670799]

Primary cell culture

Primary human blood monocytes

Human peripheral blood monocytes were isolated from the blood of healthy donors. The blood samples were collected after obtaining informed written consent from healthy volunteers as approved by The University of Sheffield Ethics Committee (Old Reference: SMBRER310, New Reference: 031330).

Monocytes were isolated by Ficoll density gradient centrifugation to purify peripheral blood mononuclear cells (PBMCs) followed by monocyte isolation using the MACS system (Miltenyi) for $CD14^+$ monocytes positive selection procedure. 80mL of blood was drawn in two 50mL-conical tubes, 40mL of the blood was dispensed then each tube was mixed with 5mL of 3.8% (w/v) tri-sodium citrate dihydrate ($Na_3C_6H_5O_7 \cdot 2H_2O$) as an anti-coagulant. The blood was layered carefully over a 50mL conical tube filled with 15mL of Ficoll-Paque Plus then centrifuged at 900xg for 20 minutes (acceleration and brake at 1). The top layer (plasma) was removed and the cloudy layer (middle layer) containing the mononuclear cells was aspirated by Pasteur pipettes and placed in a 50mL-conical tube filled with 5mL of PBS-EDTA then centrifuged at 1500 rpm for 5 minutes. We centrifuged the aspirated PBMCs to eliminate the Ficoll-Paque and some of the plasma that might be aspirated with the PBMCs layer. The soft pellet was resuspended in 10 mL of Red Blood cell lysis buffer to eliminate erythrocytes and

platelets, incubated for 5 minutes at room temperature then centrifuged again, the pellet obtained was re-suspended and counted. Finally, $CD14^+$ monocytes were isolated by $CD14^+$ positive magnetic selection using (Miltenyi Biotec Inc.) anti-human $CD14^+$ antibodies coated with micro-beads. The isolated monocytes were counted again and plated at either $1x10^6$ or $5x10^5$ cell/well in a 6-well cell culture plate with adding RPMI-1640 containing 1% (v/v) L-glutamine and supplemented with 10% (v/v) foetal bovine serum (low endotoxin & heat inactivated), and 1% (v/v) penicillin/streptomycin.

The monocyte isolation method used in this project was optimised previously by our group members, Dr. Yang Li (PhD thesis, 2019), assessed the specificity of PBMCs isolation protocol by staining monocytes for purity and activation yielding more than 90% of monocytes. Also, Dr.Chiara Niespolo (PhD thesis, 2020) from our group has assessed the $CD14^+$ monocyte purity yielding 90% monocytes among few cell debris and lymphocytes.

Human monocyte derived macrophages (hMDMs)

Monocytes were differentiated into macrophages by adding (100ng/mL) of human recombinant macrophage-colony stimulating factor (M-CSF) and incubation at 37°C, 5% CO_2 for 7 days. On day 7, MDMs were ready to prime and stimulate to produce MVs.

Established cell line:

THP-1

The human monocytic leukaemia cell line (THP-1) was purchased from ATCC (TIB-202), maintained in suspension culture in RPMI-1640 medium containing 1% (v/v) L-glutamine and supplemented with 10% (v/v) foetal bovine serum (low endotoxin & heat inactivated), and 1% (v/v) penicillin / streptomycin, and 200µM 2-mercaptoethanol, as recommended by the supplier. The culture was maintained in 20-40mL of fresh medium at 37°C & 5% CO_2, sub-cultured every two to three days, maintaining cell numbers between $8x10^5$ - $1x10^6$ cells/ml.

For microvesicle and IL-1β production:

$10.8x10^6$ of cells were cultured in 6-well plate ($1.8x10^6$ cells per well) with adding 2mL of medium (above described) in each well, then differentiated into macrophage-like cells by adding 300ng/mL of Phorbol 12-myristate 13-acetate (PMA) for 3 hours. Subsequently, the media was changed, and cells incubated for 72 hours at 37°C, 5% CO_2. After three days of rest, cells were primed with LPS and stimulated with or without BzATP.

Immortalized bone marrow derived macrophages (iBMDMs)

The murine immortalized bone marrow derived macrophage cell line (iBMDMs) was a gift from David Brough (University of Manchester, originally generated by Hornung et al 2008), maintained in DMEM media containing 4500 mg/L glucose, L-glutamine, sodium pyruvate, and sodium bicarbonate. The media was supplemented with 10% (v/v) of foetal bovine serum (low endotoxin & heat inactivated), and 1% (v/v) penicillin / streptomycin (100 U/ml Penicillin, 100 µg/ml streptomycin), and 1% (v/v) of sodium pyruvate. The culture was maintained in 10mL of fresh medium at 37°C & 5% CO_2, sub-cultured every two to three days. When the cultured cells reached around 90% confluency, cells were ready for splitting. The media was discarded and substituted with 1xPBS buffer for washing and then discarded. Subsequently, cells were scraped in fresh media using a cell scraper and the cell suspension transferred into a new 75 cm^2 culture flask and topped up with fresh media to a dilution of (1:10).

For MVs and IL-1β production:

$2x10^5$ cells were cultured in 6-well plates with 2mL of medium (described above) per well. Cells were incubated overnight at 37°C, 5% CO_2 to allow the cells to achieve a confluence of at least 70%. The next day, cells were primed with LPS and stimulated with or without BzATP.

HeLa Cell Line

The human immortalised cervical epithelial HeLa cell line was obtained (ATCC, CCL-2) were maintained in DMEM media containing 4500 mg/L glucose, and L-glutamine.

The media was supplemented with 10% (v/v) of foetal bovine serum (low endotoxin & heat inactivated), and 1% (v/v) penicillin / streptomycin (100 U/ml Penicillin, 100 µg/ml streptomycin). The culture was maintained in around 10mL of fresh medium at 37°C & 5% CO_2, sub-cultured every two to three days. When the cultured cells reached around 90% confluency, cells were ready for splitting. The media was discarded and rinsed briefly with PBS buffer and then discarded. Subsequently, cells were detached using 2-ml of 0.25 % Trypsin-EDTA (1x) for 5-10 minutes, then neutralised with complete media. Next, cells were diluted to a suitable ratio of the cell suspension, usually 1:5 to 1:10 dilution, into a 75 cm^2 culture flask as appropriate.

HeLa cells as a bioassay for IL-1 delivery:

$2x10^5$ cells were cultured in 12-well plate with 1mL of medium (described above) per well. Cells were incubated overnight at 37°C, 5% CO_2 to allow the cells to achieve a confluence of at least 70%. The next day, cells were stimulated with cell samples, IL-1β in the absence or presence of IL-1 receptor antagonist; IL-1Ra.

HeLa cell Transfection:

$1x10^5$ cells were cultured in 12-well plate with 1mL of medium (described above) per well. Cells were incubated overnight at 37°C, 5% CO_2 to allow the cells to achieve a confluence of at least 70%. The next day, cells were transfected as described below and incubated for 48 hours then hMDMs supernatants or MVs pellets were applied onto the transfected HeLa cells.

2.2.2 Microvesicle generation, isolation, and IL-1β production

Cells from both cell lines and primary hMDMs after differentiation into macrophages, were primed with 1µg/mL lipopolysaccharides (LPS) for 3 hours in order to upregulate the expression of the pro-inflammatory cytokine pro-IL-1β and the inflammasome proteins, or without LPS as controls and incubated at 37°C & 5% CO_2. The media was then removed and substituted with 400µl of 1xPBS containing magnesium and calcium. BzATP [2, 3-O-(4-benzoylbenzoyl)-ATP] is a $P2X_7$ receptors synthetic agonist, more potent and stable than ATP. BzATP was used at a final concentration of 300µM for 20 minutes. Supernatants were collected from each well in 1.5ml Eppendorfs; these were then either used to measure IL-1β release by ELISA or MVs

were isolated. The isolation of MVs was achieved by differential centrifugation, the supernatant was centrifuged twice at 1500xg, 4°C for 5 minutes to remove cells and cellular debris as well as apoptotic bodies. Next, the supernatant was collected and centrifuged once more at a high speed of 20,000xg at 4°C for 30 minutes to pellet MVs only. For the MV-depleted supernatant experiments; the supernatant obtained after isolation MVs pellet was kept for IL-1β measurements by ELISA as well as for applying it onto HeLa cells ± IL-1Ra and transfected HeLa cells. For sample storage, the MV pellets were stored at -20°C until analysis to preserve the vesicle structure from degradation while the supernatants and cell lysates were stored at -80°C.

2.2.3 P2X$_7$R selective inhibition (A 438079 hydrochloride)

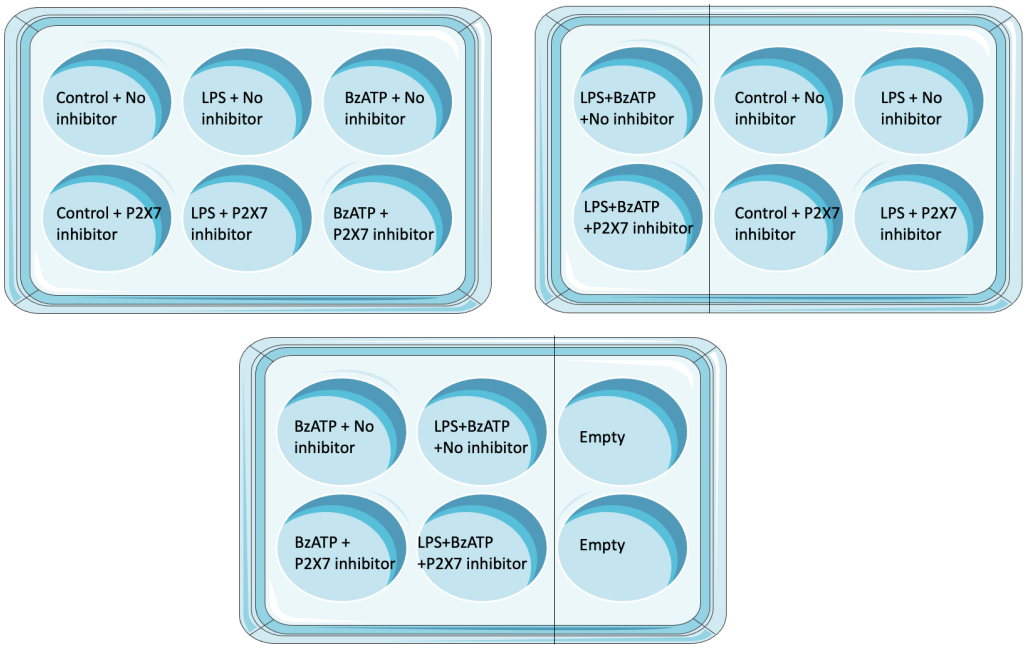

Figure 2.1: The experimental layout of the cell lines: iBMDMs/THP-1 treated with the selective P2X$_7$R inhibitor (A438079 hydrochloride).

The cell lines, THP-1 and iBMDMs, the cells were seeded in three 6-well plates and the layout for each biological replicate was as follows: Control, LPS, BzATP, LPS+BzATP and this layout was set twice, one for Flow cytometry to quantify MVs

and one for IL-1β measurements in the supernatant by ELISA (Fig. 2.1). Hence, the experiments were run in parallel. The $P2X_7R$ selective inhibitor (A 438079 hydrochloride) was used at 2.5 μM and incubated with cells for 30 minutes at 37°C prior to and during LPS priming and BzATP stimulation. Then the supernatants were collected for either directly measuring IL-1β levels in the supernatant or for MV isolation by multiple centrifugation and quantification by Flow cytometry. The lysate of the supernatant was also collected and investigated for IL-1β production by ELISA.

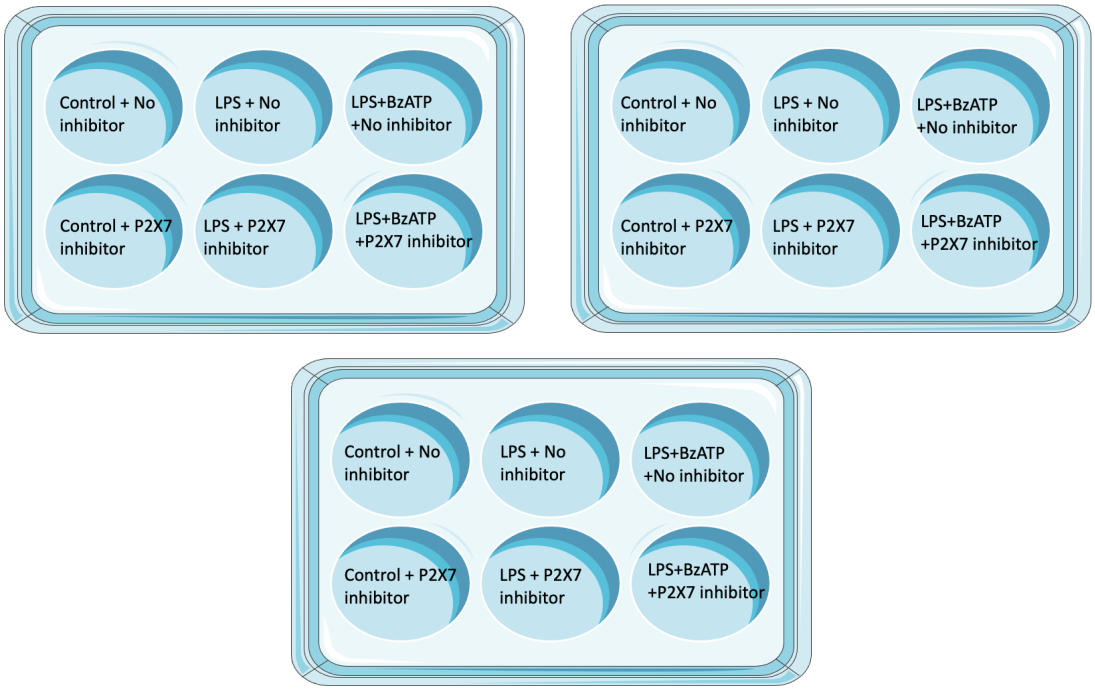

Figure 2.2: The experimental layout of the human primary macrophages (hMDMs) treated with the selective $P2X_7R$ inhibitor (A438079 hydrochloride).

The primary hMDMs were seeded in three 6-well plates ($5x10^{\wedge 5}$ cell/well) and the layout for each biological replicate (donor) was as follows: Control, LPS, LPS+BzATP and this layout was set for three purposes: one for Flow cytometry to quantify MVs and one for IL-1β measurements in the supernatant by ELISA, the last was for IL-1β measurements in the MV pellet by ELISA (Fig. 2.2). Hence, the experiments were run

in parallel. The $P2X_7R$ selective inhibitor (A438079 hydrochloride) was used at 2.5 µM and incubated with cells for 30 minutes at 37°C prior to and during LPS priming and BzATP stimulation. Then the supernatants were collected for either directly measuring IL-1β levels in the supernatant or for MVs isolation by multiple centrifugation subsequently, some for quantification by Flow cytometry and some for measuring IL-1β levels. The lysate was harvested from cells corresponding to the supernatant and investigated for IL-1β production by ELISA.

2.2.4 Caspase-1 inhibition using Ac-YVAD-cmk

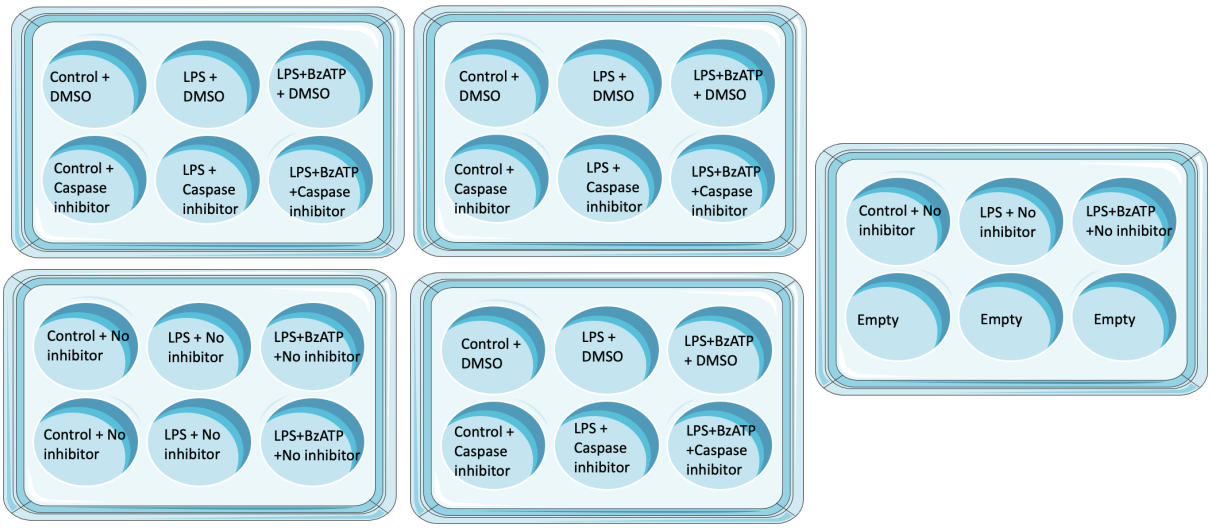

Figure 2.3: The experimental layout of the cell line iBMDMs treated with the Caspase-1 inhibitor (Ac-YVAD-cmk).

The cell line iBMDMs, the cells were seeded in five 6-well plates ($2x10^{\wedge 5}$ cell/well) and the layout for each biological replicate was as follows: Control, LPS, LPS+BzATP and this layout was set for three purposes: one for Flow cytometry to quantify MVs and one for IL-1β measurements in the supernatant by ELISA, the last was for IL-1β measurements in the MV pellet by ELISA (Fig. 2.3). Hence, the experiments were run in parallel. The Caspase-1 inhibitor (Ac-YVAD-cmk) was used at 27 µg/ml and

incubated with cells for 30 minutes at 37°C prior to LPS priming and BzATP stimulation. The cells were also incubated with the equivalent vehicle concentration of 0.2% DMSO as the caspase-1 inhibitor. The lysate was harvested from cells corresponding to the supernatant and investigated for IL-1β production by ELISA.

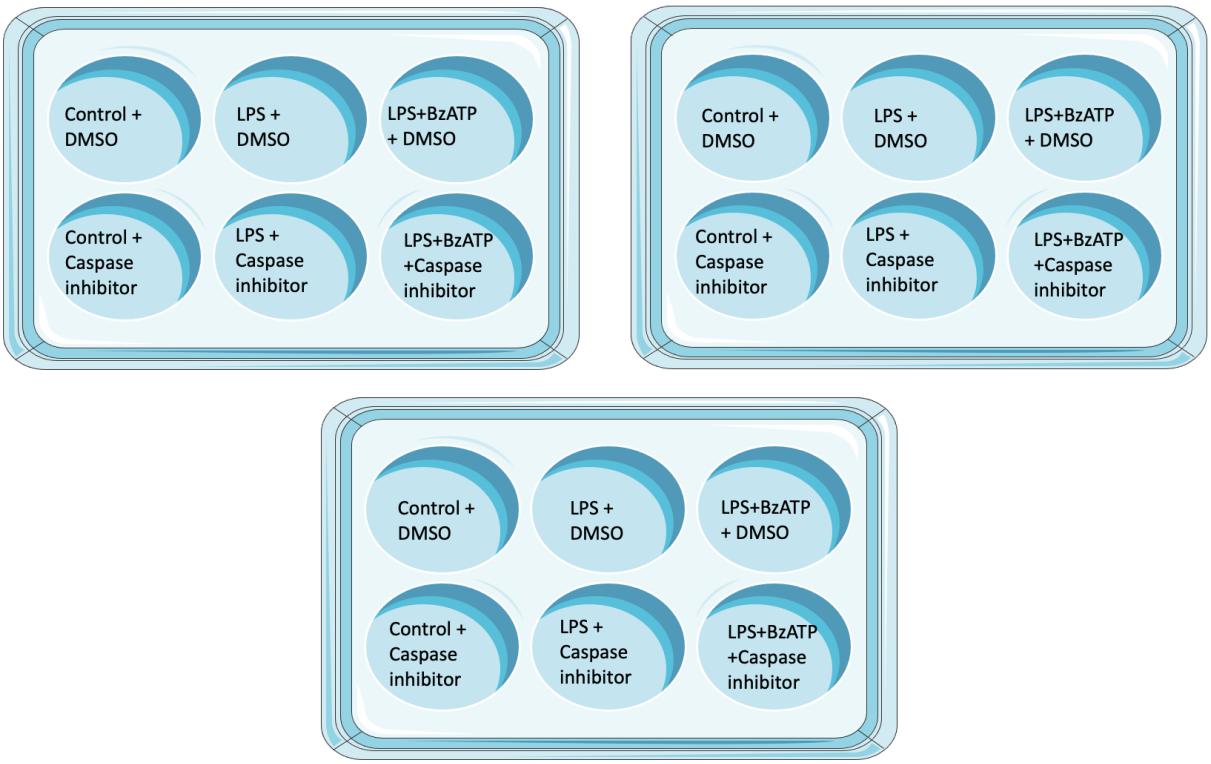

Figure 2.4: The experimental layout of the human primary macrophages (hMDMs) treated with the Caspase-1 inhibitor (Ac-YVAD-cmk).

For primary hMDMs, cells were seeded in three 6-well plates (5x10^5 cell/well) and the layout for each biological replicate (donor) was as follows: Control, LPS, LPS+BzATP and this layout was set for three purposes: one for Flow cytometry to quantify MVs and one for IL-1β measurements in the supernatant by ELISA, the last was for IL-1β measurements in the MV pellet by ELISA (Fig. 2.4). Hence, the experiments were run in parallel. The Caspase-1 inhibitor (Ac-YVAD-cmk) was used at 27 µg/ml and incubated with cells for 30 minutes at 37°C prior to LPS priming and BzATP stimulation. The cells were also incubated with the vehicle; DMSO at the same

concentration as the caspase-1 inhibitor. The lysate was harvested from cells corresponding to the supernatant (not the MVs pellet) and investigated for IL-1β production by ELISA.

2.2.5 Detection and counting of microvesicles

After isolating the MVs, their numbers were quantified by Flow cytometry. The size range of the MVs generated was determined using Nano-particle Tracking Analysis (Zetaview). In addition, the proportion of positive MVs for PS surface molecule was measured by labelling with a fluorescent Annexin V. Annexin V, is a ligand protein that has a high affinity to bind the PS surface molecule thus, a fluorescent conjugate to Annexin V was added to MVs and quantified using the Flow Cytometry.

2.2.6 Flow cytometry

Table 2.2: Reagents and materials for Flowcytometry.

Material / Reagent	Supplier [Catalogue No.]
Megamix beads	Biocytex [7801]
Annexin V binding buffer (5x), 30mL	Invitrogen [V13246]
Annexin V, Alexa Fluor ™, 488 conjugates	Invitrogen [A13201]
SPHERO™ AccuCount Particles	Spherotech Inc. [ACBP-20-10], 2.0µm

Microvesicles preparation and labelling for Flow Cytometry analysis

Microvesicle pellets were resuspended in 400µl of 1 x Annexin V Binding Buffer (by Invitrogen). In a new 1.5ml Eppendorf, 70 µl 1 x Annexin V Binding Buffer was added, then 30 µl of the MV pellets suspension was added, and was labelled with the Annexin V, Alexa Fluor™ 488 conjugate (1:20), incubated on ice for 15 minutes. Then, 10µl of the SPHERO™ AccuCount Particles (counting beads) were added and topped up again with 185µl of 1xAnnexin V Binding Buffer ending with a mixture volume of 300µl. Then, samples were analysed by Flow Cytometry to quantify the MVs numbers and determine the proportion of PS positive MVs.

The MVs were counted using BD LSR II flow cytometer analyser and calibrated using megamix beads with the following sizes 0.5µm, 0.9µm, and 3µm to serve as size reference (Fig. 2.1). The flow cytometer gates were set up according to the protocol provided by BioCytex company associated with the megamix beads.

The total MVs number and the percentage of PS positive MVs were calculated according to the SpheroTech company technical notes of calculating absolute cell count formula (https://www.spherotech.com/tech_SpheroTech_Note_15.html) which is:

(A/B) x (C/D) = Number of MVs per µL

Where:

A = number of events for the Test sample

B = number of events for the AccuCount Particles

C = number of AccuCount Particles per 50µL

D = volume of test Sample initially used in µL

To obtain the total MVs number that showed on our results figures, the result obtained from the formula above is multiplied by 400 which is the initial MVs resuspension volume.

For determining the percentage of PS-positive MVs, we followed the same steps as for the total MVs number to obtain total AnnexinV-positive MVs then, divided the total AnnexinV-positive MVs by the total MVs number and multiplied by 100.

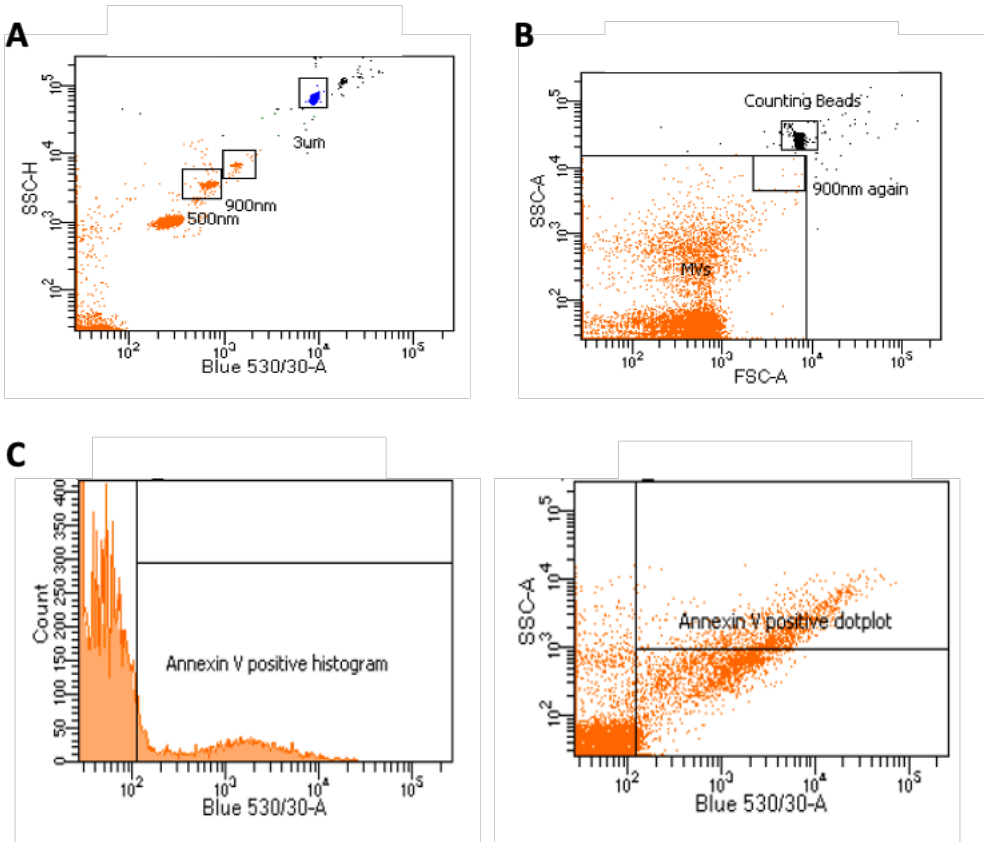

Figure 2.5: Flow cytometer gate settings to detect and count microvesicles.

(A) The flow cytometer calibration using megamix beads of varied sizes (500 nm, 900 nm, and 3µm) to detect and count the MVs. (B) The region of interest determined according to megamix bead sizes and plotted as Side scatter (SSC) versus forward scatter (FSC), MVs detecting region indicates the region of interest. (C) The MVs labelled with Annexin V, Alexa Fluor™ 488 conjugate staining detected via the filter 530/30.

2.2.7 Nano-particle Tracking Analysis (NTA)

Microvesicles preparation for Nano-particle Tracking Analysis (NTA)

Microvesicle pellets were resuspended in 100µl of PBS. The mixture for analysis was made by dilution to (1:40) in molecular water then injecting the mixture into the NTA (ZetaView) for analysis.

The MV size distribution was evaluated using Nano-particle Tracking Analysis (NTA) (ZetaView, ParticleMetrix), which works by tracking particles in the size range 100 to 1000nm where suspended in a fluid. Each particle is tracked individually through detecting the light scatter from the particle that is detected via a sensitive camera, with the size being determined by analysing the Brownian motion of each particle (Fig. 2.2). The term Brownian motion refers to the random movement of particles suspended in fluid, by diffusion. The physical principal underlying NTA to measure the particles size is based on the determination of the diffusion coefficient (D) of a particle in a given time interval (t) through quantifying the mean square displacement. The mean square displacement (x^2) is the observed movement of a certain particle between two spots per time interval registered in two dimensions. Thus, the diffusion coefficient can be calculated as follows;

$$D = \langle x,y \rangle^2/4t$$

The particle diameter (d) was determined using Stokes-Einstein's equation as follows:

$$D = 4k_BT/ 3\pi\eta d$$

Where k_B is Boltzmann's constant, T is the temperature, and η is the viscosity of the fluid.

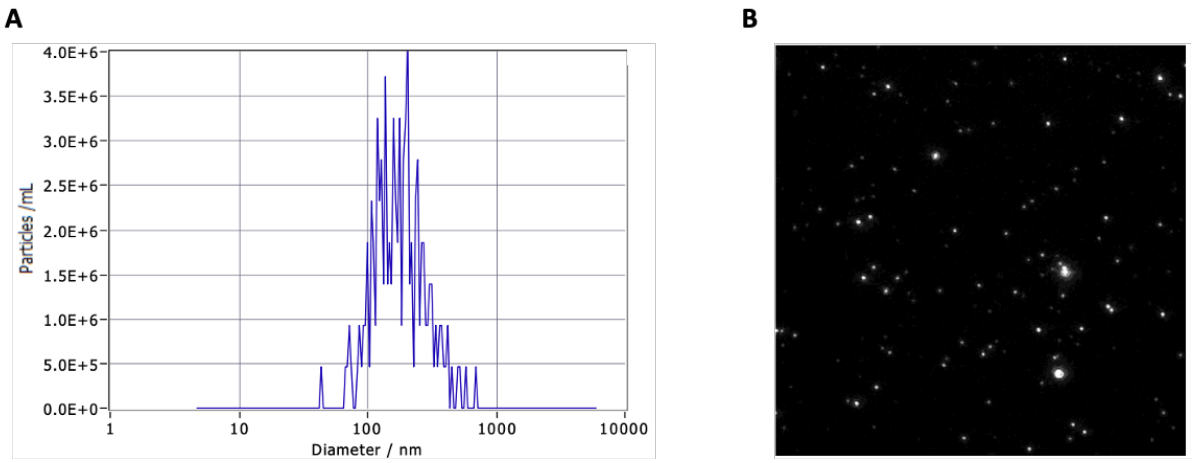

Figure 2.6: Nano-particle Tracking Analysis (ZetaView) to detect and count microvesicles.

(A) Typical histogram from a sample demonstrating the size distribution of the detected particles. (B) Typical image of a sample showing the detected particles captured by the camera.

2.2.8 Bicinchoninic acid (BCA) protein determination

The BCA protein assay is a colorimetric protein assay method relying on a chemistry involving two reactions; first, protein and copper chelation then, reducing the copper and production of a colour that is detectable. The biuret reaction occurs where cysteine, tyrosine, and tryptophan amino acids residues chelate with the cupric ions (Cu^{2+}) forming a complex in alkaline medium in the presence of sodium potassium tartrate. The reduction of copper ion by the biuret complex from cupric to cuprous is detectable from the formation of a light blue colour. The number of peptide bonds involved in the biuret reaction are proportional to the intensity of the colour produced thus, the more peptides involved the more intense the colour obtained. The second reaction involved is the chelation of two molecules of bicinchoninic acid (BCA) with one ion of the cuprous ions to produce a purple-coloured complex. This complex is measured with spectrophotometer to determine the absorbance at wavelength of 562 nm.

The protein concentration was measured to achieve equal loading in western blotting. A dilution-series of standards with known protein concentrations was run in parallel to samples helps to calculate protein concentrations in samples. This was done for each assay, as the BCA reaction is time and temperature dependent. The absorbance values obtained from the standards were plotted to generate a standard curve and the samples' concentration interpolated for the absorbance values.

The attached cells on the multi-well cell culture plates were treated with a mixture of RIPA lysis buffer and Protease inhibitor cocktail in a dilution of (1:10). RIPA buffer contains the following; 150 mM NaCl, 1.0% IGEPAL® CA-630, 0.5% sodium deoxycholate, 0.1% SDS, 50 mM Tris, pH 8.0 in order to lyse cells and maintain proteins solubility. This mixture was added onto each well with adjusted volumes according to purposes of use, i.e. western blotting for cell lysate or for MVs pellet. Next, the cells were scraped carefully until the liquid becomes viscous then transferred to microcentrifuge tubes. Bovine Serum Albumin (BSA) protein was used to generate a standard curve for ten points from 0 to 2 µg/ml. the standards and samples were prepared and assayed according to the manufacturer's protocol (Thermo Scientific™, Pierce™ BCA Protein Assay Kit).

2.2.9 Cell fixation for Scanning Electron Microscopy (SEM)

Scanning electron microscopy is a method used to visualise the topography of the surface of a biological specimen. It creates an image by focusing a beam of high energy electrons over the specimen.

For iBMDMs: 2x10^5 (cell/well) were seeded in 24-well plate on coverslips and allowed to adhere overnight. The next day cells were either primed with 1µg/ml LPS for 3 hours or non-primed as negative control. The LPS-primed cells were then stimulated with 300µM BzATP for several time points before cellular fixation; 2 minutes, 5 minutes, 10 minutes in buffer. After each time point assigned, the buffer containing BzATP was discarded and cells were fixed with 1ml of 2.5% (v/v) Glutaraldehyde-1xPBS and incubated overnight at 4°C. The next day, glutaraldehyde was discarded and replaced with 1ml of 1xPBS and incubated at 4°C before imaging.

For THP-1: 2x10^5 (cell/well) were seeded in 12-well plate on coverslips then differentiated into macrophage-like cells by adding 300ng/ml of Phorbol 12-myristate 13-acetate (PMA) for 3 hours. Subsequently, the media was changed, and cells incubated for 72 hours at 37°C, 5% CO_2. After 3 days of rest, cells were either non stimulated, as negative control, or stimulated with 300µM BzATP for several time points before cellular fixation; 2 minutes, 5 minutes, 20 minutes in 1xPBS containing calcium and magnesium. After each time point assigned, the PBS containing BzATP was discarded and cells were fixed with 1ml of 4% (w/v) Paraformaldehyde-1xPBS for 10 minutes at room temperature. After that, it was removed and cells were rinsed once with 1xPBS for 10 minutes then removed. Next, another fixative reagent was added; 1ml of 2.5% (v/v) Glutaraldehyde-1xPBS onto the cells and incubated overnight at 4°C. The next day, glutaraldehyde was discarded and replaced with 1ml of 1xPBS and incubated at 4°C before imaging.

For hMDMs: 2x10^5 (cell/well) of monocytes were seeded in 12-well plate on coverslips then differentiated into macrophage by 100ng/ml of M-CSF for 7 days. On the 7th day, the cells were treated and fixed by the same protocol of THP-1 above.

For the secondary fixation, which was carried out by our colleague Dr. Jaime Canedo,as well as the imagine. Started with 2% (v/v) aqueous osmium tetroxide. Samples were then dehydrated sequentially using 75%, 95% and 100% (v/v) ethanol

before drying using a Leica EM CPD300. When dried, samples were mounted on aluminium stubs, attached to carbon sticky tabs and coated with 25 nm of gold in an Edwards S150B sputter coater. Images to assess cell morphology were taken using TESCAN Vega 3 LMU Scanning Electron Microscope at an acceleration voltage of 10 kV.

2.2.10 Enzyme-linked Immunosorbent Assay (ELISA)

Table 2.3: Reagents and materials for ELISA.

Material / Reagent	Supplier [Catalogue No.]
Bovine Serum Albumin	Sigma-Aldrich A7906
Human IL-1 beta/IL-1F2 DuoSet ELISA	R&D [DY-201]
Mouse IL-1 beta/IL-1F2 DuoSet ELISA	R&D [DY-401]
1xPBS tablets	Thermo Scientific Oxoid [10209252]
Substrate solution ELISA	R&D [DY999]
Human IL-6 mini ELISA kit	PeproTech [900-TM16]

ELISA is a immunoassay technique used to detect and quantify target analytes such as antibodies, proteins, peptides. In this project, we used the sandwich ELISA technique to detect and quantify the cytokines IL-1β, IL-6 or IL-8. The basic principle of sandwich ELISA is to layer the target analyte between two different antibodies that are specific for that analyte's epitopes. The capture antibody adsorbs to a 96-well plate that is raised against the desired target analyte, then it captures the target analyte by recognising a specific epitope. Next, the second antibody detects a different epitope on the target analyte hence, the target analyte is sandwiched between two antibodies. The second "detection" antibody is biotin-labelled that binds to streptavidin. The streptavidin is enzyme-conjugated to horseradish peroxidase (HRP) enzyme which, when the tetramethylbenzidine (TMB) substrate is added, generates a colorimetric reaction. A dilution-series of standards with known concentrations of the protein being

detected (IL-1β, IL-6 or IL-8) were run in parallel to samples in order to quantify cytokine levels in the samples.

ELISA kits for detecting IL-1β, from both human cells and murine cells, were obtained from R&D systems company and the manufacturer's protocol was followed. ELISA kits for detecting IL-6, was obtained from PeproTech company and the manufacturer's protocol was followed. ELISA kits for detecting IL-8, was obtained from R & D company and the manufacturer's protocol was followed.

Plate preparation: a high-binding 96-well microplate was coated with 100 µl/well of capture antibody diluted in 1xPBS at room temperature overnight. The next day, the plate was washed three times with the washing buffer as described in the manufacturer's protocol then blocked with 1% (w/v) bovine serum albumin (BSA)-1xPBS adding 300 µl/well for 1 hour. Next, the plate was washed three times before sample addition.

Assay procedure: the standards were prepared according to the manufacturer's protocol and loaded 100 µl/well onto the plate along with the samples (100 µl/well) and incubated for 2 hours at room temperature. The three washes were repeated, and the detection antibody was prepared according to the manufacturer's protocol and 100 µl/well were added to the plate wells, incubated for 2 hours at room temperature, followed by three washes, and 100 µl/well of streptavidin conjugate to HRP was added and incubated for 20-30 minutes then the three washes repeated. The substrate solution TMB was prepared (1:1) and 100 µl/well were added for 20 minutes. Finally, 50 µl/well of the stop solution (2N of H_2SO_4) was used to stop the reaction. The plate was read using a Varioskan (Thermo Scientific) plate reader at 450nm to determine the optical density at 450nm of standards and samples.

The samples and standards were run in duplicates and averaged after subtracting the blanks (buffer only in place of standard or sample). The standard curve was analysed using GraphPad Prism 9.0 software by generating a four parameter logistic curve-fit, and the sample concentrations were determined by interpolation from the standard curve with confidence interval ≥ 95%.

2.2.11 Western blot

Table 2.4: Reagents and materials for Western Blot.

Material / Reagent	Supplier [Catalogue No.]
Tris Buffered Saline pH 8.0, powder	Sigma-Aldrich [T6664-10PAK]
MES SDS Running Buffer (20X)	Invitrogen [NP0002]
NuPAGE 4-12% Bis-Tris Protein Gels 10 wells, 15 wells	Invitrogen [NP0323PK2], [NP0335PK2]
NuPAGE Antioxidant	Invitrogen [NP0005]
Protein Ladder	Invitrogen [LC5925]
Human Recombinant IL-1 beta Protein	R&D [201-LB]
Rabbit Anti-Human IL-1 beta antibody (EP408Y)	Abcam [ab33774]
Goat Anti-Mouse IL-1 beta /IL-1F2 Antigen Affinity-purified Polyclonal Antibody	R&D [AF-401-NA]
ECL™ Select Western Blotting Detection Reagent	Merck [RPN2235]

Western blot was used to evaluate the size of the cytokine; IL-1β using the "XCell SureLock Mini-Cell and XCell II Blot Module" from Invitrogen™. The samples were prepared from stimulated cells and the supernatant, and their corresponding cell lysate and MV pellet. Supernatants were subjected to ultrafiltration in order to concentrate the IL-1β protein using Amicon Ultra-0.5 Centrifugal Filter Units of nominal molecular weight cut-off of either 3 kDa or 10 kDa (MerckMillipore). Cell lysates were processed as described above (see 2.2.6 BCA section) and 50 µg of the hMDMs samples' protein was loaded whilst the iBMDMs cell lysate was 25 µg. MV pellets were treated the same as the cell lysate and the protein concentration was determined by BCA technique and 12 µg of the samples' protein was used. Next, the samples were mixed with 5x loading buffer (10% SDS (w/v), 25% (v/v) beta-mercaptoethanol, 50% (v/v) glycerol, 0.01% (w/v) bromophenol blue, 0.125M Tris-HCl, pH 6.8) and heated to 100°C for 5 minutes.

The samples were loaded onto the SDS-PAGE gel (NuPAGE 4-12% Bis-Tris SDS-PAGE gel Novex (Invitrogen)) alongside the positive control (recombinant human IL-1β by Abcam), and the protein standard which was SeeBlue™ Plus2 Pre-stained Protein Standard (Invitrogen). The gel was added in the XCell SureLock Mini-Cell Electrophoresis System and ran at 120V for 70 minutes in MES SDS buffer (Invitrogen). After that, the protein transfer was carried out onto nitrocellulose membrane in the XCell II Blot Module (Invitrogen) and the addition of the transfer buffer (described in the materials above) and ran at 35V for 1 hour. The membrane was stained with Ponceau S red solution (Sigma Aldrich) was carried out for 5-10 minutes to assess efficient transfer then the membrane was washed with 1xTBS three times and blocked for 1 hour using the blocking buffer (described in the materials above) at room temperature. Next, the primary antibody was diluted in the blocking buffer and incubated with the membrane at 4°C overnight. The next day, the membrane was washed three times with 1xTBST for 5 minutes each wash. The secondary antibody was HRP conjugated (either Anti-Goat or Anti-Rabbit) and was diluted in the blocking buffer at 1:2500, incubated with the membrane for 1 hour at room temperature, while rotating for mixing. Following three washes of 5 minutes, for chemiluminescent detection the membrane was covered with ≈ 2 ml of ECL™ Select Western Blotting Detection Reagent (reagents A&B mixed equally, Merck Millipore), and incubated for 1 minute before their detection using the ChemiDoc XRS+ Imaging System (BioRad).

For hMDMs (5x10^6 Cell/Condition) where western blotting was used to evaluate the IL-1β molecular weight, Rabbit Anti-Human IL-1β primary antibody (by Abcam) was used at 1:5000 in the blocking buffer and incubated for two days at 4°C hence, the recombinant human IL-1β protein was used at 1.6 ng.

For iBMDMs (5x10^6 Cell/Condition) were used to evaluate the IL-1β molecular weight and the Goat Anti-Mouse IL-1β primary antibody (by R&D) was used at 0.4 µg/ml in the blocking buffer and incubated overnight at 4°C. The recombinant human IL-1β protein was used at 1.6 ng as a control which cross-reacts with the anti-mouse IL-1β antibody.

2.2.12 Transient transfection

Table 2.5: Reagents and materials for Transfection.

Material / Reagent	Supplier [Catalogue No.]
ON-TARGETplus Non-targeting Control Pool	Horizon Discovery [D-001810-10-20]
siGLO Green Transfection Indicator	Horizon Discovery [D-001630]
ON-TARGETplus Human MERTK siRNA	Horizon Discovery [L-003155-00-0005]
DharmaFect Transfection Reagent	Horizon Discovery [T-2001-01]

Transient transfection of siRNAs was performed in the HeLa cell line to induce MerTK knockdown. The human ON-TARGETplus MerTK siRNA (Horizon Discovery for Dharmacon) and the ON-TARGETplus Non-targeting Control Pool (Horizon Discovery for Dharmacon) were both delivered to HeLa cells seeded in 12-well plates at 25 nM final concentration using DharmaFECT transfection reagents according to the manufacturer's protocol.

2.2.13 Gene expression analysis by RT-qPCR

RNA isolation from cells was performed using the RNeasy UCP kit (Qiagen) according to manufacturer's instructions. The complementary DNA was transcribed from the total RNA using the Precision nanoScriptTM 2 RT kit (Primer design), and the manufacturer's instructions were followed. The reagents used were Precision PLUS SYBR-Green master mix (Primer design) and specific primers (listed below) designed with NCBI BLAST. The results were analysed with CFX384 C1000 Touch Thermal Cycler (Biorad). All assays were performed in triplicate and normalised to the house keeping gene GAPDH expression levels. The primers were designed and checked for specify using the BLAST Primer Design Tool (https://www.ncbi.nlm.nih.gov/tools/primer-blast/) and purchased from Merck Millipore company. The qPCR of MerTK expression in HUVECs exposed to different shear stress was done by Dr. Klaudia Kocsy, and the samples were provided by Dr. Daniela

Pirri. Whilst, the qPCR of MerTK in all HeLa cells, SMCs, and hMDMs was done by Charlotte Moss.

Gene (GenBank Accession Number)	**Forward Primer**	**Reverse Primer**
Human GAPDH (NM_002046.7)	ATTGCCCTCAACGACCACTTT	CCCTGTTGCTGTAGCCAAATTC
Human MerTK (NM_006343.3)	CGCTCTGGCGTAGAGCTAT	AGGCTGGGTTGGTGAAAACA

2.2.14 Existing data analysis

The data in chapter (4) were obtained from published microarray gene expression data using the datasets stored at the Gene Expression Omnibus (GEO) repository (https://www.ncbi.nlm.nih.gov/geo/). This data was mined to identify the MerTK receptor gene expression values which was plotted and analysed using appropriate statistical analysis (see below).

2.2.16 Statistical analysis

Data are represented as mean±SEM,or as mean±SD or as individual values, as indicated. The parametric tests, One-Way ANOVA, Two-Way ANOVA, or student t-tests were performed as indicated. For all the experiments comparisons were carried with GraphPad Prism 9 software. P values <0.05, were considered statistically significant. The N-value represents separate experiments carried out for cell lines or represents different donors/individuals for primary cells; these values are stated for each dataset presented.

Chapter 3 . Macrophage microvesicle production, interleukin-1β release and phosphatidylserine exposure in response to inflammation activation

3.1 Background and Aims

Macrophages are widely known to significantly contribute to atherosclerosis disease progression and are the most abundant type of cell present in the plaque. They play a central role in the initiation of the plaque (atherogenesis), lipid accumulation in foam cells, plaque stability and in chronic inflammation (Moore et al., 2013).

Macrophages drive atherosclerotic plaque advancement by taking up lipids and driving immune cell activation and are present in each stage of atherosclerosis. They are a key source of the proinflammatory cytokine and chemokine production in plaque inflammation including IL-1β (Barrett, 2020). Macrophage-derived MV have previously been described to contain specific cytokines (MacKenzie et al., 2001). MVs are membrane-bound vesicles, known to participate in intercellular communication influencing targeted cell function acting as signalling vectors for many physiological as well as pathological conditions. Since MVs function in intercellular communication they are likely to play a role in the pathogenesis of atherosclerosis. Cytokines participate in atherosclerotic plaque cell signalling throughout all the disease stages contributing to inflammation, cellular proliferation, migration, and death as well as vascular remodelling. To date, the role of macrophage-derived MVs in atherosclerosis is still unclear.

Previous studies have shown that human macrophages including differentiated THP-1 cells (MacKenzie et al., 2001) and peripheral blood monocyte-derived macrophages (Ward et al., 2010) release MVs in response to $P2X_7$ receptor activation with BzATP. MVs were shown to contain IL-1β (MacKenzie et al., 2001), while MVs release was dependent on BzATP stimulation with or without production of IL-1β which required LPS priming (TLR4 receptor (PRR) activating NF-κB, and upregulation of the inflammasome; (Liu et al., 2017)). MacKenzie et al. (2001) labelled and isolated MVs using annexin V, demonstrating that PS was exposed on the cell surface and

externally on MVs rapidly (within 2 minutes) following BzATP treatment. Since this time extracellular vesicle populations from various cell types have been shown to be a mix of PS negative and positive populations (Connor et al., 2010, Shet et al., 2003, Jimenez et al., 2003). This has been enabled from the use of differential centrifugation methods to isolate the total population of EVs produced by cells. We therefore set out here to use differential centrifugation methods to determine whether BzATP-stimulation of macrophages results in increased MV production and an increased PS-positive MV population (this chapter), and whether PS serves to target MVs to target cell populations via the MerTK PS-receptor (chapters 4 and 5).

Since MacKenzie et al (2001) demonstrated that macrophage IL-1β was contained in MVs, others have shown that IL-1β is secreted in a MV-independent pathway, via Gasdermin D activation (Evavold et al., 2018). It is unclear whether the two-step process of inducing inflammasome activity (LPS priming) and IL-1β release by damage-associated molecular patterns (DAMPS) including ATP, is driven predominantly by one or both of these processes. To date, no publication has been published to resolve this question.

In this chapter we set out to test the following hypotheses:

1. Macrophages treated with both LPS and BzATP will generate a higher number of MVs compared to no treatment (control), priming (LPS) only or BzATP treatment alone.
2. Macrophages treated with BzATP produce an increased proportion of PS-positive MVs compared to untreated or LPS only treated cells.
3. Macrophages release IL-1β contained within MVs, which is stimulus dependent.

The aims were to use differential centrifugation methods to isolate the complete macrophage-derived MV population. In the first instance we aimed to use a suitable macrophage-like cell line in order to provide a consistent (not donor dependent) IL-1β release response. The higher cell numbers from a cell line would enable production of high numbers of MVs to be tested for MerTK-dependent MV-targeting (chapter 5).

3.2 Microvesicle production in PMA-differentiated THP-1 cells

THP-1 cells are acute leukemic monocytic cell line derived from human, the cell line has been used previously by (MacKenzie et al., 2001) to produce IL-1β containing PS-positive MVs isolated using annexin V-pull down. In that study MVs were not isolated using differential centrifugation, and numbers and relative PS exposure were not quantified using more up to date methods of flow cytometry. We therefore set out to use THP-1 cell line to generate MVs under multiple conditions. The conditions were established to investigate the effect of the bacterial stimuli LPS alone, and the effect of activating the $P2X_7$ receptor using BzATP on the production of MVs. To assess the role of $P2X_7$ receptor in MV production, a selective $P2X_7$ inhibitor (A438079) was used. It is a competitive $P2X_7$ antagonist called 3-[[5-(2,3-Dichlorophenyl)-1H-tetrazol-1-yl] methyl] pyridine hydrochloride that prevents $P2X_7$ receptor activation, preventing ion channel opening, and Na^+/Ca^{2+} influx and blocks loss of membrane asymmetry (cell surface PS exposure) (Ward et al., 2010).

THP-1s were differentiated to macrophages using PMA (see methods) and subsequently treated for 3h with or without LPS then washed and treated with or without BzATP for 20 mins in the absence or presence of A438079 ($P2X_7$ antagonist). MVs were isolated from the cell supernatants by differential centrifugation and quantified by flow cytometry. The data shown here are experiments of three replicates and follow optimisation of several trials.

PMA-differentiated THP-1 produced MVs from all the conditions, however the results obtained were highly variable between replicates (Fig. 3.1 A). Untreated cells produced significant numbers of MVs (Figure 3.1 A) while LPS and BzATP treatments did not act to significantly alter MV numbers above the control cells. ŦHP-1 MV production was not significantly altered in the presence of the $P2X_7$ receptor antagonist, which was also highly variable across the replicates (Fig. 3.1 A). The differences between each condition with or without the use of the $P2X_7$ inhibitor were compared using repeated measures, Two-way ANOVA test followed by Tukey's correction for multiple comparisons showing there were no statistically significant differences between conditions. These preliminary data show that PMA-differentiated THP-1 cells produced MVs regardless of the stimuli used and that MV release is not upregulated following $P2X_7$ receptor activation.

We assessed the PS externalization on MV surface by using the fluorescently-labelled Annexin-V conjugate that binds to PS, quantified by flow cytometry from the same samples used to assess MV numbers. We aimed to test whether PS externalization on the MV surface is stimulus dependent, particularly $P2X_7$ receptor activation dependent as assessed by using a $P2X_7$ antagonist. The proportion of PS-positive MVs were calculated from the total MVs number obtained (Fig. 3.1 B), showing that the PS-positive MV population was a low proportion of the total population, on average, 8% ± 4.78 across all conditions. The change in proportion of PS-positive MVs was highly variable between replicates and conditions, and was not altered with $P2X_7$ receptor inhibition. This suggests that PS exposure on the MV surface in THP-1 differentiated cells is stimulus independent, where no significant differences were found between the conditions tested.

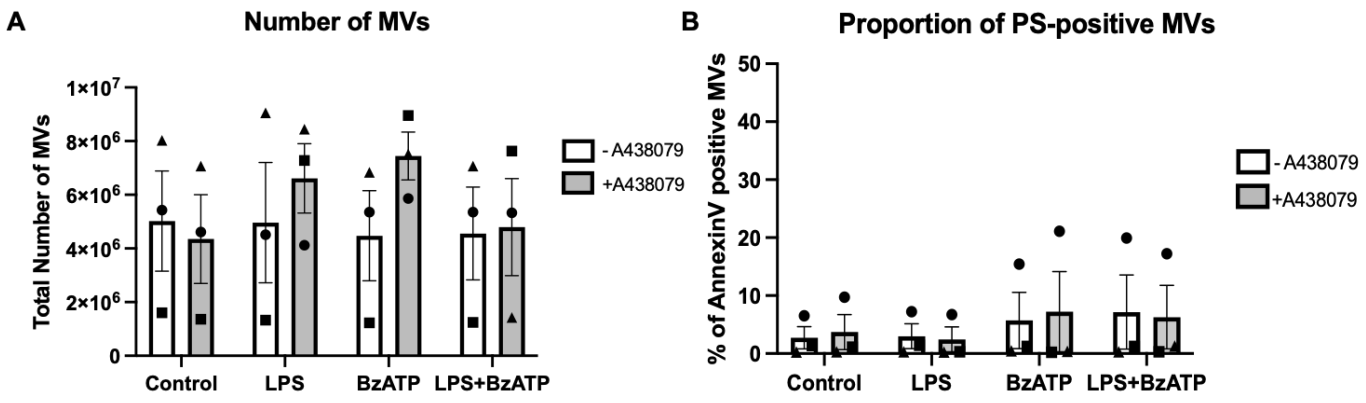

Figure 3.1: P2X$_7$R selective inhibition effect on microvesicle production from THP-1 cells.

Cells were differentiated with 300ng/ml PMA for 3 h followed by three days of resting prior exposure to the P2X$_7$R selective inhibitor 2.5μM (A438079) for 30 min then ± priming with 1μg/ml LPS for 3h followed by ± stimulation with 300μM BzATP for 20 min (N=3). A) Flow cytometry quantification of the total number of isolated MVs. B) The proportion of PS positive MVs quantified by flow cytometry and represented as percentages for the four conditions. Each symbol represents an individual replicate and is consistent in all graphs. Values are presented as mean ± SEM, analysed by Two-way ANOVA with Tukey's correction method for multiple comparisons. No significant differences were detected.

In order to refine the identification of MV production and characterised EVs produced by THP-1 cells, we visualised the cells under scanning electron microscopy before and after BzATP stimulation at several time points (Fig. 3.2). No cellular blebs were visible (as published previously in MacKenzie et al. 2001), which may have been due to the process of cellular fixation or due to the fact that blebs are retractable once the stimuli is removed (Verhoef et al., 2003).

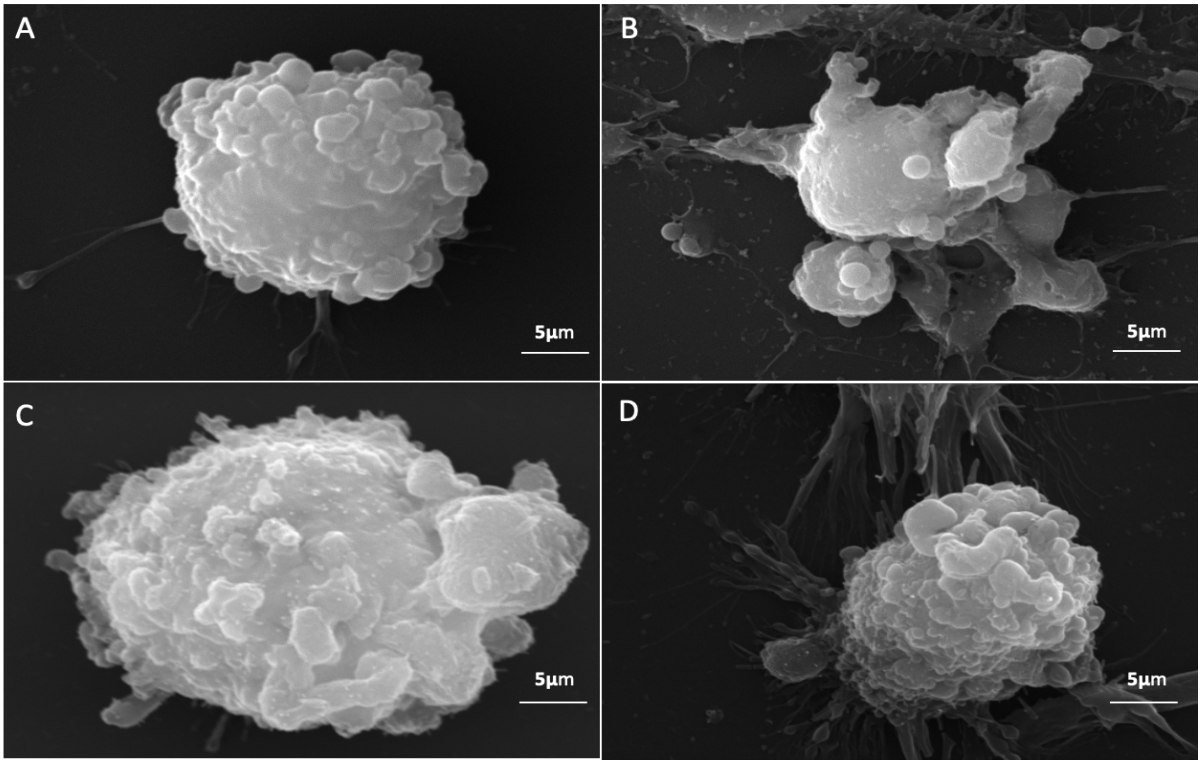

Figure 3.2: Scanning electron microscopy of control and BzATP treated THP-1 cells.

Cells were differentiated for 3 h with PMA followed by 3 days resting, then stimulated with 300µm BzATP at various time points (N=1): A) control, no BzATP; B) after 2 minutes of exposure to BzATP; C) after 5 minutes of exposure to BzATP; and D) after 20 minutes of exposure to BzATP.

In summary, THP-1 cells produce MVs under resting (control) and multiple treatment conditions. These treatment conditions do not alter the proportion of PS positive MVs such that the MV production and PS externalization occurs irrespective to the type of stimulus.

3.3 IL-1β release by PMA-differentiated THP-1 cells

Despite THP-1 cells producing MVs independently from their stimulus, we set out to investigate whether there is an increased production and release of IL-1β by PMA-differentiated THP-1 cells following LPS priming and BzATP treatment. The same conditions described above for MV quantification and the same samples were tested for IL-1β content. The supernatants and the corresponding cell lysates were collected for IL-1β quantification by ELISA (Fig. 3.3 A&B). THP-1 supernatants contained varying levels of IL-1β in the absence and presence of LPS & BzATP. They showed high variability between experimental replicates as well as between cell treatment conditions. It is notable that this variability was reduced on treatment with the $P2X_7$ inhibitor, A438079, where lower levels of IL-1β were released from the cells overall. However, this was not statistically significant, but perhaps suggestive that some IL-1β secretion may be $P2X_7$ dependent.

We also encountered issues with maintaining and growing the cells and several attempts were made including altering the media supplements and trying different batches of stocks and newly purchased cells from ATCC supplier. Despite multiple biological experiments performed, THP-1 cell production and release of IL-1β was highly variable, with high levels shown in untreated controls, with the pattern of release being inconsistent regardless of the stimuli added. For this reason we proceeded to test other cell models for more consistent responses with respect to MV production and IL-1β secretion.

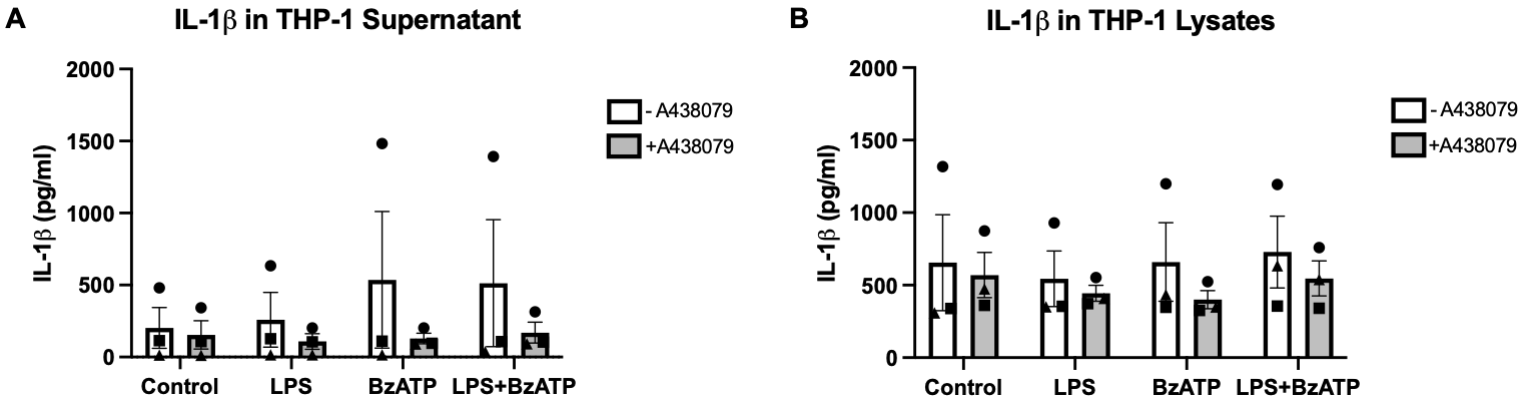

Figure 3.3: Effect of P2X$_7$R selective inhibition on IL-1β release from THP-1 cells.

Cells were differentiated with 300ng/ml PMA for 3 h followed by three days of resting prior exposure to the P2X$_7$R selective inhibitor 2.5μM (A438079) for 30 min then ± priming with 1μg/ml LPS for 3h followed by ±stimulation with 300μM BzATP for 20 min (N=3). IL-1β was measured by ELISA in the supernatant (A) or cell lysate (B). Each symbol represents an individual replicate and is consistent in all graphs. Values are presented as mean ± SEM, analysed by Two-way ANOVA with Tukey's correction method for multiple comparisons. No significant differences were detected.

3.4 Immortalised mouse Bone Marrow Derived Macrophage cell line (iBMDMs) microvesicle production is stimulus independent

Since we aimed to isolate MV-containing IL-1β, to test the role of MerTK in targeting (Chapter 5), we continued to identify a reliable cell model that can produce MVs containing IL-1β. Since PMA-differentiated THP-1 cellular MV production and IL-1β release was highly variable and inconsistent, we sought to identify and test the immortalized mouse macrophages cell line that was generated from wild type (C57BL/6) mice. The iBMDM cell line has been employed in inflammation-based studies; in particular it has been applied as an in-vitro model for IL-1β synthesis and secretion studies (Hornung et al., 2008, England et al., 2014). However, MV release by this cell line hasn't yet been studied. Investigating the mouse MDMs is important to study the behaviour of these cells, in terms of detecting and counting the MVs produced in response to LPS and BzATP stimulation and compare the results with those from human derived cells. Studying mouse cell lines will be useful for future experiments, since we aim to establish an *in vitro* system involving MerTK receptor knockdown. Thus, we investigated whether iBMDMs were able to release MVs in response to the two stimuli previously applied to THP-1. Similar to THP-1 experiments, the MV production in the presence or absence of BzATP was investigated as well as the $P2X_7$ receptor inhibition. In addition, the PS molecule externalization in their surface.

The data shown here are the results of experiments from three different biological replicates and represent the optimisation of multiple trials. The iBMDMs produced MVs in control, LPS and LPS + BzATP treatments. Compared to the THP-1 cells, variability between treatment conditions and replicates was reduced and showed greater consistency (Fig 3.4 A). However, the MV numbers were not significantly altered by the different stimulation conditions and the $P2X_7$ antagonist, added 30 minutes prior to other treatments, did not significantly alter the MV numbers. A Two-way ANOVA test was performed followed by correction for multiple comparisons (Tukey's) to test for difference between treatments; increasing the number of biological replicates by a further 2-3 tests would be optimal before making firm conclusions.

We investigated if the proportion of PS-externalised varies according to cellular treatment. Thus, MVs were incubated with the fluorescently labelled AnnexinV conjugate to detect and quantify the PS positive MVs produced as described previously. The results show considerable variability between biological replicates (Fig. 3.4 B), both for different treatments as well as in the presence of $P2X_7$ receptor inhibitor, A438079. Statistical testing showed there were no significant differences between stimuli nor between $P2X_7$ inhibition and non-inhibited conditions.

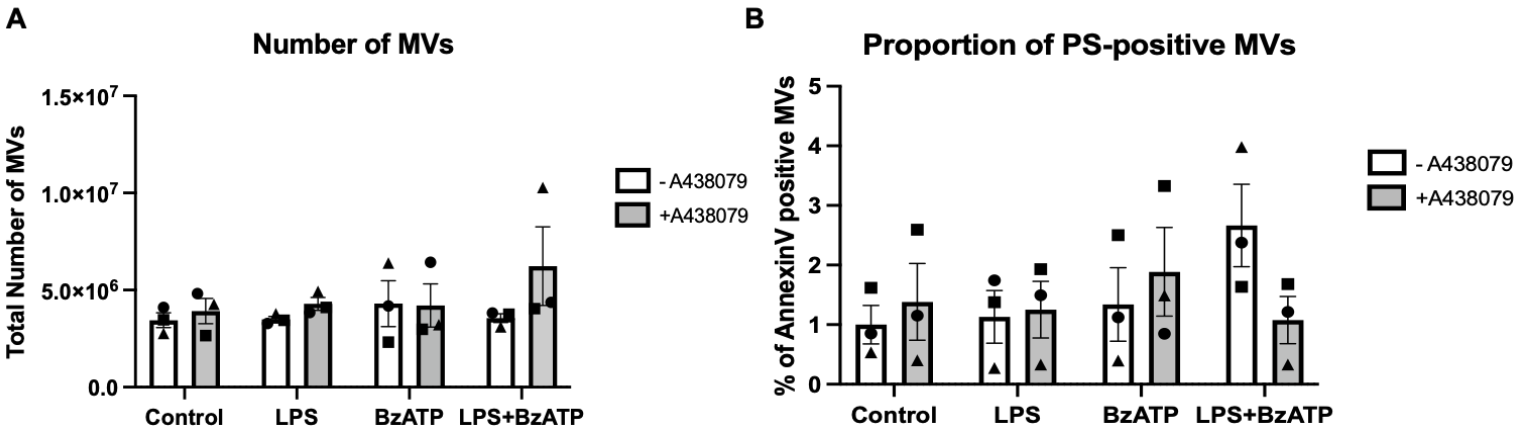

Figure 3.4: The effect of P2X7R inhibition on MV production from immortalised bone marrow-derived mouse macrophages (iBMDMs).

Macrophages were pre-treated with 2.5μM of the $P2X_7R$ selective inhibitor (A438079) for 30 min followed by treatment ± 1μg/ml LPS for 3h followed by treatment ± 300μM BzATP for 20 min (N=3). A) Flow cytometry quantification of the total number of isolated MVs. B) The proportion of phosphatidylserine positive MVs quantified by flow cytometry and represented as percentages for the four conditions. Each symbol represents an individual replicate and is consistent in all graphs. Values are presented as mean ± SEM, analysed by Two-way ANOVA with Tukey's correction for multiple comparisons test. No significant differences were detected.

Similar to the THP-1 experiments, we aimed to study the iBMDMs cell surface for the purpose of visualising cellular blebs and MV formation, characteristic of P2X7 activation, using scanning electron microscopy. Similarly to THP-1 cells, we were not able to identify noticeable differences in cellular morphology between control and following BzATP treatment, which may be a result of the fixation process (Fig. 3.5).

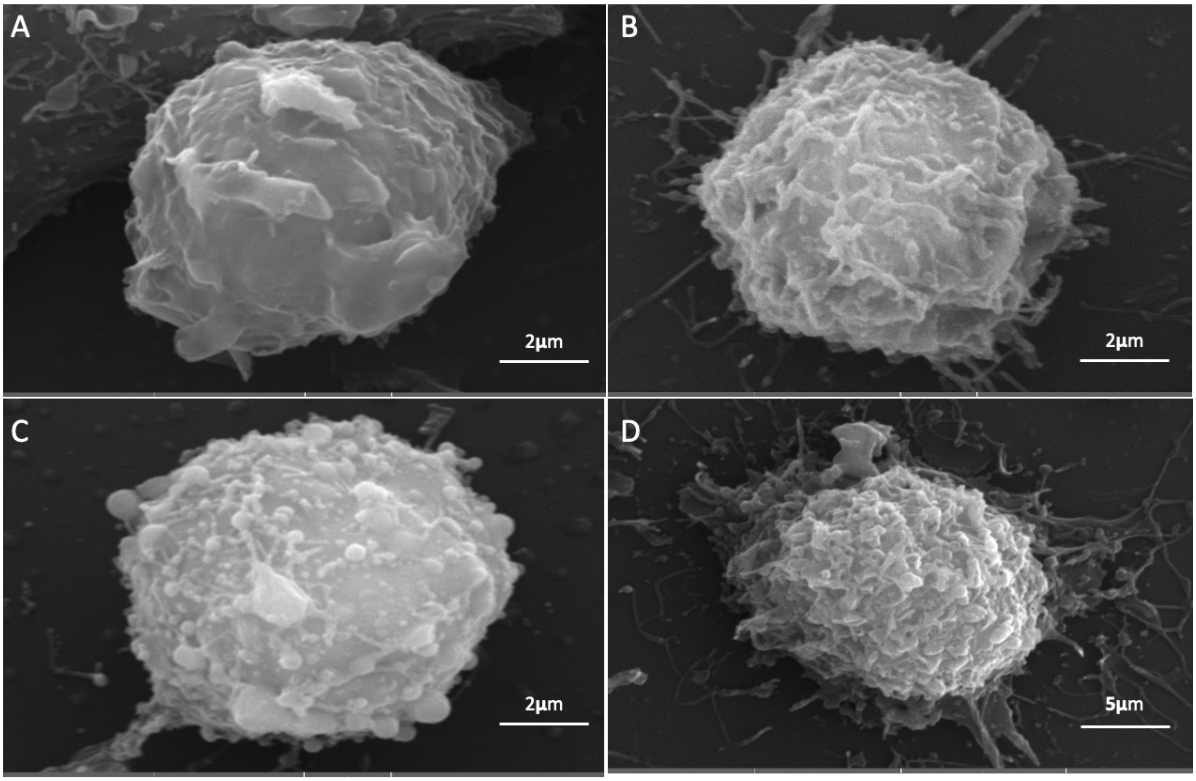

Figure 3.5: Scanning electron microscopy of control and BzATP treated iBMDMs.

Cells were stimulated with 300µM BzATP at various time points (N=1) : A) control, no BzATP; B) after 2 minutes of exposure to BzATP; C) after 5 minutes of exposure to BzATP; and D) after 10 minutes of exposure to BzATP.

3.5 IL-1β release by immortalised bone marrow derived macrophage cell line

Previously THP-1 PS-positive MVs were shown to contain IL-1β (Mackenzie et al., 2001). Since this macrophage population is a mix of PS positive and negative MVs, we wished to determine whether MVs isolated by differential centrifugation contain IL-1β and that this presents a mechanism for its release.

Initially we quantified by ELISA the IL-1β within the total supernatant and in the cell lysates to assess whether secreted and cellular levels were altered with different cell treatments (Fig. 3.6 A&B). Low but measurable concentrations of IL-1β were detected in the supernatant. These levels did not alter significantly with the different cell treatment conditions compared to control unstimulated cells. The cell lysates also contained similar concentrations of IL-1β which did not significantly increase above control for LPS treatment, although there was a small but significant decrease in the presence of BzATP (Fig. 3.6 B). This suggests that iBMDMs may have a high level of constitutive IL-1β production, where the inflammasome is not as inducible as has been reported in primary macrophages. The amounts measured of IL-1β produced and released in the cell lysate and the supernatant, respectively were highly variable between biological replicates, and the cellular response was inconsistent across the conditions tested. The presence of the $P2X_7$ antagonist did not significantly alter IL-1β production or secretion for any of the control or treatment conditions tested, suggesting production and release are not $P2X_7$-dependent.

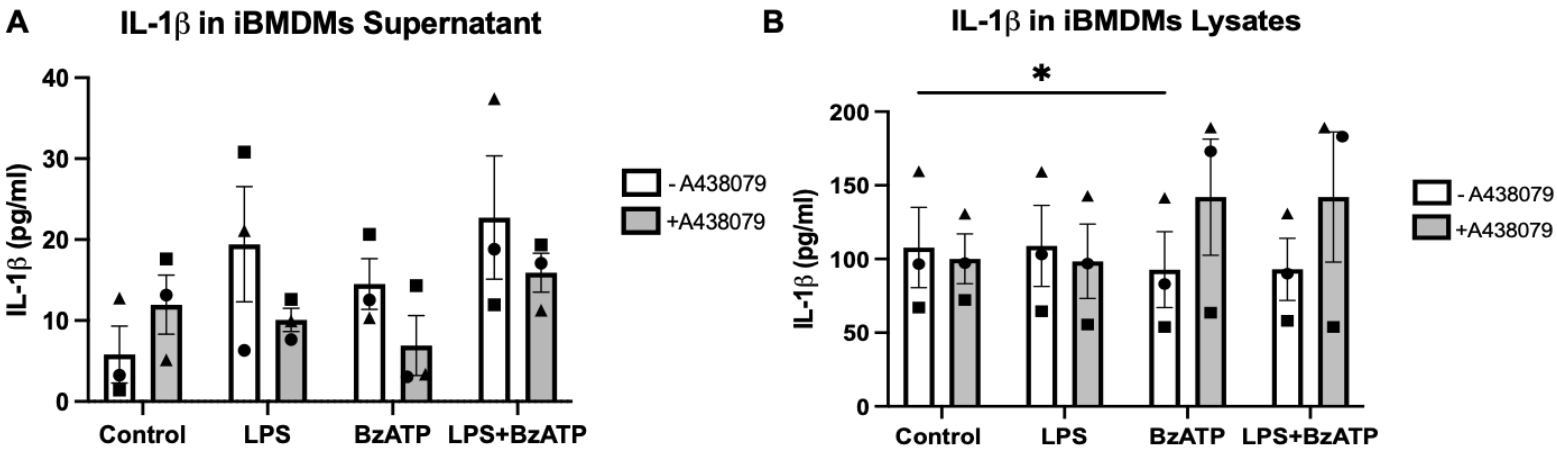

Figure 3.6: The effect of P2X7R inhibition on IL-1β release from immortalised bone marrow-derived mouse macrophages (iBMDMs).

Macrophages were pre-treated with 2.5 μM of the $P2X_7R$ selective inhibitor (A438079) for 30 min then followed by treatment ± 1 μg/ml LPS for 3 h followed by treatment ± 300 μM BzATP for 20 min (N=3). IL-1β was measured by ELISA in the supernatant (A) and cell lysate (B). Each symbol represents an individual replicate and is consistent in all graphs. Values are presented as mean ± SEM, analysed by Two-way ANOVA with Tukey's correction for multiple comparisons test. No significant differences were detected, *p=0.05.

The observations of low levels of IL-1β release were confirmed via western blot (Fig. 3.7). It showed no release of mature IL-1β (17 kDa) detected in the supernatant however, the immature form (pro-IL-1β; 31 kDa) fragment was detected in the corresponding cell lysates when cells were primed with LPS. It was also seen in the supernatant which may indicate that IL-1β was not cleaved.

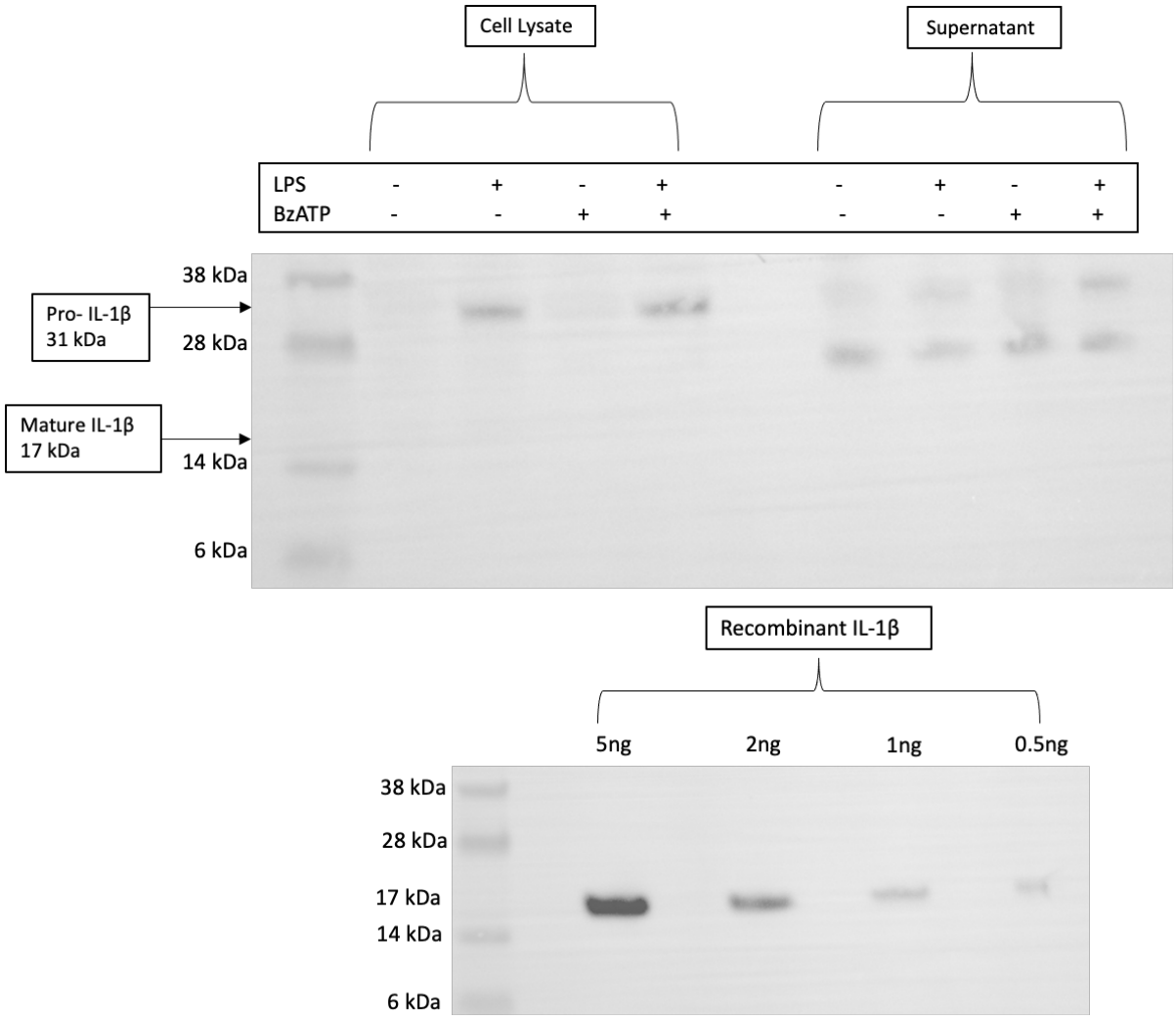

Figure 3.7: Representative western blot membrane for IL-1β.

Bone marrow-derived mouse macrophages (iBMDMs) ± priming with 1 μg/ml LPS for 3h followed by ± stimulation with 300 μM BzATP for 20 min, showing only pro-IL-1β (31 kDa) fragments expressed in the supernatant and cell lysate when primed with LPS but active IL-1β (31 kDa) was not expressed in the supernatant. Recombinant IL-1β protein was used as a positive control.

3.6 Caspase-1/Gasdermin D dependence of iBMDM IL-1β secretion and MV production

Recently, the Gasdermin-D protein has been shown to provide a conduit for IL-1β release from macrophages through pore formation in intact plasma membranes (Evavold et al., 2018). This protein requires activation, which is achieved by the caspase-1 enzyme. Since MV production by iBMDM was not significantly altered according to the stimulus, but they do release some IL-1β, we assessed whether inhibiting the caspase-1 enzyme would affect MV number or IL-1β release. As shown in Figure (3.8 A), in the presence of the caspase-1 inhibitor (Ac-YVAD-cmk) for 30 minutes prior to stimulation, the cells produced MVs but their numbers quantified were variable across the replicates and there was no statistically significant differences. We also tested whether Caspase-1 inhibition altered the proportion of MVs externalising PS molecule (Fig. 3.8B) where similar variability was observed between replicates.

In summary, this preliminarily data showed that iBMDMs cells were able to produce MVs in all the conditions tested and PS positive MVs were detected, but the numbers and proportions, appear to be irrespective of stimuli.

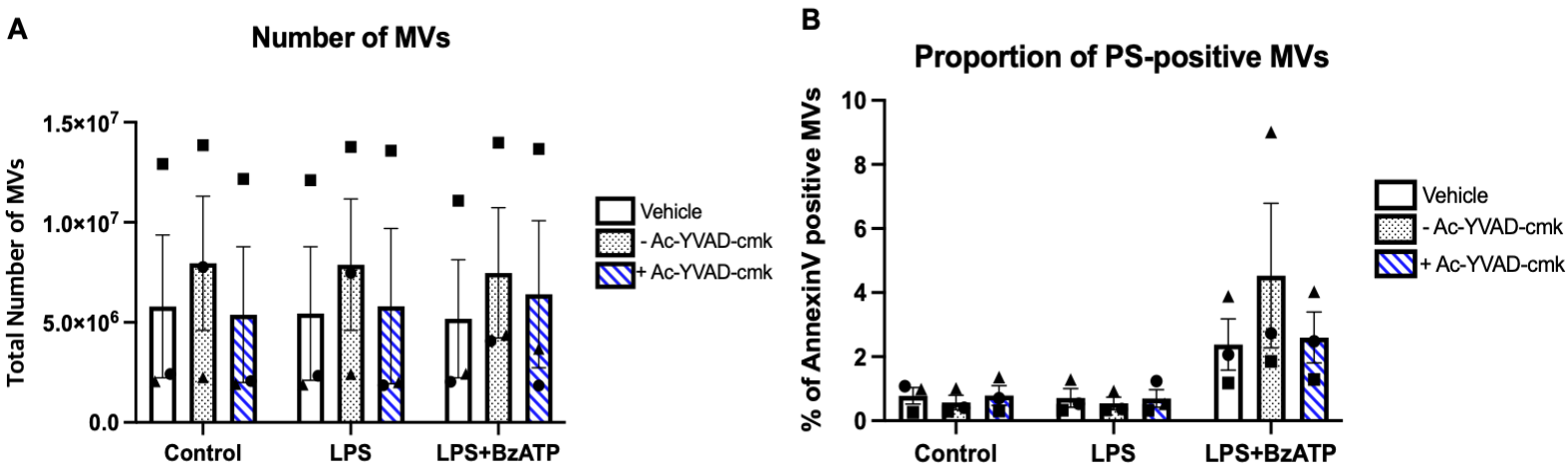

Figure 3.8: Effect of caspase-1 inhibition on MV production from iBMDMs.

Cells were pre-treated with 27µg/ml of the irreversible Caspase-1 inhibitor (Ac-YVAD-cmk) for 30 min followed by priming with 1µg/ml LPS for 3h followed by ± stimulation with 300 µM BzATP for 20 min (N=3). A) Flow cytometry quantification of the total number of isolated MVs. B) The proportion of phosphatidylserine-positive MVs quantified by flow cytometry and represented as percentages for the three conditions. Each symbol represents an individual replicate and is consistent in all graphs. Values are presented as mean ± SEM, analysed by Two-way ANOVA with Tukey's correction for multiple comparisons test. No significant differences were detected.

Investigation of whether the secretion of IL-1β detected in the MV pellets was through Gasdermin-D pore forming pathway was carried out by inhibiting the caspase enzyme. The iBMDMs were pre-treated with the caspase-1 inhibitor (Ac-YVAD-cmk) for 30 minutes or left un-treated followed by priming with either LPS alone or both LPS followed by BzATP alongside the negative control. Subsequently, the culture supernatants (Fig. 3.9 A) and their corresponding cell lysates (Fig. 3.9 C) and MV pellets (Fig. 3.9 B), were collected from parallel experiments and IL-1β levels were measured by ELISA. Very low levels of IL-1β were detected in the MV pellets irrespective of the stimuli or the presence of the caspase-1 inhibitor. However, this was only detectable in one replicate out of three and was close to the limit of detection for the ELISA assay (3.9 pg/ml). There was no IL-1β detected in the supernatant. The lysates showed detectable IL-1β from within each cell extract, although these levels are low compared to other macrophages tested (see section on human MDMs). Statistical analysis showed no significant differences between conditions (stimuli) nor between the caspase-1 inhibited and non-inhibited conditions in IL-1β levels released in the supernatant, the MV pellets or in cell lysates.

Based on several repeats, the iBMDMs were not responsive to stimuli that are known to induce IL-1β release. This could be due to the fact that cell lines do not completely mimic the primary cells and their behaviour may change with continuous culturing and when induced to become immortalised. We therefore proceeded to investigate our aims using primary cells.

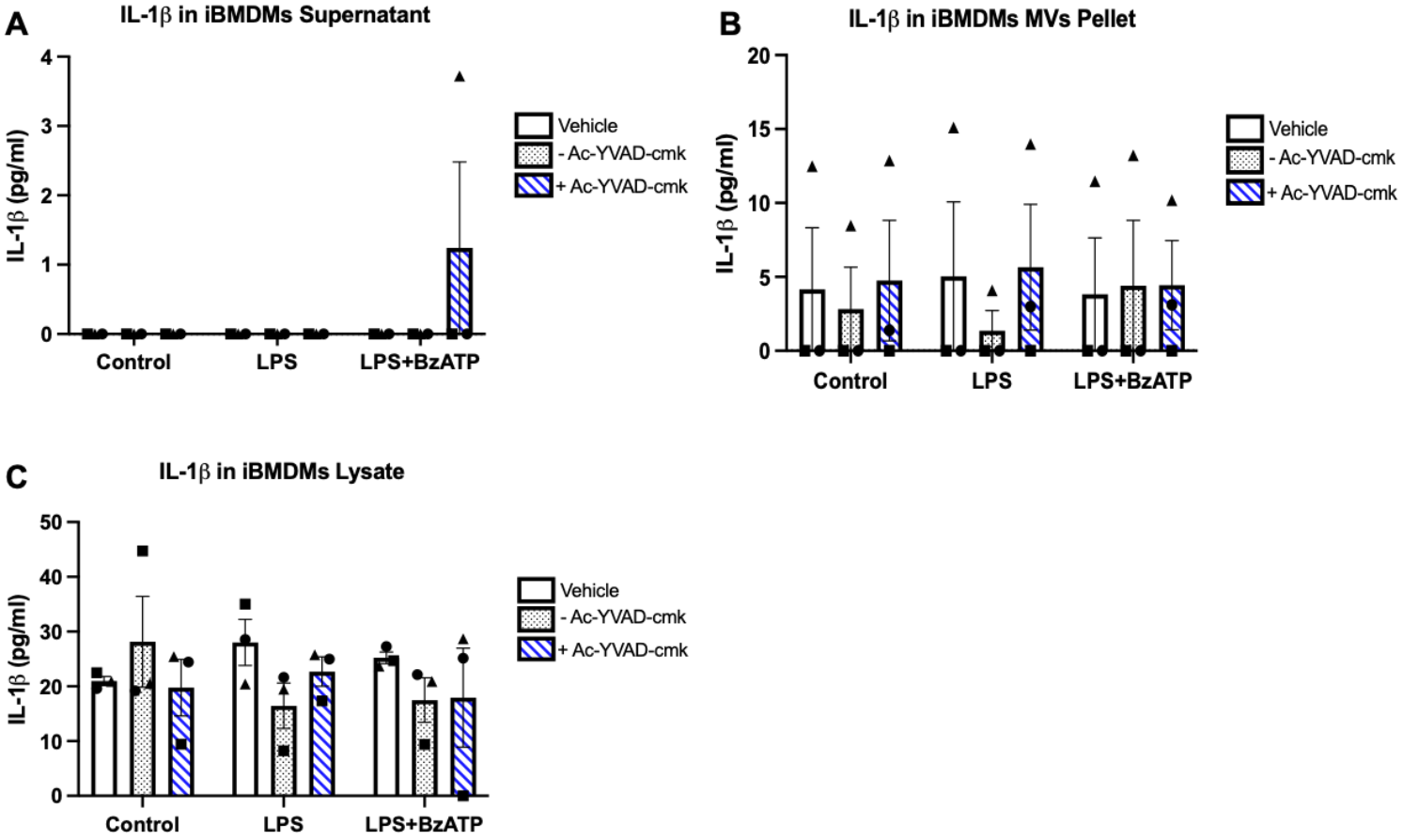

Figure 3.9: Effect of caspase-1 inhibition on IL-1β release from iBMDMs.

Cells were pre-treated with 27µg/ml of the irreversible Caspase-1 inhibitor (Ac-YVAD-cmk) for 30 min followed by priming with 1µg/ml LPS for 3h followed by ± stimulation with 300 µM BzATP for 20 min (N=3). IL-1β measured by ELISA in the supernatant (A) or in the MV pellet (B). (C) in the cell lysate. Each symbol represents an individual replicate and is consistent in all graphs. Values are presented as mean ± SEM, analysed by Two-way ANOVA with Tukey's correction for multiple comparisons test. No significant differences were detected.

3.7 Microvesicle production in primary human monocyte-derived macrophages (hMDMs)

After exploring cell lines for consistent inducible MV production and IL-β secretion in response to specific stimuli we sought to test primary macrophages. It is possible that the process of immortalisation in producing a cell line, renders these cells constitutively activated with respect to MV production and inflammatory cytokine secretion. Since we wish to understand the human biological response Human primary monocytes were isolated from healthy donors and incubated for 7 days with M-CSF in order to differentiate them into macrophages. On the seventh day, cells were unstimulated (as negative control), treated for 3 h with LPS followed by buffer or BzATP stimulation. The $P2X_7$ receptor selective antagonist, A438079 was added 30 minutes prior to any stimulation. The MVs were isolated by multiple centrifugation and counted by flow cytometry.

The results show that MVs were produced from all the stimulation conditions tested, although considerable variations were found between each donor (Fig. 3.10). Also, the $P2X_7$ antagonist did not affect the number of MVs produced under each condition. Statistical analysis showed no significant difference between the conditions tested. Interestingly, while observing the cells by transmission light under the microscope, cellular blebbing was more pronounced in the presence of BzATP treatment compared to control or LPS treated cells. This suggests that membrane blebbing requires the BzATP treatment, and fits with previously published observations where activation of the $P2X_7$ receptor triggers cytoskeletal rearrangement that leads to the formation of membrane blebs (Mackenzie et al., 2005).

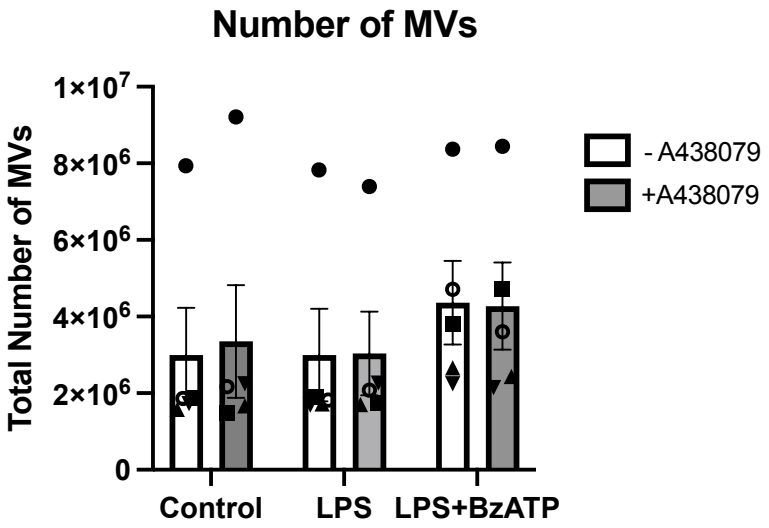

Figure 3.10: $P2X_7R$ selective inhibition effect on microvesicle production from human primary monocyte-derived macrophages (hMDMs).

Cells were exposed to the $P2X_7R$ selective inhibitor 2.5 μM (A438079) for 30 min then priming with 1 μg/ml LPS for 3 h followed by ± stimulation with 300 μM BzATP for 20 min (N=5). The figure shows flow cytometry quantification of the total number of isolated MVs. Each symbol represents a donor which correspond in upcoming graphs where $P2X_7R$ selective inhibitor was used. Values are presented as mean ± SEM, analysed by Two-way ANOVA with Tukey's correction for multiple comparisons test. No significant differences were detected.

Since we observed BzATP-dependent cell blebbing under transmission microscopy, we aimed to visualise the primary human macrophages for morphological changes and MV formation, at various time points following BzATP treatment. Cells were fixed after BzATP stimulation and imaged as shown in (Fig. 3.11). As for previous experiments using THP-1 and iBMDM cell lines, cellular blebs were not visible following this fixation and scanning microscopy processing. Since morphological changes were observed using conventional microscopy, we consider it likely that the process of cellular fixation or due to the fact that blebs are retractable once the stimuli is removed may account for these different observations which are method dependent (Verhoef et al., 2003).

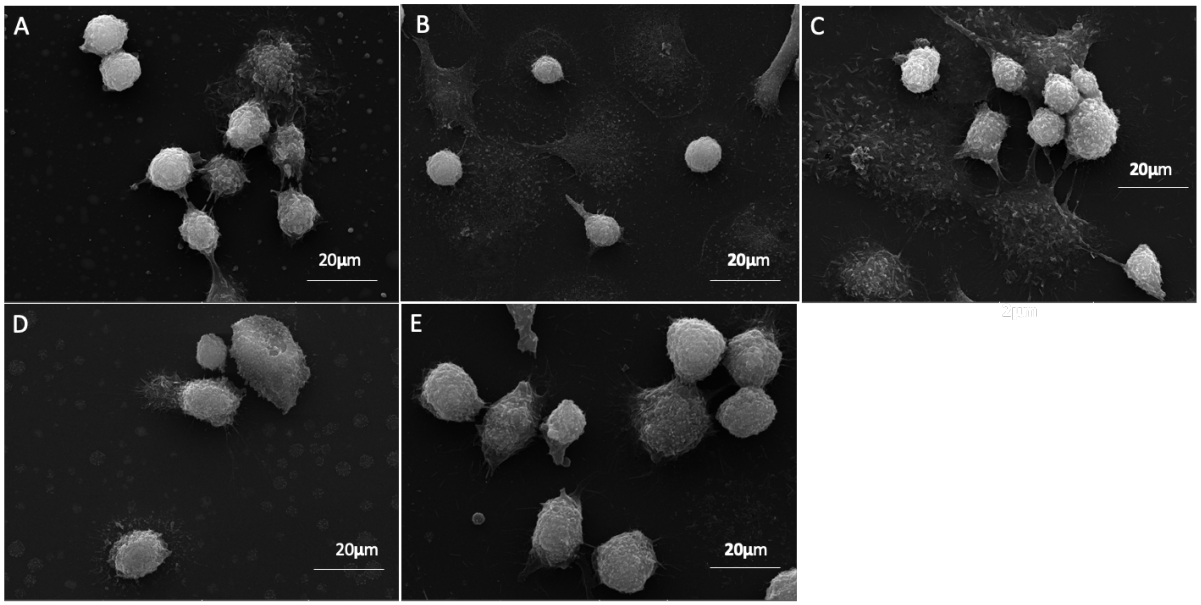

Figure 3.11: Scanning electron microscopy of human primary monocyte-derived macrophages (hMDMs).

Cells were stimulated with 300µm BzATP and fixed after 0 min (A), 2 min (B), 10 min (C), 15 min (D) and 20 min (E) exposure to BzATP, N=1.

3.8 Assessing stimulus dependence of PS-positive MV production by human MDMs

We then tested whether the PS molecule exposure on the surface of the isolated MVs from human MDMs is stimulus dependent. As previously described, MVs were labelled using Annexin V, Alexa Fluor™ 488 conjugate and the proportion of the total MV population positive for GFP fluorescence was quantified by flow cytometry. The results show that the proportion of PS positive MVs did not vary according to the different cellular treatment conditions tested including in the absence and presence of the $P2X_7$ antagonist (Fig. 3.12). There was considerable variability in the proportion of PS-positive MVs between donors. The Two-way ANOVA test has showed no significant differences between the conditions nor between the $P2X_7$ inhibited and non-inhibited conditions. A total of five donors was tested in this experiment, which given the variation among donors, may mean this test remains under-powered and further replicates would be required to confirm the preliminary conclusion that PS-exposure is independent of stimulus.

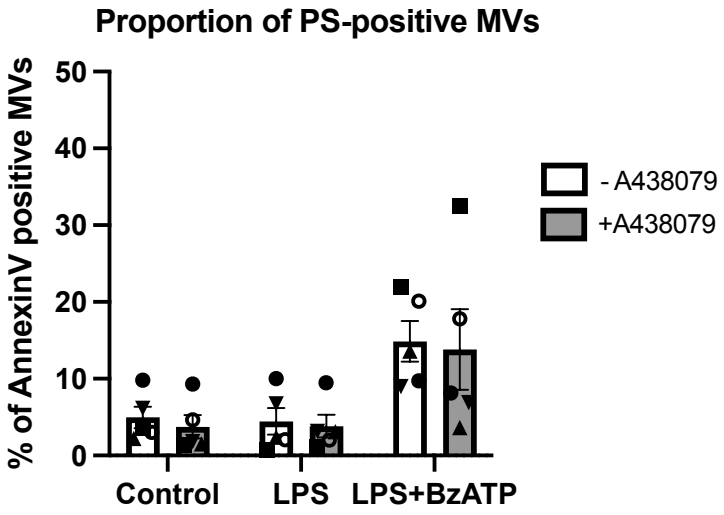

Figure 3.12: P2X$_7$R selective inhibition effect on production of PS-positive MVs from human primary monocyte-derived macrophages (hMDMs).

Cells were exposed to the P2X$_7$R selective inhibitor 2.5μM (A438079) for 30 min then primed with 1μg/ml LPS for 3 h followed by ± stimulation with 300μ M BzATP for 20 min (N=5). The figure shows the proportion of phosphatidylserine-positive MVs quantified by Flow cytometry and represented as percentages for the three conditions. Each symbol represents a donor which correspond in upcoming graphs where P2X$_7$R selective inhibitor was used. Values are presented as mean ± SEM, analysed by Two-way ANOVA with Tukey's correction for multiple comparisons test. No significant differences were detected..

3.9 Assessing Extracellular Vesicle production from human MDMs using Nanoparticle tracking

Since macrophage IL-1β secretion in MVs was described by MacKenzie et al (2001), new technologies have been developed to analyse a given population of extracellular vesicles (EVs) produced. One such technology is nanoparticle tracking analysis (ZetaView) to identify the size range of the EVs produced. We assessed the size of the MVs produced from the same conditions used previously including: untreated control, LPS-primed with or without subsequent BzATP stimulation for 20 minutes. The size distribution of MVs obtained was between 100 – 700 nm, with a shift towards overall small size of MVs i.e. below 400nm (Fig. 3.13 A,B,C), and the average median size between 120-240 nm which are classified as small sized MVs (Fig. 3.13 D). Our data of macrophage-derived MV size range is between 100-1000nm which is consistent with earlier publications in the literature (Cai et al., 2018).

These preliminary results suggest that MVs are produced by hMDMs and can be effectively isolated by differential centrifugation for detection and analysis by nanoparticle tracking. The MV population produced by hMDMs both in terms of size and PS exposure is stimulus independent and probably the focus should be on the content of these MVs rather than their numbers.

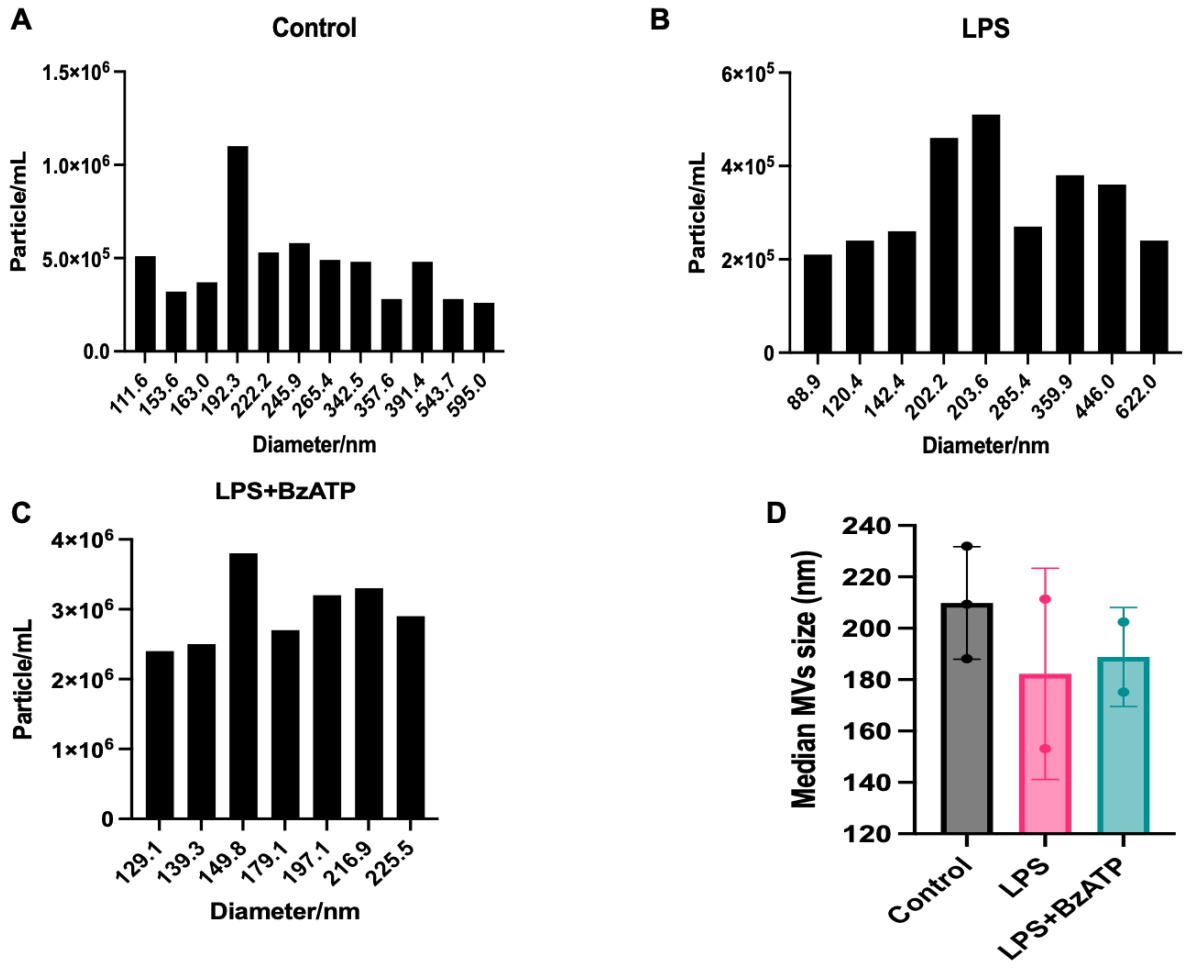

Figure 3.13: Nanoparticle tracking analysis to assess the size of extracellular vesicles isolated from human primary monocyte-derived macrophages (hMDMs).

Data shown are representative for a macrophages derived from a single donor. After priming with 1µg/ml LPS for 3h followed by stimulation with 300µM BzATP for 20min, MVs were isolated by multiple centrifugation, MVs size distribution obtained from A) control untreated cells; B) LPS-primed cells. C) LPS-primed followed by BzATP stimulation sample. D) Median MV size according to cell treatment where bars show the average from the 3 hMDMs donors, whilst each dot represents the average median MVs size per donor detected by the NTA instrument from at least two cycles per sample/condition. Values in (D) are presented as mean±SD.

3.10 hMDMs release MVs that contain IL-1β in response to LPS priming and $P2X_7$ receptor activation

After verifying that hMDMs primary cells were able to produce MVs, we proceeded to investigate the IL-1β synthesis and release in these macrophages. We measured IL-1β release in both the complete supernatant and in the MV pellet to assess the proportion of IL-1β secretion that is MV associated compared to the total released. We measured the corresponding IL-1β levels in the cell lysates to compare cellular production to release. We hypothesised that stimulating LPS-primed macrophages with BzATP will produce IL-1β containing MVs.

We compared control, LPS primed with and without subsequent BzATP treatment in hMDMs with and without 30 minutes pre-treatment with the $P2X_7$ receotor antagonist, A438079. MDMs from different human donors were run in parallel. Stimulation of LPS-primed hMDMs with BzATP showed increased IL-1β into the supernatant compared to control and LPS only treatments (Fig.3.14 A). There was considerable donor variability in the IL-1β levels. What is notable is that the levels of IL-1β were consistently increased in LPS and LPS+BzATP treated supernatants, MV pellets and lysate samples (Fig. 3.14 A,B,C). Whilst MV numbers were high in untreated and treated cells, the IL-1β production and release is inducible. The THP-1 and iBMDMs showed high baseline constitutive IL-1β production and were less inducible compared to these human MDM primary cells. Intracellular production of IL-1β was inducible and significantly increased with LPS treatment when measured in the hMDM cell lysates. The amount of IL-1β released through MVs from the LPS-primed cells without further BzATP treatment is considerable compared to the control. This might be explained by the endogenous release of ATP by the cells when exposed to DAMP signal (Sakaki et al., 2013).

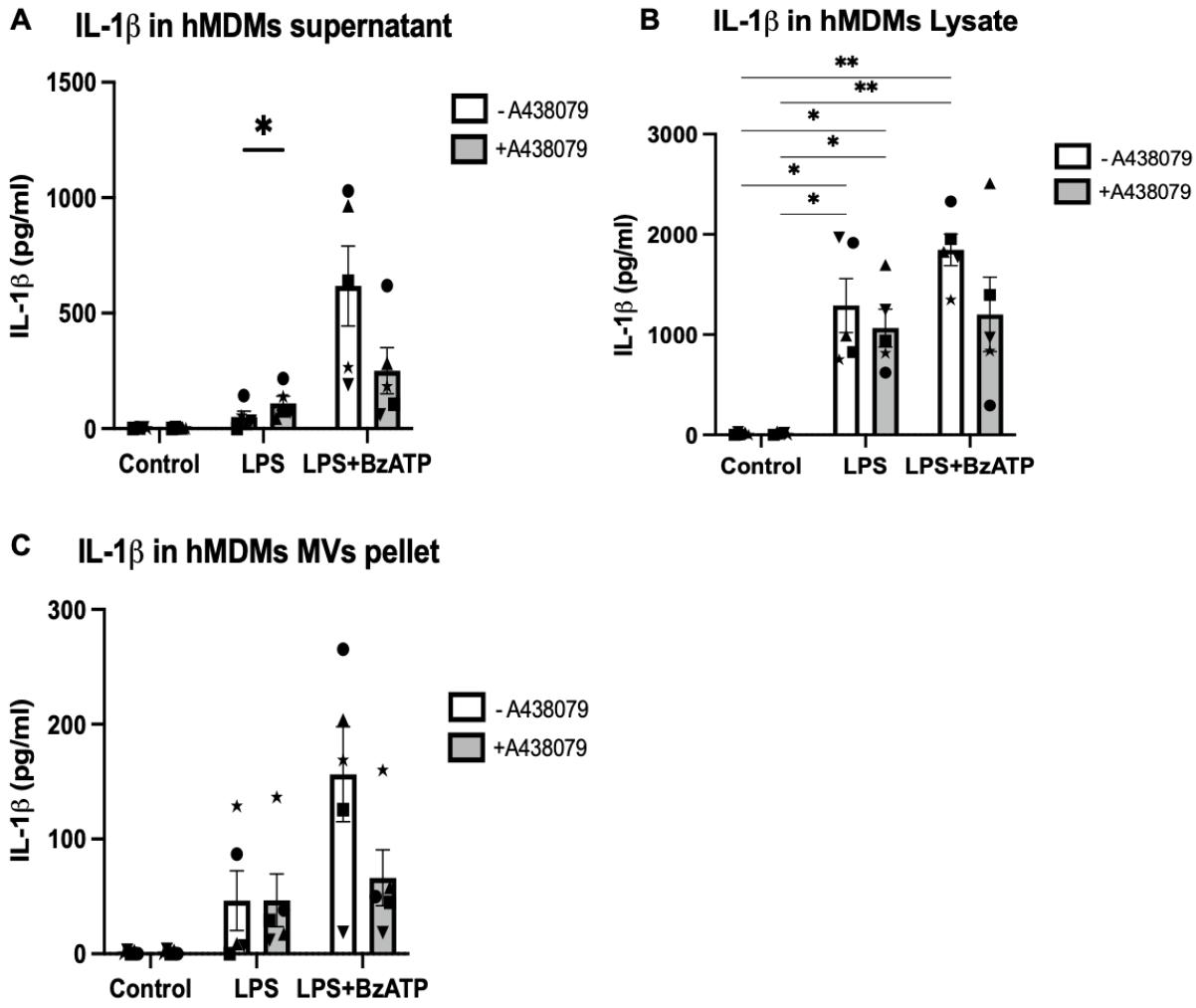

Figure 3.14: P2X$_7$R selective inhibition effect on IL-1β release from human primary monocyte-derived macrophages (hMDMs).

Cells were pre-treated with the P2X$_7$R selective inhibitor 2.5μM (A438079) for 30 minutes then priming with 1μg/ml LPS for 3h followed by ±stimulation with 300μM BzATP for 20min (N=5). IL-1β was measured by ELISA. A) The released IL-1β in the supernatant. B) The IL-1β concentrations in the cell lysate. C) MVs pellet isolated by multiple centrifugation to quantify the released IL-1β. Each symbol represents a donor which correspond in previous graphs where P2X$_7$R selective inhibitor was used. Values are presented as mean ± SEM, analysed by Two-way ANOVA with Tukey's correction for multiple comparisons test. No significant differences were detected, ns or *p<0.05 or **p<0.005.

In the presence of the $P2X_7$ antagonist, A438079, there was variable hMDM IL-1β production and release. The bars shown in Fig. 3.14 show that the average levels were generally lower for LPS/LPS+BzATP treated cells, supernatant and MV pellet in the presence of A438079 (except LPS only on supernatant levels, which were higher in its presence) (Fig. 3.14 A,C). However, these changes were not statistically significantly different from in the absence of the $P2X_7$ receptor antagonist. This may be due to the donor variability meaning that a higher replicate number is required to identify a true $P2X_7$ receptor dependence, or that some, or all, of the production and secretion is independent of $P2X_7$ receptor activation.

Comparing levels of IL-1β between hMDM supernatants, MV pellets and lysate samples there were approximately 4-fold higher concentrations of IL-1β in the total supernatants (average of 750 pg/ml) compared the MV pellet (average of 170 pg/ml). MV pellets were resuspended in the same volume as the supernatant samples, so the concentrations were proportionally comparable. These preliminarily data suggest that MV release is a pathway for IL-1β secretion, but much of the IL-1β released into the supernatant is not associated with MVs that were isolated using differential centrifugation methods, and may represent free, non-MV associated IL-1β.

IL-1β is produced in an inactive 31kDa precursor; it requires processing by the caspase-1 enzyme in order to cleave it to its active form. Commercial ELISA kits do not distinguish between pro-IL-1β and active IL-1β. In order to investigate whether the released IL-1β detected by ELISA was the cleaved and active form, western blot was carried out to analyse MV pellets, culture supernatants and the corresponding cell lysates (Fig. 3.15). Recombinant active IL-1β was used as a positive control, visible in the 2 left lanes loaded with samples. No detectable IL-1β band was visible in the MV pellet samples with or without stimulation. This may be due to lower concentrations of IL-1β secreted in the MV pellets (as measured by ELISA, see above). The total hMDM supernatant from LPS-primed and BzATP treated cells, showed 17 kDa active IL-1β, which was not detected in the absence of LPS/BzATP, showing inducible production of active IL-1β. In the corresponding cell lysates, IL-1β was detected at 31 kDa i.e. pro-IL-1β in the cell fraction. The band was visibly much larger and denser for LPS/BzATP treated hMDMs compared to untreated control cell lysates, again showing induction of IL-1β production.

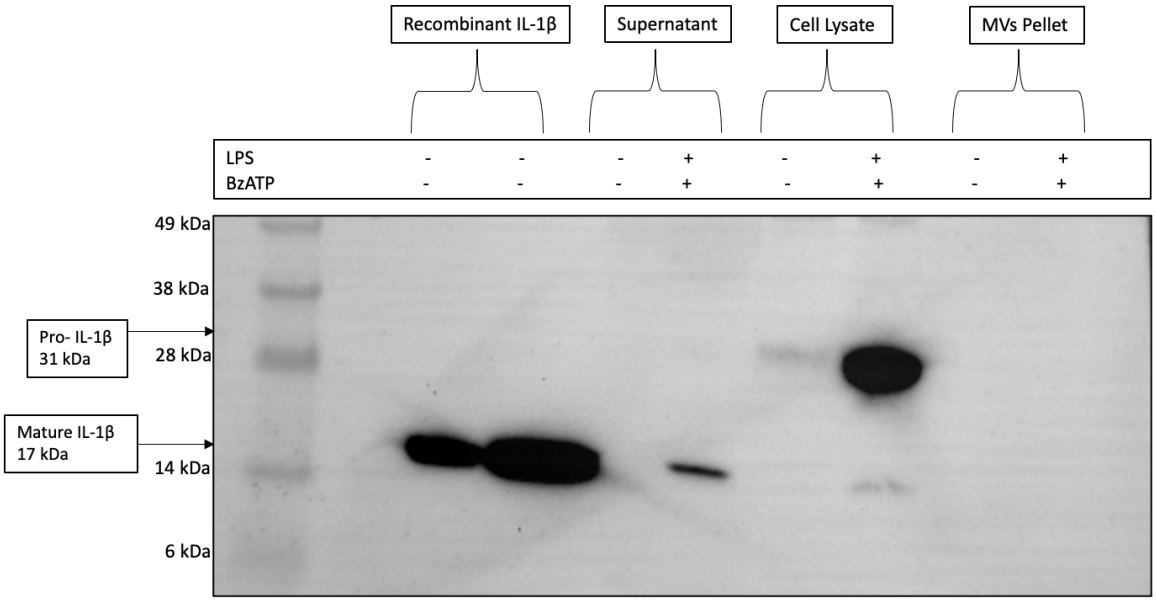

Figure 3.15: Western blotting to IL-1β from control and LPS/BzATP treated human primary monocyte-derived macrophages (hMDMs).

Supernatant, cell lysates and MVs were collected from human MDMs without (-) and with (+) 1μg/ml LPS 3h and 300μM BzATP for 20min treatment. Pro-IL-1β is 31 kDa and mature IL-1β is 17 kDa indicated to the left. Recombinant IL-1β protein was used as a positive control (left lane) loaded at 1.6 ng.

3.11 Effect of Caspase-1/Gasdemin-D inhibition on MV production and IL-1β release in human MDMs

Gasdermin-D has been shown to provide a conduit for IL-1β release from macrophages through pore formation in intact plasma membranes, via activation of the caspase-1 enzyme (Evavold et al., 2018). hMDM MV numbers were not significantly altered according to the stimulus. These cells do release IL-1β, some of which is MV-associated and a larger proportion is not MV-associated. The release of non-MV associated IL-1β may be dependent on the Gasdermin-D pore formation pathway. We therefore assessed whether inhibiting the caspase-1 enzyme, which inhibits the Gasdermin-D pore formation, would affect the number of MVs released or IL-1β released from hMDMs.

The hMDMs were pre-treated with the caspase-1 inhibitor (Ac-YVAD-cmk) for 30 minutes or left untreated followed by priming with either LPS alone or both LPS followed by BzATP alongside the negative control. The caspase-1 inhibition did not significantly alter the number of MVs produced (Fig. 3.16 A) or the proportion of PS-positive MVs under any of the treatment conditions (Fig. 3.16 B). These data suggest that caspase-1 /Gasdermin-D inhibition did not interfere with the MV production.

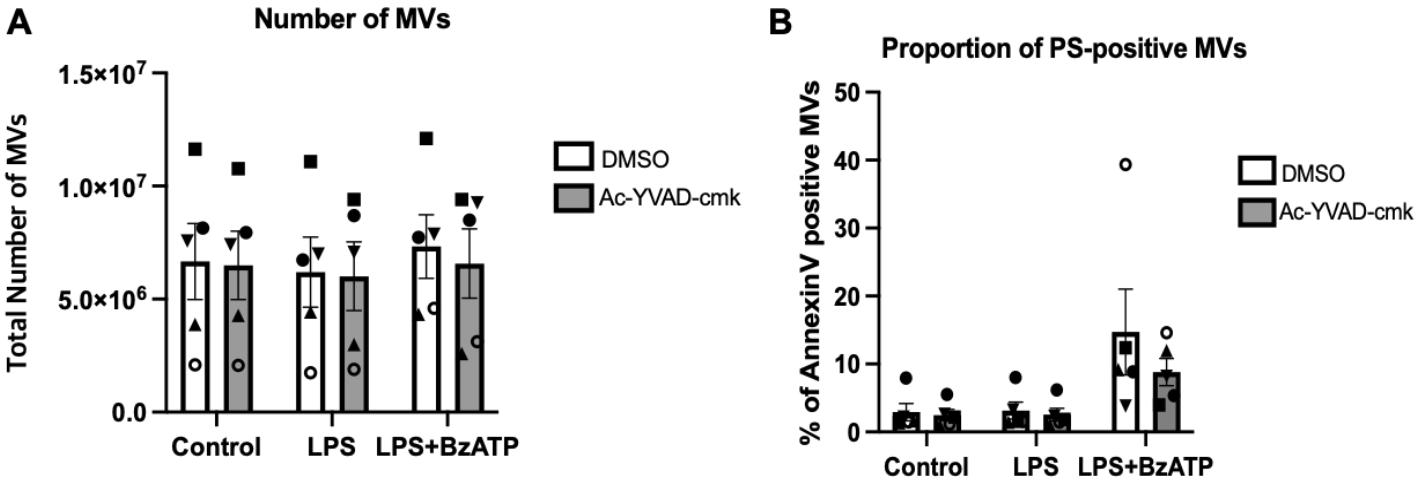

Figure 3.16: Caspase-1 inhibition effect on microvesicle production from human primary monocyte-derived macrophages (hMDMs).

Cells were pre-treated with the Caspase-1 irreversible inhibitor 27µg/ml (Ac-YVAD-cmk) for 30 minutes then priming with 1µg/ml LPS for 3h followed by ±stimulation with 300µM BzATP for 20min (N=5). A) Flow cytometry quantification of the total number of isolated MVs by multiple centrifugation. B) The proportion of phosphatidylserine-positive MVs quantified by flow cytometry and represented as percentages for the three conditions. Each symbol represents a donor which correspond in upcoming graphs where caspase-1 (Ac-YVAD-cml) inhibitor was used. Values are presented as mean ± SEM, analysed by Two-way ANOVA with Tukey's correction for multiple comparisons test. No significant differences were detected.

Human MDM supernatants, MV pellets, and cell lysates were collected from cells treated in the absence and presence of the caspase-1 inhibitor ± LPS/BzATP and IL-1β levels were measured by ELISA. The IL-1β measurements obtained from the culture supernatant and MV pellets were markedly variable between each donor, likely due to donor heterogeneity. The caspase-1 enzyme inhibition had no effect on IL-1β secretion in the supernatant nor in the MV pellets obtained and Two-Way ANOVA analysis showed no significant difference (Fig. 3.17 A&C). The cell lysates corresponding to the supernatants and MV pellets was tested for IL-1β levels to further assess if caspase-1 inhibition affects cellular IL-1β production. Caspase-1 inhibition resulted in a reduction in the mean levels of IL-1β in hMDM cell lysates suggesting an inhibition of IL-1β synthesis. However, statistical analysis did not show any significant differences, potentially due to low number of donors tested (N=5). These preliminarily findings suggest that IL-1β release is not predominantly mediated by gasdermin-D and other routes for IL-1β are involved including MV release.

These data suggest the MVs released from hMDMs contain IL-1β, and that MV release is indeed a conduit for IL-1β secretion as suggested in the literature previously (Mackenzie et al., 2001). In addition, the hMDMs provide a suitable *in-vitro* cell model to produce and isolate IL-1β-containing MVs to proceed with the investigation of how MVs target cells and deliver IL-1β (chapter 5). The human primary macrophages also serve as a suitable model to study IL-1β production and release.

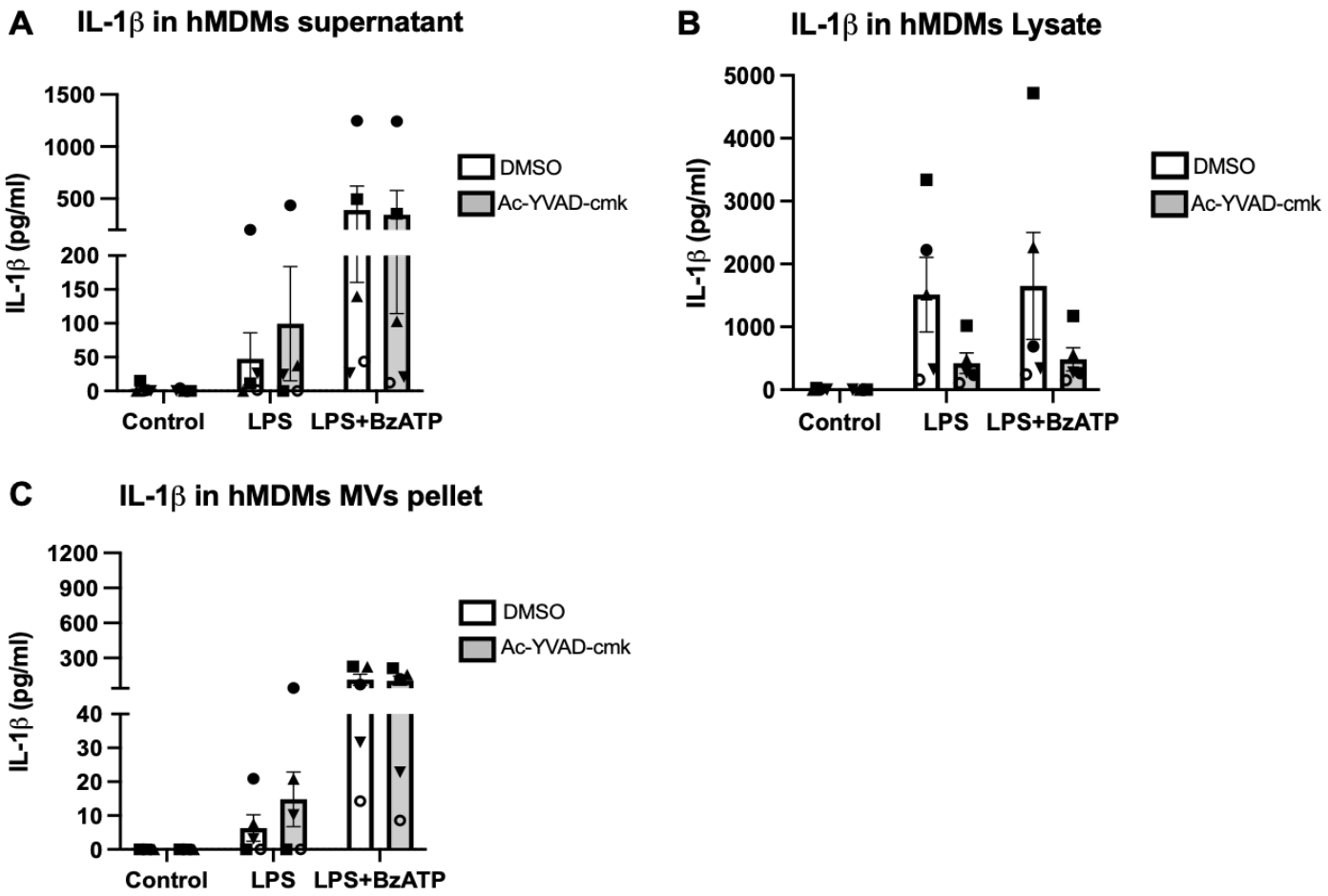

Figure 3.17: Caspase-1 inhibition effect on IL-1β release from human primary monocyte-derived macrophages (hMDMs).

Cells were pre-treated with the Caspase-1 irreversible inhibitor 27µg/ml (Ac-YVAD-cmk) for 30 minutes then priming with 1µg/ml LPS for 3h followed by ±stimulation with 300µM BzATP for 20min (N=5). IL-1β was measured by ELISA. A) The released IL-1β in the supernatant. B) The IL-1β concentrations in the corresponding cell lysate. C) MVs pellet isolated by multiple centrifugation to quantify the released IL-1β. Each symbol represents a donor which correspond in previous graphs where caspase-1 (Ac-YVAD-cmk) inhibitor was used. Values are presented as mean ± SEM, analysed by Two-way ANOVA with Tukey's correction for multiple comparisons test. No significant differences were detected.

3.12 Discussion

It is well appreciated that MVs are released from various cell types and under both physiological and pathological states and their production may be a regulated mechanism functioning in inter-cellular communication. Microvesicles have been implicated in several diseases, and in particular in cardiovascular diseases such as atherosclerosis (Shantsila et al., 2010).

In the present study, we have demonstrated that MVs were produced from various cell sources including human primary macrophages and the two cell lines; THP-1 and immortalised mouse BMDMs, under multiple in vitro treatment conditions. Variability in the number of MVs produced in both primary and cell line macrophages was pronounced between each replicate (experiment). In addition, the numbers of MVs that were released seems to be stimulus-independent i.e. MVs were produced even under the basal control condition. This can be due to several possible explanations such as the fact that MVs are produced in both physiological and pathological states. Firstly, the number of MVs released may not be an indication of the cell state but rather the content of these MVs released as they function to transfer information to neighbouring cells. The second possible explanation might be that endogenously released ATP that has acted through $P2X_7$ receptors induces MVs production. Macrophages when under stress tend to release ATP as 'danger signal' in inflammatory states to initiate the innate immune response. Studies have shown there is a link between Toll-like receptors (TLR) associated signalling and ATP release in macrophages, particularly LPS-primed macrophages i.e. TLR-4 associated signalling (Ren et al., 2014, Dosch et al., 2019). The ATP released extracellularly may activate purinergic receptors in an autocrine or paracrine manner leading to MVs production. A third possible explanation is the involvement of other purinergic receptors -that haven't been studied yet- in the shedding of MVs. Release of IL-1β containing MVs via $P2X_7$ receptor activation by ATP in macrophages has been extensively studied (Pizzirani et al., 2007, Bianco et al., 2005, MacKenzie et al., 2001). Therefore, we attempted to inhibit $P2X_7$ receptor activation but this had no effect on MV production or release leading us to a fourth possible explanation - the involvement of other pathways. A study has shown that cytokine stimulation leads to MV shedding in a microglial cell line (Colombo et al., 2018). MVs are present in body fluids and circulate

in the blood of healthy individuals, denoting that cells are capable of producing MVs even in the absence of any pathogen or inflammatory stimulus (Ratajczak et al., 2006). Ultimately, the release of MVs by un-stimulated cells is a general feature of macrophages also, suggesting that MV shedding is an intrinsic and constitutively active mechanism used in intercellular communication.

Cell blebbing is a feature of cellular activation in response to chemical or mechanical stimuli. They are spherical protrusions formed when the cytoskeleton cleaved and plasma membrane is protruded by pressure outward (Charras and Paluch, 2008, Norman et al., 2010). Extensive cellular blebbing has been seen within 30-90 seconds after cells stimulated with ATP, preceding MV shedding (Mackenzie et al., 2001). The fact that cell blebs are retractable (Norman et al., 2010) may explain the absence of blebs when we sought to capture them under scanning electron microscopy. Also, the fixation procedure or reagents used may led to their retraction or inability to be detected. If time had allowed, we would have imaged cells under live light microscopy to record and capture the induction of cellular blebbing produced by BzATP stimulation that was observed during these experiments. The reason we chose scanning electron microscopy was to attempt to capture cells undergoing MV production as well as blebbing. This was shown in MacKenzie et al. (2001), but these were P2X7 overexpressing HEK293T cells, and not macrophages used in our investigations.

The MVs produced in this study were heterogenous in terms of exposing PS molecules on their surface; some MVs produced were lacked the PS molecule as they were not labelled by Annexin V-Alexa Fluor-488. This suggests that macrophages indeed produce heterogeneous populations of MVs, the majority of which were PS-negative. The MacKenzie et al. (2001) study showing IL-1β is contained in MVs used annexin V-bead pull-down methods to isolate MVs, hence the population of MVs was selective and not representative of the overall population of MVs produced by macrophages, compared to our investigation where the total MV population was isolated by differential centrifugation. The presence of PS-negative MVs from some macrophages and platelets was identified in other studies (Bernimoulin et al., 2009, Connor et al., 2010). The detection of MVs lacking PS could result from different experimental procedures such as MV collection or storage, presence of proteins that interact with PS, fusion with other vesicles, MV labelling techniques, or due to sub-threshold flow cytometry detection. Traditionally PS-exposure has been shown to be a characteristic

hallmark of apoptosis. One study found that following apoptosis in endothelial cells there was an increased proportion of annexin-V positive MVs compared to control non-apoptotic cellular MVs (Jimenez et al., 2003). In this study we used relatively short LPS and BzATP treatments (3h and 20 min, respectively), which have previously been shown not to induce cell death in other cell-types, such as HEK293Ts (MacKenzie et al., 2001) and human monocytes (Ward et al., 2010). The PS-negative macrophage-derived MVs lacking surface PS in our results, is the first report to show this in human macrophages. The results we obtained showed externalisation of PS was not affected by the stimulation conditions and non-stimulated cells have also produced PS positive MVs. However, a study demonstrated that the longer the incubation of cells with LPS, the more PS positive MVs generated (Lee et al., 2017), which may be associated with apoptosis induction over longer incubation times.

Cell lines such as THP-1 have been widely used as an *in vitro* model mimicking human monocytes to generate MVs and has succeeded to resemble primary monocytes and macrophages when treated to differentiate. From our data, we noticed the cell line MV response was not consistent and highly variable throughout the study. The pattern of cellular vesiculation as well as the IL-1β release were variable and inconsistent. This appeared to be altered between each passage of both cell lines; THP-1 and the murine iBMDMs, although further studies would be required to validate this idea based on observations. It can be due to local environmental changes such as CO_2 levels, temperature changes. These changes in the cell lines sensitivity and their response to stimuli are anticipated as those cells were cultured in an artificial nature mimicking the human body's environment. Although, the use of the THP-1 cell line has several advantages over the use of primary cells, the most significant of these is that THP-1 cells have the same genetic background compared to primary cells taken from blood of human volunteers. Primary human monocytes may have been exposed to varying inflammatory stimuli or pathogens prior to isolation and are more difficult to access or to obtain in large numbers (Schildberger et al., 2013). The primary macrophages have also showed inter-individual variability likely due to genetic variation, age, gender and inflammatory or pathogen background. In the case of human MDMs, it is possible that increasing the number of experimental replicates and/or donors would lower the variation and may have revealed some statistically significant differences. In this study, however, the cell line MV numbers and IL-1β secretion responses do not mimic

primary cells and were in fact more variable and inconsistent. For this reason we decided to use primary macrophages.

Established cell lines derived from mice have not been used frequently in the literature as a model for MV generation, unlike human cell lines such as THP-1. Researchers have successfully generated and studied MVs from mouse derived macrophages; for instance, RAW 264.7 murine macrophage cell line used to test the MV production by this cell line under different stimuli such as LPS and Poly (I:C), a TLR3 ligand, and CpG oligonucleotide, TLR9 ligand (Gauley and Pisetsky, 2010). We also have effectively induced murine macrophages to produce MVs suggesting that MVs play important roles in inflammation and that macrophages are primary mediators in innate immunity. Although, researchers used the immortalized mouse BMDMs stimulated with LPS to measure secreted IL-1β, these studies did not measure MV production (England et al., 2014).

Several lines of study have shown that MVs are considered as an important mechanism to package and deliver IL-1β to target cells. The mechanism of IL-1β production after stimulation of monocytes/macrophages with LPS and BzATP was sufficiently evident in the literature. Although, how IL-1β production is linked to the number of MVs produced and whether changing the type of stimulus will affect the IL-1β production has not been reported. More recent investigations on IL-1β secretion from macrophages have focused on the Gasdermin-D pore formation pathway, while the role of MVs as a route of secretion and delivery of IL-1β has not been documented in primary macrophages. Several reports suggest that MVs act to deliver packaged IL-1β through, speculating that this is via vesicle fusion with the target cell membrane, or through ligand-receptor interaction. However, the mechanism of IL-1β delivery from MVs has not been specifically demonstrated and still requires further investigation.

Chapter 4 . Cell type and stimulus dependent differential expression of the MerTK phosphatidylserine receptor target in relation to the atherosclerotic plaque

4.1 Background and Rationale

Atherosclerosis is a chronic inflammatory disease involving multiple cell types, cytokines, and chemokines that participate in the pathophysiology of the disease initiation and progression. Each of the cell types presented in the atherosclerotic plaque can express and secrete diverse groups of cytokines and chemokines, as well as responding to them. Key cell types that are involved in atherosclerosis pathogenicity will be focused on in this chapter, specifically: monocytes, macrophages, endothelial cells, and smooth muscle cells.

Monocytes/macrophages contribute throughout the different stages of atherosclerotic disease. Their role starts when blood-borne monocytes are recruited via activated endothelial cells promoting their entry into the subendothelial space where they subsequently differentiate into macrophages. Following that macrophages form foam via phagocytosis of oxLDL. The accumulation of internalised macrophage lipid is key to plaque progression. When lipid processing is overwhelmed, macrophages undergo necrosis resulting in the “necrotic core” of the plaque. Macrophages release cytokines and growth factors, in turn exerting multiple effects on other cells in the plaque. Since macrophages have been shown previously to release the early pro-inflammatory cytokine IL-1β within PS-positive MVs, we propose that targeting of IL-1β may occur via the MerTK phosphatidylserine receptor. To understand which cells within the atherosclerotic plaque may be a target for PS-positive MVs, we aimed to determine the relative gene expression of the MerTK receptor on a variety of atherosclerotic plaque cells.

Endothelial cells are one of the main cells participating in the early stages of atherosclerosis. The primary step initiating atherogenesis and propagating plaque progression beyond, is endothelial dysfunction/activation (Lusis, 2000). Endothelial dysfunction/activation occurs as a result of disturbed blood flow, injury, inflammation

from infection, nicotine, increased circulating glucose and lipid. Endothelial activation leads to: 1) increased vascular permeability thus, lipid retention and accumulation in the intima, 2) enhanced endothelial cell expression of adhesion molecules increasing immune cell (including monocyte) recruitment, 3) endothelial cell secretion of chemokines and cytokines activating circulating monocytes and T-cells, as well as sub-endothelial plaque vascular smooth muscle cells, macrophages/foam cells and T-cells (Lusis, 2000). Macrophages contribute to maintaining endothelial cell inflammatory activation by secreting a number of cytokines including interleukins, and tumour necrosis factor (TNF).

Vascular smooth muscle cells (VSMCs) are also one of the main cells present in the plaque at all stages. They promote plaque growth and contribute to plaque remodelling and stabilization as well as fibrous cap formation (Basatemur et al., 2019). Macrophages exert multiple effects on VSMCs leading to their proliferation and migration. For instance, macrophage release a potent chemotactic and growth regulatory molecule called platelet-derived growth factor (PDGF) contributing to SMCs migration and proliferation (Ross et al., 1990). In addition, macrophage affect their production of collagen via releasing extracellular matrix metalloproteinases (MMPs), and it also promotes SMCs apoptosis in late atherosclerotic stages via several mechanisms (Bennett et al., 2016, Boyle et al., 2002).

Considerable evidence has emerged indicating that bacterial or viral infections contribute to triggering myocardial infarction and stroke. Observations from many studies have linked respiratory tract infections with increased risk of myocardial infarction. It is thought that the inflammatory response caused by the infection may act to destabilise the atherosclerotic plaque, leading to increased chance of rupture (Ward et al., 2009). Interestingly, studies have shown that respiratory infections enhanced atherosclerosis progression and was dependent upon the activation of TLR4 receptors via the ligand LPS (Vink et al., 2002). The cells involved in maintaining lung homeostasis and serve as physical barrier against inhaled pathogens and toxins, are lung epithelial cells and alveolar macrophages. Both of these cell types are capable of producing and secreting a plethora of inflammatory and immune cells mediators into the circulation that may contribute to worsening atherosclerotic plaque and weakening the plaque cap structure making it more vulnerable to rupture. We therefore included

these cells to assess MerTK gene expression as they may serve as a target for circulatory MVs loaded with cytokines.

Hypothesis: The phosphatidylserine receptor, MerTK, is expressed on cells that are targets for cytokine-containing PS-positive microvesicles. Expression of MerTK is altered under pro-inflammatory and atherosclerosis-promoting conditions.

Aim 1: assess the relative gene expression of MerTK receptor in the cells that participate in atherosclerosis including endothelial cells, macrophages, and vascular smooth muscle cells (illustrated in Figure 4.1). To compare relative expression of MerTK in cell lines to be used to investigate whether the MerTK receptor is targeted by MVs containing IL-1β (chapter 5).

Aim 2: determine whether MerTK receptor gene expression is regulated in these cells under different stimuli that are present in the atherosclerotic plaque.

We have compared MerTK expression in a variety of cell extracts using qPCR and have used published datasets to analyse and investigate the MerTK receptor gene expression in different cell-types under a variety of conditions in order to test the above hypothesis.

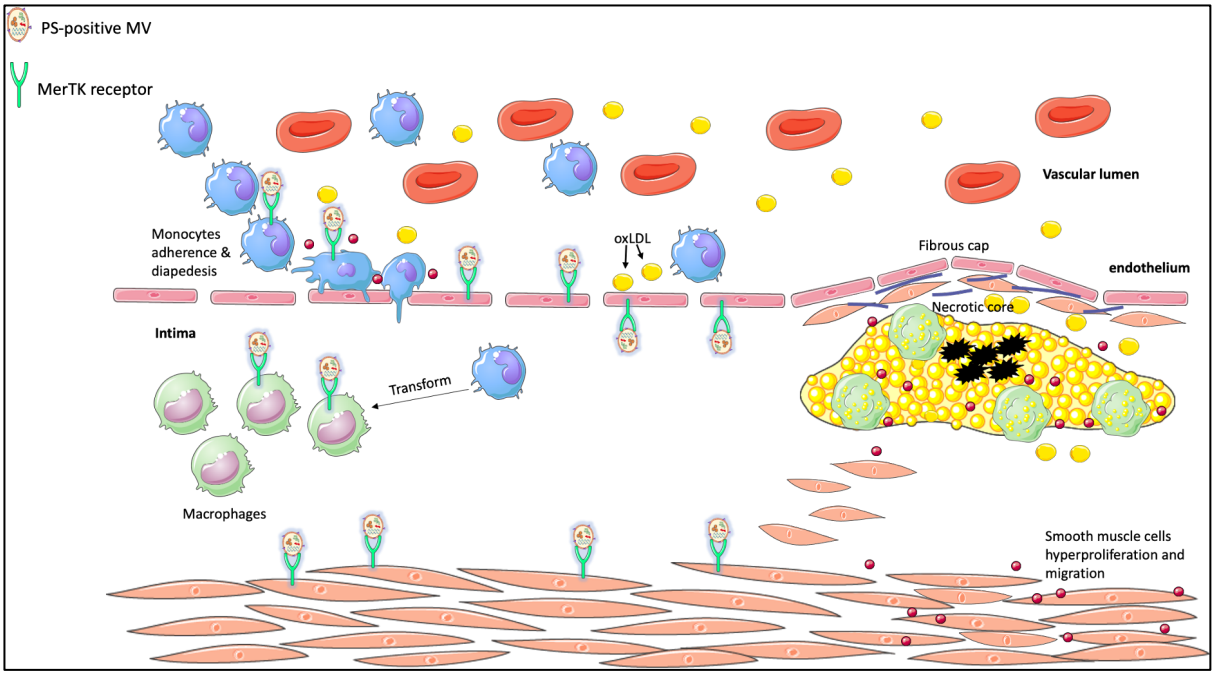

Figure 4.1: Potential macrophage-derived microvesicle MerTK receptor targets in the atherosclerotic plaque.

This schematic illustrates our hypothesis of how PS-positive macrophage-derived MVs are targeted to MerTK receptors on cells present in the atherosclerotic plaque including monocytes, endothelial cells, macrophages, and vascular smooth muscle cells.

4.2 Endogenous MerTK receptor expression in human cells

MerTK receptor gene has been reported to be expressed in a variety of tissues and organs but mainly in myeloid immune cells, such as monocyte and macrophage. We sought to explore the MerTK mRNA expression using the Human Protein Atlas dataset (https://www.proteinatlas.org/ENSG00000153208-MERTK/celltype). For single cell RNA from all cell types, we chose to report the consensus normalised expression; NX, which is the normalised mRNA expression levels obtained from three different datasets. The first dataset is the Human Protein Atlas (HPA), the second is the Genotype-Tissue Expression (GTEx), an online portal for tissue-specific gene expression and regulation, lastly we accessed the Functional Annotation of Mammalian Genome (FANTOM5) Atlas.

Specific data has been extracted to compare mRNA expression of MerTK receptor in different cells and tissues related to atherosclerosis. We focused on cells that participate largely in atherosclerosis development i.e. monocyte, macrophage, endothelial cell, smooth muscle cell, as well as alveolar macrophages, responsive to inhaled pathogens. The MerTK expression is reported here as the mean from cell types across various tissues (see Fig. 4.2). The data revealed all of these cells do express MerTK receptor with the highest expression in alveolar macrophages type II (20 NX) and macrophages (16.83 NX) whilst monocytes do not seem express the receptor (0 NX) (Fig. 4.2).

We also sought to explore the MerTK mRNA expression in different cell types from specific tissues such as heart muscle and the lung (Fig. A & B respectively). The data from HPA dataset of the heart muscle revealed the highest MerTK mRNA expression was in the mixed immune cells; 18.8 pTPM (1 million transcripts per kilobase million), followed by SMCs; 16.1 pTPM and ECs; 8.25 pTPM (averaged from two clusters of cells) whilst cardiomyocytes expressed the least; 1.28 pTPM (averaged from five clusters of cells) (Fig. 4.3 A). In lungs, it revealed that macrophage and alveolar macrophage (both types: I & II) as well as endothelial cells express MerTK receptor with the highest expression in alveolar macrophage type II (averaged from two clusters); 27.15 pTPM followed by macrophage (averaged from two clusters); 22.7 pTPM, Ecs; 15.4 pTPM and lastly alveolar macrophage type I; 5.4 pTPM (Fig. 4.3 B).

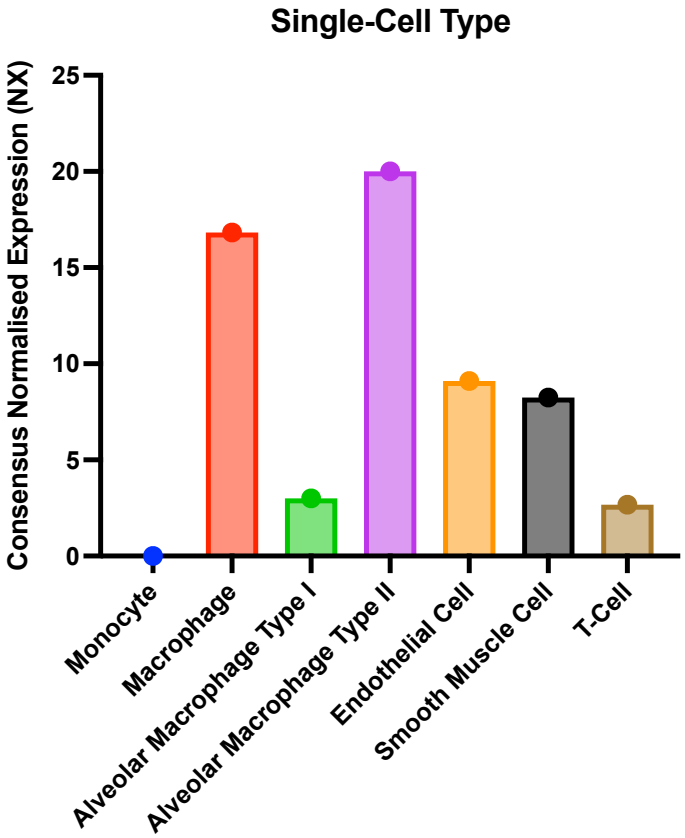

Figure 4.2: Normalised MerTK gene expression levels in Cell Types presented as means across various tissues.

The average of MerTK gene expression in macrophage was from 6 tissues: testis, prostate, pancreas, Kidney, Skin, Lung. While in endothelial cells this was from 9 tissues: heart muscle, testis, prostate, pancreas, Kidney, Skin, Liver, Eye, Placenta. And in the smooth muscle cell was from 4 tissues: Heart muscle, Pancreas, Prostate, skin. T-cell levels were averaged was from 6 tissues: Liver, Lung, Kidney, Colon, Skin, Prostate. The consensus normalised expression; NX, is obtained from combining data from three datasets; HPA, GTEx, and FANTOM5.

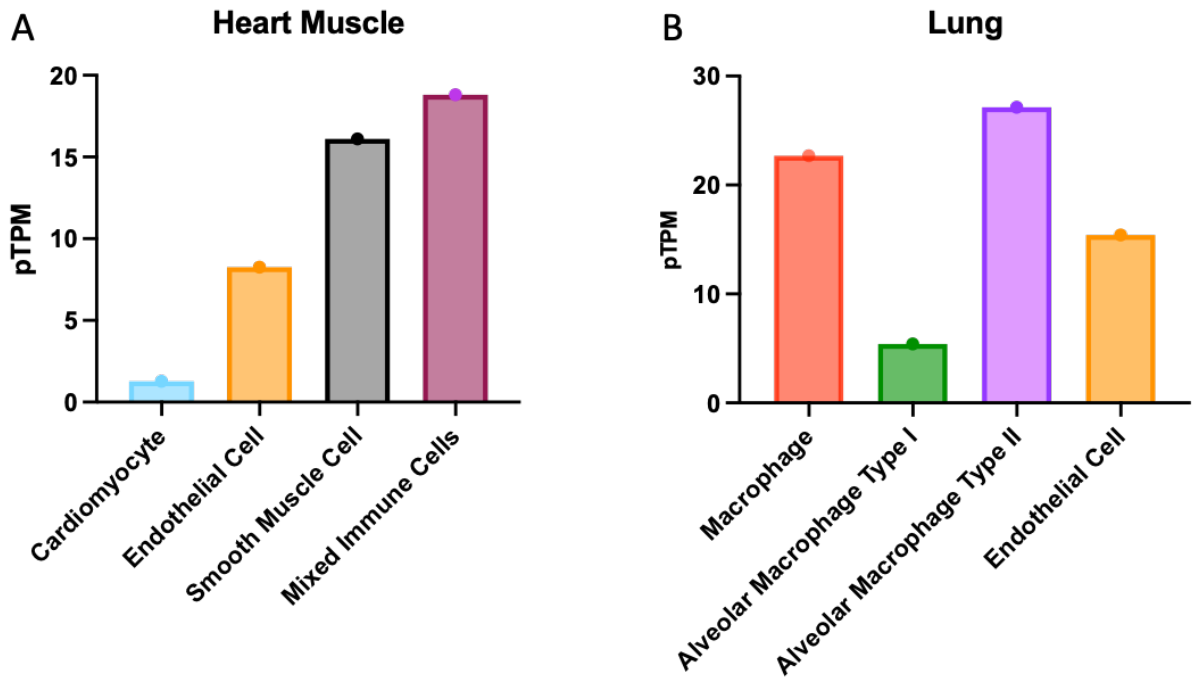

Figure 4.3: MerTK mRNA expression different cell types relating to immunity and atherosclerosis.

The MerTK mRNA expression was extracted from the Human Protein Atlas data set presented in cell types as pTPM (transcripts per million protein coding genes for each of the single cell clusters) from Heart muscle (A) and in the Lungs (B). Cell clusters were manually annotated based on clusters expressing known markers of immune cells (where “Mixed immune cells” are shown for Heart). Alveolar macrophages were defined as distinct clusters according to expressed markers.

4.3 Determining the MerTK receptor gene expression pattern in human primary cells and HeLa cell line

Monocyte-derived macrophages (hMDMs)

Macrophages key roles played in atherosclerosis are coupled to their plasticity that influence them to acquire tailored properties in response to local stimuli in plaques such as cytokines, lipid derivatives and cellular debris. In general, macrophage phenotype spectrum was initially identified at two extremes of activation with distinct properties and activators i.e. either pro-inflammatory or anti-inflammatory phenotypes. The classical macrophage phenotype, M1 which is pro-inflammatory contributing to promoting inflammation, while the alternative macrophage phenotype, M2 is anti-inflammatory contributing to resolving inflammation (Sica and Mantovani, 2012). However, recent studies have discovered diverse intermediate phenotypes of macrophages involved in atherosclerotic plaque in response to its microenvironment cues encountered. It demonstrates that macrophage phenotypes are on a broad activation continuum spectrum that is dependent on the stimuli in the plaque (Cochain et al., 2018). We sought to focus on the two classical in-vitro phenotypes of macrophages M1 and M2 to determine MerTK receptor gene expression due to limited time. From healthy donors, monocytes were isolated and then differentiated into hMDMs via incubation with 100 ng/ml M-CSF for 7 days. Subsequently, they were polarised towards both M1 and M2 as well as the unpolarised or resting M0 as control. Hence, hMDMs were stimulated for 24 hours with either 100ng/ml LPS and 20 ng/ml IFN-γ (for M1 phenotype) or with 20ng/ml of IL-4 (for M2 phenotype). M0 denotes the M-CSF-treated hMDMs with no subsequent polarisation as control. Next, total RNA was isolated, reverse transcribed and RT-qPCR was carried out. The data obtained are presented as delta Ct values i.e. the Ct values normalised to the housekeeping gene GAPDH, and are inversely correlated to the gene expression levels (Fig. 4.4). The data indicates detectable MerTK expression in hMDMs which appears to reduce with both M1 and M2 macrophage polarisation compared to the unpolarised state, M0

(Fig. 4.4). This is suggestive that MerTK receptor function may be dampened during inflammation and resolution although, more replicates and further investigations are needed to test this fully.

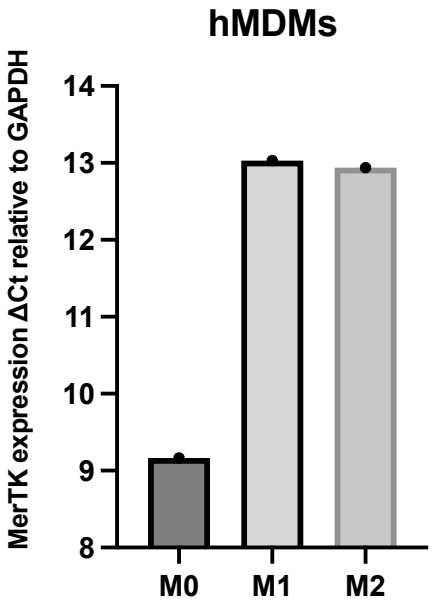

Figure 4.4: Relative MerTK expression in polarised human monocyte-derived macrophages by RT-qPCR.

Human primary monocyte-derived macrophages (hMDMs) either un-polarised (untreated, M0) or polarised towards an inflammatory M1 phenotype by treatment both LPS and IFN-γ or anti-inflammatory M2 phenotype using IL-4, respectively for 24 hours. Values are presented as delta Ct values relative to the housekeeping gene GAPDH. (N=1).

Endothelial Cells

The blood flow, whether it is laminar or oscillatory, exerts force that is parallel to the surface of the endothelium and is called shear stress. The shear stress can also be defined as the force exerted on the vessel wall and the surface of the lining endothelium due to the friction of blood flowing. The hemodynamic shear stress has been implicated in the development of atherosclerosis by mediating vascular remodelling at sites of disturbed blood flow. The flow pattern in the blood vessel near branches or arterial bifurcation is disturbed and irregular generating low and oscillatory shear stress; these areas are susceptible to developing atherosclerosis (Zarins et al., 1983). On the other hand, vessels with unidirectional and regular blood flow generate high and laminar shear stress and less prone to disease (Bharadvaj et al., 1982). Therefore, we have analysed the gene expression of MerTK receptor in primary human umbilical vein endothelial cells (HUVECs) exposed to either; 1) laminar or regular shear stress, or to 2) oscillatory or irregular shear stress for 72 hours in orbital shaker, relative to static condition as control. Total RNA was isolated from HUVECs and the gene expression was analysed by RT-qPCR. Similarly, the data obtained are presented as delta Ct values i.e. the Ct values normalised to the housekeeping gene GAPDH, inversely correlated to the gene expression levels (Fig. 4.5). These data showed that MerTK was downregulated significantly when cells were exposed to shear stress (One-Way ANOVA, $p=0.03$). The post hoc test, Tukey's showed a significant downregulation of MerTK gene expression between high, laminar shear stress compared to cells under static conditions. Statistical differences between low, oscillatory shear stress and static was not significant nor between the low and high shear stress. This is potentially due to the small sample size ($N=3$). This suggests that MerTK receptor may play a protective role against inflammation that has been proposed in the literature (Cai et al., 2017, Waterborg et al., 2018), as the high, laminar shear stress is athero-protective.

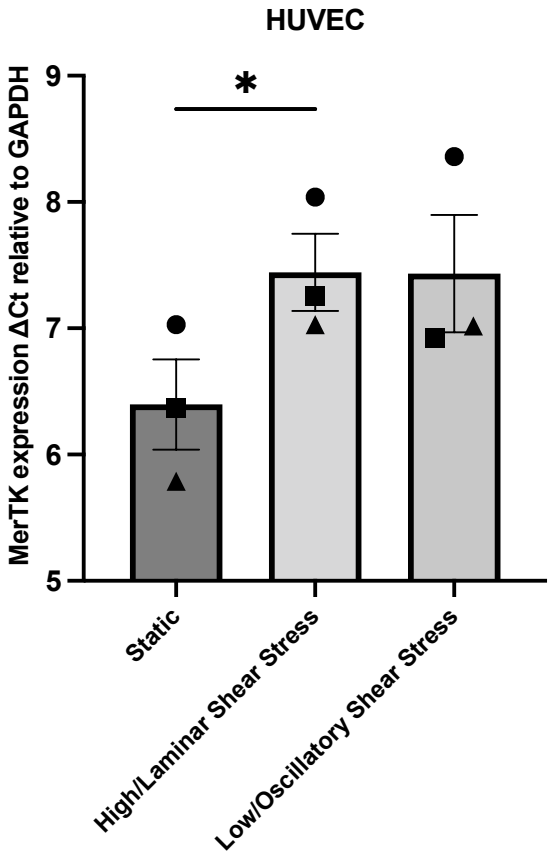

Figure 4.5: Relative MerTK expression in endothelial cells subjected to shear stress, by RT-qPCR.

Primary human umbilical vein endothelial cells (HUVECs) exposed for 72 hours to either high and laminar shear stress or low and oscillatory shear stress compared to static conditions. Each replicate is matched by shape. Values are presented as delta Ct values relative to the housekeeping gene GAPDH (N=3), and analysed by one-Way ANOVA, Tukey's multiple comparison test, ns or *p<0.05.

Human Epithelial Cell Line; HeLa

Prior to proceeding with investigating whether MVs target MerTK receptor, we sought to determine the receptor expression in the HeLa cell line by RT-qPCR. HeLa cells are highly responsive to IL-1β and therefore a suitable cell line to measure the effect of IL-1β containing MVs on IL-6/IL-8 production in the absence and presence of MerTK knockdown. It is important to determine whether HeLa cells do in fact express MerTK, to determine whether we are able to test the role of this receptor in MV targeting. The results showed that HeLa cells express detectable MerTK receptor (Fig. 4.6).

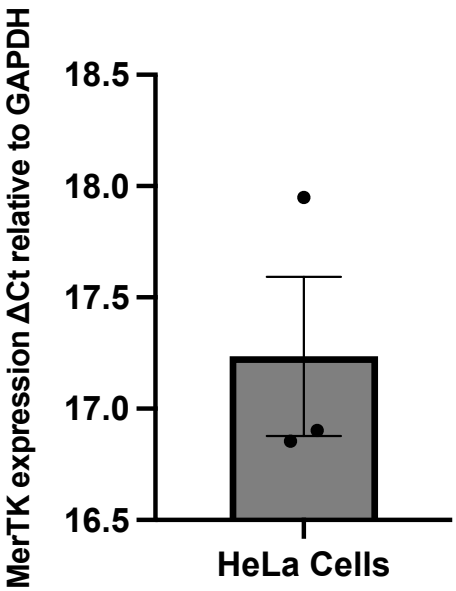

Figure 4.6: Assessment of MerTK RNA expression in HeLa cell line by RT-qPCR.

HeLa cells from different passages showing MerTK receptor gene expression (N=3). Values are presented as mean ± SEM.

Comparison of MerTK relative expression across different cells using RT-qPCR

We wished to compare relative expression of MerTK in the different cells and conditions tested by our own qPCR (Fig. 4.7) prior to comparing this in published datasets.

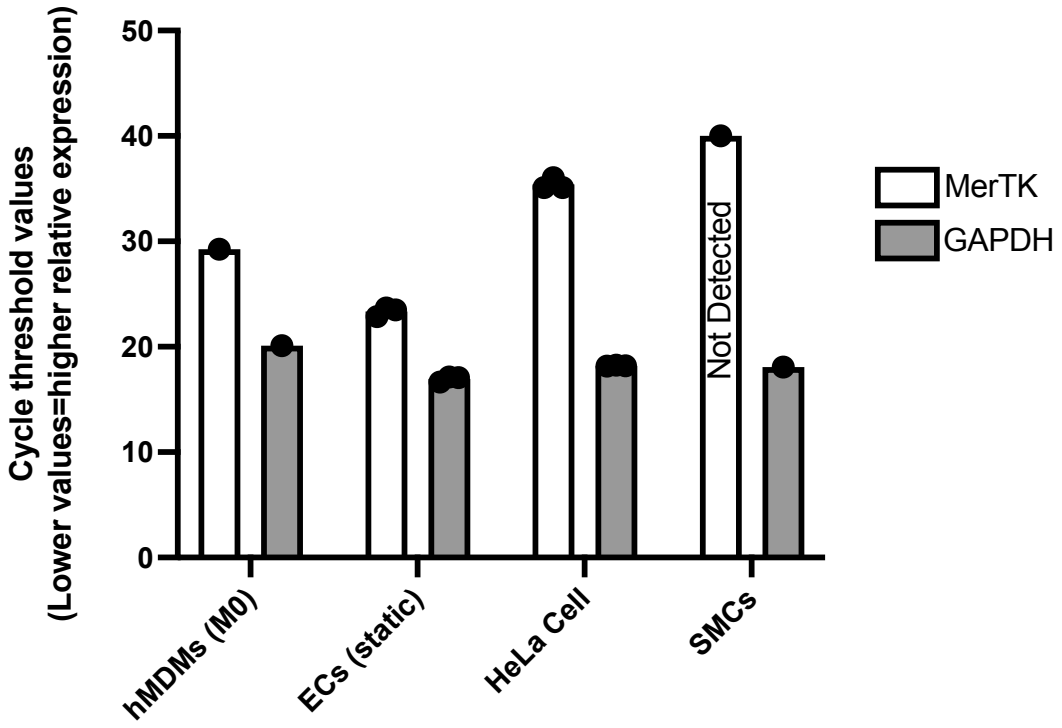

Figure 4.7: Comparison of relative MerTK expression in different cells by RT-qPCR.

The figure presents the cycle threshold values of: primary human smooth muscle cells (SMCs), human epithelial cell line; HeLa, primary human umbilical vein endothelial cells (HUVECs) static conditions, and unpolarised (M0) hMDMs. Values are presented as the Ct values relative to the housekeeping gene GAPDH.

4.4 Analysis of published datasets to assess MerTK receptor expression in Endothelial Cells

In this section we have used published datasets from microarrays to extract and analyse data to explore our own specific hypotheses. These data have not been extracted and used previously to explore these questions and therefore provide new and previously unpublished results.

4.4.1 Determining whether MerTK expression is upregulated in TNF-inflammatory activated endothelial cells

Tumour necrosis factor (TNF) is a pro-inflammatory cytokine that exerts multiple effects on cells present in the atherosclerotic plaque, endothelial cells in particular. TNF is pivotal in mediating inflammatory response and innate immunity through inducing vascular endothelial cell dysfunction/activation and monocyte recruitment and subsequently cellular invasion. It has been shown that TNF stimulates endothelial cells to express leukocyte adhesion molecules such as E-selectin, vascular cell adhesion molecule (VCAM-1) and intercellular adhesion molecule (ICAM-1), and intercellular adhesion molecule (Zhang et al., 2020). TNF stimulates endothelial oxidative stress, production of intracellular reactive oxygen species (ROS) which upregulates expression of monocyte chemoattractant protein-1; MCP-1 (Zeiher et al., 1995). One of the best-characterised endothelial TNF signalling cascades is activation of mitogen-activated protein kinase MAPK signalling and the nuclear factor κB (NF-κB) transcription factor (Hiscott et al., 1993, Ho et al., 2008). NF-κB activation induces production and release of cytokines including interleukins and chemokines. In the atherosclerotic plaque these cytokines activate monocyte adhesion, migration and entry to the vascular intima, apoptosis (Laster et al., 1988) and endothelial and vascular smooth muscle cell proliferation (Ligresti et al., 2011, Selzman et al., 1999). TNF therefore plays a key role in atherosclerosis activating endothelial cells, initiating angiogenesis and promoting inflammation in the arterial plaque which can result in plaque rupture in later stage atherosclerosis.

Since plaque macrophages may produce IL-1β containing PS-positive MVs, they may preferentially target inflammation-primed endothelial cells.

Hypothesis: The pro-inflammatory cytokine TNF increases expression of MerTK on endothelial cells. In turn, upregulated MerTK may provide a target for PS-positive MVs.

Datasets analysed: The response to inflammatory TNF was investigated in two endothelial cell subtypes (Viemann et al., 2006): Human microvascular endothelial cells (HMEC) and macrovascular human umbilical vein endothelial cells (HUVEC). Endothelial cells were stimulated with 2 ng/ml of human recombinant TNF-α for 5 hours. The gene expression profile was determined using oligonucleotide microarray technique.

Results: obtained showed differences in response to stimulation between the two endothelial cell subtypes. MerTK receptor gene expression was downregulated in HUVECs stimulated with TNF-α compared to the control ($p<0.005$), whereas the microvascular endothelial cells (HMEC-1) results did not show significant difference in MerTK expression (Fig. 4.8).

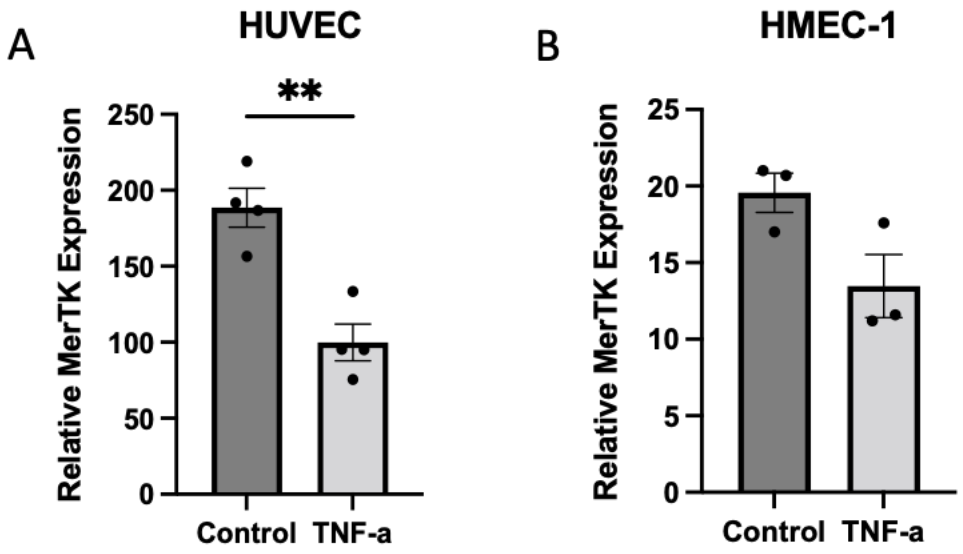

Figure 4.8: Comparison of MerTK RNA expression in response to TNF, extracted from microarray data (Viemann et al., 2006).

A) macrovascular Human umbilical vein endothelial cells (HUVECs) (N=4), B) human microvascular endothelial cells (HMEC-1) (N=3), non-treated versus treated with 2ng/ml of human recombinant TNF-α for 5 hours. Values are presented as mean $\pm$ SEM, analysed by two-tailed paired t-test, ns or ** $p<0.005$,.

Summary: TNF inhibits the expression of MerTK in HUVEC Instead, downregulated endothelial MerTK under TNF-induced inflammation may reflect a feedback mechanism to prevent the anti-thrombotic effects of MerTK receptor in atherosclerosis or to dampen inflammation from PS-positive MVs. To test this hypothesis more fully, it would be interesting to test MerTK expression and protein levels in human arterial endothelial cells, and to stain for MerTK in non-diseased and atherosclerotic arteries.

4.4.2 Determining whether MerTK expression is upregulated in Interleukin-1 inflammatory activated endothelial cells

Interleukin-1α/β are pro-inflammatory cytokines widely known to play key roles in atherosclerosis (chapter 1, section 1.3.2). Endothelial cell dysfunction is the first step initiating atherosclerosis since the endothelium act as a barrier protecting the vessels. IL-1 is released by multiple cells present in the plaque such as macrophage, T lymphocyte, smooth muscle cell and the endothelial cell itself. IL-1 activates endothelial cells to express adhesion molecules on their surface such as VCAM-1 (Singh et al., 2005) and the chemokine MCP-1 (Rollins et al., 1990) as well as other prothrombotic mediators including tissue factor (TF) (Bevilacqua et al., 1984). In addition, ECs stimulated with IL-1 induce chemokines such as CX3C, thereby furthering leukocyte recruitment and attraction to the site of inflammation (Bazan et al., 1997). These effects are a result of IL-1 activating the transcription factor NF-κB that induce the gene expression of several mediators of the inflammatory response (Gimbrone and Garcia-Cardena, 2016, Rollins et al., 1990).

The IL-1 may be released by plaque macrophages contained in PS-positive MVs which target the endothelium via MerTK receptor.

Hypothesis: IL-1 treatment upregulates MerTK expression in endothelial cells.

Dataset Analysed: HUVECs were cultured and treated with 100U/mL human IL-1. Total RNA was isolated from the cells at different time points after IL-1 stimulation: 0.5, 1, 2.5, and 6 hours. The gene expression profile was determined using oligonucleotide microarray technique (Mayer et al., 2004).

Results: Data obtained showed MerTK expression appears to be downregulated at 2.5 and 6 h following IL-1 stimulation compared to control, 30 minute and 1 h IL-1 exposure (Fig. 4.9). Further replicates are required to determine whether these changes are reproducible and statistically significantly different.

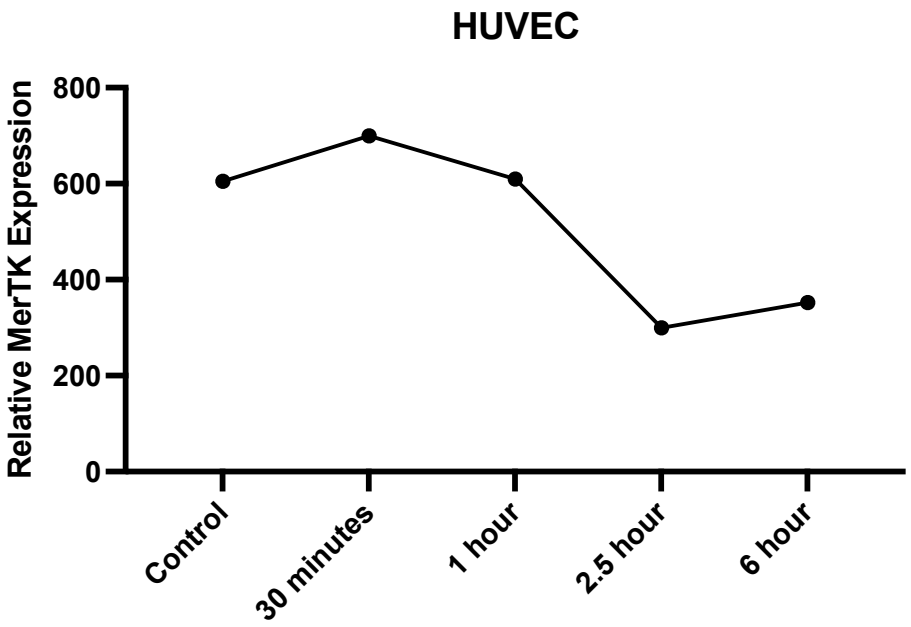

Figure 4.9: Assessment of MerTK RNA expression in response to IL-1 from microarray data (Mayer et al., 2004).

Human umbilical vein endothelial cell (HUVECs) stimulated with human IL-1 cytokine at 100U/mL at different time points versus non-treated cells as control. single dataset provided, so no statistics were performed.

Summary: The apparent inhibitory effect of IL-1 on the expression of MerTK in HUVECs suggests rejecting the proposed hypothesis. It would be interesting to assess the effect of IL-1 on arterial endothelial cells which are more relevant to atherosclerosis compared to cells from veins. This may suggest that free IL-1 (i.e. not contained in MVs) may downregulate MerTK expression in endothelial cells. The effect of PS-positive MV-delivered IL-1β on arterial endothelial MerTK expression has yet to be explored and would be interesting to test.

4.4.3 Determining the effect of shear stress and intraluminal pressure on MerTK expression in endothelial cells

The vessel wall is exposed to biomechanical forces; blood flow and blood pressure forces, this is due the pulsatile flow of blood pumped by the heart to supply different organs/tissues. The physiological haemodynamic shear stress in a healthy artery is estimated between 10 to 20 dynes/cm^2. In contrast, the pulsatile blood pressure exerts a perpendicular force to the vascular wall, which is the intraluminal pressure and known as circumferential stress and is estimated between 1 to 2x10^6 dynes/cm^2 (Kwak et al., 2014). Disturbed or static blood flow induce endothelial apoptosis, a resultant loss of barrier function, which predisposes the arterial site to atherogenesis (Davies et al., 1986), whilst high laminar shear stress inhibits endothelial apoptosis (Dimmeler et al., 1996). Disturbed blood flow activates endothelial MAPK signalling and the transcription factors activator protein-1 (AP-1) and NF-κB that regulate expression of adhesion molecules and inflammatory cytokines/chemokines (Lan et al., 1994). Similarly, high intraluminal blood pressure activates the endothelium resulting in inflammatory pathway activation, including activation of NF-κB thereby increasing surface expression of adhesion molecules ICAM-1 and P-selectin, as increased cytokines and chemokines like MCP-1 (Wang et al., 2004).

Since disturbed blood flow has been shown to activate and sustain development of atherosclerosis, it is important to understand its effect on endothelial MerTK expression, which may serve as a target for PS-positive IL-1b containing MVs.

Hypothesis: disturbed, low and oscillatory shear stress associated with arterial branches and bifurcations increases the expression of endothelial MerTK.

Datasets Analysed:

Dataset 1: HUVECs were tested from pooled-donors from four different batches cultured and exposed to different blood flow; normal shear stress 15 dynes/cm^2 (LSS15), or high shear stress 75 dynes/cm^2 (LSS75) using parallel-plate fluid flow chamber for 24 hours. Total RNA was isolated from the cells. The gene expression profile was determined using oligonucleotide microarray technique (White et al., 2011).

Dataset 2: Sixteen paired intact conduit human umbilical veins were perfused for six hours under four defined forces settings. The first setting included sixteen paired veins exposed to low shear stress (<2 dynes/cm^2) or high shear stress (25 dynes/cm^2) with constant normal intraluminal pressure of 20 mm Hg. The second setting included sixteen paired veins exposed to high intraluminal pressure (40 mm Hg) or normal intraluminal pressure (20 mm Hg) with constant normal shear stress of 10 dynes/cm^2. HUVECs were isolated and RNA was extracted and pooled as duplicate for analysis with microarray (Andersson et al., 2005).

Results: Analysis of extracted expression levels from dataset 1 shows there was no significant difference in MerTK gene expression between HUVECs exposed to normal shear stress and high shear stress (Fig. 4.10 A). The MerTK expression detected in cells exposed to normal shear stress were more varied compared to expression in high shear stress-exposed cells. Analysis of data obtained from dataset 2 showed no apparent difference in MerTK expression between the four different biomechanical forces settings (Fig. 4.10 B). More replicates are required to determine whether the differential forces alter MerTK expression and in order to be able to test this statistically.

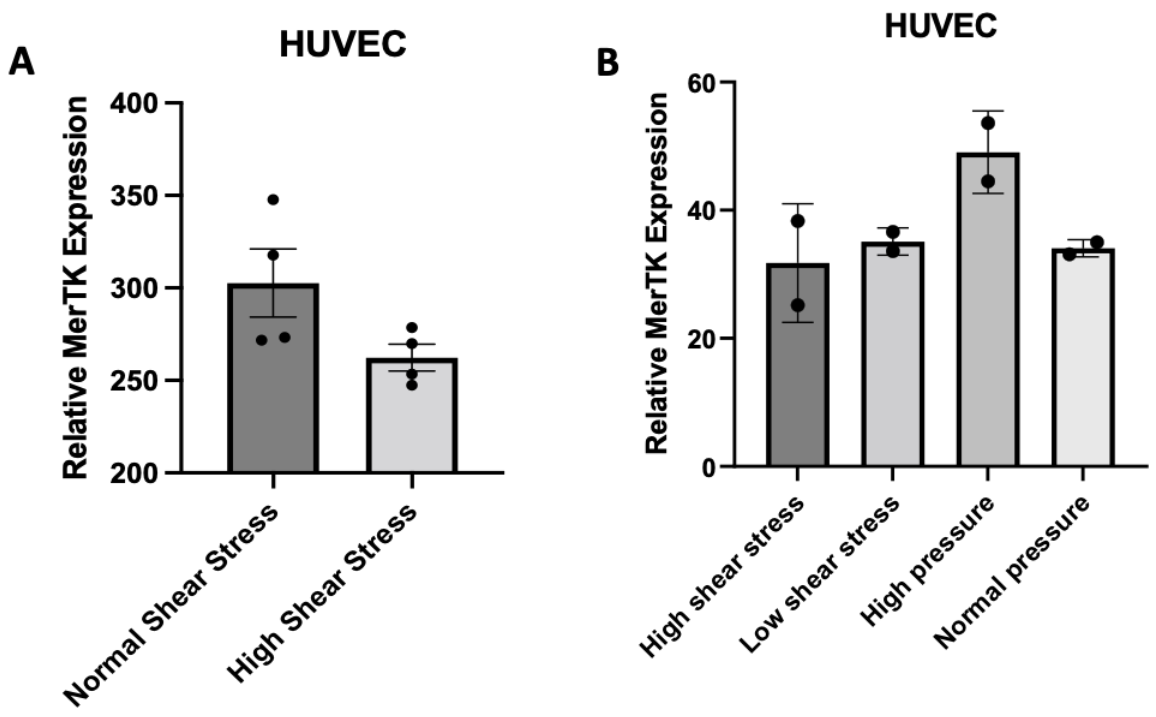

Figure 4.10: Assessment of MerTK RNA expression under biomechanical forces; wall shear stress and intraluminal pressure from microarray data.

A) Exposed to either normal shear stress or high shear stress for 24 hours (N=4) (White et al., 2011), B) Exposed to either high or low shear stress, high or normal intraluminal pressure for 6 hours (N=2) (Andersson et al., 2005). Values are presented as mean ± SEM for A, and as mean ± SD for B, analysed by two-tailed paired t-test for A, and analysed by One-Way ANOVA with Tukey's correction method for multiple comparison test for B, where all comparisons were not significant, $p>0.05$.

Summary: The data obtained suggest no effect of shear stress and/or intraluminal pressure on MerTK receptor gene expression. The MerTK receptor may require prolonged exposure to low/disturbed flow in order to alter its gene expression significantly in Ecs (i.e. longer than 24 hours). Full testing of this hypothesis requires further investigation; currently little is known about the involvement of MerTK receptor in atherosclerosis development.

4.4.4 Determining the effect of interferons on MerTK expression in endothelial cells

Interferons [IFNs] are a family of cytokines known to regulate immune responses in many diseases including atherosclerosis. They are highlighted as key mediators participating in many processes involved in the early stages of atherosclerosis and can be found in abundance in the plaque. Their roles in atherosclerosis have been a matter of debate since they possess both pro-inflammatory and anti-inflammatory properties. IFNs are involved in promoting endothelial dysfunction: IFN-γ participates in enhancing exposure of adhesion molecules ICAM-1, VCAM-1, P-selectin and E-selectin on endothelial cells (Zhang et al., 2011), in turn inducing leukocyte recruitment and adhesion to the endothelium and subsequently migration to the vascular intima. IFN-α, IFN-β and IFN-γ are anti-angiogenic cytokines inducing EC apoptosis via upregulating specific genes (Indraccolo et al., 2007).

This leads us to explore whether IFNs regulate MerTK receptor gene expression in endothelial cells, which may serve to target PS-positive IL-1β containing MVs.

Hypothesis: IFNs stimulate endothelial upregulation of MerTK gene expression.

Dataset Analysed: The response to inflammatory IFNs was investigated in HUVECs taken from three groups of pooled donors. ECs were either non-treated [control] or treated with IFN-α and IFN-γ both at a dose of 1000 IU/ml for five hours. Each biological replicate consisted of four different donors, and pooled together before hybridization thus, donor number in total is 12. RNA was isolated from the cells and the gene expression profile was determined using oligonucleotide microarray technique (Indraccolo et al., 2007).

Results: Datasets extracted and analysed showed no significant differences in MerTK gene expression between non-treated control and either IFN-α and IFN-γ treated Ecs (Fig. 4.11).

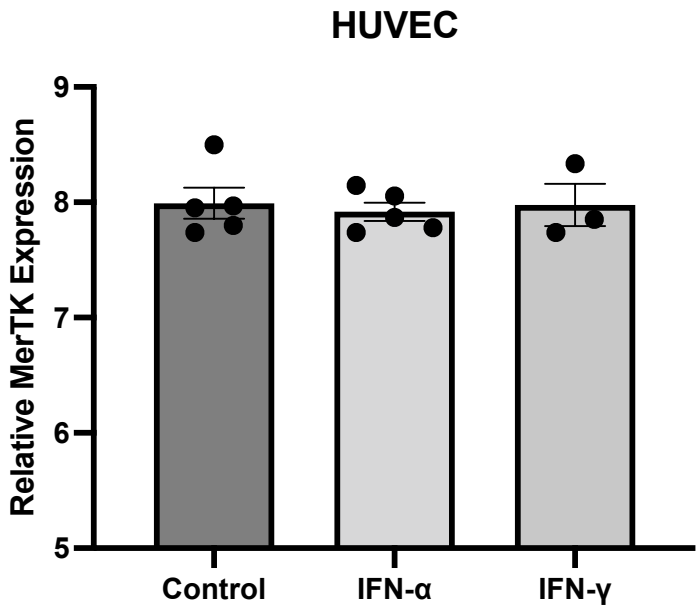

Figure 4.11: Endothelial MerTK expression in response to IFN treatment, from microarray data (Indraccolo et al., 2007).

Human umbilical vein endothelial cells (HUVECs) non-treated versus treated with 1000U/l of human recombinant IFN-α and IFN-γ for 5 hours. Values are presented as mean $\pm$ SEM (N=3-5,technical replicates of a pool of 12 donors), analysed by One-way ANOVA with Dunnett's correction method for multiple comparisons, where all comparisons were not significant, $p>0.05$.

Summary: The results suggest that IFN-α and IFN-γ may not regulate endothelial MerTK gene expression and IFNs and therefore may not affect MV targeting to ECs. IFNs convey a dual anti-inflammatory and pro-inflammatory role, so may not regulate mechanisms of IL-1 targeting.

4.4.5 Determining the effect of oxidised low-density lipoprotein (oxLDL) on MerTK expression in endothelial cells

Oxidative modification of LDL is an important process attributing to its pro-atherosclerotic behaviour. When high levels of circulatory oxLDL come in contact with the endothelium, it binds to their scavenger receptor; lectin-like low-density lipoprotein receptor, LOX-1. The binding and uptake of oxLDL leads to endothelial cell activation contributes to atherosclerosis initiation and progression, by upregulating cell adhesion molecules exposure (Khan et al., 1995), cytokine/chemokine release such as MCP-1 (Navab et al., 1991) and apoptosis (Lu et al., 2009). This is achieved primarily through oxLDL binding to LOX-1 and signalling to activate transcription factors including NF-κB and AP-1; these in turn upregulate cytokines, chemokines and adhesion molecule exposure (Yurdagul et al., 2016).

Oxidised LDL activates endothelial cells during the inflammatory response (Khan et al., 1995). Hence it may play a role in upregulating MerTK as a target for PS-positive IL-1β containing MVs.

Hypothesis: MerTK gene expression is upregulated in endothelial cells exposed to oxLDL.

Dataset Analysed: The expression of MerTK was investigated in immortalised human arterial endothelial cell line (HAECT) over-expressing GFP. The experiment design was as follows: three replicates of cells treated with 50ug/ml OxLDL over the time points 2h, 6h, 12h and 24h. These were compared to three replicates of non-treated cells over the time points: 2h, 6h, 12h and 24h. Cells were not treated with oxLDL at 0h in both treated and control conditions (Mattaliano et al., 2009).

Results: The extracted and analysed data showed that MerTK gene expression was not affected when cells were treated with 50μg/ml oxLDL, compared to untreated control cells. There was no statistical significant difference between the overall mean MerTK expression over the time course for the oxLDL treated cells compared to the overall mean of untreated cells, nor for oxLDL treated ECs over time, compared to the control when analysed by Two-way ANOVA. The Šídák's multiple comparison test showed no significant differences between control and treated samples for individual time points (Fig. 4.12).

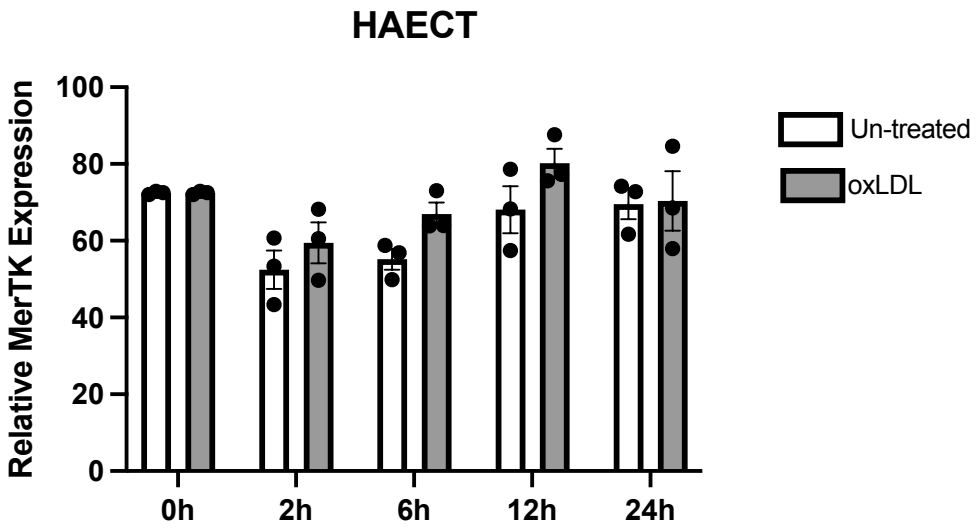

Figure 4.12: Assessment of endothelial MerTK RNA expression in the absence and presence of oxLDL from microarray data (Mattaliano et al., 2009).

Human aortic endothelial cell line (HAECT) (N=3), non-treated versus treated with 50ug/ml of oxLDL for different time points. Values are presented as mean ± SEM. Two-Way ANOVA followed by Šídák's multiple comparison test. There were no significant differences between control and treated samples for individual time points.

Summary: The data suggest that MerTK gene expression does not change when ECs are exposed to oxLDL over time, suggesting that the endothelium may upregulate the MerTK receptor target for PS-positive IL-1β-containing MVs.

4.5 Analysis of deposited datasets to assess MerTK receptor expression in Macrophages

Macrophages and IL-1 play a key role in atherosclerosis disease progression. While this project has tested the role of macrophages in secreting IL-1β-containing PS-positive MVs, it is conceivable that these MVs play a role in targeting surrounding macrophages in the plaque in order to augment the inflammatory environment. A variety of cytokines and mediators are released from macrophages that may influence the expression of the MerTK receptor, which in turn may affect the targeting of IL-1β-containing MVs.

4.5.1 Determining the effect of Interleukins on MerTK expression in monocytes and macrophages

IL-1 cytokines can induce a series of intracellular signalling events that lead to activation of transcription factors such as NF-κB which is turn lead to increase the gene expression of a diverse of cytokines and chemokines including IL-1α, IL-1β, IL-6, IL8, MCP-1 and others (Liu et al., 2017).

Similarly, IL-6 has been reported to participate in atherosclerosis progression and participate in plaque initiation and disruption (Yudkin et al., 2000). A study have indicated the role of IL-6 in the development of macrophages and vascular smooth muscle cells stimulating their growth (Ikeda et al., 1991) (Jenkins et al., 2004). Another study has suggested the use of anti-IL-6 therapy in reducing atherosclerotic plaque size in LDL receptor knockout mice, supporting the involvement of IL-6 in cell proliferation (Akita et al., 2017).

In contrast, IL-10 is a potent anti-inflammatory cytokine that dampens inflammatory response and interferes with the progression of atherosclerosis. IL-10 is detected in both the early and the late stages of plaque formation inhibiting diverse processes that contribute to atherosclerotic. It has shown that IL-10 inhibits the cytokines production from macrophages such as IL-1β, IL-6, TNF, and others via inhibiting the activation of

NF-κB (Lentsch et al., 1997, Malefyt et al., 1991). It also decreases macrophage foam cell apoptosis hence participating in decreased the atherosclerotic lesion size (Pinderski et al., 2002). Moreover, IL-10 interferes with the macrophage ability to modulate the extracellular matrix by preventing their production of matrix metalloproteinases (Lacraz et al., 1995).

Therefore, it is of importance to understand how interleukins may participate in PS-positive MV targeting through modulating MerTK gene expression.

Hypothesis: interleukins increase the gene expression of MerTK in macrophages.

Datasets Analysed:

1. Human monocyte-derived macrophages (hMDMs) were prepared from peripheral blood mononuclear cells (PBMCs) obtained from five healthy donors and stimulated for 4 hours with either 15ng/ml of IL-1 or 25ng/ml of IL-6 or non-stimulated as control. RNA was isolated and gene expression profiling was carried out via microarray (Jura et al., 2008).
2. Human monocytes isolated from PBMCs obtained from four healthy donors were either treated with 10ng/ml of IL-10 for 24h or without treatment as control, gene expression profiles were determined by microarray (Teles et al., 2013).

Results: Analysed data showed no significant differences in MerTK gene expression between hMDMs treated with IL-1 and non-treated cells, nor between IL-6 treated and non-treated cells (Fig. 4.13 A). In contrast, IL-10 has significantly upregulated the gene expression of MerTK receptor in human primary monocytes (Fig. 4.13 B).

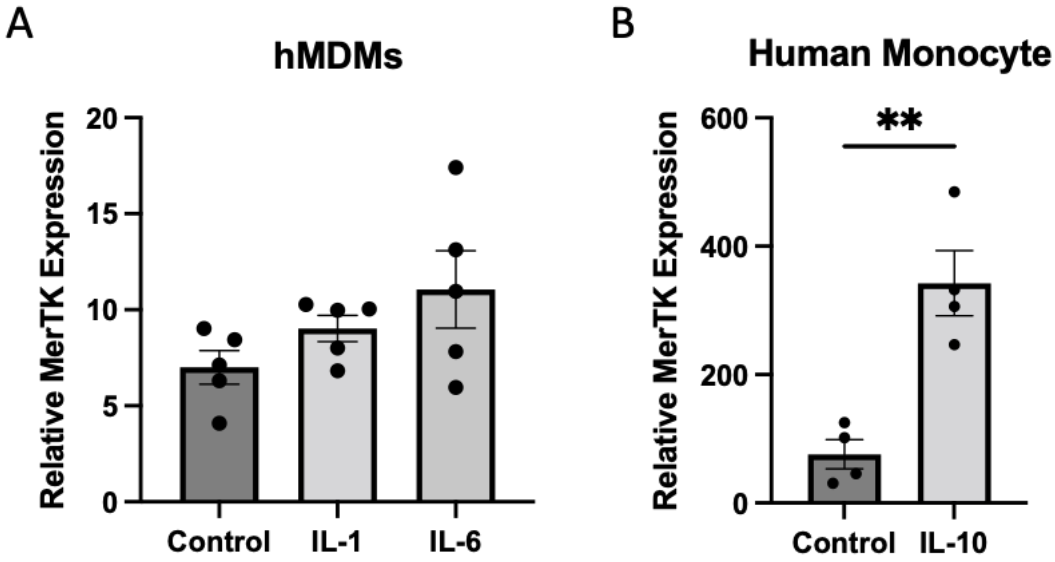

Figure 4.13: Assessment of MerTK RNA expression in response to interleukins from microarray data.

A) hMDMs obtained from healthy donors, treated with either 50ng/ml of IL-1 or 25ng/ml of IL-6 or non-treated as control (N=5) (Jura et al., 2008), Values are presented as mean ± SEM, analysed by One-Way ANOVA with Dunnett's correction method for multiple comparisons test, where all comparisons were not significant, $p>0.05$. B) Human monocytes obtained from healthy donors, treated with 10ng/ml of IL-10 or only media as control for 24 hours (N=4) (Telese et al., 2013), Values are presented as mean ± SEM, analysed by two-tailed paired t-test, **$p<0.005$.

Summary: The data obtained from IL-1 and IL-6 stimulation suggest that these pro-inflammatory cytokines do not regulate MerTK gene expression in macrophages. On the other hand, anti-inflammatory IL-10 has significantly increased MerTK gene expression in monocytes. This may suggest that IL-10 upregulation of MerTK in monocytes would offer an increased level of targets to PS-positive MVs aiding in delivering their content to the target cell. As this data was from monocytes only, it would be interesting to extend this to testing the effect of IL-10 in macrophages both in culture and obtained from atherosclerotic plaques on MerTK gene expression. The effect may be IL-10 specific across monocytic/macrophage cells or may be unique to the undifferentiated monocyte.

4.5.2 Effect of IFNs on MerTK expression in monocyte-derived macrophages (hMDMs)

IFNs possess a variety of pro-atherogenic properties that regulate immune responses in atherosclerosis. A main effect on macrophages in atherosclerosis is enhancing their expression of scavenger receptors such as SR-A leading to oxLDL uptake and formation of foam cells (Boshuizen et al., 2016, Li et al., 2011). IFNs also enhance the expression of chemokines receptors on macrophages such as CCR2 and CCR5 that basically bind MCP-1 chemokines and promote their recruitment to atherosclerotic sites and adhesion to endothelial cells (Goossens et al., 2010). IFN-γ specifically, is responsible for macrophage expression of chemokines including CCL3,4,5, and CXCL9,10,11 inducing immune cell chemotaxis (Read et al., 2019). Moreover, the deletion of the downstream target of IFN-γ signalling i.e. STAT1, resulted in reduced foam cell formation as well as macrophage apoptosis (Agrawal et al., 2007). Therefore, IFNs participate in increasing the atherosclerotic lesion size by regulating macrophage recruitment and increasing lipid uptake.

Hence, it is important to investigate the role of IFNs in MerTK gene expression regulation to test whether they may contribute in PS-positive MV targeting.

Hypothesis: IFN-γ upregulates MerTK expression in hMDMs .

Dataset Analysed: Three independent pools of RNA obtained from hMDMs that were isolated from total of 12 healthy human donors, were either unstimulated or stimulated with 100U/ml of IFN-γ for either 3 hours or 24 hours. Total RNA was then isolated and gene expression profile was assessed by microarray (Hu et al., 2005).

Results: The data obtained showed no statistical significant difference in MerTK gene expression between un-stimulated and IFN-γ stimulated hMDMs (Fig. 4.14).

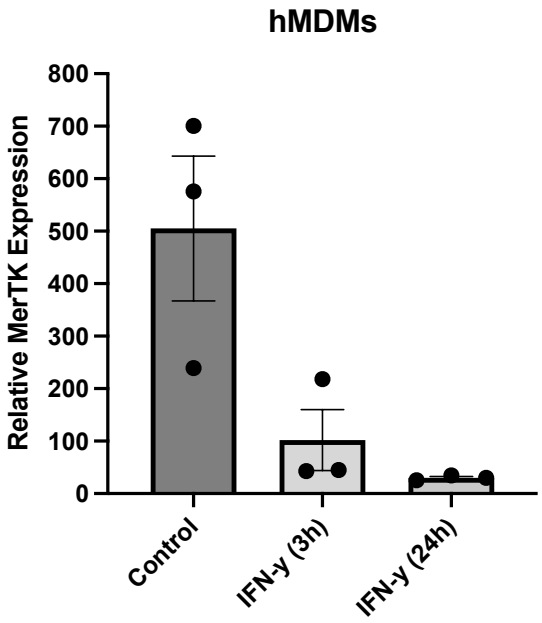

Figure 4.14: Assessment of MerTK RNA expression in hMDMs in response to IFN from microarray data (Hu et al., 2005).

Three RNA pooled samples of hMDMs obtained from 12 healthy donors, treated with either 100U/ml of IFN-γ for either 3h or 24h, and non-treated as control, Values are presented as mean ± SEM, analysed by One-Way ANOVA with Dunnett's correction method for multiple comparisons test, where all comparisons were not significant, $p>0.05$.

Summary: There was no statistically significant difference in MerTK expression between control and IFN-γ treated hMDMs. However, the expression values of MerTK receptor showed high inter-individual variability, particularly in control untreated cells; this variability was notably reduced when hMDMs were stimulated with IFN-γ for 24 hours (Fig. 4.14). It is possible that the high variability in the untreated cells has meant that a real reduction in MerTK following IFN-γ treatment is not detectable when analysed statistically. An increase in the biological replicates as well as, assessing macrophages from atherosclerotic plaques may give more insight into IFN-γ regulation of MerTK expression.

4.5.3 Assessing MerTK expression in Vascular Smooth Muscle Cells

VSMCs are a target of IL-1 in the atherosclerotic plaque, where inflammatory stimulation results in VSMC proliferation, migration to the plaque surface, and development of the atherosclerotic plaque structure.

Several human VSCM datasets were tested for MerTK expression (GSE109859, GSE59740, GSE185784). In each dataset and under all conditions, MerTK was found to be undetectable in this cell type.

4.6 Analysis of datasets to assess MerTK receptor expression in Lung Epithelial Cells and Alveolar Macrophages

IL-1β containing PS-positive MVs are likely to be produced in other tissues where pathogens are exposed to macrophages. Since infections such as pneumonia are linked to an increased risk of plaque rupture it is possible that MVs produced in the lung may enter the circulation and interact with arterial atherosclerotic plaques. They may also act locally within the lung tissue so we aimed to determine whether MerTK expression alters in lung epithelial cells and alveolar macrophages.

4.6.1 Determining the effect of the bacterial endotoxin (LPS) on MerTK expression in alveolar macrophages

LPS is a gram-negative bacterial endotoxin that present in the outer membrane of their cell wall. It acts as an antigen inducing inflammatory response via activating the toll-like receptor; TLR4 that is expressed on myeloid cells such as the macrophages. TLR4 activation leads to diverse intracellular signalling pathways involving activation the transcription factor; NF-κB that trigger the biosynthesis of inflammatory mediators (Lu et al., 2008). LPS has been implicated in several diseases including respiratory diseases. The lower respiratory tract primary immune response is the resident alveolar macrophages which offers the first line of cellular defence to clear the respiratory tract from invading pathogens and/or pollutants (Sibille and Reynolds, 1990).

Several studies reported an association between respiratory tract infection and atherosclerotic plaque rupture leading to myocardial infarction (Keller et al., 2008, Naghavi et al., 2003). We sought to determine whether LPS from respiratory infections regulates the MerTK receptor expression on alveolar macrophages, which may serve as a target for PS-positive MVs.

Hypothesis: LPS increases MerTK gene expression in alveolar macrophages.

Dataset Analysed: Reynier et al 2012, conducted a human *in vivo* study in seven healthy human subjects to investigate the effects of LPS treatment on alveolar macrophages. Each subject was challenged with instilled LPS 10ml (concentration was not specified) in one segment of the lung via bronchoscopy and instilled sterile saline (10ml) in the contralateral lung segment was used for intra-individual comparison i.e. to serve as a control. Bronchoalveolar lavage was carried out after six hours of treatment and alveolar macrophages were isolated for RNA extraction and gene expression profiling was carried out via microarray (Reynier et al., 2012).

Results: Analysed data showed no significant difference in MerTK gene expression between control and LPS treated alveolar macrophages (Fig. 4.15).

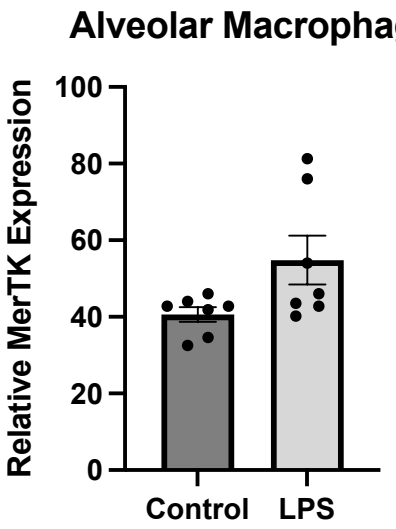

Figure 4.15: Assessment of MerTK RNA expression in response to LPS in human alveolar macrophages, from microarray data (Reynier et al., 2012).

Alveolar macrophages obtained by bronchioalveolar lavage from healthy human subjects, challenged with intra-bronchial either 10ml of LPS or 10ml of sterile saline in the contralateral segment (N=7). Values are presented as mean ± SEM, analysed by two-tailed paired t-test, where comparisons were not significant, $p>0.05$.

Summary: LPS does not alter MerTK gene expression in macrophages. Although, would be interesting if more subjects were tested to confirm the effect of LPS on MerTK gene expression as it showed inter-individual variability in the response to LPS, relative to control, and statistical tests gave a p value of 0.05.

4.6.2 Effect of LPS and TNF on MerTK expression in bronchial epithelial cells

Bronchial epithelial cells play essential roles in pulmonary immune homeostasis and act as defensive barrier against external pollutants and pathogens. Bacterial and viral infections of the pulmonary tract lead to activation of the immune response mediated by epithelial cells. The bacterial endotoxin, LPS is capable of activating the transcription factor, NF-κB in bronchial epithelial cells, which in turn leads to production of a variety of cytokines and chemokines responsible for the immune response (Inui et al., 2018). TNF can also activate bronchial epithelial cells to produce and secret pro-inflammatory cytokines such as interleukins IL-6 and IL-8 (Inui et al., 2018). This is mainly through activating the mitogen-activated protein kinases (MAPK) pathway as well as, the transcription factor NF-κB that transduce intracelular signals leading to diverse responses including cytokines production (Lee et al., 2013, Krunkosky et al., 2000). Therefore, the effects of LPS and TNF on bronchial epithelial cells may augment inflammatory response systematically affecting the atherosclerotic plaque. Investigating whether LPS and TNF may affect the MerTK receptor gene expression would give insight on whether MerTK is involved in inflammation and also whether it serves as a target for PS-positive MVs.

Hypothesis: MerTK is upregulated in bronchial epithelial cells exposed to LPS or TNF.

Dataset Analysed: Human bronchial epithelial cell line (Beas-2B) were either un-stimulated or stimulated with 1μg/ml LPS or with 20ng/ml TNF for 4 hours. Total RNA was isolated and gene expression profile was determined by microarray (Hu et al., 2012).

Results: The data obtained showed no significant change in MerTK gene expression when bronchial epithelial cells were stimulated with TNF or with LPS (Fig. 4.16).

Summary: The effect of TNF and LPS on MerTK gene expression was not elucidated properly due to low number of biological replicates.

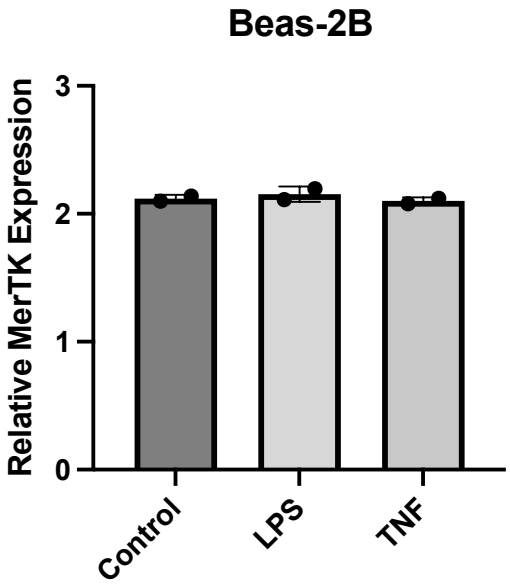

Figure 4.16: Assessment of relative MerTK expression in response to LPS and TNF in human lung epithelial cells, using microarray data (Hu et al., 2012).

Human bronchial epithelial cell line (Beas-2B) (N=2), treated with either 1μg/ml of LPS or 20ng/ml of TNF for 4h, and non-treated as control. Values are presented as mean ± SD.

4.6.3 Effect of rhinovirus and influenza virus on MerTK expression in human bronchial epithelial cells

Respiratory tract infections have been linked to increased risk of myocardial infarction and stroke (Ward et al., 2009). Seasonal influenza infection is found to be associated with high risk of developing acute myocardial infarction and ischemic heart disease mortality (Madjid et al., 2007). It was also shown that systemic respiratory infection are associated with a substantially high risk of myocardial infarction during the first three days of infection, the risk then decreases gradually (Smeeth et al., 2004). This association may be linked to provoking the systemic inflammatory responses that are driven by inflammatory cells and pro-inflammatory mediators in the circulation during respiratory tract infections.

Therefore, we sought to investigate whether these pathogens regulate MerTK receptor expression in human bronchial epithelial cells to predict whether MerTK may participate in the inflammatory state.

Hypothesis: MerTK receptor gene expression is upregulated in bronchial epithelial post-infection.

Dataset Analysed: Human bronchial epithelial cells (Beas-2B) were infected with 300 μl of diluted rhinovirus strain RV16 or influenza virus strain H1N1 in culture media (the multiplicity of infection used was 2 for each virus) and incubated for several times points; 2h, 4h, 8h, 12h, 24h, 36h, 48h, 60h, 72h along with non-infected cells as control. Each time point was of five biological replicates. After each assigned time point, total RNA was isolated and gene expression profile was determined by microarray (Kim et al., 2015).

Results: Both data obtained from Beas-2B infected with Rhinovirus and/or Influenza Virus showed no significant change in MerTK gene expression compared to non-infected control. The expression of MerTK has increased over time post-infection in both the Rhinovirus infected cells and non-infected control (Fig. 4.17 A). Similarly, Beas-2B infected with Influenza Virus showed no significant alteration in MerTK expression and increased over time post-infection in both infected and non-infected control (Fig. 4.17 B).

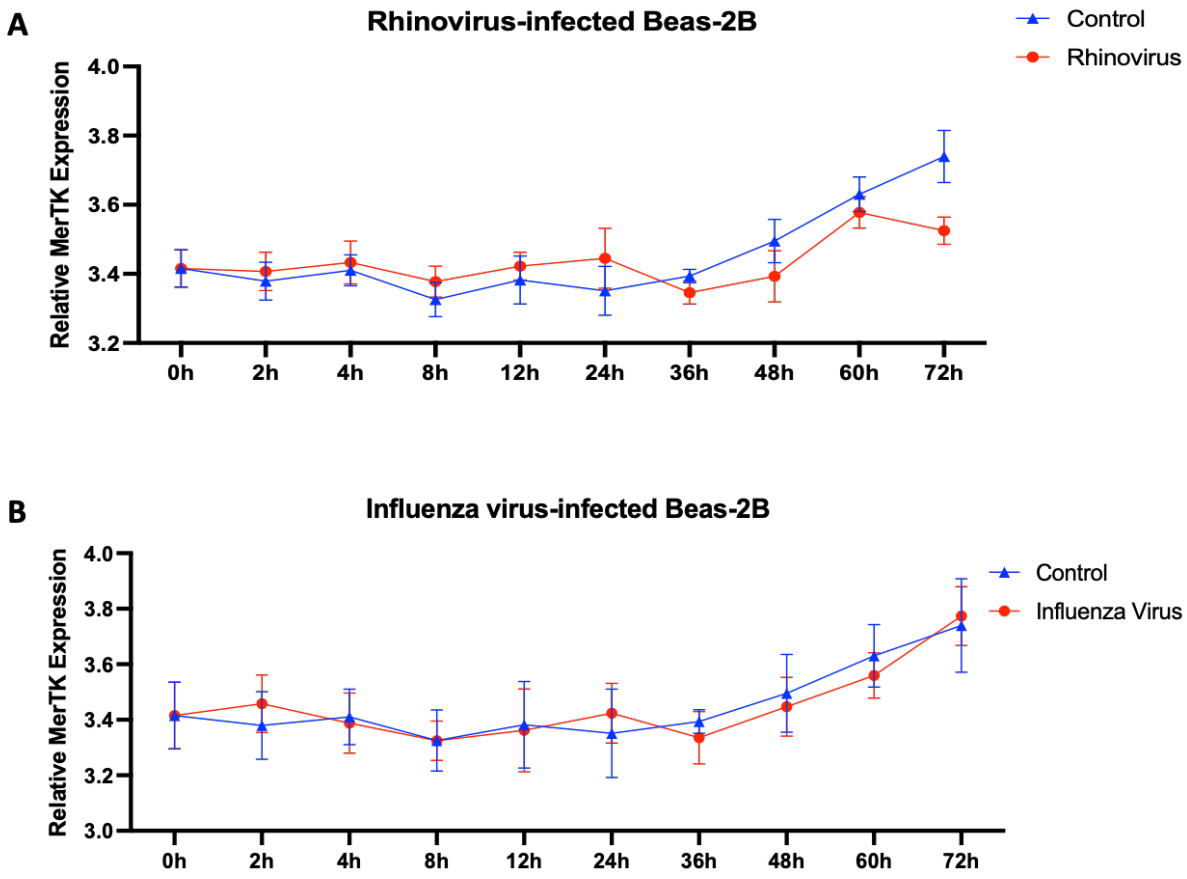

Figure 4.17: MerTK expression in response to viral infection in human bronchial epithelial cells, from microarray data (Kim et al., 2015).

Human bronchial epithelial cell line (Beas-2B) for non-infected control or infected with 300µl of diluted viruses (the multiplicity of infection used was 2 for each virus); A) Rhinovirus or B) influenza virus for multiple time points. Values are presented as mean ± SEM (N=5), analysed by Two-Way ANOVA with Šídák's correction method for multiple comparisons test, where all comparisons were not significant, $p>0.05$.

Summary: These data suggest that MerTK expression is not altered in Beas-2B post-infection with either Rhinovirus or the Influenza Virus nor post-infection over time. This supports the role of MerTK as anti-inflammatory receptor and it may also participate in MV targeting. Further investigations are needed to prove whether MerTK is involved in PS-positive MV binding.

4.7 Summary and Discussion

The overall aim of this project has been to test whether PS-positive MVs containing IL-1β are targeted to the PS-receptor, MerTK. In order to understand which cells express MerTK and which conditions lead to changes in its expression, we assessed whether expression of MerTK is altered in a variety of cells involved in initiating and progressing atherosclerosis. We used deposited datasets to investigate this, since a large source of data is available from a variety of studies, that have not sought to specifically quantify and compare changes in MerTK. A summary of these findings is outlined in Table 4.1.

Table 4.1: Summary of human cell types assessed for MerTK expression.

Category	Cell Type	Treatment	MerTK Expression	Reference
Endothelial Cell	HUVECs	TNF-α	Downregulated	(Viemann et al., 2006)
	HUVECs	IL-1	Downregulated	(Mayer et al., 2004)
	HUVECs	High Shear stress	No change	(White et al., 2011)
	HUVECs	Low Shear Stress	No change	(Andersson et al., 2005)
	HUVECs	High intraluminal pressure	No change	(Andersson et al., 2005)
	HUVECs	IFN-γ & IFN-α	No change	(Indraccolo et al., 2007)
	HMEC-1	TNF-α	No change	(Viemann et al., 2006)
	HAECT	oxLDL	No change	(Mattaliano et al., 2009)
Monocyte	Primary Monocyte	IL-10	Upregulated	(Teles et al., 2013)
Macrophage	Primary hMDMs	IL-1	No change	(Jura et al., 2008)
	Primary hMDMs	IL-6	No change	(Jura et al., 2008)
	Primary hMDMs	IFN-γ	No change	(Hu et al., 2005)
Vascular Smooth Muscle Cells	Human primary VSCMs	WNT5a, IL-1β, PDGF-BB, TGFβ1, TNFα	Not detectable in control or treated	Section 4.5.3 above

Alveolar Macrophage	Alveolar Macrophage	LPS	No change	(Reynier et al., 2012)
Bronchial Epithelial Cell	Beas-2B	LPS	No change	(Hu et al., 2012)
Bronchial Epithelial Cell	Beas-2B	TNF	No change	(Hu et al., 2012)
Bronchial Epithelial Cell	Beas-2B	Rhinovirus infection	No change	(Kim et al., 2015)
Bronchial Epithelial Cell	Beas-2B	Influenza Virus infection	No change	(Kim et al., 2015)

The MerTK receptor has been reported to be involved in removing apoptotic cells and is crucial for homeostasis of immune responses (Cai et al., 2017, Waterborg et al., 2018). MerTK receptor is activated via “eat me” signals which involves the cell externalising PS molecule on its surface. However, it is unknown whether MerTK is involved in binding MVs exposing PS on their surface. We aimed to identify the MerTK receptor expression in cells involved in atherosclerosis disease alongside with cells critical for pulmonary immune homeostasis. The results comparing MerTK gene expression are relative values and depend on the technologies used to detect mRNA (in this case all studies were using microarrays). In general our results suggest that MerTK receptor plays a role in attenuating inflammation, which is in line to what has been published with respect to its role in clearance and resolution of inflammation (Camenisch et al., 1999, Zhang et al., 2019).

The results from ECs exposed to cytokines released in the atherosclerotic plaque some have shown some downregulation of MerTK expression while some experiments showed no difference between cell treatment conditions. Likewise, the data we analysed from the literature regarding ECs exposed to shear stress and/or intraluminal pressure have suggested no significant difference in MerTK expression. This is consistent with our own data where we used qPCR to compare MerTK in HUVECs exposed to high, laminar versus low, oscillatory shear stress, where no changes in mRNA levels were found. Our qPCR did find a decrease in MerTK expression was in ECs exposed to high shear stress compared to static. Taken

together, these data show that the endothelium expresses MerTK, which is upregulated under certain conditions, suggesting that these cells may provide a target for MVs exposing PS on their surface.

Macrophages were also found to express MerTK. Similarly to ECs, macrophage MerTK expression was not markedly altered under a variety of treatment conditions. In a recent study, polarisation of macrophages toward M2 (M-CSF + IL-4) was shown to be associated with increased MerTK expression (Giroud et al., 2020). Our own qPCR data did not show significant changes in MerTK expression when polarised. Due to lack of time, we had low sample size, and more replicates from more donors would mean we could address this question fully and make robust comparisons. Interestingly, human primary monocyte from published microarray data, showed significantly upregulated MerTK when treated with IL-10, which is anti-inflammatory cytokine.

We did not observe MerTK expression from human primary smooth muscle cells, nor in microarray data published from smooth muscle cell. We looked for MerTK in some datasets, all of which showed it was undetected. In contrast, the Human Protein Atlas (HPA) reported MerTK receptor expression in smooth muscle cells. The HPA did not distinguish between different smooth muscle cell types, while we focused on vascular smooth muscle cells which are relevant to our question relating to a role in atherosclerosis. Overall this strongly suggests that vascular smooth muscle cells are not a target for PS-exposed MVs if MerTK plays a role in this targeting process.

The MerTK expression in both human alveolar macrophages and human bronchial epithelial cells (Beas-2B cell line), was not altered by either LPS or TNF treatment nor post infection with both Rhinovirus and Influenza Virus. This may fit more closely with a role for MerTK in the resolution phase rather than the inflammatory phase of innate immunity.

Collectively, MerTK receptor gene expression is cell type dependent. Our own comparison of CT values from qPCR in different cells shows a higher expression in macrophage and endothelial cells compared to HeLa cells, and an absence of expression in VSMCs, fitting with other datasets we tested. Modulation of MerTK expression by a variety of stimuli did not alter MerTK to a large extent. Whether these cells expressing MerTK receptor occurs in all stages of atherosclerosis and how the

receptor would participate in the disease progression or regression is still unknown. Analysis of single cell RNA-seq from macrophages, and other cells taken in situ directly from diseased and non-diseased arteries, would help address this question more fully. This is something our research group is actively investigating and we hope that such data will be available in the future.

The exact function of MerTK receptor in atherosclerosis is still not fully investigated and more data are needed in this context. For instance, the phagocytic role of MerTK receptor has been linked to atherosclerosis only to participate in progressing the atherosclerotic plaque necrotic core (Thorp et al., 2008). However, deficiency of the other member of TAM family; Axl receptor, did not affect the progression of the plaque (Subramanian et al., 2016). Whereas the role of the third member of TAM family; Tyro3, has not been reported in atherosclerosis in the literature. This might be due to the fact that it is mainly expressed in the brain (Mark et al., 1994). The method used for MerTK receptor detection in this chapter is based on the mRNA level only. A study showed that LPS enhance the proteolysis of MerTK to produce a soluble form of Mer protein that act as a decoy receptor (Sather et al., 2007). Therefore, other detecting methods for the MerTK protein level such as western blot or immunohistochemistry will evaluate the presence of a functional protein hence, give more comprehensive insight into the role of MerTK receptor. It is of interest to understand whether MerTK receptor provides a target for MVs exposing PS molecule not only in the context of atherosclerosis but rather in general as this would give more insight into how MVs contribute in inter-cellular communication and even if MerTK might offer a suitable therapeutic target in diseased states.

Chapter 5 . Microvesicle delivery of IL-1β to responsive cells and MerTK dependence of vesicle targeting

5.1 Introduction/Hypothesis

Interleukin-1β serves as a key messenger in the pathogenesis of atherosclerosis as it induces inflammatory functions on cells that participate in the plaque initiation and progression. IL-1β exerts multiple actions on endothelial cells in atherosclerosis including upregulation of chemoattractant MCP-1 and induction of adhesion molecules ICAM and VCAM. This in turn leads to leukocyte recruitment, adhesion, and eventually migration into the intima progressing plaque formation. Multiple mechanisms for IL-1β release were proposed in the literature. The 'protected release' is our focus in this thesis which is the of MVs directly from the macrophage plasma membrane loaded with IL-1β (MacKenzie et al., 2001). This process is proceeded by parental cell membrane phospholipid rearrangement of the inner and outer leaflets which allows the exposure of the PS molecule on the surface thus expressed on the shed MVs surface (Ridger et al., 2017). Phosphatidylserine exposure on MVs may serve functionally to allow uptake and internalization of MVs by targeted cells. It is important to understand the underlying molecular machinery of MV cargo delivery, as it reveals the role of MVs in the pathophysiology of atherosclerosis and may prove of therapeutic value. Various mechanisms of MV targeting have been suggested in the literature including membrane fusion (Parolini et al., 2009) endocytosis (Svensson et al., 2013), and phagocytosis (Feng et al., 2010) (see also section 1.7). It remains unknown how macrophage derived MVs containing IL-1β interact with the endothelium or other target cells to deliver their cargo.

The MerTK receptor belonging to the TAM receptor tyrosine kinase subfamily has been widely shown to bind to PS exposed on apoptotic cell membranes (Scott et al., 2001). The PS molecule exposed on the surface of apoptotic cells serves as a ligand for the MerTK receptor. Therefore, our own group used a MerTK deficient zebrafish line and found that MerTK deficiency showed reduced IL-1β targeting of an inflammatory response in the head region of the fish following tailfin injury. We were

also able to image macrophage-derived MVs in the circulation. This led us to consider that MerTK may be a target for IL-1β containing MVs.

We **hypothesised that the MerTK receptor is involved in PS-positive MV targeting**. We therefore wished to test this in a mammalian *in vitro* cell based system to investigate the specificity of this mechanism.

We aimed to test whether MVs containing IL-1β are delivered to target cells through a receptor-ligand interaction. We used HeLa cells, an epithelial cell line, as a reporter bioassay sensitive to IL-1β delivery, which was also amenable to siRNA transfection to achieve knockdown of MerTK. We used IL-6 secretion as the response measured to IL-1β exposure. This was implemented by applying macrophage-derived MVs into HeLa cells in the presence or absence of IL-1 receptor antagonist (IL-1Ra) to assess HeLa cell response to IL-1β by measuring IL-6 levels. In addition, this was performed with or without MerTK receptor knockdown to the dependence of IL-1β delivery on MerTK receptor expression.

5.2 Results

5.2.1 Optimisation of HeLa cell line as a bioassay responsive to IL-1b

Testing the sensitivity of IL-6 and IL-8 production in response to IL-1b in HeLa cells

IL-1β acts on the Type 1 IL-1 cell surface receptor to induce the production of downstream inflammatory cytokines such as IL-6 and IL-8 due to signalling and activation of the transcription factor NF-κB (Yu et al., 2020). Thus, we set out to measure the time and concentration dependence of IL-1β-stimulation of HeLa cells for IL-6 and IL-8 release measured using ELISA.

In order to identify the responsiveness of HeLa cells to IL-1β for release of both IL-6 and IL-8, we used recombinant IL-1β treatment in order to test known concentrations of IL-1β in a concentration dependence assay. We wished to determine whether HeLa cells are more sensitive to IL-8 or IL-6 production and which cytokine production shows a typical dose-response relationship, before applying macrophage-derived MVs.

To assess the time-course of IL-8 and IL-6 production, HeLa cells were treated with human recombinant IL-1β at 10 ng/ml over different time points over the typical range described in the literature (Yang et al., 2008, Legrand-Poels et al., 2000). We observed that after 6 hours of IL-1β stimulation, HeLa cells produced significant levels of IL-6, compared to earlier time points (Fig. 5.1 A) as measured by ELISA.

Next, we aimed to evaluate the dose-response effect of IL-1β on HeLa cell production of IL-6 and IL-8. We aimed to test within the range of IL-1β levels found to be produced by hMDMs, since we need the bioassay to be sensitive to these levels. Therefore concentrations were selected ranging from 1pg/ml to 10 ng/ml. This dose-response effect was performed in the absence and presence of the IL-1 receptor antagonist (IL-1Ra) on IL-6 (Fig. 5.1 B&C) and IL-8 (Fig. 5.2 A&B) release by HeLa cells for 6 hours as measured by ELISA. Note that in Figures (5.1 C) and (5.2 B) the IL-1β doses of 100 pg/ml and 300 pg/ml were not tested with IL-1Ra as there was not enough IL-1Ra available for this test.

The amount of IL-8 secreted by HeLa cells in response to lower doses of IL-1β did not alter above control, until a concentration of 100pg/ml IL-1β where the response was maximal, following a steep dose-response curve of an “all-or-nothing” response (Fig. 5.2). For IL-6 release in response to IL-1β, this showed a higher sensitivity to lower concentrations of IL-1β, over a range of concentrations between 3 to 100 pg/ml (Fig. 5.1 B). Due to lack of time to repeat these experiments, we decided to proceed with IL-6 as a reporter assay for IL-1β stimulation along with using IL-1Ra at a concentration of 200ng/ml which was sufficient to block IL-1β-induced IL-6 release across all concentrations of IL-1β tested in HeLa cells (red line, Figure 5.1).

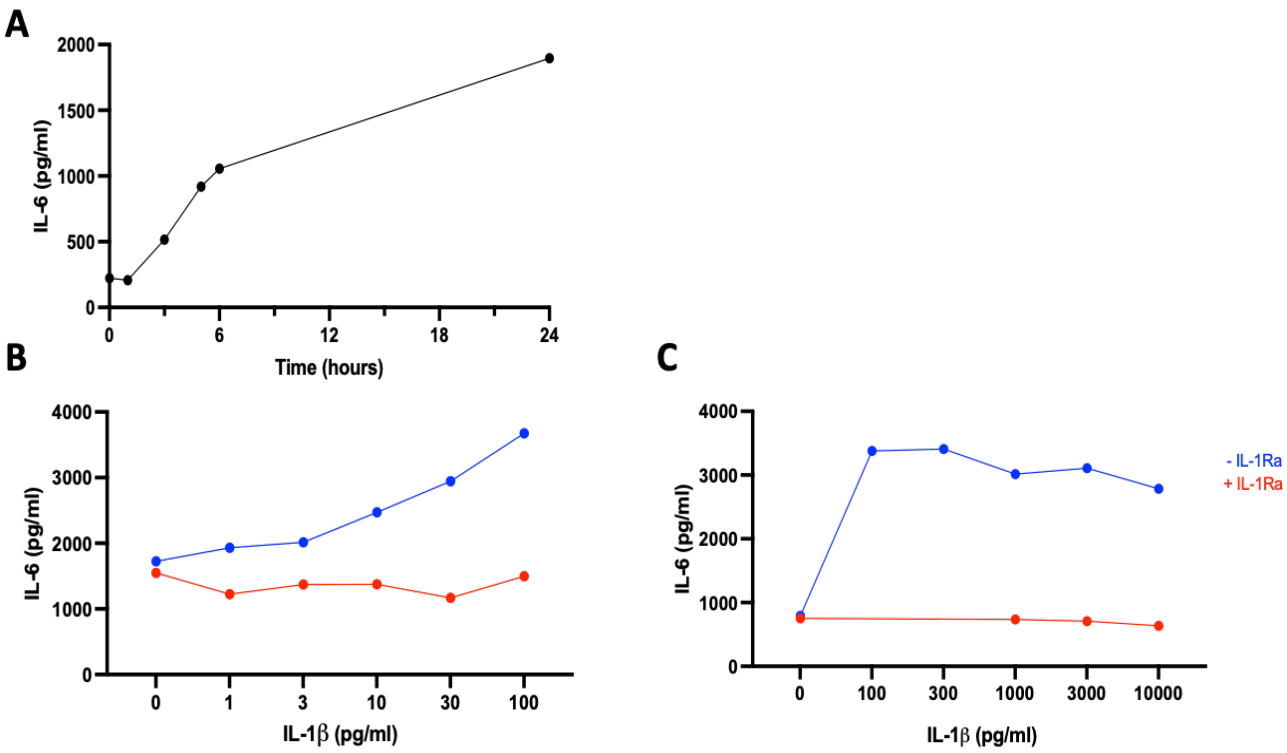

Figure 5.1: IL-6 release from HeLa cells in response to IL-1β measured by ELISA.

HeLa cells were treated with 10ng/ml IL-1β at different time points from 0 to 24 hrs (A), with IL-6 measured in the supernatant samples by ELISA. Cells were treated with increasing concentrations of IL-1β with released IL-6 measured by ELISA from the supernatant: B) stimulated with increasing concentrations (0-100pg/ml) of IL-1β ± IL-1Ra of 200 ng/ml for 6 hours; C) stimulated with increasing concentrations (0-10,000pg/ml) of IL-1β ± IL-1Ra at 20 ug/ml for 6 hours. (N=1).

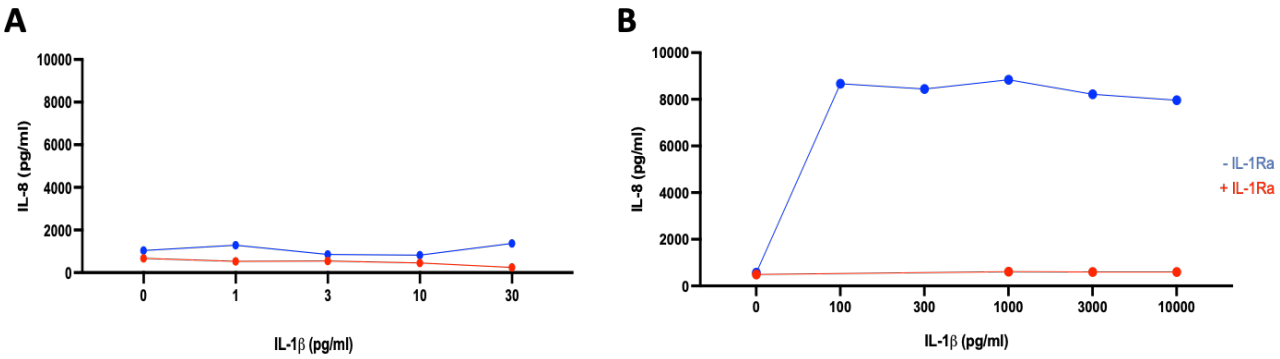

Figure 5.2: IL-8 release from HeLa cells in response to IL-1β measured by ELISA.

HeLa cells were treated with increasing concentrations of IL-1β with released IL-8 measured by ELISA from the supernatant: A) stimulated with increasing concentrations (0-30pg/ml) of IL-1β ± IL-1Ra of 200 ng/ml for 6 hours; B) stimulated with increasing concentrations (0-10,000pg/ml) of IL-1β ± IL-1Ra at 20 ug/ml for 6 hours. (N=1).

Optimisation of siRNA knockdown of MerTK in HeLa cells

Before we proceeded to silence the MerTK receptor gene expression, we sought to test the efficiency of the transfection. HeLa cell were transfected with siGlo a green fluorescent transfection indicator of siRNA delivery, using Dharmafect-1 transfection reagent. After 24h following transfection cells were imaged and compare to un-transfected control cells (Fig. 5.3 B&A, respectively). This showed that the transfection process was successful as the siGlo indicator is localised intracellularly to the majority of cells in the field of view.

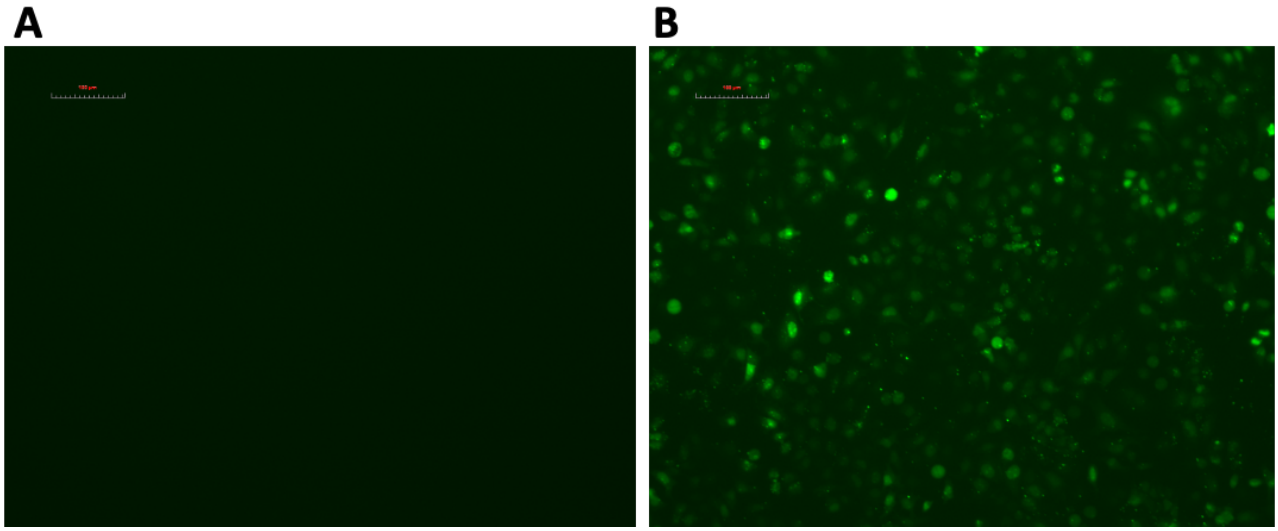

Figure 5.3: siGlo transfection of HeLa cell line.

HeLa cells were transfected with siGlo Green Transfection Indicator (for siRNAs) at 25 nM and non-transfected cells. Images were taken at 24 hours after transfection. A) non-transfected (negative control). B) Transfected with RNA siGlo. The images are representative of n=2 with two technical replicates for each.

We then tested the efficiency and optimal time of siRNA-mediated MerTK gene silencing in HeLa cells. We used SMARTpool siRNAs (Dharmacon), a pool of 4 optimised siRNAs targeted to human MerTK. The MerTK knockdown efficiency was measured at the RNA level using qPCR, at 24 hrs and 48 hrs post-transfection (Fig. 5.4). We did not assess this at later time points, due to the rapid growth time of HeLa cells where over-confluence might confound their use in the IL-6 reporter assay when subsequently treating with hMDM MV samples. MerTK gene expression reduction was efficient 48 hours post-transfection with knockdown percentage of 92.7% while the reduction was 81.4% in 24 hours post-transfection. We therefore proceeded to use 48 hours post-transfection in subsequent experiments, since this showed a higher MerTK knockdown efficiency.

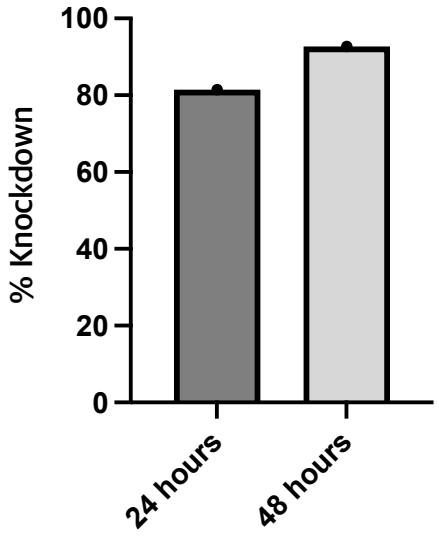

Figure 5.4: Assessment of siRNA-mediated MerTK gene silencing efficiency in HeLa cell line.

HeLa cells were transfected with 25 nM of non-targeting control siRNAs and SMART-pool siRNAs targeting MerTK. The expression of MerTK was measured by qPCR at 24 hours and 48 hours post transfection. The efficiency of knockdown was calculated by comparing MerTK expression in non-targeting control cells to MerTK siRNA-treated cells. Data shown is n=1.

5.2.2 Delivery of IL-1β-containing MVs to IL-1β responsive HeLa target cells

hMDMs shed IL-1β-containing microvesicles

hMDMs release IL-1β through MVs, but the larger proportion of IL-1β is not MV-associated (see Chapter 3). We have observed donor variability in the amount of IL-1β measured in the MVs. Therefore, we sought to assess the amount of IL-1β contained in MVs produced from hMDMs isolated from each human donor prior to applying those onto HeLa cells. hMDMs were isolated and differentiated from three different human donors. Cells were untreated (control), LPS-primed with or without subsequent BzATP stimulation. MVs were isolated by multiple centrifugation then, IL-1β levels were assessed by ELISA in total supernatant, in MV pellets, and in supernatant depleted of MVs (Fig. 5.5). This showed that the majority of IL-1β that was produced from LPS-primed and BzATP stimulated cells, was not released through MVs but rather was found in the MV-depleted supernatant when compared to the total supernatant or depleted supernatant.

This information on relative IL-1β levels in each fraction links directly to the samples applied to the HeLa cell bioassay (± IL-1Ra or ± MerTK knockdown), responsive to IL-1β using IL-6 production as a response. The same donor samples were used in the IL-6 bioassay, where these IL-1β levels were measured by ELISA; i.e. the same symbols are used corresponding to the same donor across the graphs presented for IL-1β levels and for their targeting to HeLa cells measured by IL-6 responses. The experimental plan for measuring targeting of hMDM supernatant and MV samples to HeLa cells is shown in Figure (5.6).

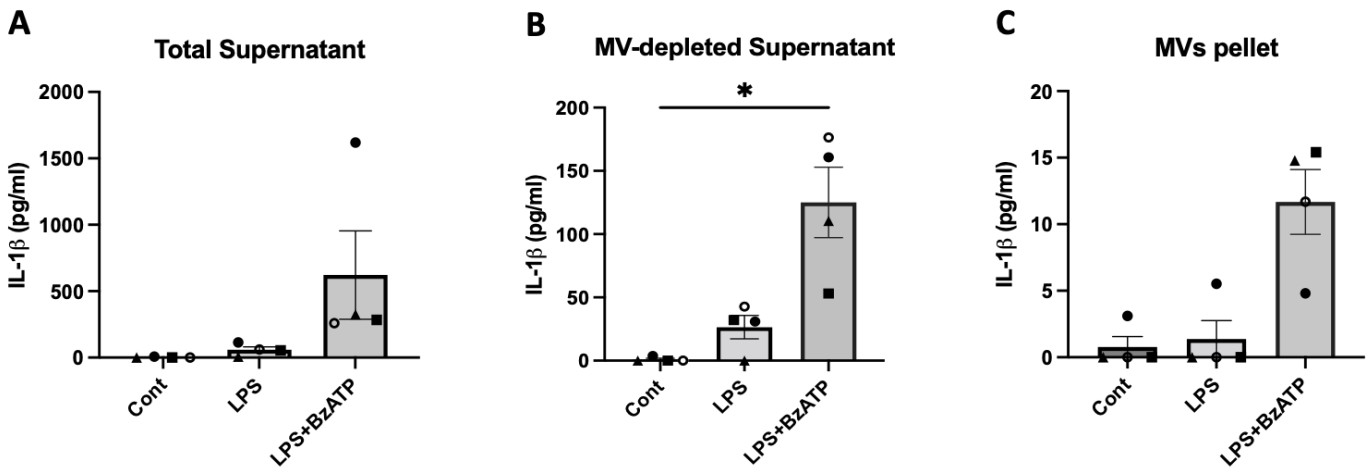

Figure 5.5: IL-1β release in MV and MV-depleted fractions from human primary monocyte-derived macrophages (hMDMs) measured by ELISA.

hMDMs were untreated (control) or primed with 1µg/ml LPS for 3h followed by ± stimulation with 300µM BzATP for 20min (N=4). Supernatants were collected and tested, or in parallel were separated by differential centrifugation to obtain a pellet containing MVs or the supernatant depleted of MVs. The IL-1β levels in each fraction were measured by ELISA: A) in the total supernatant. B) in the MV-depleted supernatant. C) in the MV pellet obtained by differential centrifugation. Each symbol represents a donor and is the same symbol by donor corresponding across each graph. Values are presented as mean±SEM, analysed by One-way ANOVA with Tukey's correction for multiple comparisons test, *$p<0.05$ or, ns where $p>0.05$.

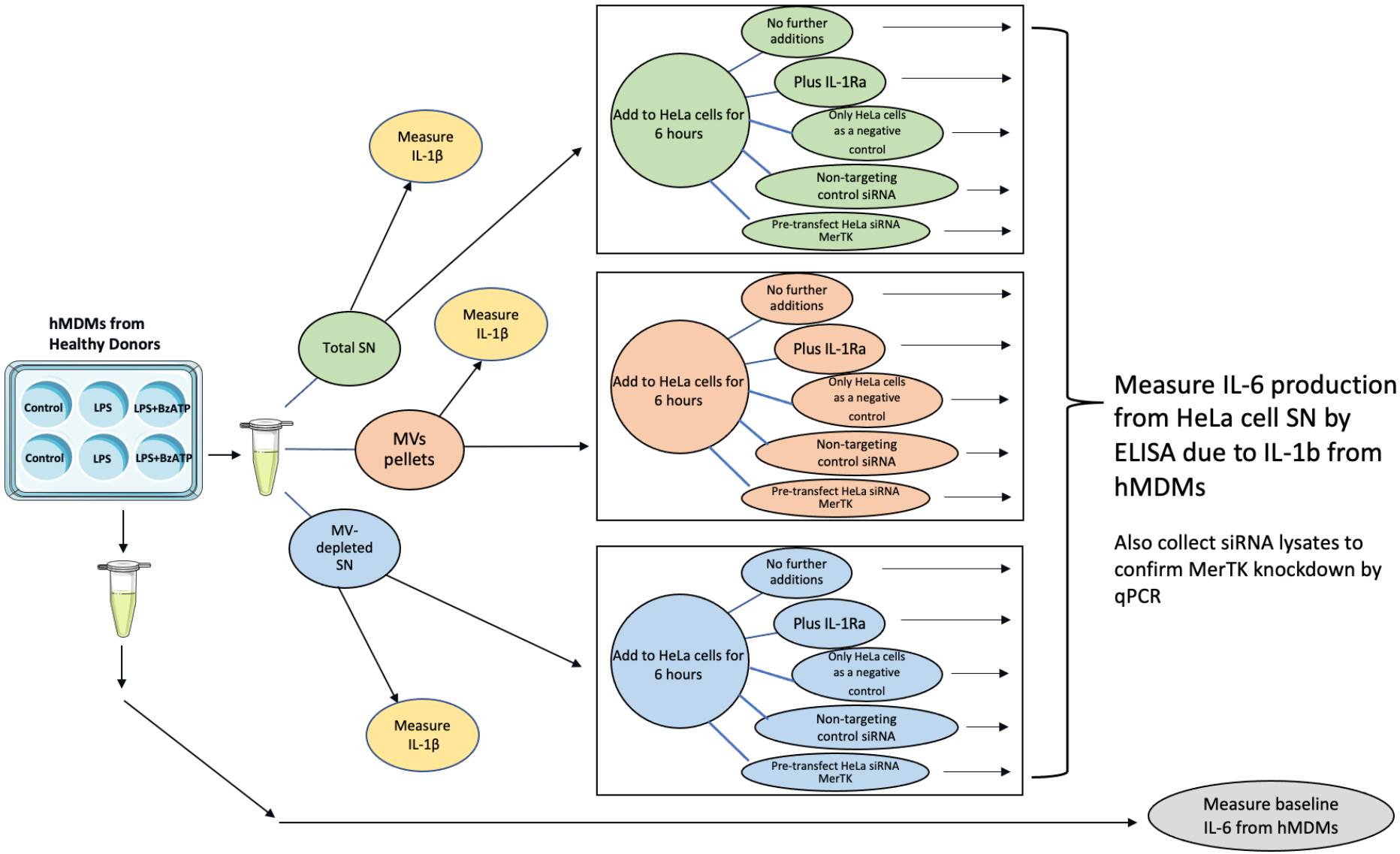

Figure 5.6: Schematic diagram of experimental plan. A summary of the experiments that were performed and presented in this chapter.

After confirming that IL-1β is contained in MVs, even if in lower proportions to the total production, we proceeded to use the *in vitro* IL-1β responsive reporter assay i.e. the HeLa cell IL-6 production, when incubated with hMDMs IL-1β-containing MVs/supernatants. This was implemented via applying the hMDMs IL-1β-containing MVs/supernatants onto HeLa cells for 6 hours and the released IL-6 was measured by ELISA (Fig. 5.7). MVs were isolated by multiple centrifugation from primary hMDMs with the following conditions established; non primed/treated, LPS-primed only, LPS-primed and BzATP treated as described in Chapter 3. We intended to apply the IL-1β-containing MVs and the total supernatant as well as the MV-depleted supernatant, in order to compare the HeLa cell response i.e. IL-6 levels from each, as outlined in the overall plan (Fig. 5.6), where each donor hMDM were used in the bioassay ± IL-1Ra (to evaluate IL-1β specific responsiveness) and ± MerTK knockdown.

These hMDM samples were applied onto HeLa cells in the presence of absence of the IL-1Ra, in order to assess the proportion of IL-6 response that is specific to IL-1β for 6 hour incubation with hMDM samples (Fig. 5.7 A,B,C). The data showed that HeLa cells do secrete IL-6 in response to IL-1β from hMDMs supernatants. This includes IL-1β-containing MVs although, the IL-6 levels were lower and variable between replicates and not statistically significantly different. However, the release of IL-6 in the absence of IL-1Ra from HeLa incubated with the total supernatant (which was not subjected to differential centrifugation) of LPS-primed and BzATP treated hMDMs showed a significant increase when compared to the control (Fig. 5.7 A). HeLa cells incubated with the IL-1β-containing MVs, released IL-6 (Fig. 5.7 C) which was entirely abolished in the presence of IL-1Ra; this effect was not significant statistically, although this is likely due to the noise and variability in the IL-6 response in the absence of IL-1Ra, since all IL-1Ra treatments blocked all IL-6 production.

The hMDM samples transferred to HeLa cells may contain IL-6 produced by the hMDMs cells themselves. Therefore the levels of IL-6 in the hMDM supernatants were tested as shown in Figure (5.7 F). The hMDM supernatants treated with LPS both in the absence and presence of BzATP, contained IL-6 (although the levels were variable between donors), suggesting that hMDMs secreted IL-6 in response to LPS; this is unsurprising as TLR4 signalling upregulates IL-6 transcription. In order to more accurately assess the HeLa cell response to IL-1β contained in the hMDM MVs/supernatants the hMDM IL-6 baseline was subtracted from the IL-6 released by HeLa cells in response to the hMDM sample incubations (Fig. 5.7 D,E). The IL-6 levels

after baseline subtraction were highly variable between donors and were not significant statistically. This partially reflects the variability in the IL-6 baseline production by hMDMs. The subtraction was not performed on the HeLa IL-6 response to MV pellets data since IL-6 is secreted by a conventional ER-Golgi secretion pathway, and therefore unlikely to be present within the pelleted MVs. This assumption is likely to hold true, as IL-1Ra completely blocked the HeLa IL-6 response to MVs without baseline subtraction, while this was not the case for total and depleted supernatants before baseline subtraction.

Taken together, the data suggest that HeLa cells released IL-6 in response to the hMDMs IL-1β containing MVs/supernatant. IL-1Ra appeared to inhibit the IL-6 response, although this was not statistically significantly different, likely due to donor variability in IL-1β production as seen in the IL-1β ELISA measurements (Fig. 5.5), as well as in baseline IL-6 production by hMDMs. More replicates are needed to identify whether these differences are statistically significant in order to draw firm conclusions.

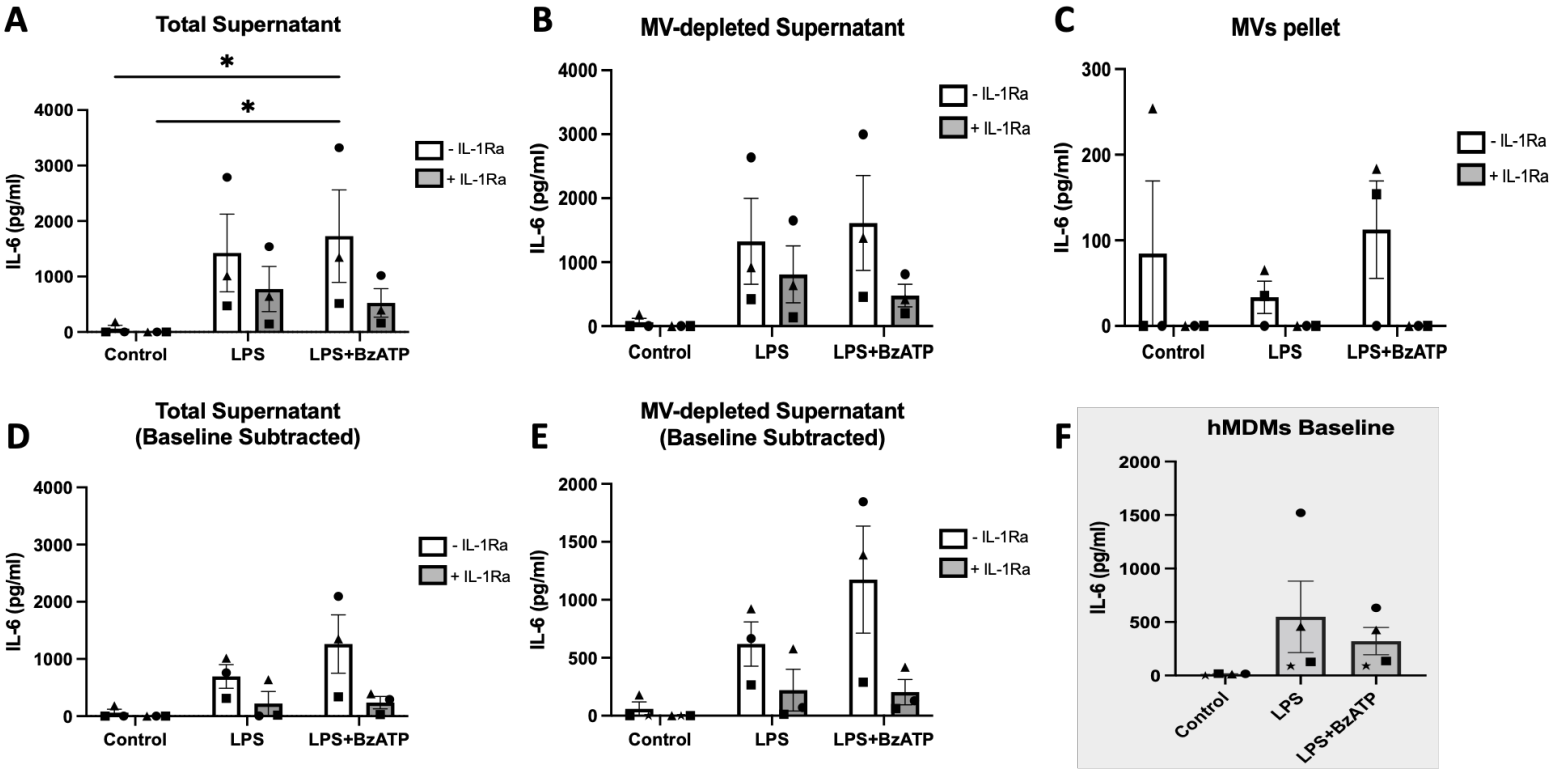

Figure 5.7: IL-6 release from HeLa cells after incubation with hMDMs supernatant and MV fractions.

HeLa cells were incubated for 6h ± IL-1Ra with hMDM samples, of :A) total supernatant; B) MV-depleted supernatant; C) MV pellets. followed by IL-6 measured in HeLa supernatants by ELISA. D & E show IL-6 measurements from A & B after subtraction of the IL-6 measured in the hMDM supernatants without addition to HeLa cells (i.e. baseline IL-6 levels). F) hMDM release of IL-6 following control, LPS or LPS+BzATP treatment. Each symbol represents a single donor matches the symbols corresponding across all figures in this section. Data is mean±SEM for (N=3 donors), analysed by Two-way ANOVA with Tukey's correction for multiple comparisons test, *$p<0.05$, ns $p>0.05$.

We sought to assess the effect of siRNA-mediated knockdown of MerTK in HeLa cells on IL-6 release following incubation with hMDM IL-1β-containing MVs/supernatant (see plan in Fig. 5.6). Thus, HeLa cells were transiently transfected with the MerTK siRNA and non-targeting siRNA as a negative control for 48 hours prior to the incubation with hMDMs IL-1β containing MVs/supernatant for 6 hours. The MerTK knockdown efficiency was evaluated in each experiment by qPCR presented in Table 5.1 below, averaging 91% knockdown efficiency across all experiments.

Table 5.1: The efficiency of MerTK gene siRNA-mediated knockdown

Experiment	Symbol	$2^{-\Delta\Delta CT}$	% Knockdown
1	●	0.153	84.6 %
2	■	0.0632	93.6%
3	▲	0.0526	94.7 %

Knockdown of MerTK produced no change in HeLa cell IL-6 production from total supernatants (Fig. 5.8 A), but a significant increase in IL-6 production by HeLa cells was seen following incubation with MV pellets from hMDM for control, LPS, LPS+BzATP treatments, respectively (Figure 5.8 C). The control hMDM vesicle-depleted supernatants also showed an increase in IL-6 production for MerTK knockdown compared to the siNT control (Fig. 5.8 B). This indicates that MerTK depletion may contribute to augmenting the inflammatory response.

Collectively, these data suggest that IL-1β containing MVs are not targeted to HeLa cells via the MerTK receptor when using IL-6 as a biological assay for IL-1β responsiveness. Further validation of these results in primary cells is required to draw firm conclusions.

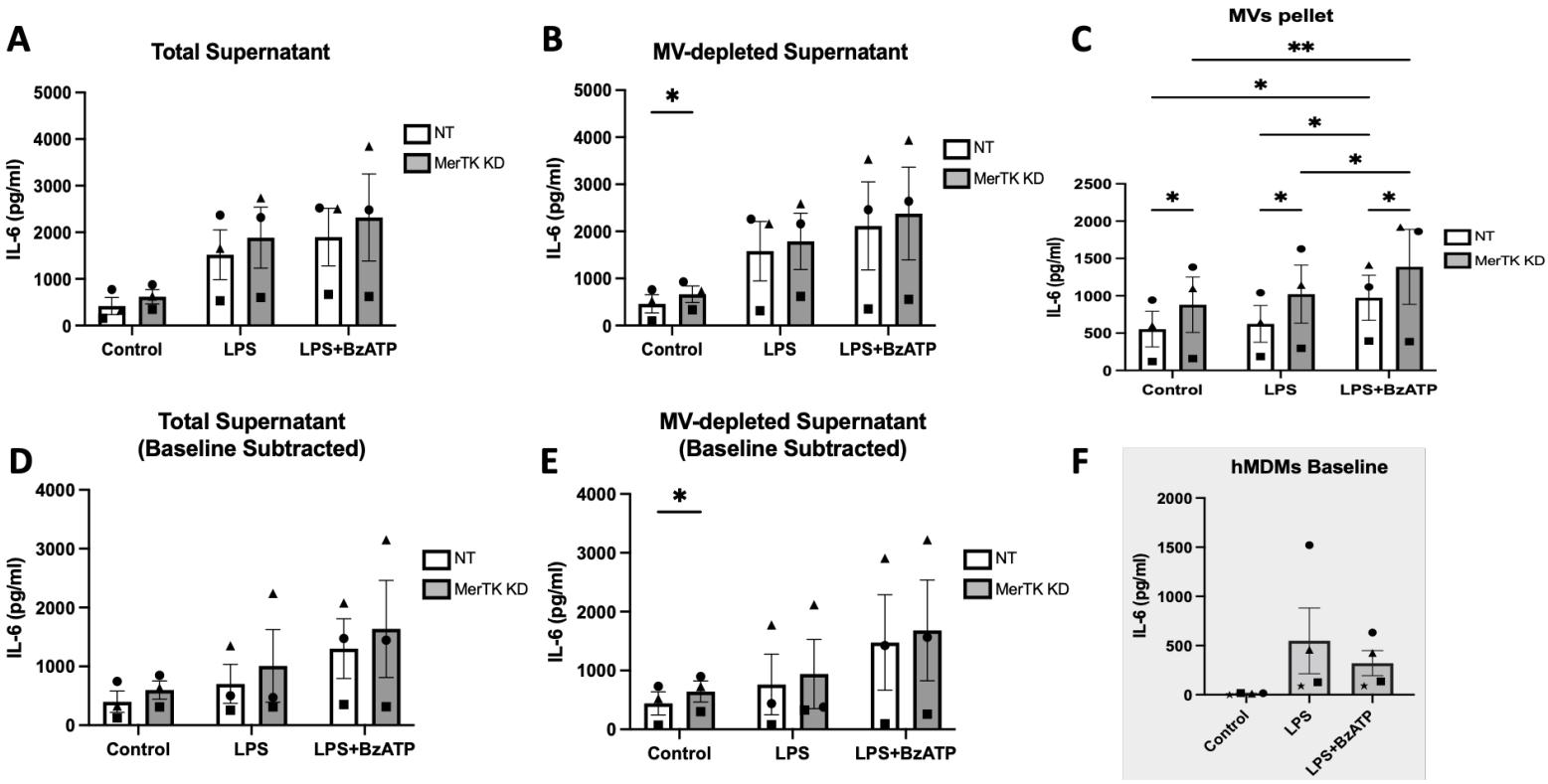

Figure 5.8: Assessment of the effects of MerTK receptor depletion on IL-6 release from HeLa cells after incubation with hMDMs supernatants by ELISA.

siRNA-mediated MerTK knockdown in HeLa cells for 48 hours, subsequently incubated with hMDMs: A) total supernatant. B) MV-depleted supernatant. C) MVs pellets. Each for 6 hours (N=3), and the released IL-6 was measured by ELISA. The figures D & E show IL-6 measurements from A & B after the hMDMs baseline subtraction. F) represents the hMDMs baseline release of IL-6 from the three conditions. Each symbol represents a donor and is corresponding in all figures. Values are presented as mean±SEM, analysed by Two-way ANOVA with Tukey's correction for multiple comparisons test, *p<0.05, **p<0.005, ns p>0.05.

5.1 Discussion

The MerTK receptor is activated by its ligands Protein S and Gas6 (Nagata et al., 1996), that bind to the PS molecule externalized on the cell surface (Nakano et al., 1997) leading to downstream signalling to mediate apoptotic cell clearance (Scott et al., 2001). Here we explored the involvement of the MerTK receptor in targeting PS-positive IL-1β-containing MVs and its contribution to IL-1β delivery to the target cell. This was carried out on an optimised *in vitro* IL-1β responsive cell model of HeLa cell IL-6 production. In parallel we tested MV-associated IL-1β release from primary hMDMs prior to incubation with HeLa, and found that the majority of IL-1β was not contained in MVs. This indicates that MV shedding is not a major secretory pathway for IL-1β as reported by Mackenzie et al. (2001), compared to other MV-independent release mechanisms. Such mechanisms involved in MV-independent IL-1β secretion in macrophages have been proposed in the literature. One of those is the $P2X_7$ receptor-mediated membrane permeabilization through the pore forming protein gasdermin D allowing the exportation of IL-1β (Evavoled et al., 2018). The other is also $P2X_7$ receptor-mediated process to form multivesicular bodies that exocytose exosomes entrapping IL-1β (Qu et al., 2007). The amount of IL-1β measured in the MV-depleted supernatant was lower than the amount in total supernatant, which may have been due to degradation of the cytokine during the process of MV isolation. We cannot exclude the possibility that IL-1β in the MVs is also subject to degradation during this process.

Knockdown of MerTK in HeLa cells prior to incubating with hMDMs MVs/supernatants resulted in an increased inflammatory IL-6 secretion response compared to the non-targeting siRNA control, suggesting that MerTK receptor may confer anti-inflammatory properties (see chapter 4). Importantly this suggests that IL-1β targeting to HeLa cells is not dependent on MerTK, as IL-6 production would have been decreased if targeting had been dependent on this receptor. The expression of MerTK may dampen the inflammatory response and silencing its expression resulted in more IL-6 release. This effect is similar to studies reported where deletion of MerTK led to exacerbation of immune responses (Waterborg et al., 2018, Cai et al., 2017). However, these observations require further investigation and validation in primary cells such as endothelial cells alongside the use of MerTK small molecule inhibitors such as

monoclonal antibodies. It is important to note that the PS-positive MVs produced by hMDMs were low in number (see chapter 3) where they accounted for a low proportion of the MVs isolated from hMDMs. This may suggest that MVs target cells through other molecular machinery rather than through the MerTK receptor, including membrane fusion (Parolini et al., 2009) endocytosis (Svensson et al., 2013), and phagocytosis (Feng et al., 2010).

It is of importance to understand whether the PS molecule is participating in MVs cargo delivery. The involvement of the PS molecule itself, in MVs targeting was not investigated due to lack of time. The use of tools such as annexin V or enriching the PS-positive MV fraction using annexin V biotin-strepatividin bead pull-down as performed previously by MacKenzie et al. (2001), would be appropriate to extend this work. We also aimed to assess the internalisation of MVs using surface labelling techniques to track this process.

Collectively, this data suggests that the majority of macrophage released IL-1β is not MV-associated and that MVs containing IL-1β do not appear to depend on MerTK expression to target IL-1β to HeLa cells.

Chapter 6 . General Discussion

MVs are shed from plasma membrane protrusions as a result of cytoskeletal remodelling followed by their release into the extracellular space. They were described to function as mediators of inter-cellular crosstalk in both healthy and pathological states through exchange of biologically active materials inside as well as expressed on their surfaces (Ratajczak et al., 2006, Beaudoin and Grondin, 1991). Of note, their release has been widely linked to all stages of atherosclerosis disease (Badimon et al., 2017). MVs have the potential to induce inflammation in atherosclerosis by delivering biological cargo including lipids, molecular materials, and inflammatory cytokines such as IL-1β. MVs containing IL-1β were previously shown to express the PS molecule on their outer surface (MacKenzie et al., 2001). Multiple cell types are involved in atherosclerotic plaque development and stability; MVs are derived from cells including monocytes and macrophages, the latter being one of the most abundant within the developed plaque (Leroyer et al., 2007). The tyrosine kinase receptor, MerTK, has been identified as a key PS-receptor (Nakano et al., 1997). In addition, our group obtained preliminary data to show attenuated IL-1β targeting following tailfin injury in zebrafish lacking the MerTK receptor. We therefore set out to test the hypothesis that PS-positive macrophage-derived IL-1β-containing MVs target endothelial cells via the MerTK receptor.

In this project, we focused on investigating whether MV production from macrophages is stimulus dependent alongside determining their relative IL-1β content. A previous study by Mackenzie et al. (2001) showed that macrophage-derived MVs contain IL-1β and their production was dependent on LPS-priming followed by $P2X_7$ receptor activation by ATP. However, the MVs isolation and characterisation analysis used in that study were different from our methodological analysis. For instance, they selectively isolated only the PS-exposing MVs using annexin V pull downs, and vesicles were not quantified using standardised methods such as bead-calibrated flow cytometry and nano-particle tracking analysis. There is also a gap in our knowledge regarding the shedding of PS-positive MVs from macrophages under those specific stimuli; LPS and BzATP. Thus, in this project we used more up-to-date MV isolation and characterisation methods. We isolated macrophage-derived MVs by differential

centrifugation methods and quantified MVs by bead-calibrated flow cytometry and found their production was stimuli independent. In contrast, some studies have shown that MV production is inducible from monocytes and macrophages using stimuli such as IFN (Cai et al., 2018), LPS and cholesterol (Liu et al., 2007), and IL-4 (Colombo et al., 2018). MV shedding has been shown to occur under basal conditions where they play a role in inter-cellular communication in response to their surrounding microenvironment (Beaudoin and Grondin, 1991).

We also found that the proportion of PS-positive MVs produced was not altered according to stimulus as determined by fluorescent annexin V labelling measured by flow cytometry. The MV population is considered heterogeneous in terms of PS molecule externalisation to the MV surface. PS externalisation has classically been considered a hallmark “eat-me” signal of cellular apoptosis (Fadok et al., 1992). More recently PS exposure was shown to occur in the absence of cell death. For example, $P2X_7$ induced PS exposure was shown to be a reversible phenomenon, dependent on stimulus strength and duration and not related to cell death (MacKenzie et al., 2005). The heterogeneity of PS exposure on MVs remains poorly understood. However, some studies have linked PS externalisation to specific stimuli, such as to cholesterol enrichment (Liu et al., 2007). It has been reported previously that some cells produced MVs that lack the PS moleucle on their surface (Bernimoulin et al., 2009, Connor et al., 2010). Our results show for the first time that primary human macrophages produce PS-negative MVs.

Determination of IL-1β content in MVs is important to understand the relative contribution of MVs in IL-1β release and delivery and their role in atherosclerotic plaque inflammation. IL-1β is produced when macrophages are primed with LPS leading to activation of NF-κB to induce the upregulation of inactive IL-1β (Pro-IL-1β). A second signal such as ATP is required to activate the inflammasome and caspase-1 to cleave pro-IL-1β into the mature form for activity at the IL-1β Type1 receptor when secreted. We found that IL-1β secretion within MVs was upregulated following LPS and BzATP treatment of human monocyte-derived macrophages, in line with previous findings (MacKenzie et al., 2001). The content of MVs is dependent on their surrounding microenvironment. For example, Gomez et al. (2020) showed that neutrophil-derived MVs contained increasing levels of specific miRNAs (miR155)

when cells were exposed to certain stimuli, including high fat diet and inflammatory conditions.

While we showed that macrophage-derived MVs contain IL-1β when stimulated with LPS followed by ATP, the majority of IL-1β released was not MV-associated and the levels of the IL-1β detected in those MV pellets were low compared to those detected in the MV-depleted supernatant. Several mechanisms of IL-1β release have been proposed in the literature since the process of MV shedding was shown by Mackenzie et al. (2001), one of those is the release of exosomes entrapping IL-1β (Qu et al., 2007). Recent findings show that the pyroptosis regulatory protein; Gasdermin D is involved in MV-independent IL-1β release. Studies have demonstrated that macrophage pyroptosis is induced following LPS or bacterial infections due to the activation of the pore forming protein Gasdermin D, accompanied by IL-1β release following cell death (Shi et al., 2015,(Kayagaki et al., 2015). More recent publications demonstrated release of IL-1β through the pore forming protein Gasdermin D from macrophages while maintaining viability (Evavold et al., 2018).

There are no previous studies exploring whether MerTK might be a target for PS-positive MVs. We explored this question for the first time; our preliminarily findings suggest that MerTK knockdown did not inhibit MV-mediated IL-1β-targeting detected through measuring induction of IL-6 release from HeLa cells.

Study limitations and future directions

It is important to mention that some experiments in our study need further expansion in order to be adequately powered statistically and to subsequently draw firm conclusions. This includes the investigation of IL-1β release from LPS primed macrophages after purinergic receptor activation in the absence and presence of the $P2X_7$ receptor inhibitor, A438079. It would have been useful to have increased the donor numbers for these experiments and to have tested the $P2X_7$ dependence of MV produced IL-1β and MV-independently secreted IL-1β. Alternatively, other $P2X_7$ receptor inhibitors could be investigated such as oxidized ATP and KN-62 or inhibitory monoclonal antibodies against $P2X_7$ receptor. If the BzATP induced IL-1β secretion was not found to be $P2X_7$ independent, it would be important to determine whether

other purinergic receptors contribute to MV shedding using specific molecular inhibitors of P2X and P2Y receptors.

The exploration of which model of IL-1β release constitute the major pathway in hMDMs would give more insight into how this cytokine target cells in the atherosclerotic plaque. This could be achieved through investigating the pathways proposed in the literature i.e. the exocytosis of exosomes entrapping IL-1β (Qu et al., 2007), and the Gasdermin D mediated pore formation and subsequently IL-1β release (Evavolde et al., 2018). Investigating whether IL-1β is released through exosomes can be achieved via isolating the pellet by ultracentrifugation method (at 100,000xg for 1 hour) and assaying the samples with either Western Blot or ELISA for IL-1β content. Alternatively, the pellet containing exosomes can be identified via western blot or immunohistochemistry for the common specific exosomes surface markers such as the tetraspanins including CD81, CD63, and CD9, together with IL-1β (Jiang et al., 2020). The exploration of IL-1β release through caspase-1 mediated cleavage of Gasdermin D have been carried out in this project but would also requires more replicates in order to be able to draw firm conclusions. We used the caspase-1 inhibitor, Ac-YVAD-cmk, which was limited to inhibiting caspase-1 primarily, and is involved in the canonical pathway of inflammasome activation and assembly. It has been proposed that other caspases in macrophage can cleave and activate Gasdermin D such as caspase-4 and 5, and caspase-11 in mice macrophages (Platnich et al., 2018). Therefore, further investigation is required to compare the contribution of Gasdermin D mediated release of IL-1β versus MVs shedding mechanism. For instance, using the pan-caspase, z-VAD-fmk, to further inhibit the caspase-4 and 5 or siRNA-mediated Gasdermin D or caspase gene siRNA knockdown methods. Recently disulfiram was identified as a Gasdermin D inhibitor, which may prove a useful tool, both experimentally and therapeutically to treat inflammatory disease (Hu et al., 2020). Moreover, other stimuli involved in IL-1β release can be tested to compare relative contribution of IL-1β secretion from MVs and from Gasdermin D pathway, such as the inflammasome inducer, nigericin. The IL-1β contained in the shed MVs was not detectable via western blotting, most likely due to low levels released as measured in ELISA. This is potentially due to the fact that IL-1β levels were limited by the cell numbers isolated from healthy participants as a result of the restricted volume of blood we were allowed to collect.

Determination of MV content with respect to IL-1β is of importance to investigate the role of MVs in IL-1β delivery. A study has shown that ATP stimulation of microglial cells had a great impact on the EVs contents (Drago et al., 2017). Therefore, proteomic and lipid analysis of MVs with and without LPS/ATP stimulation would give more insight into the extent of their contribution to atherosclerotic plaque inflammation. In addition, determining the number of MVs produced and measuring the vesicular IL-1β following various stimuli, and the proportion of PS-positive MVs produced would help in understanding the impact of MVs in atherosclerosis disease.

The visualisation of MVs and assessment of their temporal properties via electron microscopy was not investigated fully in this project due to lack of time. Further cell fixation protocol optimisation is needed. The electron microscopy analysis offers the opportunity to assess MV size and sample purity, i.e. containing sufficient MVs, as there is a chance of an overlap between MVs and exosomes. Importantly, we would wish to validate MV biogenesis mechanisms through labelling the plasma membrane, for example, using PKH labelling. This would enable tracking of MVs pinching off from the cell membrane using fluorescent video microscopy.

In this project, the investigation of the MerTK receptor role in targeting PS-positive MVs was performed using the HeLa cell line. While this was repeated 3-4 times, ideally we would require more replicates to reach high statistical power, considering the donor variability particularly in the baseline IL-6 production. Investigating the targeting of MVs to endothelial cells would be more relevant to atherosclerosis; in addition these cells express more of the endogenous MerTK compared to HeLa cells. Although, endothelial cell transfection would be more challenging to achieve high efficiency compared to HeLa cells, this would be the logical next step in this study.

Our study included the investigation of both populations of MVs, PS negative and positive MVs to investigate the role of MerTK in MV targeting. It would be more relevant to our hypothesis to test PS-positive MVs in the MerTK knockdown by isolating these MVs using the annexin V pull down method. Alternatively, the annexin V protein itself can be used to inhibit the PS-positive MV targeting as it competes to bind the PS molecule. Testing cell lines with MerTK permanent knockdown may give more insight into the role of MerTK in MV targeting. Considering other components of the MerTK receptor complex, i.e. its ligands: Gas6 and Protein-S in the future experiments may

have an impact on the results obtained, as our experiments were limited to testing the MerTK only. This can be tested in the presence and absence of inhibitors such as inhibitors for the other parts of the PS receptor TAM complex / protein S or Gas6 or monoclonal antibodies against MerTK.

In conclusion, macrophage-derived MVs are detectable in cell line models of monocyte/macrophages as well as in primary hMDMs. The data suggest that MV production is stimulus independent, and are a mixed population with respect to PS exposure where the proportion of PS positive MVs is not stimulus dependent. The production of IL-1β containing MVs requires two stimuli: LPS (TLR4 receptor) & ATP (Purinergic receptors). Interestingly, the human donor-derived primary macrophages offer the most consistent ATP-dependent IL-1β MVs production, compared to cultured monocytic cell lines. The expression of MerTK receptor was detected in endothelial cells and macrophages but absent in vascular smooth muscle cells for cell-types compared in relation to the atherosclerotic plaque. MerTK expression did not appear to be altered in response to a variety of conditions relevant to the plaque. Finally, IL-1β containing MVs do not appear to be targeted to cells via the MerTK receptor.

References:

ADINOLFI, E., CALLEGARI, M. G., FERRARI, D., BOLOGNESI, C., MINELLI, M., WIECKOWSKI, M. R., PINTON, P., RIZZUTO, R. & DI VIRGILIO, F. 2005. Basal activation of the P2X(7) ATP receptor elevates mitochondrial calcium and potential, increases cellular ATP levels, and promotes serum-independent growth. *Molecular Biology of the Cell,* 16**,** 3260-3272.

AGRAWAL, S., FEBBRAIO, M., PODREZ, E., CATHCART, M. K., STARK, G. R. & CHISOLM, G. M. 2007. Signal transducer and activator of transcription 1 is required for optimal foam cell formation and atherosclerotic lesion development. *Circulation,* 115**,** 2939-2947.

AKITA, K., ISODA, K., SATO-OKABAYASHI, Y., KADOGUCHI, T., KITAMURA, K., OHTOMO, F., SHIMADA, K. & DAIDA, H. 2017. An Interleukin-6 Receptor Antibody Suppresses Atherosclerosis in Atherogenic Mice. *Frontiers in Cardiovascular Medicine,* 4.

ALLSOPP, R. C. & EVANS, R. J. 2015. Contribution of the Juxtatransmembrane Intracellular Regions to the Time Course and Permeation of ATP-gated P2X7 Receptor Ion Channels. *Journal of Biological Chemistry,* 290**,** 14556-14566.

ANDERSSON, M., KARLSSON, L., SVENSSON, P. A., ULFHAMMER, E., EKMAN, M., JERNAS, M., CARLSSON, L. M. S. & JERN, S. 2005. Differential global gene expression response patterns of human endothelium exposed to shear stress and intraluminal pressure. *Journal of Vascular Research,* 42**,** 441-452.

ANDREI, C., DAZZI, C., LOTTI, L., TORRISI, M. R., CHIMINI, G. & RUBARTELLI, A. 1999. The secretory route of the leaderless protein interleukin 1 beta involves exocytosis of endolysosome-related vesicles. *Molecular Biology of the Cell,* 10**,** 1463-1475.

ASATRYAN, L., KHOJA, S., RODGERS, K. E., ALKANA, R. L., TSUKAMOTO, H. & DAVIES, D. L. 2015. Chronic ethanol exposure combined with high fat diet up-regulates P2X7 receptors that parallels neuroinflammation and neuronal loss in C57BL/6J mice. *Journal of Neuroimmunology,* 285**,** 169-179.

BADIMON, L., SUADES, R., ARDERIU, G., PENA, E., CHIVA-BLANCH, G. & PADRO, T. 2017. Microvesicles in Atherosclerosis and Angiogenesis: From Bench to Bedside and Reverse. *Frontiers in Cardiovascular Medicine,* 4.

BARRETT, T. J. 2020. Macrophages in Atherosclerosis Regression. *Arteriosclerosis Thrombosis and Vascular Biology,* 40**,** 20-33.

BARRY, O. P., PRATICO, D., SAVANI, R. C. & FITZGERALD, G. A. 1998. Modulation of monocyte-endothelial cell interactions by platelet microparticles. *Journal of Clinical Investigation,* 102**,** 136-144.

BASATEMUR, G. L., JORGENSEN, H. F., CLARKE, M. C. H., BENNETT, M. R. & MALLAT, Z. 2019. Vascular smooth muscle cells in atherosclerosis. *Nature Reviews Cardiology,* 16**,** 727-744.

BAZAN, J. F., BACON, K. B., HARDIMAN, G., WANG, W., SOO, K., ROSSI, D., GREAVES, D. R., ZLOTNIK, A. & SCHALL, T. J. 1997. A new class of membrane-bound chemokine with a CX(3)C motif. *Nature,* 385**,** 640-644.

BEAUDOIN, A. R. & GRONDIN, G. 1991. SHEDDING OF VESICULAR MATERIAL FROM THE CELL-SURFACE OF EUKARYOTIC CELLS - DIFFERENT CELLULAR PHENOMENA. *Biochimica Et Biophysica Acta,* 1071**,** 203-219.

BEHRENS, E. M., GADUE, P., GONG, S. Y., GARRETT, S., STEIN, P. L. & COHEN, P. L. 2003. The mer receptor tyrosine kinase: expression and function suggest a role in innate immunity. *European Journal of Immunology,* 33**,** 2160-2167.

BENNETT, M. R., SINHA, S. & OWENS, G. K. 2016. Vascular Smooth Muscle Cells in Atherosclerosis. *Circulation Research,* 118**,** 692-702.

BENSEN, J. T., DAWSON, P. A., MYCHALECKYJ, J. C. & BOWDEN, D. W. 2001. Identification of a novel human cytokine gene in the interleukin gene cluster on chromosome 2q12-14. *Journal of Interferon and Cytokine Research,* 21**,** 899-904.

BERCKMANS, R. J., NIEUWLAND, R., BOING, A. N., ROMIJN, F., HACK, C. E. & STURK, A. 2001. Cell-derived microparticles circulate in healthy humans and support low grade thrombin generation. *Thrombosis and Haemostasis,* 85**,** 639-646.

BERNIMOULIN, M., WATERS, E. K., FOY, M., STEELE, B. M., SULLIVAN, M., FALET, H., WALSH, M. T., BARTENEVA, N., GENG, J. G., HARTWIG, J. H., MAGUIRE, P. B. & WAGNER, D. D. 2009. Differential stimulation of monocytic cells results in distinct populations of microparticles. *Journal of Thrombosis and Haemostasis,* 7**,** 1019-1028.

BEVILACQUA, M. P., POBER, J. S., MAJEAU, G. R., COTRAN, R. S. & GIMBRONE, M. A. 1984. INTERLEUKIN-1 (IL-1) INDUCES BIOSYNTHESIS AND CELL-SURFACE EXPRESSION OF PROCOAGULANT ACTIVITY IN HUMAN VASCULAR ENDOTHELIAL-CELLS. *Journal of Experimental Medicine,* 160**,** 618-623.

BHARADVAJ, B. K., MABON, R. F. & GIDDENS, D. P. 1982. STEADY FLOW IN A MODEL OF THE HUMAN CAROTID BIFURCATION .1. FLOW VISUALIZATION. *Journal of Biomechanics,* 15**,** 349-362.

BIANCHI, B. R., LYNCH, K. J., TOUMA, E., NIFORATOS, W., BURGARD, E. C., ALEXANDER, K. M., PARK, H. S., YU, H. X., METZGER, R., KOWALUK, E., JARVIS, M. F. & VAN BIESEN, T. 1999. Pharmacological characterization of recombinant human and rat P2X receptor subtypes. *European Journal of Pharmacology,* 376**,** 127-138.

BIANCO, F., CERUTI, S., COLOMBO, A., FUMAGALLI, M., FERRARI, D., PIZZIRANI, C., MATTEOLI, M., DI VIRGILIO, F., ABBRACCHIO, M. P. & VERDERIO, C. 2006. A role for P2X(7) in microglial proliferation. *Journal of Neurochemistry,* 99**,** 745-758.

BIANCO, F., PRAVETTONI, E., COLOMBO, A., SCHENK, U., MOLLER, T., MATTEOLI, M. & VERDERIO, C. 2005. Astrocyte-derived ATP induces vesicle shedding and IL-1 beta release from microglia. *Journal of Immunology,* 174**,** 7268-7277.

BORING, L., GOSLING, J., CLEARY, M. & CHARO, I. F. 1998. Decreased lesion formation in CCR2(-/-) mice reveals a role for chemokines in the initiation of atherosclerosis. *Nature,* 394**,** 894-897.

BOSHUIZEN, M. C. S., HOEKSEMA, M. A., NEELE, A. E., VAN DER VELDEN, S., HAMERS, A. A. J., VAN DEN BOSSCHE, J., LUTGENS, E. & DE WINTHER, M. P. J. 2016. Interferon-beta promotes macrophage foam cell formation by altering both cholesterol influx and efflux mechanisms. *Cytokine,* 77**,** 220-226.

BOULANGER, C. M., LOYER, X., RAUTOU, P.-E. & AMABILE, N. 2017. Extracellular vesicles in coronary artery disease. *Nature Reviews Cardiology,* 14**,** 259-272.

BOYETTE, L. B., MACEDO, C., HADI, K., ELINOFF, B. D., WALTERS, J. T., RAMASWAMIL, B., CHALASANI, G., TABOAS, J. M., LAKKIS, F. G. & METES, D. M. 2017. Phenotype, function, and differentiation potential of human monocyte subsets. *Plos One,* 12.

BOYLE, J. J., WEISSBERG, P. L. & BENNETT, M. R. 2002. Human macrophage-induced vascular smooth muscle cell apoptosis requires NO enhancement of Fas/Fas-L interactions. *Arteriosclerosis Thrombosis and Vascular Biology,* 22**,** 1624-1630.

BRODSKY, S. V., ZHANG, F., NASJLETTI, A. & GOLIGORSKY, M. S. 2004. Endothelium-derived microparticles impair endothelial function in vitro. *American Journal of Physiology-Heart and Circulatory Physiology,* 286**,** H1910-H1915.

BUELL, G. N., TALABOT, F., GOS, A., LORENZ, J., LAI, E., MORRIS, M. A. & ANTONARAKIS, S. E. 1998. Gene structure and chromosomal localization of the human P2X(7) receptor. *Receptors & Channels,* 5**,** 347-+.

BURKE, A. P., KOLODGIE, F. D., FARB, A., WEBER, D. K., MALCOM, G. T., SMIALEK, J. & VIRMANI, R. 2001. Healed plaque ruptures and sudden coronary death - Evidence that subclinical rupture has a role in plaque progression. *Circulation,* 103**,** 934-940.

BURNSTOCK, G. 2007. Purine and pyrimidine receptors. *Cellular and Molecular Life Sciences,* 64**,** 1471-1483.

CAI, B. & KASIKARA, C. 2020. TAM receptors and their ligand-mediated activation: Role in atherosclerosis. *Tam Receptors in Health and Disease,* 357**,** 21-33.

CAI, B., THORP, E. B., DORAN, A. C., SANSBURY, B. E., DAEMEN, M. J. A. P., DORWEILER, B., SPITE, M., FREDMAN, G. & TABAS, I. 2017. MerTK receptor cleavage promotes plaque necrosis and defective resolution in atherosclerosis. *Journal of Clinical Investigation,* 127**,** 564-568.

CAI, C., KOCH, B., MORIKAWA, K., SUDA, G., SAKAMOTO, N., RUESCHENBAUM, S., AKHRAS, S., DIETZ, J., HILDT, E., ZEUZEM, S., WELSCH, C. & LANGE, C. M. 2018. Macrophage-Derived Extracellular Vesicles Induce Long-Lasting Immunity Against Hepatitis C Virus Which Is Blunted by Polyunsaturated Fatty Acids. *Frontiers in Immunology,* 9.

CAMARE, C., PUCELLE, M., NEGRE-SALVAYRE, A. & SALVAYRE, R. 2017. Angiogenesis in the atherosclerotic plaque. *Redox Biology,* 12**,** 18-34.

CAMENISCH, T. D., KOLLER, B. H., EARP, H. S. & MATSUSHIMA, G. K. 1999. A novel receptor tyrosine kinase, Mer, inhibits TNF-alpha production and lipopolysaccharide-induced endotoxic shock. *Journal of Immunology,* 162**,** 3498-3503.

CHARRAS, G. & PALUCH, E. 2008. Blebs lead the way: how to migrate without lamellipodia. *Nature Reviews Molecular Cell Biology,* 9**,** 730-736.

CHESSELL, I. P., SIMON, J., HIBELL, A. D., MICHEL, A. D., BARNARD, E. A. & HUMPHREY, P. P. A. 1998. Cloning and functional characterisation of the mouse P2X(7) receptor. *Febs Letters,* 439**,** 26-30.

CHISTIAKOV, D. A., OREKHOV, A. N. & BOBRYSHEV, Y. V. 2015. Contribution of neovascularization and intraplaque haemorrhage to atherosclerotic plaque progression and instability. *Acta Physiologica,* 213**,** 539-553.

COCHAIN, C., VAFADARNEJAD, E., ARAMPATZI, P., PELISEK, J., WINKELS, H., LEY, K., WOLF, D., SALIBA, A.-E. & ZERNECKE, A. 2018. Single-Cell RNA-Seq Reveals the Transcriptional Landscape and Heterogeneity of Aortic

Macrophages in Murine Atherosclerosis. *Circulation Research,* 122**,** 1661-1674.
COLLO, G., NEIDHART, S., KAWASHIMA, E., KOSCOVILBOIS, M., NORTH, R. A. & BUELL, G. 1997. Tissue distribution of the P2X(7) receptor. *Neuropharmacology,* 36**,** 1277-1283.
COLOMBO, F., BASTONI, M., NIGRO, A., PODINI, P., FINARDI, A., CASELLA, G., RAMESH, M., FARINA, C., VERDERIO, C. & FURLAN, R. 2018. Cytokines Stimulate the Release of Microvesicles from Myeloid Cells Independently from the P2X7 Receptor/Acid Sphingomyelinase Pathway. *Frontiers in Immunology,* 9.
CONNOR, D. E., EXNER, T., MA, D. D. F. & JOSEPH, J. E. 2010. The majority of circulating platelet-derived microparticles fail to bind annexin V, lack phospholipid-dependent procoagulant activity and demonstrate greater expression of glycoprotein Ib. *Thrombosis and Haemostasis,* 103**,** 1044-1052.
CONTRERAS, F. X., SANCHEZ-MAGRANER, L., ALONSO, A. & GONI, F. M. 2010. Transbilayer (flip-flop) lipid motion and lipid scrambling in membranes. *Febs Letters,* 584**,** 1779-1786.
D'SOUZA, A., BURCH, A., DAVE, K. M., SREERAM, A., REYNOLDS, M. J., DOBBINS, D. X., KAMTE, Y. S., ZHAO, W., SABATELLE, C., JOY, G. M., SOMAN, V., CHANDRAN, U. R., SHIVA, S. S., QUILLINAN, N., HERSON, P. S. & MANICKAM, D. S. 2021. Microvesicles transfer mitochondria and increase mitochondrial function in brain endothelial cells. *Journal of Controlled Release,* 338**,** 505-526.
DASGUPTA, S. K., LE, A., CHAVAKIS, T., RUMBAUT, R. E. & THIAGARAJAN, P. 2012. Developmental Endothelial Locus-1 (Del-1) Mediates Clearance of Platelet Microparticles by the Endothelium. *Circulation,* 125**,** 1664-1672.
DAVIES, P. F., REMUZZI, A., GORDON, E. J., DEWEY, C. F. & GIMBRONE, M. A. 1986. TURBULENT FLUID SHEAR-STRESS INDUCES VASCULAR ENDOTHELIAL-CELL TURNOVER INVITRO. *Proceedings of the National Academy of Sciences of the United States of America,* 83**,** 2114-2117.
DAWICKI, D. D., MCGOWANJORDAN, J., BULLARD, S., POND, S. & ROUNDS, S. 1995. EXTRACELLULAR NUCLEOTIDES STIMULATE LEUKOCYTE ADHERENCE TO CULTURED PULMONARY-ARTERY ENDOTHELIAL-CELLS. *American Journal of Physiology-Lung Cellular and Molecular Physiology,* 268**,** L666-L673.
DE SALLES, E. M., DE MENEZES, M. N., SIQUEIRA, R., DA SILVA, H. B., AMARAL, E. P., CASTILLO-MENDEZ, S. I., CUNHA, I., CASSADO, A. D. A., VIEIRA, F. S., NICHOLAS OLIVIERI, D., TADOKORO, C. E., ALVAREZ, J. M., COUTINHO-SILVA, R. & D'IMPERIO-LIMA, M. R. 2017. P2X7 receptor drives Th1 cell differentiation and controls the follicular helper T cell population to protect against Plasmodium chabaudi malaria. *Plos Pathogens,* 13.
DEL CONDE, I., SHRIMPTON, C. N., THIAGARAJAN, P. & LOPEZ, J. A. 2005. Tissue-factor-bearing microvesicles arise from lipid rafts and fuse with activated platelets to initiate coagulation. *Blood,* 106**,** 1604-1611.
DIMMELER, S., HAENDELER, J., RIPPMANN, V., NEHLS, M. & ZEIHER, A. M. 1996. Shear stress inhibits apoptosis of human endothelial cells. *Febs Letters,* 399**,** 71-74.
DINARELLO, C. A. 2011. Interleukin-1 in the pathogenesis and treatment of inflammatory diseases. *Blood,* 117**,** 3720-3732.

DINARELLO, C. A. 2018. Overview of the IL-1 family in innate inflammation and acquired immunity. *Immunological Reviews,* 281**,** 8-27.
DING, J., WANG, K., LIU, W., SHE, Y., SUN, Q., SHI, J., SUN, H., WANG, D.-C. & SHAO, F. 2016. Pore-forming activity and structural autoinhibition of the gasdermin family. *Nature,* 535**,** 111-+.
DISTLER, J. H. W., HUBER, L. C., HUEBER, A. J., REICH, C. F., GAY, S., DISTLER, O. & PISETSKY, D. S. 2005. The release of microparticles by apoptotic cells and their effects on macrophages. *Apoptosis,* 10**,** 731-741.
DONNELLY-ROBERTS, D. L., NAMOVIC, M. T., HAN, P. & JARVIS, M. F. 2009. Mammalian P2X7 receptor pharmacology: comparison of recombinant mouse, rat and human P2X7 receptors. *British Journal of Pharmacology,* 157**,** 1203-1214.
DOSCH, M., ZINDEL, J., JEBBAWI, F., MELIN, N., SANCHEZ-TALTAVULL, D., STROKA, D., CANDINAS, D. & BELDI, G. 2019. Connexin-43-dependent ATP release mediates macrophage activation during sepsis. *Elife,* 8.
DRAGO, F., LOMBARDI, M., PRADA, I., GABRIELLI, M., JOSHI, P., COJOC, D., FRANCK, J., FOURNIER, I., VIZIOLI, J. & VERDERIO, C. 2017. ATP Modifies the Proteome of Extracellular Vesicles Released by Microglia and Influences Their Action on Astrocytes. *Frontiers in Pharmacology,* 8.
ENGLAND, H., SUMMERSGILL, H. R., EDYE, M. E., ROTHWELL, N. J. & BROUGH, D. 2014. Release of Interleukin-1 alpha or Interleukin-1 beta Depends on Mechanism of Cell Death. *Journal of Biological Chemistry,* 289**,** 15942-15950.
EVAVOLD, C. L., RUAN, J., TAN, Y., XIA, S., WU, H. & KAGAN, J. C. 2018. The Pore-Forming Protein Gasdermin D Regulates Interleukin-1 Secretion from Living Macrophages. *Immunity,* 48**,** 35-+.
FADOK, V. A., VOELKER, D. R., CAMPBELL, P. A., COHEN, J. J., BRATTON, D. L. & HENSON, P. M. 1992. EXPOSURE OF PHOSPHATIDYLSERINE ON THE SURFACE OF APOPTOTIC LYMPHOCYTES TRIGGERS SPECIFIC RECOGNITION AND REMOVAL BY MACROPHAGES. *Journal of Immunology,* 148**,** 2207-2216.
FAILLE, D., EL-ASSAAD, F., MITCHELL, A. J., ALESSI, M. C., CHIMINI, G., FUSAI, T., GRAU, G. E. & COMBES, V. 2012. Endocytosis and intracellular processing of platelet microparticles by brain endothelial cells. *Journal of Cellular and Molecular Medicine,* 16**,** 1731-1738.
FENG, D., ZHAO, W.-L., YE, Y.-Y., BAI, X.-C., LIU, R.-Q., CHANG, L.-F., ZHOU, Q. & SUI, S.-F. 2010. Cellular Internalization of Exosomes Occurs Through Phagocytosis. *Traffic,* 11**,** 675-687.
FERRARI, D., CHIOZZI, P., FALZONI, S., DALSUSINO, M., MELCHIORRI, L., BARICORDI, O. R. & DIVIRGILIO, F. 1997. Extracellular ATP triggers IL-1 beta release by activating the purinergic P2Z receptor of human macrophages. *Journal of Immunology,* 159**,** 1451-1458.
FERREIRA, A. C., PETER, A. A., MENDEZ, A. J., JIMENEZ, J. J., MAURO, L. M., CHIRINOS, J. A., GHANY, R., VIRANI, S., GARCIA, S., HORSTMAN, L. L., PUROW, J., JY, W., AHN, Y. S. & DE MARCHENA, E. 2004. Postprandial hypertriglyceridemia increases circulating levels of endothelial cell microparticles. *Circulation,* 110**,** 3599-3603.
FOLCO, E. J., SUKHOVA, G. K., QUILLARD, T. & LIBBY, P. 2014. Moderate Hypoxia Potentiates Interleukin-1 beta Production in Activated Human Macrophages. *Circulation Research,* 115**,** 875-883.

GAULEY, J. & PISETSKY, D. S. 2010. The release of microparticles by RAW 264.7 macrophage cells stimulated with TLR ligands. *Journal of Leukocyte Biology,* 87**,** 1115-1123.
GAUTIER, E. L., HUBY, T., WITZTUM, J. L., OUZILLEAU, B., MILLER, E. R., SAINT-CHARLES, F., AUCOUTURIER, P., CHAPMAN, M. J. & LESNIK, P. 2009. Macrophage Apoptosis Exerts Divergent Effects on Atherogenesis as a Function of Lesion Stage. *Circulation,* 119**,** 1795-U186.
GEISSMANN, F., JUNG, S. & LITTMAN, D. R. 2003. Blood monocytes consist of two principal subsets with distinct migratory properties. *Immunity,* 19**,** 71-82.
GIMBRONE, M. A., JR. & GARCIA-CARDENA, G. 2016. Endothelial Cell Dysfunction and the Pathobiology of Atherosclerosis. *Circulation Research,* 118**,** 620-636.
GIROUD, P., RENAUDINEAU, S., GUDEFIN, L., CALCEI, A., MENGUY, T., ROZAN, C., MIZRAHI, J., CAUX, C., DUONG, V. & VALLADEAU-GUILEMOND, J. 2020. Expression of TAM-R in Human Immune Cells and Unique Regulatory Function of MerTK in IL-10 Production by Tolerogenic DC. *Frontiers in Immunology,* 11.
GLASS, C. K. & WITZTUM, J. L. 2001. Atherosclerosis: The road ahead. *Cell,* 104**,** 503-516.
GOICHOT, B., GRUNEBAUM, L., DESPREZ, D., VINZIO, S., MEYER, L., SCHLIENGER, J. L., LESSARD, M. & SIMON, C. 2006. Circulating procoagulant microparticles in obesity. *Diabetes & Metabolism,* 32**,** 82-85.
GOMEZ, I., WARD, B., SOUILHOL, C., RECARTI, C., ARIAANS, M., JOHNSTON, J., BURNETT, A., MAHMOUD, M., LE ANH, L., WEST, L., LONG, M., PARRY, S., WOODS, R., HULSTON, C., BENEDIKTER, B., NIESPOLO, C., BAZAZ, R., FRANCIS, S., KISS-TOTH, E., VAN ZANDVOORT, M., SCHOBER, A., HELLEWELL, P., EVANS, P. C. & RIDGER, V. 2020. Neutrophil microvesicles drive atherosclerosis by delivering miR-155 to atheroprone endothelium. *Nature Communications,* 11.
GOOSSENS, P., GIJBELS, M. J. J., ZERNECKE, A., EIJGELAAR, W., VERGOUWE, M. N., VAN DER MADE, I., VANDERLOCHT, J., BECKERS, L., BUURMAN, W. A., DAEMEN, M. J. A. P., KALINKE, U., WEBER, C., LUTGENS, E. & DE WINTHER, M. P. J. 2010. Myeloid Type I Interferon Signaling Promotes Atherosclerosis by Stimulating Macrophage Recruitment to Lesions. *Cell Metabolism,* 12**,** 142-153.
GRAHAM, D. K., DAWSON, T. L., MULLANEY, D. L., SNODGRASS, H. R. & EARP, H. S. 1994. CLONING AND MESSENGER-RNA EXPRESSION ANALYSIS OF A NOVEL HUMAN PROTOONCOGENE, C-MER. *Cell Growth & Differentiation,* 5**,** 647-657.
GREEN, J. P., SOUILHOL, C., XANTHIS, I., MARTINEZ-CAMPESINO, L., BOWDEN, N. P., EVANS, P. C. & WILSON, H. L. 2018. Atheroprone flow activates inflammation via endothelial ATP-dependent P2X7-p38 signalling. *Cardiovascular Research,* 114**,** 324-335.
GU, B. J., RATHSAM, C., STOKES, L., MCGEACHIE, A. B. & WILEY, J. S. 2009. Extracellular ATP dissociates nonmuscle myosin from P2X(7) complex: this dissociation regulates P2X(7) pore formation. *American Journal of Physiology-Cell Physiology,* 297**,** C430-C439.
GU, B. J., SAUNDERS, B. M., JURSIK, C. & WILEY, J. S. 2010. The P2X(7)-nonmuscle myosin membrane complex regulates phagocytosis of

nonopsonized particles and bacteria by a pathway attenuated by extracellular ATP. *Blood,* 115**,** 1621-1631.
GU, B. J., SAUNDERS, B. M., PETROU, S. & WILEY, J. S. 2011. P2X(7) Is a Scavenger Receptor for Apoptotic Cells in the Absence of Its Ligand, Extracellular ATP. *Journal of Immunology,* 187**,** 2365-2375.
GU, B. J., ZHANG, W. Y., BENDALL, L. J., CHESSELL, I. P., BUELL, G. N. & WILEY, J. S. 2000. Expression of P2X(7) purinoceptors on human lymphocytes and monocytes: evidence for nonfunctional P2X(7) receptors. *American Journal of Physiology-Cell Physiology,* 279**,** C1189-C1197.
GUHA, S., BALTAZAR, G. C., COFFEY, E. E., TU, L.-A., LIM, J. C., BECKEL, J. M., PATEL, S., EYSTEINSSON, T., LU, W., O'BRIEN-JENKINS, A., LATIES, A. M. & MITCHELL, C. H. 2013. Lysosomal alkalinization, lipid oxidation, and reduced phagosome clearance triggered by activation of the P2X7 receptor. *Faseb Journal,* 27**,** 4500-4509.
HAPPONEN, K. E., TRAN, S., MORGELIN, M., PRINCE, R., CALZAVARINI, S., ANGELILLO-SCHERRER, A. & DAHLBACK, B. 2016. The Gas6-Axl Protein Interaction Mediates Endothelial Uptake of Platelet Microparticles. *Journal of Biological Chemistry,* 291**,** 10586-10601.
HILGENDORF, I., SWIRSKI, F. K. & ROBBINS, C. S. 2015. Monocyte Fate in Atherosclerosis. *Arteriosclerosis Thrombosis and Vascular Biology,* 35**,** 272-279.
HISCOTT, J., MAROIS, J., GAROUFALIS, J., DADDARIO, M., ROULSTON, A., KWAN, I., PEPIN, N., LACOSTE, J., NGUYEN, H., BENSI, G. & FENTON, M. 1993. CHARACTERIZATION OF A FUNCTIONAL NF-KAPPA-B SITE IN THE HUMAN INTERLEUKIN-1-BETA PROMOTER - EVIDENCE FOR A POSITIVE AUTOREGULATORY LOOP. *Molecular and Cellular Biology,* 13**,** 6231-6240.
HO, A. W. Y., WONG, C. K. & LAM, C. W. K. 2008. Tumor necrosis factor-alpha up-regulates the expression of CCL2 and adhesion molecules of human proximal tubular epithelial cells through MAPK signaling pathways. *Immunobiology,* 213**,** 533-544.
HORNUNG, V., BAUERNFEIND, F., HALLE, A., SAMSTAD, E. O., KONO, H., ROCK, K. L., FITZGERALD, K. A. & LATZ, E. 2008. Silica crystals and aluminum salts activate the NALP3 inflammasome through phagosomal destabilization. *Nature Immunology,* 9**,** 847-856.
HOSSEINKHANI, B., VAN DEN AKKER, N. M. S., MOLIN, D. G. M. & MICHIELS, L. 2020. (Sub)populations of extracellular vesicles released by TNF-alpha -triggered human endothelial cells promote vascular inflammation and monocyte migration. *Journal of Extracellular Vesicles,* 9.
HU, J. J., LIU, X., XIA, S., ZHANG, Z., ZHANG, Y., ZHAO, J., RUAN, J., LUO, X., LOU, X., BAI, Y., WANG, J., HOLLINGSWORTH, L. R., MAGUPALLI, V. G., ZHAO, L., LUO, H. R., KIM, J., LIEBERMAN, J. & WU, H. 2020. FDA-approved disulfiram inhibits pyroptosis by blocking gasdermin D pore formation. *Nature Immunology,* 21**,** 736-+.
HU, P., WANG, X., HAITSMA, J. J., FURMLI, S., MASOOM, H., LIU, M., IMAI, Y., SLUTSKY, A. S., BEYENE, J., GREENWOOD, C. M. T. & DOS SANTOS, C. 2012. Microarray Meta-Analysis Identifies Acute Lung Injury Biomarkers in Donor Lungs That Predict Development of Primary Graft Failure in Recipients. *Plos One,* 7.

HU, X. Y., PARK-MIN, K. H., HO, H. H. & IVASHKIV, L. B. 2005. IFN-gamma-primed macrophages exhibit increased CCR2-dependent migration and altered IFN-gamma responses mediated by Stat1. *Journal of Immunology,* 175**,** 3637-3647.

HUANG, M. D., RIGBY, A. C., MORELLI, X., GRANT, M. A., HUANG, G. Q., FURIE, B., SEATON, B. & FURIE, B. C. 2003. Structural basis of membrane binding by Gla domains of vitamin K-dependent proteins. *Nature Structural Biology,* 10**,** 751-756.

IKEDA, U., IKEDA, M., OOHARA, T., OGUCHI, A., KAMITANI, T., TSURUYA, Y. & KANO, S. 1991. INTERLEUKIN-6 STIMULATES GROWTH OF VASCULAR SMOOTH-MUSCLE CELLS IN A PDGF-DEPENDENT MANNER. *American Journal of Physiology,* 260**,** H1713-H1717.

INDRACCOLO, S., PFEFFER, U., MINUZZO, S., ESPOSITO, G., RONI, V., MANDRUZZATO, S., FERRARI, N., ANFOSSO, L., DELL'EVA, R., NOONAN, D. M., CHIECO-BIANCHI, L., ALBINI, A. & AMADORI, A. 2007. Identification of genes selectively regulated by IFNs in endothelial cells. *Journal of Immunology,* 178**,** 1122-1135.

INSULL, W., JR. 2009. The Pathology of Atherosclerosis: Plaque Development and Plaque Responses to Medical Treatment. *American Journal of Medicine,* 122**,** S3-S14.

INUI, T., WATANABE, M., NAKAMOTO, K., SADA, M., HIRATA, A., NAKAMURA, M., HONDA, K., OGAWA, Y., TAKATA, S., YOKOYAMA, T., SARAYA, T., KURAI, D., WADA, H., ISHII, H. & TAKIZAWA, H. 2018. Bronchial epithelial cells produce CXCL1 in response to LPS and TNF alpha: A potential role in the pathogenesis of COPD. *Experimental Lung Research,* 44**,** 323-331.

ISODA, K., SAWADA, S., ISHIGAMI, N., MATSUKI, T., MIYAZAKI, K., KUSUHARA, M., IWAKURA, Y. & OHSUZU, F. 2004. Lack of interleukin-1 receptor antagonist modulates plaque composition in apolipoprotein E-deficient mice. *Arteriosclerosis Thrombosis and Vascular Biology,* 24**,** 1068-1073.

JANKS, L., SHARMA, C. V. R. & EGAN, T. M. 2018. A central role for P2X7 receptors in human microglia. *Journal of Neuroinflammation,* 15.

JENKINS, B. J., GRAIL, D., INGLESE, M., QUILICI, C., BOZINOVSKI, S., WONG, P. & ERNST, M. 2004. Imbalanced gp130-dependent signaling in macrophages alters macrophage colony-stimulating factor responsiveness via regulation of c-fms expression. *Molecular and Cellular Biology,* 24**,** 1453-1463.

JIANG, Z., LIU, G. & LI, J. 2020. Recent Progress on the Isolation and Detection Methods of Exosomes. *Chemistry-an Asian Journal,* 15**,** 3973-3982.

JIMENEZ, J. J., JY, W., MAURO, L. M., SODERLAND, C., HORSTMAN, L. L. & AHN, Y. S. 2003. Endothelial cells release phenotypically and quantitatively distinct microparticles in activation and apoptosis. *Thrombosis Research,* 109**,** 175-180.

JURA, J., WEGRZYN, P., KOROSTYNSKI, M., GUZIK, K., OCZKO-WOJCIECHOWSKA, M., JARZAB, M., KOWALSKA, M., PIECHOTA, M., PRZEWLOCKI, R. & KOJ, A. 2008. Identification of interleukin-1 and interleukin-6-responsive genes in human monocyte-derived macrophages using microarrays. *Biochimica Et Biophysica Acta-Gene Regulatory Mechanisms,* 1779**,** 383-389.

KARASAWA, A. & KAWATE, T. 2016. Structural basis for subtype-specific inhibition of the P2X7 receptor. *Elife,* 5.

KAYAGAKI, N., STOWE, I. B., LEE, B. L., O'ROURKE, K., ANDERSON, K., WARMING, S., CUELLAR, T., HALEY, B., ROOSE-GIRMA, M., PHUNG, Q. T., LIU, P. S., LILL, J. R., LI, H., WU, J., KUMMERFELD, S., ZHANG, J., LEE, W. P., SNIPAS, S. J., SALVESEN, G. S., MORRIS, L. X., FITZGERALD, L., ZHANG, Y., BERTRAM, E. M., GOODNOW, C. C. & DIXIT, V. M. 2015. Caspase-11 cleaves gasdermin D for non-canonical inflammasome signalling. *Nature,* 526**,** 666-671.

KELLER, T. T., VAN DER MEER, J. J., TEELING, P., VAN DER SLUIJS, K., IDU, M. M., RIMMELZWAAN, G. F., LEVI, M., VAN DER WAL, A. C. & DE BOER, O. J. 2008. Selective expansion of influenza a virus-specific T cells in symptomatic human carotid artery atherosclerotic plaques. *Stroke,* 39**,** 174-179.

KEYEL, P. A., TKACHEVA, O. A., LARREGINA, A. T. & SALTER, R. D. 2012. Coordinate Stimulation of Macrophages by Microparticles and TLR Ligands Induces Foam Cell Formation. *Journal of Immunology,* 189**,** 4621-4629.

KHAN, B. V., PARTHASARATHY, S. S., ALEXANDER, R. W. & MEDFORD, R. M. 1995. MODIFIED LOW-DENSITY-LIPOPROTEIN AND ITS CONSTITUENTS AUGMENT CYTOKINE-ACTIVATED VASCULAR CELL-ADHESION MOLECULE-1 GENE-EXPRESSION IN HUMAN VASCULAR ENDOTHELIAL-CELLS. *Journal of Clinical Investigation,* 95**,** 1262-1270.

KIM, M., JIANG, L. H., WILSON, H. L., NORTH, R. A. & SURPRENANT, A. 2001. Proteomic and functional evidence for a P2X(7) receptor signalling complex. *Embo Journal,* 20**,** 6347-6358.

KIM, T.-K., BHEDA-MALGE, A., LIN, Y., SREEKRISHNA, K., ADAMS, R., ROBINSON, M. K., BASCOM, C. C., TIESMAN, J. P., ISFORT, R. J. & GELINAS, R. 2015. A systems approach to understanding human rhinovirus and influenza virus infection. *Virology,* 486**,** 146-157.

KIRII, H., NIWA, T., YAMADA, Y., WADA, H., SAITO, K., IWAKURA, Y., ASANO, M., MORIWAKI, H. & SEISHIMA, M. 2003. Lack of interleukin-1 beta decreases the severity of atherosclerosis in ApoE-deficient mice. *Arteriosclerosis Thrombosis and Vascular Biology,* 23**,** 656-660.

KRUNKOSKY, T. M., FISCHER, B. M., MARTIN, L. D., JONES, N., AKLEY, N. J. & ADLER, K. B. 2000. Effects of TNF-alpha on expression of ICAM-1 in human airway epithelial cells in vitro - Signaling pathways controlling surface and gene expression. *American Journal of Respiratory Cell and Molecular Biology,* 22**,** 685-692.

KWAK, B. R., BAECK, M., BOCHATON-PIALLAT, M.-L., CALIGIURI, G., DAEMENS, M. J. A. P., DAVIES, P. F., HOEFER, I. E., HOLVOET, P., JO, H., KRAMS, R., LEHOUX, S., MONACO, C., STEFFENS, S., VIRMANI, R., WEBER, C., WENTZEL, J. J. & EVANS, P. C. 2014. Biomechanical factors in atherosclerosis: mechanisms and clinical implications. *European Heart Journal,* 35**,** 3013-+.

LACRAZ, S., NICOD, L. P., CHICHEPORTICHE, R., WELGUS, H. G. & DAYER, J. M. 1995. IL-10 INHIBITS METALLOPROTEINASE AND STIMULATES TIMP-1 PRODUCTION IN HUMAN MONONUCLEAR PHAGOCYTES. *Journal of Clinical Investigation,* 96**,** 2304-2310.

LAN, Q. X., MERCURIUS, K. O. & DAVIES, P. F. 1994. STIMULATION OF TRANSCRIPTION FACTORS NF-KAPPA-B AND AP1 IN ENDOTHELIAL-CELLS SUBJECTED TO SHEAR-STRESS. *Biochemical and Biophysical Research Communications,* 201**,** 950-956.

LAPPING-CARR, G., GEMEL, J., MAO, Y., SPARKS, G., HARRINGTON, M., PEDDINTI, R. & BEYER, E. C. 2021. Circulating extracellular vesicles from patients with acute chest syndrome disrupt adherens junctions between endothelial cells. *Pediatric Research,* 89**,** 776-784.
LASTER, S. M., WOOD, J. G. & GOODING, L. R. 1988. TUMOR NECROSIS FACTOR CAN INDUCE BOTH APOPTIC AND NECROTIC FORMS OF CELL-LYSIS. *Journal of Immunology,* 141**,** 2629-2634.
LEE, I. T., LIN, C.-C., CHENG, S.-E., HSIAO, L.-D., HSIAO, Y.-C. & YANG, C.-M. 2013. TNF-alpha Induces Cytosolic Phospholipase A(2) Expression in Human Lung Epithelial Cells via JNK1/2-and p38 MAPK-Dependent AP-1 Activation. *Plos One,* 8.
LEE, J., WEN, B., CARTER, E. A., COMBES, V., GRAU, G. E. R. & LAY, P. A. 2017. Infrared spectroscopic characterization of monocytic microvesicles (microparticles) released upon lipopolysaccharide stimulation. *Faseb Journal,* 31**,** 2817-2827.
LEGRAND-POELS, S., SCHOONBROODT, S. & PIETTE, J. 2000. Regulation of interleukin-6 gene expression by pro-inflammatory cytokines in a colon cancer cell line. *Biochemical Journal,* 349**,** 765-773.
LEMKE, G. & ROTHLIN, C. V. 2008. Immunobiology of the TAM receptors. *Nature Reviews Immunology,* 8**,** 327-336.
LENTSCH, A. B., SHANLEY, T. P., SARMA, V. & WARD, P. A. 1997. In vivo suppression of NF-kappa B and preservation of I kappa B alpha by interleukin-10 and interleukin-13. *Journal of Clinical Investigation,* 100**,** 2443-2448.
LEON, B., LOPEZ-BRAVO, M. & ARDAVIN, C. 2005. Monocyte-derived dendritic cells. *Seminars in Immunology,* 17**,** 313-318.
LEROYER, A. S., ISOBE, H., LESECHE, G., CASTIER, Y., WASSEF, M., MALLAT, Z., BINDER, B. R., TEDGUI, A. & BOULANGER, C. M. 2007. Cellular origins and thrombogenic activity of microparticles isolated from human atherosclerotic plaques. *Journal of the American College of Cardiology,* 49**,** 772-777.
LEROYER, A. S., RAUTOU, P. E., SILVESTRE, J. S., CASTIER, Y., LESECHE, G., DEVUE, C., DURIEZ, M., BRANDES, R. P., LUTGENS, E., TEDGUI, A. & BOULANGER, C. M. 2008. CD40 ligand+ microparticles from human atherosclerotic plaques stimulate endothelial proliferation and angiogenesis. *Journal of the American College of Cardiology,* 52**,** 1302-1311.
LEW, E. D., OH, J., BURROLA, P. G., LAX, I., ZAGORSKA, A., TRAVES, P. G., SCHLESSINGER, J. & LEMKE, G. 2014. Differential TAM receptor-ligand-phospholipid interactions delimit differential TAM bioactivities. *Elife,* 3.
LI, J., FU, Q., CUI, H., QU, B., PAN, W., SHEN, N. & BAO, C. 2011. Interferon-alpha Priming Promotes Lipid Uptake and Macrophage-Derived Foam Cell Formation A Novel Link Between Interferon-alpha and Atherosclerosis in Lupus. *Arthritis and Rheumatism,* 63**,** 492-502.
LI, Y., WITTCHEN, E. S., MONAGHAN-BENSON, E., HAHN, C., EARP, H. S., DOERSCHUK, C. M. & BURRIDGE, K. 2019. The role of endothelial MERTK during the inflammatory response in lungs. *Plos One,* 14.
LIBBY, P. 2002. Inflammation in atherosclerosis. *Nature,* 420**,** 868-874.
LIBBY, P., BURING, J. E., BADIMON, L., HANSSON, C. K., DEANFIELD, J., BITTENCOURT, M. S., TOKGOZOGLU, L. & LEWIS, E. F. 2019. Atherosclerosis. *Nature Reviews Disease Primers,* 5.

LIBBY, P. & RIDKER, P. M. 2004. Inflammation and atherosclerosis: Role of C-reactive protein in risk assessment. *American Journal of Medicine,* 116**,** 9-16.
LIBBY, P., WARNER, S. J. C. & FRIEDMAN, G. B. 1988. INTERLEUKIN-1 - A MITOGEN FOR HUMAN VASCULAR SMOOTH-MUSCLE CELLS THAT INDUCES THE RELEASE OF GROWTH-INHIBITORY PROSTANOIDS. *Journal of Clinical Investigation,* 81**,** 487-498.
LIGRESTI, G., APLIN, A. C., ZORZI, P., MORISHITA, A. & NICOSIA, R. F. 2011. Macrophage-Derived Tumor Necrosis Factor-alpha Is an Early Component of the Molecular Cascade Leading to Angiogenesis in Response to Aortic Injury. *Arteriosclerosis Thrombosis and Vascular Biology,* 31**,** 1151-U555.
LIU, M.-L., REILLY, M. P., CASASANTO, P., MCKENZIE, S. E. & WILLIAMS, K. J. 2007. Cholesterol enrichment of human monocyte/macrophages induces surface exposure of phosphatidylserine and the release of biologically-active tissue factor - Positive microvesicles. *Arteriosclerosis Thrombosis and Vascular Biology,* 27**,** 430-435.
LIU, T., ZHANG, L., JOO, D. & SUN, S.-C. 2017. NF-kappa B signaling in inflammation. *Signal Transduction and Targeted Therapy,* 2.
LIU, X., ZHANG, Z., RUAN, J., PAN, Y., MAGUPALLI, V. G., WU, H. & LIEBERMAN, J. 2016. Inflammasome-activated gasdermin D causes pyroptosis by forming membrane pores. *Nature,* 535**,** 153-+.
LOMBARDI, M., MANTIONE, M. E., BACCELLIERI, D., FERRARA, D., CASTELLANO, R., CHIESA, R., ALFIERI, O. & FOGLIENI, C. 2017. P2X7 receptor antagonism modulates IL-1 beta and MMP9 in human atherosclerotic vessels. *Scientific Reports,* 7.
LOVELACE, M. D., GU, B. J., EAMEGDOOL, S. S., WEIBLE, M. W., II, WILEY, J. S., ALLEN, D. G. & CHAN-LING, T. 2015. P2X7 Receptors Mediate Innate Phagocytosis by Human Neural Precursor Cells and Neuroblasts. *Stem Cells,* 33**,** 526-541.
LOYER, X., VION, A.-C., TEDGUI, A. & BOULANGER, C. M. 2014. Microvesicles as Cell-Cell Messengers in Cardiovascular Diseases. *Circulation Research,* 114**,** 345-353.
LU, J., YANG, J.-H., BURNS, A. R., CHEN, H.-H., TANG, D., WALTERSCHEID, J. P., SUZUKI, S., YANG, C.-Y., SAWAMURA, T. & CHEN, C.-H. 2009. Mediation of Electronegative Low-Density Lipoprotein Signaling by LOX-1 A Possible Mechanism of Endothelial Apoptosis. *Circulation Research,* 104**,** 619-627.
LU, Y.-C., YEH, W.-C. & OHASHI, P. S. 2008. LPS/TLR4 signal transduction pathway. *Cytokine,* 42**,** 145-151.
LUSIS, A. J. 2000. Atherosclerosis. *Nature,* 407**,** 233-241.
MACKENZIE, A., WILSON, H. L., KISS-TOTH, E., DOWER, S. K., NORTH, R. A. & SURPRENANT, A. 2001. Rapid secretion of interleukin-1 beta by microvesicle shedding. *Immunity,* 15**,** 825-835.
MACKENZIE, A. B., YOUNG, M. T., ADINOLFI, E. & SURPRENANT, A. 2005. Pseudoapoptosis induced by brief activation of ATP-gated P2X(7) receptors. *Journal of Biological Chemistry,* 280**,** 33968-33976.
MADJID, M., MILLER, C. C., ZARUBAEV, V. V., MARINICH, I. G., KISELEV, O. I., LOBZIN, Y. V., FILIPPOV, A. E. & CASSCELLS, S. W., III 2007. Influenza epidemics and acute respiratory disease activity are associated with a surge in autopsy-confirmed coronary heart disease death: results from 8 years of autopsies in 34 892 subjects. *European Heart Journal,* 28**,** 1205-1210.

MALEFYT, R. D., ABRAMS, J., BENNETT, B., FIGDOR, C. G. & DEVRIES, J. E. 1991. INTERLEUKIN-10(IL-10) INHIBITS CYTOKINE SYNTHESIS BY HUMAN MONOCYTES - AN AUTOREGULATORY ROLE OF IL-10 PRODUCED BY MONOCYTES. *Journal of Experimental Medicine,* 174**,** 1209-1220.

MALLAT, Z., HUGEL, B., OHAN, J., LESECHE, G., FREYSSINET, J. M. & TEDGUI, A. 1999. Shed membrane microparticles with procoagulant potential in human atherosclerotic plaques - A role for apoptosis in plaque thrombogenicity. *Circulation,* 99**,** 348-353.

MANFIOLETTI, G., BRANCOLINI, C., AVANZI, G. & SCHNEIDER, C. 1993. THE PROTEIN ENCODED BY A GROWTH ARREST-SPECIFIC GENE (GAS6) IS A NEW MEMBER OF THE VITAMIN-K-DEPENDENT PROTEINS RELATED TO PROTEIN-S, A NEGATIVE COREGULATOR IN THE BLOOD-COAGULATION CASCADE. *Molecular and Cellular Biology,* 13**,** 4976-4985.

MARK, M. R., SCADDEN, D. T., WANG, Z. G., GU, Q. M., GODDARD, A. & GODOWSKI, P. J. 1994. RSE, A NOVEL RECEPTOR-TYPE TYROSINE KINASE WITH HOMOLOGY TO AXL/UFO, IS EXPRESSED AT HIGH-LEVELS IN THE BRAIN. *Journal of Biological Chemistry,* 269**,** 10720-10728.

MARTINON, F., BURNS, K. & TSCHOPP, J. 2002. The inflammasome: A molecular platform triggering activation of inflammatory caspases and processing of proIL-beta. *Molecular Cell,* 10**,** 417-426.

MARUI, N., OFFERMANN, M. K., SWERLICK, R., KUNSCH, C., ROSEN, C. A., AHMAD, M., ALEXANDER, R. W. & MEDFORD, R. M. 1993. VASCULAR CELL-ADHESION MOLECULE-1 (VCAM-1) GENE-TRANSCRIPTION AND EXPRESSION ARE REGULATED THROUGH AN ANTIOXIDANT SENSITIVE MECHANISM IN HUMAN VASCULAR ENDOTHELIAL-CELLS. *Journal of Clinical Investigation,* 92**,** 1866-1874.

MATTALIANO, M. D., HUARD, C., CAO, W., HILL, A. A., ZHONG, W., MARTINEZ, R. V., HARNISH, D. C., PAULSEN, J. E. & SHIH, H. H. 2009. LOX-1-dependent transcriptional regulation in response to oxidized LDL treatment of human aortic endothelial cells. *American Journal of Physiology-Cell Physiology,* 296**,** C1329-C1337.

MAUSE, S. F. & WEBER, C. 2010. Microparticles Protagonists of a Novel Communication Network for Intercellular Information Exchange. *Circulation Research,* 107**,** 1047-1057.

MAYER, H., BILBAN, M., KURTEV, V., GRUBER, F., WAGNER, O., BINDER, B. R. & DE MARTIN, R. 2004. Deciphering regulatory patterns of inflammatory gene expression from interleukin-1-stimulated human endothelial cells. *Arteriosclerosis Thrombosis and Vascular Biology,* 24**,** 1192-1198.

MESRI, M. & ALTIERI, D. C. 1999. Leukocyte microparticles stimulate endothelial cell cytokine release and tissue factor induction in a JNK1 signaling pathway. *Journal of Biological Chemistry,* 274**,** 23111-23118.

MICHEL, A. D., CHESSELL, I. P. & HUMPHREY, P. P. A. 1999. Ionic effects on human recombinant P2X(7) receptor function. *Naunyn-Schmiedebergs Archives of Pharmacology,* 359**,** 102-109.

MICHEL, A. D. & FONFRIA, E. 2007. Agonist potency at P2X(7) receptors is modulated by structurally diverse lipids. *British Journal of Pharmacology,* 152**,** 523-537.

MIYANISHI, M., TADA, K., KOIKE, M., UCHIYAMA, Y., KITAMURA, T. & NAGATA, S. 2007. Identification of Tim4 as a phosphatidylserine receptor. *Nature,* 450**,** 435-439.
MOBARREZ, F., ANTONIEWICZ, L., BOSSON, J. A., KUHL, J., PISETSKY, D. S. & LUNDBACK, M. 2014. The Effects of Smoking on Levels of Endothelial Progenitor Cells and Microparticles in the Blood of Healthy Volunteers. *Plos One,* 9.
MONACK, D. M., DETWEILER, C. S. & FALKOW, S. 2001. Salmonella pathogenicity island 2-dependent macrophage death is mediated in part by the host cysteine protease caspase-1. *Cellular Microbiology,* 3**,** 825-837.
MOORE, K. J., SHEEDY, F. J. & FISHER, E. A. 2013. Macrophages in atherosclerosis: a dynamic balance. *Nature Reviews Immunology,* 13**,** 709-721.
MOREL, O., JESEL, L., FREYSSINET, J.-M. & TOTI, F. 2011. Cellular Mechanisms Underlying the Formation of Circulating Microparticles. *Arteriosclerosis Thrombosis and Vascular Biology,* 31**,** 15-26.
MULVIHILL, E., SBORGI, L., MARI, S. A., PFREUNDSCHUH, M., HILLER, S. & MUELLER, D. J. 2018. Mechanism of membrane pore formation by human gasdermin-D. *Embo Journal,* 37.
NAGATA, K., OHASHI, K., NAKANO, T., ARITA, H., ZONG, C., HANAFUSA, H. & MIZUNO, K. 1996. Identification of the product of growth arrest-specific gene 6 as a common ligand for Axl, Sky, and Mer receptor tyrosine kinases. *Journal of Biological Chemistry,* 271**,** 30022-30027.
NAGHAVI, M., WYDE, P., LITOVSKY, S., MADJID, M., AKHTAR, A., NAGUIB, S., SIADATY, M. S., SANATI, S. & CASSCELLS, W. 2003. Influenza infection exerts prominent inflammatory and thrombotic effects on the atherosclerotic plaques of apolipoprotein E-deficient mice. *Circulation,* 107**,** 762-768.
NAHRENDORF, M., SWIRSKI, F. K., AIKAWA, E., STANGENBERG, L., WURDINGER, T., FIGUEIREDO, J.-L., LIBBY, P., WEISSLEDER, R. & PITTET, M. J. 2007. The healing myocardium sequentially mobilizes two monocyte subsets with divergent and complementary functions. *Journal of Experimental Medicine,* 204**,** 3037-3047.
NAKANO, T., ISHIMOTO, Y., KISHINO, J., UMEDA, A., INOUE, K., NAGATA, K., OHASHI, K., MIZUNO, K. & ARITA, H. 1997. Cell adhesion to phosphatidylserine mediated by a product of growth arrest-specific gene 6. *Journal of Biological Chemistry,* 272**,** 29411-29414.
NAVAB, M., IMES, S. S., HAMA, S. Y., HOUGH, G. P., ROSS, L. A., BORK, R. W., VALENTE, A. J., BERLINER, J. A., DRINKWATER, D. C., LAKS, H. & FOGELMAN, A. M. 1991. MONOCYTE TRANSMIGRATION INDUCED BY MODIFICATION OF LOW-DENSITY-LIPOPROTEIN IN COCULTURES OF HUMAN AORTIC-WALL CELLS IS DUE TO INDUCTION OF MONOCYTE CHEMOTACTIC PROTEIN-1 SYNTHESIS AND IS ABOLISHED BY HIGH-DENSITY-LIPOPROTEIN. *Journal of Clinical Investigation,* 88**,** 2039-2046.
NICKLIN, M. J. H., HUGHES, D. E., BARTON, J. L., URE, J. M. & DUFF, G. W. 2000. Arterial inflammation in mice lacking the interleukin 1 receptor antagonist gene. *Journal of Experimental Medicine,* 191**,** 303-311.
NOMURA, S., SUZUKI, M., KATSURA, K., XIE, G. L., MIYAZAKI, Y., MIYAKE, T., KIDO, H., KAGAWA, H. & FUKUHARA, S. 1995. PLATELET-DERIVED MICROPARTICLES MAY INFLUENCE THE DEVELOPMENT OF

ATHEROSCLEROSIS IN DIABETES-MELLITUS. *Atherosclerosis,* 116**,** 235-240.
NORMAN, L. L., BRUGUES, J., SENGUPTA, K., SENS, P. & ARANDA-ESPINOZA, H. 2010. Cell blebbing and membrane area homeostasis in spreading and retracting cells (vol 99, pg 1726, 2010). *Biophysical Journal,* 99**,** 2715-2715.
OREKHOV, A. N., BOBRYSHEV, Y. V. & CHISTIAKOV, D. A. 2014. The complexity of cell composition of the intima of large arteries: focus on pericyte-like cells. *Cardiovascular Research,* 103**,** 438-451.
OTZEN, D. E., BLANS, K., WANG, H. B., GILBERT, G. E. & RASMUSSEN, J. T. 2012. Lactadherin binds to phosphatidylserine-containing vesicles in a two-step mechanism sensitive to vesicle size and composition. *Biochimica Et Biophysica Acta-Biomembranes,* 1818**,** 1019-1027.
PAKALA, R. 2004. Serotonin and thromboxane A2 stimulate platelet-derived microparticle-induced smooth muscle cell proliferation. *Cardiovascular radiation medicine,* 5**,** 20-6.
PAROLINI, I., FEDERICI, C., RAGGI, C., LUGINI, L., PALLESCHI, S., DE MILITO, A., COSCIA, C., IESSI, E., LOGOZZI, M., MOLINARI, A., COLONE, M., TATTI, M., SARGIACOMO, M. & FAIS, S. 2009. Microenvironmental pH Is a Key Factor for Exosome Traffic in Tumor Cells. *Journal of Biological Chemistry,* 284**,** 34211-34222.
PASSLICK, B., FLIEGER, D. & ZIEGLERHEITBROCK, H. W. L. 1989. IDENTIFICATION AND CHARACTERIZATION OF A NOVEL MONOCYTE SUBPOPULATION IN HUMAN PERIPHERAL-BLOOD. *Blood,* 74**,** 2527-2534.
PELEGRIN, P. & SURPRENANT, A. 2006. Pannexin-1 mediates large pore formation and interleukin-1 beta release by the ATP-gated P2X(7) receptor. *Embo Journal,* 25**,** 5071-5082.
PENG, K., LIU, L., WEI, D., LV, Y., WANG, G., XIONG, W., WANG, X., ALTAF, A., WANG, L., HE, D., WANG, H. & QU, P. 2015. P2X7R is involved in the progression of atherosclerosis by promoting NLRP3 inflammasome activation. *International Journal of Molecular Medicine,* 35**,** 1179-1188.
PFEIFFER, Z. A., AGA, M., PRABHU, U., WATTERS, J. J., HALL, D. J. & BERTICS, P. J. 2004. The nucleotide receptor P2X7 mediates actin reorganization and membrane blebbing in RAW 264.7 macrophages via p38 MAP kinase and Rho. *Journal of Leukocyte Biology,* 75**,** 1173-1182.
PINDERSKI, L. J., FISCHBEIN, M. P., SUBBANAGOUNDER, G., FISHBEIN, M. C., KUBO, N., CHEROUTRE, H., CURTISS, L. K., BERLINER, J. A. & BOISVERT, W. A. 2002. Overexpression of interleukin-10 by activated T lymphocytes inhibits atherosclerosis in LDL receptor-deficient mice by altering lymphocyte and macrophage phenotypes. *Circulation Research,* 90**,** 1064-1071.
PISCOPIELLO, M., SESSA, M., ANZALONE, N., CASTELLANO, R., MAISANO, F., FERRERO, E., CHIESA, R., ALFIERI, O., COMI, G., FERRERO, M. E. & FOGLIENI, C. 2013. P2X7 receptor is expressed in human vessels and might play a role in atherosclerosis. *International Journal of Cardiology,* 168**,** 2863-2866.
PIZZIRANI, C., FERRARI, D., CHIOZZI, P., ADINOLFI, E., SANDONA, D., SAVAGLIO, E. & DI VIRGILIO, F. 2007. Stimulation of P2 receptors causes release of IL-1 beta-loaded microvesicles from human dendritic cells. *Blood,* 109**,** 3856-3864.

PLATNICH, J. M., CHUNG, H., LAU, A., SANDALL, C. F., BONDZI-SIMPSON, A., CHEN, H.-M., KOMADA, T., TROTMAN-GRANT, A. C., BRANDELLI, J. R., CHUN, J., BECK, P. L., PHILPOTT, D. J., GIRARDIN, S. E., HO, M., JOHNSON, R. P., MACDONALD, J. A., ARMSTRONG, G. D. & MURUVE, D. A. 2018. Shiga Toxin/Lipopolysaccharide Activates Caspase-4 and Gasdermin D to Trigger Mitochondrial Reactive Oxygen Species Upstream of the NLRP3 Inflammasome. *Cell Reports,* 25**,** 1525-U20.

POZNYAK, A. V., NIKIFOROV, N. G., MARKIN, A. M., KASHIRSKIKH, D. A., MYASOEDOVA, V. A., GERASIMOVA, E. V. & OREKHOV, A. N. 2021. Overview of OxLDL and Its Impact on Cardiovascular Health: Focus on Atherosclerosis. *Frontiers in Pharmacology,* 11.

PRESTON, R. A., JY, W., JIMENEZ, J. J., MAURO, L. M., HORSTMAN, L. L., VALLE, M., AIME, G. & ALM, Y. S. 2003. Effects of severe hypertension on endothelial and platelet microparticles. *Hypertension,* 41**,** 211-217.

QU, Y., FRANCHI, L., NUNEZ, G. & DUBYAK, G. R. 2007. Nonclassical IL-1 beta secretion stimulated by P2X7 receptors is dependent on inflammasome activation and correlated with exosome release in murine macrophages. *Journal of Immunology,* 179**,** 1913-1925.

RAJAMAKI, K., NORDSTROM, T., NURMI, K., AKERMAN, K. E. O., KOVANEN, P. T., OORNI, K. & EKLUND, K. K. 2013. Extracellular Acidosis Is a Novel Danger Signal Alerting Innate Immunity via the NLRP3 Inflammasome. *Journal of Biological Chemistry,* 288**,** 13410-13419.

RAMEL, D., GAYRAL, S., SARTHOU, M.-K., AUGE, N., NEGRE-SALVAYRE, A. & LAFFARGUE, M. 2019. Immune and Smooth Muscle Cells Interactions in Atherosclerosis: How to Target a Breaking Bad Dialogue? *Frontiers in Pharmacology,* 10.

RASSENDREN, F., BUELL, G. N., VIRGINIO, C., COLLO, G., NORTH, R. A. & SURPRENANT, A. 1997. The permeabilizing ATP receptor, P2X(7) - Cloning and expression of a human cDNA. *Journal of Biological Chemistry,* 272**,** 5482-5486.

RATAJCZAK, J., WYSOCZYNSKI, M., HAYEK, F., JANOWSKA-WIECZOREK, A. & RATAJCZAK, M. Z. 2006. Membrane-derived microvesicles: important and underappreciated mediators of cell-to-cell communication. *Leukemia,* 20**,** 1487-1495.

RATAJCZAK, M. Z. & RATAJCZAK, J. 2020. Extracellular microvesicles/exosomes: discovery, disbelief, acceptance, and the future? *Leukemia,* 34**,** 3126-3135.

READ, S. A., WIJAYA, R., RAMEZANI-MOGHADAM, M., TAY, E., SCHIBECI, S., LIDDLE, C., LAM, V. W. T., YUEN, L., DOUGLAS, M. W., BOOTH, D., GEORGE, J. & AHLENSTIEL, G. 2019. Macrophage Coordination of the Interferon Lambda Immune Response. *Frontiers in Immunology,* 10.

REN, H., TENG, Y., TAN, B., ZHANG, X., JIANG, W., LIU, M., JIANG, W., DU, B. & QIAN, M. 2014. Toll-Like Receptor-Triggered Calcium Mobilization Protects Mice against Bacterial Infection through Extracellular ATP Release. *Infection and Immunity,* 82**,** 5076-5085.

REYNIER, F., DE VOS, A. F., HOOGERWERF, J. I., BRESSER, P., VAN DER ZEE, J. S., PAYE, M., PACHOT, A., MOUGIN, B. & VAN DER POLL, T. 2012. Gene Expression Profiles in Alveolar Macrophages Induced by Lipopolysaccharide in Humans. *Molecular Medicine,* 18**,** 1303-1311.

RIDGER, V. C., BOULANGER, C. M., ANGELILLO-SCHERRER, A., BADIMON, L., BLANC-BRUDE, O., BOCHATON-PIALLAT, M.-L., BOILARD, E., BUZAS, E.

I., CAPORALI, A., DIGNAT-GEORGE, F., EVANS, P. C., LACROIX, R., LUTGENS, E., KETELHUTH, D. F. J., NIEUWLAND, R., TOTI, F., TUNON, J., WEBER, C., HOEFER, I. E., LIP, G. Y. H., WERNER, N., SHANTSILA, E., TEN CATE, H., THOMAS, M. & HARRISON, P. 2017. Microvesicles in vascular homeostasis and diseases Position Paper of the European Society of Cardiology (ESC) Working Group on Atherosclerosis and Vascular Biology. *Thrombosis and Haemostasis,* 117**,** 1296-1316.

RIDKER, P. M. 2016. From C-Reactive Protein to Interleukin-6 to Interleukin-1 Moving Upstream To Identify Novel Targets for Atheroprotection. *Circulation Research,* 118**,** 145-156.

RIDKER, P. M., EVERETT, B. M., THUREN, T., MACFADYEN, J. G., CHANG, W. H., BALLANTYNE, C., FONSECA, F., NICOLAU, J., KOENIG, W., ANKER, S. D., KASTELEIN, J. J. P., CORNEL, J. H., PAIS, P., PELLA, D., GENEST, J., CIFKOVA, R., LORENZATTI, A., FORSTER, T., KOBALAVA, Z., VIDA-SIMITI, L., FLATHER, M., SHIMOKAWA, H., OGAWA, H., DELLBORG, M., ROSSI, P. R. F., TROQUAY, R. P. T., LIBBY, P., GLYNN, R. J. & GRP, C. T. 2017. Antiinflammatory Therapy with Canakinumab for Atherosclerotic Disease. *New England Journal of Medicine,* 377**,** 1119-1131.

RIDKER, P. M., HOWARD, C. P., WALTER, V., EVERETT, B., LIBBY, P., HENSEN, J., THUREN, T. & GRP, C. P. I. 2012. Effects of Interleukin-1 beta Inhibition With Canakinumab on Hemoglobin A1c, Lipids, C-Reactive Protein, Interleukin-6, and Fibrinogen A Phase IIb Randomized, Placebo-Controlled Trial. *Circulation,* 126**,** 2739-+.

ROBBINS, C. S., CHUDNOVSKIY, A., RAUCH, P. J., FIGUEIREDO, J.-L., IWAMOTO, Y., GORBATOV, R., ETZRODT, M., WEBER, G. F., UENO, T., VAN ROOIJEN, N., MULLIGAN-KEHOE, M. J., LIBBY, P., NAHRENDORF, M., PITTET, M. J., WEISSLEDER, R. & SWIRSKI, F. K. 2012. Extramedullary Hematopoiesis Generates Ly-6C(high) Monocytes That Infiltrate Atherosclerotic Lesions. *Circulation,* 125**,** 364-U415.

ROLLINS, B. J., YOSHIMURA, T., LEONARD, E. J. & POBER, J. S. 1990. CYTOKINE-ACTIVATED HUMAN ENDOTHELIAL-CELLS SYNTHESIZE AND SECRETE A MONOCYTE CHEMOATTRACTANT, MCP-1/JE. *American Journal of Pathology,* 136**,** 1229-1233.

ROSS, R. 1999. Mechanisms of disease - Atherosclerosis - An inflammatory disease. *New England Journal of Medicine,* 340**,** 115-126.

ROSS, R., MASUDA, J., RAINES, E. W., GOWN, A. M., KATSUDA, S., SASAHARA, M., MALDEN, L. T., MASUKO, H. & SATO, H. 1990. LOCALIZATION OF PDGF-B PROTEIN IN MACROPHAGES IN ALL PHASES OF ATHEROGENESIS. *Science,* 248**,** 1009-1012.

RUBARTELLI, A., COZZOLINO, F., TALIO, M. & SITIA, R. 1990. A NOVEL SECRETORY PATHWAY FOR INTERLEUKIN-1-BETA, A PROTEIN LACKING A SIGNAL SEQUENCE. *Embo Journal,* 9**,** 1503-1510.

SAKAKI, H., TSUKIMOTO, M., HARADA, H., MORIYAMA, Y. & KOJIMA, S. 2013. Autocrine Regulation of Macrophage Activation via Exocytosis of ATP and Activation of P2Y11 Receptor. *Plos One,* 8.

SARLON-BARTOLI, G., BENNIS, Y., LACROIX, R., PIERCECCHI-MARTI, M. D., BARTOLI, M. A., ARNAUD, L., MANCINI, J., BOUDES, A., SARLON, E., THEVENIN, B., LEROYER, A. S., SQUARCIONI, C., MAGNAN, P. E., DIGNAT-GEORGE, F. & SABATIER, F. 2013. Plasmatic Level of Leukocyte-Derived Microparticles Is Associated With Unstable Plaque in Asymptomatic

Patients With High-Grade Carotid Stenosis. *Journal of the American College of Cardiology,* 62**,** 1436-1441.
SATHANOORI, R., SWARD, K., OLDE, B. & ERLINGE, D. 2015. The ATP Receptors P2X7 and P2X4 Modulate High Glucose and Palmitate-Induced Inflammatory Responses in Endothelial Cells. *Plos One,* 10.
SATHER, S., KENYON, K. D., LEFKOWITZ, J. B., LIANG, X., VARNUM, B. C., HENSON, P. M. & GRAHAM, D. K. 2007. A soluble form of the Mer receptor tyrosine kinase inhibits macrophage clearance of apoptotic cells and platelet aggregation. *Blood,* 109**,** 1026-1033.
SAVIO, L. E. B., MELLO, P. D. A., DA SILVA, C. G. & COUTINHO-SILVA, R. 2018. The P2X7 Receptor in Inflammatory Diseases: Angel or Demon? *Frontiers in Pharmacology,* 9.
SCANU, A., MOLNARFI, N., BRANDT, K. J., GRUAZ, L., DAYER, J. M. & BURGER, D. 2008. Stimulated T cells generate microparticles, which mimic cellular contact activation of human monocytes: differential regulation of pro- and anti-inflammatory cytokine production by high-density lipoproteins. *Journal of Leukocyte Biology,* 83**,** 921-927.
SCHILDBERGER, A., ROSSMANITH, E., EICHHORN, T., STRASSL, K. & WEBER, V. 2013. Monocytes, peripheral blood mononuclear cells, and THP-1 cells exhibit different cytokine expression patterns following stimulation with lipopolysaccharide. *Mediators of inflammation,* 2013**,** 697972-697972.
SCOTT, R. S., MCMAHON, E. J., POP, S. M., REAP, E. A., CARICCHIO, R., COHEN, P. L., EARP, H. S. & MATSUSHIMA, G. K. 2001. Phagocytosis and clearance of apoptotic cells is mediated by MER. *Nature,* 411**,** 207-211.
SELZMAN, C. H., SHAMES, B. D., MCINTYRE, R. C., BANERJEE, A. & HARKEN, A. H. 1999. The NF kappa B inhibitory peptide, I kappa B alpha, prevents human vascular smooth muscle proliferation. *Annals of Thoracic Surgery,* 67**,** 1227-1231.
SEMAN, M., ADRIOUCH, S., SCHEUPLEIN, F., KREBS, C., FREESE, D., GLOWACKI, G., DETERRE, P., HAAG, F. & KOCH-NOLTE, F. 2003. NAD-induced T cell death: ADP-ribosylation of cell surface proteins by ART2 activates the cytolytic P2X7 purinoceptor. *Immunity,* 19**,** 571-582.
SEN, P., WALLET, M. A., YI, Z., HUANG, Y., HENDERSON, M., MATHEWS, C. E., EARP, H. S., MATSUSHIMA, G., BALDWIN, A. S., JR. & TISCH, R. M. 2007. Apoptotic cells induce Mer tyrosine kinase-dependent blockade of NTF-kappa B activation in dendritic cells. *Blood,* 109**,** 653-660.
SHANTSILA, E., KAMPHUISEN, P. W. & LIP, G. Y. H. 2010. Circulating microparticles in cardiovascular disease: implications for atherogenesis and atherothrombosis. *Journal of Thrombosis and Haemostasis,* 8**,** 2358-2368.
SHET, A. S., ARAS, O., GUPTA, K., HASS, M. J., RAUSCH, D. J., SABA, N., KOOPMEINERS, L., KEY, N. S. & HEBBEL, R. P. 2003. Sickle blood contains tissue factor-positive microparticles derived from endothelial cells and monocytes. *Blood,* 102**,** 2678-2683.
SHI, J., ZHAO, Y., WANG, K., SHI, X., WANG, Y., HUANG, H., ZHUANG, Y., CAI, T., WANG, F. & SHAO, F. 2015. Cleavage of GSDMD by inflammatory caspases determines pyroptotic cell death. *Nature,* 526**,** 660-665.
SHI, X.-X., ZHENG, K.-C., SHAN, P.-R., ZHANG, L., WU, S.-J. & HUANG, Z.-Q. 2021. Elevated circulating level of P2X7 receptor is related to severity of coronary artery stenosis and prognosis of acute myocardial infarction. *Cardiology Journal,* 28**,** 453-459.

SHIEH, C.-H., HEINRICH, A., SERCHOV, T., VAN CALKER, D. & BIBER, K. 2014. P2X7-dependent, but differentially regulated release of IL-6, CCL2, and TNF-alpha in cultured mouse microglia. *Glia,* 62**,** 592-607.
SHIMOKAWA, H., ITO, A., FUKUMOTO, Y., KADOKAMI, T., NAKAIKE, R., SAKATA, M., TAKAYANAGI, T., EGASHIRA, K. & TAKESHITA, A. 1996. Chronic treatment with interleukin-1 beta induces coronary intimal lesions and vasospastic responses in pigs in vivo - The role of platelet-derived growth factor. *Journal of Clinical Investigation,* 97**,** 769-776.
SIBILLE, Y. & REYNOLDS, H. Y. 1990. MACROPHAGES AND POLYMORPHONUCLEAR NEUTROPHILS IN LUNG DEFENSE AND INJURY. *American Review of Respiratory Disease,* 141**,** 471-501.
SICA, A. & MANTOVANI, A. 2012. Macrophage plasticity and polarization: in vivo veritas. *Journal of Clinical Investigation,* 122**,** 787-795.
SINGH, R. J. R., MASON, J. C., LIDINGTON, E. A., EDWARDS, D. R., NUTTALL, R. K., KHOKHA, R., KNAUPER, V., MURPHY, G. & GAVRILOVIC, J. 2005. Cytokine stimulated vascular cell adhesion molecule-1 (VCAM-1) ectodomain release is regulated by TIMP-3. *Cardiovascular Research,* 67**,** 39-49.
SMEDLUND, K. & VAZQUEZ, G. 2008. Involvement of Native TRPC3 Proteins in ATP-Dependent Expression of VCAM-1 and Monocyte Adherence in Coronary Artery Endothelial Cells. *Arteriosclerosis Thrombosis and Vascular Biology,* 28**,** 2049-2055.
SMEETH, L., THOMAS, S. L., HALL, A. J., HUBBARD, R., FARRINGTON, P. & VALLANCE, P. 2004. Risk of myocardial infarction and stroke after acute infection or vaccination. *New England Journal of Medicine,* 351**,** 2611-2618.
STACHON, P., HEIDENREICH, A., MERZ, J., HILGENDORF, I., WOLF, D., WILLECKE, F., VON GARLEN, S., ALBRECHT, P., HAERDTNER, C., EHRAT, N., HOPPE, N., REINOEHL, J., MUEHLEN, C. V. Z., BODE, C., IDZKO, M. & ZIRLIK, A. 2017. P2X(7) Deficiency Blocks Lesional Inflammasome Activity and Ameliorates Atherosclerosis in Mice. *Circulation,* 135**,** 2524-2533.
STEVENSON, F. T., TORRANO, F., LOCKSLEY, R. M. & LOVETT, D. H. 1992. INTERLEUKIN-1 - THE PATTERNS OF TRANSLATION AND INTRACELLULAR-DISTRIBUTION SUPPORT ALTERNATIVE SECRETORY MECHANISMS. *Journal of Cellular Physiology,* 152**,** 223-231.
STITT, T. N., CONN, G., GORE, M., LAI, C., BRUNO, J., RADZIEJEWSKI, C., MATTSSON, K., FISHER, J., GIES, D. R., JONES, P. F., MASIAKOWSKI, P., RYAN, T. E., TOBKES, N. J., CHEN, D. H., DISTEFANO, P. S., LONG, G. L., BASILICO, C., GOLDFARB, M. P., LEMKE, G., GLASS, D. J. & YANCOPOULOS, G. D. 1995. THE ANTICOAGULATION FACTOR PROTEIN-S AND ITS RELATIVE, GAS6, ARE LIGANDS FOR THE TYRO 3/AXL FAMILY OF RECEPTOR TYROSINE KINASES. *Cell,* 80**,** 661-670.
SUBRAMANIAN, M., PROTO, J. D., MATSUSHIMA, G. K. & TABAS, I. 2016. Deficiency of AXL in Bone Marrow-Derived Cells Does Not Affect Advanced Atherosclerotic Lesion Progression. *Scientific Reports,* 6.
SURPRENANT, A. & NORTH, R. A. 2009. Signaling at Purinergic P2X Receptors. *Annual Review of Physiology,* 71**,** 333-359.
SURPRENANT, A., RASSENDREN, F., KAWASHIMA, E., NORTH, R. A. & BUELL, G. 1996. The cytolytic P-2Z receptor for extracellular ATP identified as a P-2X receptor (P2X(7)). *Science,* 272**,** 735-738.

SVENSSON, K. J., CHRISTIANSON, H. C., WITTRUP, A., BOURSEAU-GUILMAIN, E., LINDQVIST, E., SVENSSON, L. M., MORGELIN, M. & BELTING, M. 2013. Exosome Uptake Depends on ERK1/2-Heat Shock Protein 27 Signaling and Lipid Raft-mediated Endocytosis Negatively Regulated by Caveolin-1. *Journal of Biological Chemistry,* 288**,** 17713-17724.

SWIRSKI, F. K., LIBBY, P., AIKAWA, E., ALCAIDE, P., LUSCINSKAS, F. W., WEISSLEDER, R. & PITTET, M. J. 2007. Ly-6C(hi) monocytes dominate hypercholesterolemia-associated monocytosis and give rise to macrophages in atheromata. *Journal of Clinical Investigation,* 117**,** 195-205.

TACKE, F. & RANDOLPH, G. J. 2006. Migratory fate and differentiation of blood monocyte subsets. *Immunobiology,* 211**,** 609-618.

TAKEUCHI, O. & AKIRA, S. 2010. Pattern Recognition Receptors and Inflammation. *Cell,* 140**,** 805-820.

TELES, R. M. B., GRAEBER, T. G., KRUTZIK, S. R., MONTOYA, D., SCHENK, M., LEE, D. J., KOMISOPOULOU, E., KELLY-SCUMPIA, K., CHUN, R., IYER, S. S., SARNO, E. N., REA, T. H., HEWISON, M., ADAMS, J. S., POPPER, S. J., RELMAN, D. A., STENGER, S., BLOOM, B. R., CHENG, G. & MODLIN, R. L. 2013. Type I Interferon Suppresses Type II Interferon-Triggered Human Anti-Mycobacterial Responses. *Science,* 339**,** 1448-1453.

TENG, F. & FUSSENEGGER, M. 2021. Shedding Light on Extracellular Vesicle Biogenesis and Bioengineering. *Advanced Science,* 8.

TETE, S., TRIPODI, D., ROSATI, M., CONTI, F., MACCAURO, G., SAGGINI, A., CIANCHETTI, E., CARAFFA, A., ANTINOLFI, P., TONIATO, E., CASTELLANI, M. L., CONTI, P. & THEOHARIDES, T. C. 2012. IL-37 (IL-1F7) THE NEWEST ANTI-INFLAMMATORY CYTOKINE WHICH SUPPRESSES IMMUNE RESPONSES AND INFLAMMATION. *International Journal of Immunopathology and Pharmacology,* 25**,** 31-38.

THORNBERRY, N. A., BULL, H. G., CALAYCAY, J. R., CHAPMAN, K. T., HOWARD, A. D., KOSTURA, M. J., MILLER, D. K., MOLINEAUX, S. M., WEIDNER, J. R., AUNINS, J., ELLISTON, K. O., AYALA, J. M., CASANO, F. J., CHIN, J., DING, G. J. F., EGGER, L. A., GAFFNEY, E. P., LIMJUCO, G., PALYHA, O. C., RAJU, S. M., ROLANDO, A. M., SALLEY, J. P., YAMIN, T. T., LEE, T. D., SHIVELY, J. E., MACCROSS, M., MUMFORD, R. A., SCHMIDT, J. A. & TOCCI, M. J. 1992. A NOVEL HETERODIMERIC CYSTEINE PROTEASE IS REQUIRED FOR INTERLEUKIN-1-BETA PROCESSING IN MONOCYTES. *Nature,* 356**,** 768-774.

THORP, E., CUI, D., SCHRIJVERS, D. M., KURIAKOSE, G. & TABAS, I. 2008. Mertk receptor mutation reduces efferocytosis efficiency and promotes apoptotic cell accumulation and plaque necrosis in atherosclerotic lesions of Apoe(-/-) mice. *Arteriosclerosis Thrombosis and Vascular Biology,* 28**,** 1421-1428.

TSUJIOKA, H., IMANISHI, T., IKEJIMA, H., KUROI, A., TAKARADA, S., TANIMOTO, T., KITABATA, H., OKOCHI, K., ARITA, Y., ISHIBASHI, K., KOMUKAI, K., KATAIWA, H., NAKAMURA, N., HIRATA, K., TANAKA, A. & AKASAKA, T. 2009. Impact of Heterogeneity of Human Peripheral Blood Monocyte Subsets on Myocardial Salvage in Patients With Primary Acute Myocardial Infarction. *Journal of the American College of Cardiology,* 54**,** 130-138.

VAN DER LAAN, A. M., TER HORST, E. N., DELEWI, R., BEGIENEMAN, M. P. V., KRIJNEN, P. A. J., HIRSCH, A., LAVAEI, M., NAHRENDORF, M.,

HORREVOETS, A. J., NIESSEN, H. W. M. & PIEK, J. J. 2014. Monocyte subset accumulation in the human heart following acute myocardial infarction and the role of the spleen as monocyte reservoir. *European Heart Journal,* 35**,** 376-385.

VAN GILS, J. M., DERBY, M. C., FERNANDES, L. R., RAMKHELAWON, B., RAY, T. D., RAYNER, K. J., PARATHATH, S., DISTEL, E., FEIG, J. L., ALVAREZ-LEITE, J. I., RAYNER, A. J., MCDONALD, T. O., O'BRIEN, K. D., STUART, L. M., FISHER, E. A., LACY-HULBERT, A. & MOORE, K. J. 2012. The neuroimmune guidance cue netrin-1 promotes atherosclerosis by inhibiting the emigration of macrophages from plaques. *Nature Immunology,* 13**,** 136-143.

VANWIJK, M. J., VANBAVEL, E., STURK, A. & NIEUWLAND, R. 2003. Microparticles in cardiovascular diseases. *Cardiovascular Research,* 59**,** 277-287.

VERHOEF, P. A., ESTACION, M., SCHILLING, W. & DUBYAK, G. R. 2003. P2X7 receptor-dependent blebbing and the activation of Rho-effector kinases, caspases, and IL-1 beta release. *Journal of Immunology,* 170**,** 5728-5738.

VERMES, I., HAANEN, C., STEFFENSNAKKEN, H. & REUTELINGSPERGER, C. 1995. A NOVEL ASSAY FOR APOPTOSIS - FLOW CYTOMETRIC DETECTION OF PHOSPHATIDYLSERINE EXPRESSION ON EARLY APOPTOTIC CELLS USING FLUORESCEIN-LABELED ANNEXIN-V. *Journal of Immunological Methods,* 184**,** 39-51.

VIEMANN, D., GOEBELER, M., SCHMID, S., NORDHUES, U., KLIMMEK, K., SORG, C. & ROTH, J. 2006. TNF induces distinct gene expression programs in microvascular and macrovascular human endothelial cells. *Journal of Leukocyte Biology,* 80**,** 174-185.

VINCI, R., PEDICINO, D., BONANNI, A., D'AIELLO, A., SEVERINO, A., PISANO, E., PONZO, M., CANONICO, F., CIAMPI, P., RUSSO, G., DI SARIO, M., MONTONE, R. A., TRANI, C., CONTE, C., GRIMALDI, M. C., CRIBARI, F., MASSETTI, M., CREA, F. & LIUZZO, G. 2021. A Novel Monocyte Subset as a Unique Signature of Atherosclerotic Plaque Rupture. *Frontiers in Cell and Developmental Biology,* 9.

VINK, A., SCHONEVELD, A. H., VAN DER MEER, J. J., VAN MIDDELAAR, B. J., SLUIJTER, J. P. G., SMEETS, M. B., QUAX, P. H. A., LIM, S. K., BORST, C., PASTERKAMP, G. & DE KLEIJN, D. P. V. 2002. In vivo evidence for a role of toll-like receptor 4 in the development of intimal lesions. *Circulation,* 106**,** 1985-1990.

VIRGINIO, C., MACKENZIE, A., NORTH, R. A. & SURPRENANT, A. 1999. Kinetics of cell lysis, dye uptake and permeability changes in cells expressing the rat P2X(7) receptor. *Journal of Physiology-London,* 519**,** 335-346.

WANG, H., NAGHAVI, M., ALLEN, C., BARBER, R. M., BHUTTA, Z. A., CARTER, A., CASEY, D. C., CHARLSON, F. J., CHEN, A. Z., COATES, M. M., COGGESHALL, M., DANDONA, L., DICKER, D. J., ERSKINE, H. E., FERRARI, A. J., FITZMAURICE, C., FOREMAN, K., FOROUZANFAR, M. H., FRASER, M. S., PULLMAN, N., GETHING, P. W., GOLDBERG, E. M., GRAETZ, N., HAAGSMA, J. A., HAY, S. I., HUYNH, C., JOHNSON, C., KASSEBAUM, N. J., KINFU, Y., KULIKOFF, X. R., KUTZ, M., KYU, H. H., LARSON, H. J., LEUNG, J., LIANG, X., LIM, S. S., LIND, M., LOZANO, R., MARQUEZ, N., MENSAH, G. A., MIKESELL, J., MOKDAD, A. H., MOONEY, M. D., NGUYEN, G., NSOESIE, E., PIGOTT, D. M., PINHO, C., ROTH, G. A.,

SALOMON, J. A., SANDAR, L., SILPAKIT, N., SLIGAR, A., SORENSEN, R. J. D., STANAWAY, J., STEINER, C., TEEPLE, S., THOMAS, B. A., TROEGER, C., VANDERZANDEN, A., VOLLSET, S. E., WANGA, V., WHITEFORD, H. A., WOLOCK, T., ZOECKLER, L., ABATE, K. H., ABBAFATI, C., ABBAS, K. M., ABD-ALLAH, F., ABERA, S. F., ABREU, D. M. X., ABU-RADDAD, L. J., ABYU, G. Y., ACHOKI, T., ADELEKAN, A. L., ADEMI, Z., ADOU, A. K., ADSUAR, J. C., AFANVI, K. A., AFSHIN, A., AGARDH, E. E., AGARWAL, A., AGRAWAL, A., KIADALIRI, A. A., AJALA, O. N., AKANDA, A. S., AKINYEMI, R. O., AKINYEMIJU, T. F., AKSEER, N., AL LAMI, F. H., ALABED, S., AL-ALY, Z., ALAM, K., ALAM, N. K. M., ALASFOOR, D., ALDHAHRI, S. F., ALDRIDGE, R. W., ALEGRETTI, M. A., ALEMAN, A. V., ALEMU, Z. A., ALEXANDER, L. T., et al. 2016. Global, regional, and national life expectancy, all-cause mortality, and cause-specific mortality for 249 causes of death, 1980-2015: a systematic analysis for the Global Burden of Disease Study 2015. *Lancet,* 388**,** 1459-1544.

WANG, H., NAWATA, J., KAKUDO, N., SUGIMURA, K., SUZUKI, J., SAKUMA, M., IKEDA, J. & SHIRATO, K. 2004. The upregulation of ICAM-1 and P-selectin requires high blood pressure but not circulating renin-angiotensin system in vivo. *Journal of Hypertension,* 22**,** 1323-1332.

WARD, J. R., WEST, P. W., ARIAANS, M. P., PARKER, L. C., FRANCIS, S. E., CROSSMAN, D. C., SABROE, I. & WILSON, H. L. 2010. Temporal Interleukin-1 beta Secretion from Primary Human Peripheral Blood Monocytes by P2X7-independent and P2X7-dependent Mechanisms. *Journal of Biological Chemistry,* 285**,** 23145-23156.

WARD, J. R., WILSON, H. L., FRANCIS, S. E., CROSSMAN, D. C. & SABROE, I. 2009. Translational Mini-Review Series on Immunology of Vascular Disease: Inflammation, infections and Toll-like receptors in cardiovascular disease. *Clinical and Experimental Immunology,* 156**,** 386-394.

WATERBORG, C. E. J., BEERMANN, S., BROEREN, M. G. A., BENNINK, M. B., KOENDERS, M. I., VAN LENT, P. L. E. M., VAN DEN BERG, W. B., VAN DER KRAAN, P. M. & VAN DE LOO, F. A. J. 2018. Protective role of the Mer Tyrosine Kinase via Efferocytosis in Rheumatoid Arthritis Models. *Frontiers in Immunology,* 9.

WHITE, S. J., HAYES, E. M., LEHOUX, S., JEREMY, J. Y., HORREVOETS, A. J. G. & NEWBY, A. C. 2011. Characterization of the Differential Response of Endothelial Cells Exposed to Normal and Elevated Laminar Shear Stress. *Journal of Cellular Physiology,* 226**,** 2841-2848.

WILDGRUBER, M., ASCHENBRENNER, T., WENDORFF, H., CZUBBA, M., GLINZER, A., HALLER, B., SCHIEMANN, M., ZIMMERMANN, A., BERGER, H., ECKSTEIN, H.-H., MEIER, R., WOHLGEMUTH, W. A., LIBBY, P. & ZERNECKE, A. 2016. The "Intermediate" CD14(++)CD16(+) monocyte subset increases in severe peripheral artery disease in humans. *Scientific Reports,* 6.

WILHELM, K., GANESAN, J., MUELLER, T., DUERR, C., GRIMM, M., BEILHACK, A., KREMPL, C. D., SORICHTER, S., GERLACH, U. V., JUETTNER, E., ZERWECK, A., GAERTNER, F., PELLEGATTI, P., DI VIRGILIO, F., FERRARI, D., KAMBHAM, N., FISCH, P., FINKE, J., IDZKO, M. & ZEISER, R. 2010. Graft-versus-host disease is enhanced by extracellular ATP activating P2X(7)R. *Nature Medicine,* 16**,** 1434-U117.

WOOLLARD, K. J. & GEISSMANN, F. 2010. Monocytes in atherosclerosis: subsets and functions. *Nature Reviews Cardiology,* 7**,** 77-86.

XIAO, H., LU, M., LIN, T. Y., CHEN, Z., CHEN, G., WANG, W.-C., MARIN, T., SHENTU, T.-P., WEN, L., GONGOL, B., SUN, W., LIANG, X., CHEN, J., HUANG, H.-D., PEDRA, J. H. F., JOHNSON, D. A. & SHYY, J. Y. J. 2013. Sterol Regulatory Element Binding Protein 2 Activation of NLRP3 Inflammasome in Endothelium Mediates Hemodynamic-Induced Atherosclerosis Susceptibility. *Circulation,* 128**,** 632-642.

YAMAMOTO, M., KAMATSUKA, Y., OHISHI, A., NISHIDA, K. & NAGASAWA, K. 2013. P2X7 receptors regulate engulfing activity of non-stimulated resting astrocytes. *Biochemical and Biophysical Research Communications,* 439**,** 90-95.

YANG, H.-T., COHEN, P. & ROUSSEAU, S. 2008. IL-1 beta-stimulated activation of ERK1/2 and p38 alpha MAPK mediates the transcriptional up-regulation of IL-6, IL-8 and GRO-alpha in HeLa cells. *Cellular Signalling,* 20**,** 375-380.

YIP, L., WOEHRLE, T., CORRIDEN, R., HIRSH, M., CHEN, Y., INOUE, Y., FERRARI, V., INSEL, P. A. & JUNGER, W. G. 2009. Autocrine regulation of T-cell activation by ATP release and P2X(7) receptors. *Faseb Journal,* 23**,** 1685-1693.

YU, H., LIN, L., ZHANG, Z., ZHANG, H. & HU, H. 2020. Targeting NF-kappa B pathway for the therapy of diseases: mechanism and clinical study. *Signal Transduction and Targeted Therapy,* 5.

YUAN, X., PENG, X., LI, Y. & LI, M. 2015. Role of IL-38 and Its Related Cytokines in Inflammation. *Mediators of Inflammation,* 2015.

YUANA, Y., STURK, A. & NIEUWLAND, R. 2013. Extracellular vesicles in physiological and pathological conditions. *Blood Reviews,* 27**,** 31-39.

YUDKIN, J. S., KUMARI, M., HUMPHRIES, S. E. & MOHAMED-ALI, V. 2000. Inflammation, obesity, stress and coronary heart disease: is interleukin-6 the link? *Atherosclerosis,* 148**,** 209-214.

YURDAGUL, A., JR., SULZMAIER, F. J., CHEN, X. L., PATTILLO, C. B., SCHLAEPFER, D. D. & ORR, A. W. 2016. Oxidized LDL induces FAK-dependent RSK signaling to drive NF-kappa B activation and VCAM-1 expression. *Journal of Cell Science,* 129**,** 1580-1591.

ZAGORSKA, A., TRAVES, P. G., LEW, E. D., DRANSFIELD, I. & LEMKE, G. 2014. Diversification of TAM receptor tyrosine kinase function. *Nature Immunology,* 15**,** 920-U226.

ZARINS, C. K., GIDDENS, D. P., BHARADVAJ, B. K., SOTTIURAI, V. S., MABON, R. F. & GLAGOV, S. 1983. CAROTID BIFURCATION ATHEROSCLEROSIS QUANTITATIVE CORRELATION OF PLAQUE LOCALIZATION WITH FLOW VELOCITY PROFILES AND WALL SHEAR-STRESS. *Circulation Research,* 53**,** 502-514.

ZEIHER, A. M., FISSLTHALER, B., SCHRAYUTZ, B. & BUSSE, R. 1995. NITRIC-OXIDE MODULATES THE EXPRESSION OF MONOCYTE CHEMOATTRACTANT PROTEIN-1 IN CULTURED HUMAN ENDOTHELIAL-CELLS. *Circulation Research,* 76**,** 980-986.

ZHANG, B., LU, H., JIANG, A., WU, H., FANG, L. & LV, Y. 2019. MerTK Downregulates Lipopolysaccharide-Induced Inflammation Through SOCS1 Protein but Does Not Affect Phagocytosis of Escherichia coli in Macrophages. *Inflammation,* 42**,** 113-123.

ZHANG, J., ALCAIDE, P., LIU, L., SUN, J., HE, A., LUSCINSKAS, F. W. & SHI, G.-P. 2011. Regulation of Endothelial Cell Adhesion Molecule Expression by Mast Cells, Macrophages, and Neutrophils. *Plos One,* 6.

ZHANG, J., LI, S., LI, L., LI, M., GUO, C., YAO, J. & MI, S. 2015. Exosome and Exosomal MicroRNA: Trafficking, Sorting, and Function. *Genomics Proteomics & Bioinformatics,* 13**,** 17-24.
ZHANG, X., BISHAWI, M., ZHANG, G., PRASAD, V., SALMON, E., BREITHAUPT, J. J., ZHANG, Q. & TRUSKEY, G. A. 2020. Modeling early stage atherosclerosis in a primary human vascular microphysiological system. *Nature Communications,* 11.